International Rotating Equipment Conference

6th EFRC Conference

Pump Users
International Forum 2008

Compressor Users
International Forum 2008

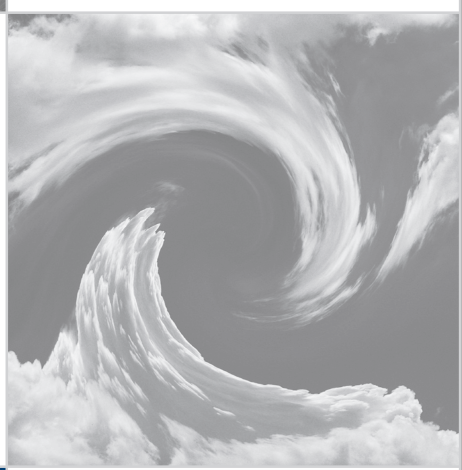

EFRC
EUROPEAN FORUM
for RECIPROCATING
COMPRESSORS

Düsseldorf, 28th–29th October 2008

PROCEEDINGS

Content

Session 31: Design and Engineering I

Session 32: Pulsations & Vibrations I

Session 33: Design & Engineering II

Session 34: Fundamentals

Session 35: Design & Engineering III

Session 36: Operations & Maintenance I

Session 37: EFRC Meeting

Session 38: Valves

Session 39: Operations & Maintenance II

Session 40: Design & Engineering IV

Session 41: Pulsations & Vibrations II

The erection of very large 4- and 6-cylinder reciprocating compressors

by:
Lau G.M. Koop
Technology Department
THOMASSEN COMPRESSION SYSTEMS
Rheden
The Netherlands

6th EFRC Conference
October 28th / 29th, 2008, Dusseldorf

Abstract:
The trend in the application of Hydrogen compressors is that the drive power of the individual compressors, is increasing to values of more than 10,000 kW. The expectation is that it may even rise to 20,000kW. The total weight of compressor and driver can be around 250 tons. The compressors used for these applications have physical dimensions and weights that require special know how for the installation and alignment to be able to obtain a stable and well aligned drive train.

In this paper the following points of special interest will be highlighted
The foundation loads:
- Static and dynamic, weights and free forces and moments
- Compressor and driver starting torques

Erection of the compressor and driver
- Sole plates
- Hoisting
- Alignment
- Commissioning

Vibrations
- Vibration measurements frame
- Vibration measurements cross head guide

1. Introduction

The demand for hydrogen at high pressure is constantly increasing. This requires an increasing compression power. For economical and efficiency reasons it is recommendable to apply a small number of large compressors instead of a large number of small ones. In order to satisfy the market, big compressors with high output have been developed and designed already several years ago. The dimensions and weight's of these compressors require special handling and care. It is obvious that driving torques and forces and compressor based dynamic forces on the foundation increase with the frame size of the compressors and motors. Erection of these machines has therefore been subject of discussion within our company, in order to acquire a procedure that in the end will ensure a vibration free compressor train.

Fig 1.1: Example of very large compressor

2. Foundation loads

The concrete foundation of a reciprocating compressor and anchor bolts determine for a greater part the vibration behaviour and the stability of the alignment. It must support the time varying loads, and therewith, limit the dynamic motion (vibration). The combined compressor and concrete mass as well as their stiffness must limit the vibration and deformation of the compressor structure.

Relevant foundation loads:

- Compressor and driver deadweights
- Driving torque
- Oscillating torques
- Free forces and moments
- Gas forces and frame deformations

2.1 Definitions

Foundation loads:
These are the weight loads of all components, and the time varying loads generated by compressor and driver.
Anchor bolts:
Anchor bolts are used for anchoring the sole plates to the concrete. They are cast in deep pockets
Hold down bolts:
Hold down bolts clamp the equipment feet on the soleplates.
Anchor bolts loads:
The anchor bolts must be able to transfer all the time varying forces to the foundation. The anchor bolts must be prestressed to such an extent that slippage is avoided.
Driving torque:
This is the torque generated by the E-motor to drive the compressor crankshaft. It causes a twisting torque in the foundation between motor and driver.
Oscillating torque:
The oscillations in the driving torque or the compressor torque. They cause dynamic loading of the anchor bolts, and dynamic twisting of the foundation.
Free forces and moments:
Caused by inertia forces of the moving parts in the compressor.
Gas forces:
In a double-acting cylinder, the instantaneous net compressive gas force acting on the piston rod equals the difference between head end and crank end gas forces. The head end and crank end pressures vary continuously and the differential force takes both positive and negative (inward and outward) net values during each cycle of piston motion.

2.2 Compressor parts and weights

The weight's of compressor and motor are considerable. This paragraph summarizes the weight's of the main components of a typical large 6 cylinder compressor. The table in fig. 2.1 indicates the weight's of the separate components.
Frame and crankshaft: approximately 40 tons
Crosshead guide with crosshead, connecting rod, cylinder, piston and valves: approximately 50 tons.
Complete electric motor approximately 90 tons.
These weights must be carried by the sole plates and the grouting.

WEIGHTS		
FRAME AND CRANKSHAFT		383.000 N
CROSSHEADGUIDE AND DISTANCE PIECE		
	6 x 68.670 - N =	412.020 N
CYLINDER 1	φ525 - mm	84.000 N
CYLINDER 2	φ740 - mm	101.000 N
CYLINDER 3	φ525 - mm	84.000 N
CYLINDER 4	φ740 - mm	101.000 N
CYLINDER 5	φ410 - mm	31.000 N
CYLINDER 6	φ410 - mm	31.000 N
PULSATION DAMP. SUCTION STAGE 1 CYL.5		11.000 N
PULSATION DAMP. SUCTION STAGE 1 CYL.6		11.000 N
PULSATION DAMP. SUCTION STAGE 2		62.500 N
PULSATION DAMP. SUCTION STAGE 3		50.000 N
PULSATION DAMP. DISCHARGE STAGE 1 CYL.5		14.000 N
PULSATION DAMP. DISCHARGE STAGE 1 CYL.6		14.000 N
PULSATION DAMP. DISCHARGE STAGE 2		63.500 N
PULSATION DAMP. DISCHARGE STAGE 3		70.000 N
AUXILIARIES		15.000 N
COMPRESSOR WEIGHT Z3		1.538.020 N
E-MOTOR INCL.ROTOR Z2 (ROTOR	330.000 N)	897.000 N
FLYWHEEL Z4		29.000 N
TOTAL WEIGHT Z1		2.464.020 N

Fig 2.1: Table with weights

The total weight of one compressor installation is about 250 tons.

2.3 Driving Torque

The E-motor is of the single bearing type and drives the compressor through a rigid flanged connection. The flywheel is mounted between the flanges. The reaction of this torque is transferred to the foundation block by the anchor bolts of the crosshead guides and the E-motor stator. In figure 2.2 the effect of dead weight and torque on the anchor bolt load is illustrated.

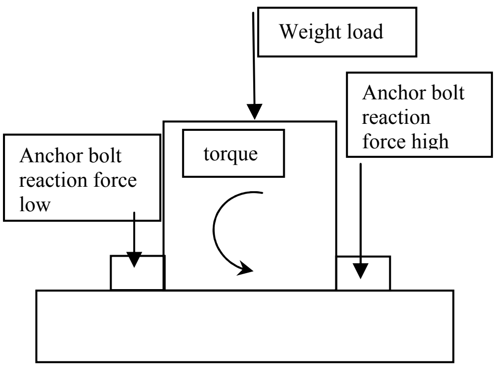

Fig 2.2: Anchor bolt loading

2.4 Oscillating torques

The oscillations in torque arise from 2 different sources:

a. The oscillations caused by the gas- and inertia forces consisting of harmonics of the compressor speed and are continuously present. They generally have amplitudes equal to the value of the static driving torque. This means that torque reversal during one revolution may occur.
b. Short circuit and starting torques These torques are transient. Short circuit and starting torques generated by the motor driver are considerable and can have values of 4-5 times the static driving torque. The stator generates a reaction force of equal magnitude, which is transferred through the anchor- and foundation bolts and soleplate, to the foundation.

In figure 2.3 a example is given of a typical starting torque characteristic. The oscillations decay within a few seconds: the main frequencies being one and two times the power frequency.

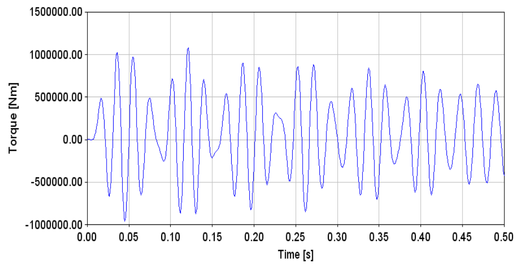

Fig 2.3: Transient starting torque at Motor stator

2.5 Free forces and moments

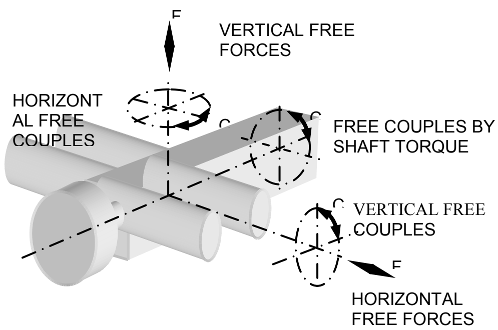

Fig2.4: Free forces and moments

Figure 2.4 shows the directions and the planes of the forces and moments caused by the moving parts in the compressor.

Free forces are induced by the unequal reciprocating masses of opposed pistons. These forces can be balanced by adding dummy masses to the crosshead of the respective cylinders.

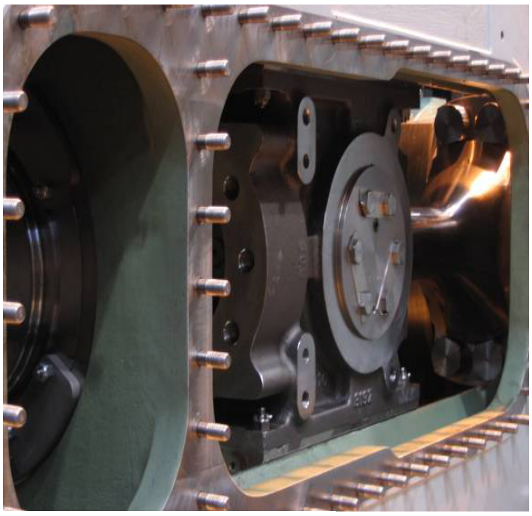

Fig 2.5: Oscillating masses

Free Moments are caused by:

a. The mutual offset of balanced opposed cylinders. The moments will cause an oscillating rocking motion of the concrete in the horizontal plane. They consist mainly of components of rotating and two times rotating speed (fundamental and 2nd harmonic). The fundamental components can be partly compensated by adding counterweights on the crankshaft webs. In case of a six-cylinder compressor these moments can be internally compensated by choosing the correct crank angles. The 2nd harmonic components can be reduced by minimizing the weight of the reciprocating masses, or in case of a four-cylinder compressor, by choosing suitable crank angles. As the mass of a crosshead (fig. 2.5) and piston of a large compressors is considerable (up to 1600 kg), a substantial 2nd order rocking moment will occur. In the table 2.6 a value of 8.55 kNm (Ch2) is given.

b. Off centre rotating masses. These moments solely consist of 1st order components. They can be compensated for by counterweighting the crankshaft.

c. Irregularities in the drive torque act in the vertical plane normal to the shaft axis. They are caused by the compression, expansion and mass forces on the piston rod. The irregularity of the rotating speed is reduced by the mass inertia of mainly the flywheel and the driver rotor. Despite this influence torque oscillations induce reaction forces in the bolting and foundation.

In table 2.6 below, values for free forces and moments generated by a large 4-cylinder compressor are presented. The horizontal rocking moment (Ch1) is 222 kNm, a considerable value despite the fact that it has already been reduced by counterweights. It is transmitted to the foundation by friction and shear in the foundation bolts. This requires attention to ensure that bolting does not fail by fatigue. Further it can be read that there are considerable harmonic amplitudes in the driving torque (Cs harmonics). These torques cause dynamic stretching on the foundation bolts. The motor short circuit torque will introduce large impulsive forces on the foundation bolts of the motor stator.

COMPRESSOR SPEED n_o =			323	RPM					
Fh_1	$(n = n_o)$	=	59.66	kN	Ch_1	$(n = n_o)$	=	221.88	kNm
Fh_2	$(n = 2 \times n_o)$	=	7.03	kN	Ch_2	$(n = 2 \times n_o)$	=	8.55	kNm
Fv_1	$(n = n_o)$	=	0	kN	Cv_1	$(n = n_o)$	=	17.72	kNm
HIGHEST OCCURING VALUES OF Cs HARMONICS:									
Cs_1	$(n = n_o)$	=	74.79	kNm					
Cs_2	$(n = 2 \times n_o)$	=	24.79	kNm					
Cs_3	$(n = 3 \times n_o)$	=	30.65	kNm					
Cs_4	$(n = 4 \times n_o)$	=	26.55	kNm					
HIGHEST VALUE OF SHAFT TORQUE VARIATION, PEAK TO PEAK							=	222.22	kNm
STEADY TORQUE BETWEEN COMPRESSOR AND DRIVER,						Cs_o	=	190.00	kNm
MOTOR SHORT CIRCUIT TORQUE,						Cs_m	=	1400	kNm

Table 2.6 Free Forces and moment for a 4-cylinder compressor

2.6 Gasforces

The gas forces in the cylinder cause alternating tension and compression forces in the crosshead guide and crankcase. These forces are internally balanced within the compressor structure. However the structure is not infinitely rigid, and stretching will occur. This leads to load transmission via the hold down and anchor bolts, to the concrete foundation, the amplitude of which is dependent on the ratio of rigidity of concrete to compressor structure.

The F.E. distortion picture in figure 2.7 shows the deformation of a cast crosshead guide support. It shows clearly that the anchor bolts are also subjected to dynamic loads. Intimate contact between sole plate and support, and the flexibility of the support determine for the greater part the amplitude of the dynamic load.

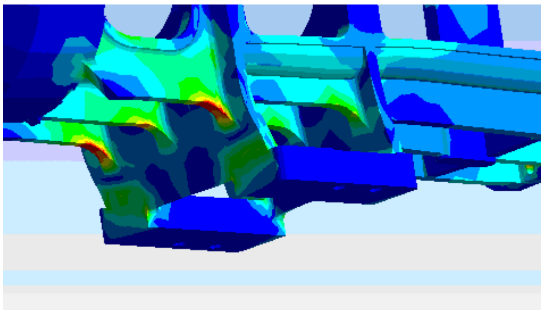

Fig 2.7: Deformation crosshead guide support

Clearances and/or misalignments are unacceptable, as these immediately lead to high dynamic loading with an increased risk of fatigue as well as increased dynamic displacements. These displacements manifest themselves at the outside of a compressor frame as vibrations. Measured vibrations are usually seismic and a summation of vibrations caused by forces and moments, and mechanical deformations of the structures caused by the gas forces.

3. Erection of compressor and driver

A very common and relative easy way to erect a compressor installation, is to ship, lift and install the completely assembled compressor including the soleplates. The alignment and grouting is then executed with the compressor in place on the foundation. Screw type jacks are used to align the machine in vertical and horizontal directions.

Large and heavy compressors are erected in a different way than the smaller frame sizes.. The TCS procedure is to install and grout the sole plates for large compressor frames prior to the installation of the frame. Of course the proper alignment of these plates on the concrete is of great significance in such a case. The sole plates are aligned with the use of precision spirit levels and/or laser alignment equipment. This is a time consuming activity, but it rewards itself when the heavy frames and crossheads can be installed without extensive shimming or aligning with the help of jacks.

Advantages and features of separate alignment of sole plates and equipment:

a. Large weights require heavy cranes. When the frame can be placed on sole plates directly, the crane occupation is limited.
b. Long shaft arrangements require accurate alignment.
c. Large concrete areas: laser alignment allows better correction and levelling possibilities.
d. Distance between anchor and hold down bolts is relatively large yielding relatively higher bending moments in the sole plates than with smaller machines. The thickness of the sole plates must be suitably chosen to accept these moments with minimal distortions, consistent with long term stability and reliability. This automatically results in large and heavy soleplates.
e. Once sole plates are almost perfectly aligned, the frame can be put in place in a relative short time period, and requires no time consuming vertical shimming or jacking.
f. Machines are not shipped fully assembled. The frames with crankshaft, and crosshead guides with cylinders are packed separately. In assembled condition they simply would not fit in sea containers and would require very special road transport facilities.
g. The relative heavy crosshead guides can then all be separately aligned to the already aligned and stable frame. They can also be separately grouted.

3.1 Sole plates

The sole plates carry the load imposed on the equipment feet. The figures 3.1 and 3.2 show the separate plates and relative alignment. Demonstrated are the precision techniques employed to assure the required degree of accuracy.

Fig 3.1: Sole plate alignment

Fig 3.2: Sole plate alignment

3.2 Hoisting

The compressor and driver are not shipped in assembled condition. Physical dimensions and weight's give restraints for transport. At site these parts must be put in place by relative heavy cranes.

Fig 3.3: Hoisting frame

The drive train of a 6-cylinder crankshaft, and rotor shaft can have a length of 10.5 m consisting of a system of 7 in line bearings, all of which have to be aligned in accordance manufacturers specifications. These are stringent to ensure a low wear and a long life in addition to ensuring long term machine reliability.

A flywheel is installed between the crankshaft and motor flange to reduce the speed irregularity. This flywheel is heavy, and may typically weigh 30 tons . The load of this flywheel is carried by the 1st and 2nd compressor bearing and partly by the Electric motor bearing. Precision alignment means that the flywheel weight is correctly distributed over the bearings and misalignment loads on bearings minimised.

Fig 3.4: Lifting Electric motor

Fig 3.5: Lifting Electric motor

Fig 3.6: Lifting flywheel

3.3 Alignment

As the machines are large, they are normally not shipped fully assembled. The crosshead guides and cylinders are packed separately. This means that the crosshead guides have to be site mounted and aligned. In many cases this is done by using precision spirit levels. The alignment of the crosshead guides to the crankcase is critical. Rod drop measurement during turn over in cold condition, is a method to confirm the alignment after installation. The method is described in the API 618 and the allowable values for the rod drop are calculated during the design stage of the compressor.

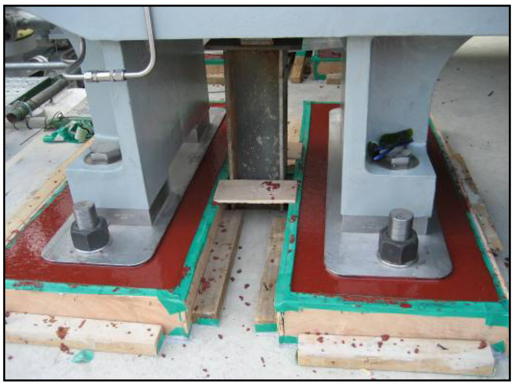

Fig 3.7: Cylinder and crosshead guide alignment

Alignment of the electric motor shaft is shown in fig 3.8. The electric motor rotor is aligned against the flywheel and crankshaft of the compressor, and thereafter the stator and rotor with respect to each other. Criteria for alignment are: the air gap of the electric motor should normally be to within 0.1 mm, and the crank web deflections to within 0.02 mm.

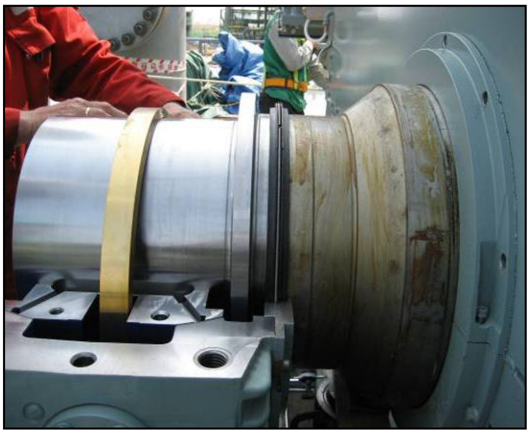

Fig 3.8: Alignment electric motor bearing

4. Measured vibrations after installation

After installation, the compressors are commissioned. During these runs the vibrations can and are often measured at several locations. Locations which give most information on the proper alignment, erection of the compressor train, integrity and design of the concrete foundation, are on the frame. Vibration measurements on crosshead guides supply mostly information on the machine condition . The cylinder cover vibration can give information on the gasforces inside the cylinder, and therewith the loading of the cylinder.

In the following paragraphs an example is be given showing vibration levels in bar charts from measurements on three identical compressors. The compressors are large frame size 4-cylinder compressors, which have been erected in accordance with the procedures outlined in this paper. From these charts it can be concluded that the vibrations of the 3 machines are very comparable and the levels measured on compressor C generally lowest.

4.1 Vibrations on crossheadguide

Measurements on the crosshead guides give information on the mechanical integrity of the compressor part itself, and should be measured by fixed accelerometers. Trending the measured acceleration will supply information on developing or imminent mechanical failures or periodical mechanical contact between parts yielding recognisable impact loads.

Figure 4.1 shows the crosshead guide acceleration per cylinder for compressor B and C (no data available for compressor A).

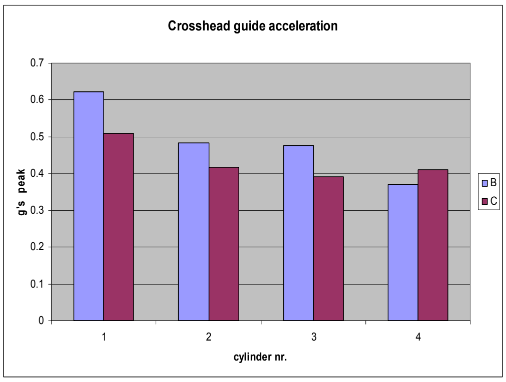

Fig 4.1: Crosshead guide acceleration

4.2 Frame vibrations

Typical locations for measurement on the frame are the frame feet, locations opposite main bearings on the shaft centreline, and the top of the frame. These measurements can be performed with hand held equipment. The vibrations are normally presented as vibration velocity. Comparison of the vibrations on parallel operating and identical compressors, will reveal significant differences between machines. Frame measurements often form part of a commissioning procedure and provides baseline values for future reference.

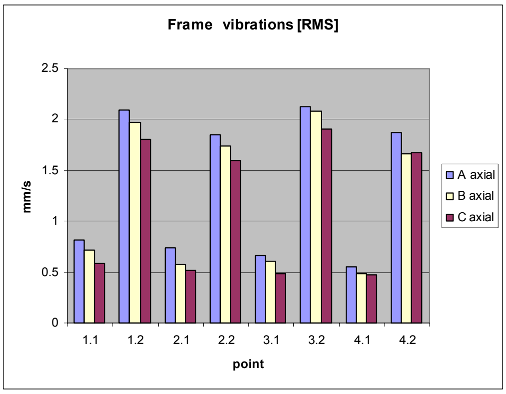

Fig 4.2: Frame vibrations

Figure 4.2 indicates that the frame vibrations of the three identical parallel machines is almost identical. This tends to confirm that the installation of the machines on the foundations has been correctly performed as the values are consistent per measuring point and closely comparable. Significant differences would have served as an alert for installation deviations and/or errors

4.3 Cylinder cover

Cylinder cover vibrations are the resultant of the stretching of the compressor structure resulting from the gas forces, as well the vibrations of the frame and concrete foundation . The gas force is the leading factor in these vibrations, which are mostly presented in vibration velocity ptp. It should be noted that these vibrations must be recorded from a rigid location. Not in the center of the cover.

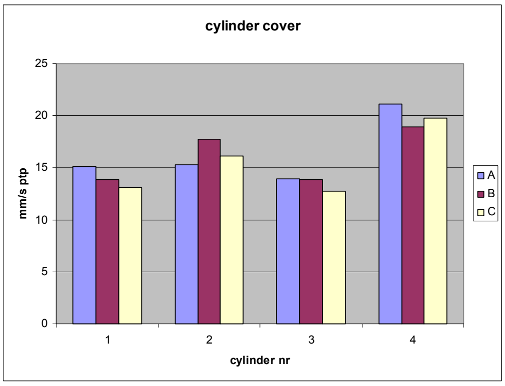

Fig 4.3: Cylinder cover vibrations

4.4 Assessment of vibrations

The assessment of the measured vibrations, should be done for each part. Frame vibrations should normally not exceed 5.3 mm/s RMS value vibration. The cylinder cover vibrations design value is 10.7 mm/s RMS (appr. 28 mm/s ptp velocity.) The crossheadguide base value is determined during commissioning the compressor at full load. It is generally presented as an impact value (acceleration mm/s^2 or g's).

Currently within a research project sponsored by the EFRC vibration criteria for compressors and process equipment are being examined and formulated.

5. Summary

- All mentioned loads in chapter 2 are transferred to and through the concrete foundations by the hold down bolts, anchor bolts and the friction forces between the soleplates and the frame feet. This implies that great accuracy is required in adjustment and alignment of the sole plates, as it is a critical interface in this force transmission path. When misalignment and/or gaps are present, this will immediately result in machine increased vibration levels and restless running behaviour.
- The outlined procedures and techniques have in practice proved themselves as being first of all, practical.
- In addition it offers advantages in convenience, accuracy, erection time and equipment demands, all of which makes it a preferred installation technique for machines of large size and weight.

EUROPEAN
FORUM
for
RECIPROCATING
COMPRESSORS

Use of modern control systems in compressor stations

by:

Dipl.-Volkswirt Ulrich Dirkmann
RWE Energy AG
Dortmund
Germany
Ulrich.Dirkmann@RWE.com

Dipl.-Ing. Burkhard Lenth
RWE Energy AG
Dortmund
Germany
Burkhard.Lenth@RWE.com

Dipl.-Ing. Joachim Wermeling
RWE WWE NS GmbH
Gronau-Epe
Germany
Joachim.Wermeling@RWE.com

6th Conference of the EFRC

October 28 – 29, 2008, Dusseldorf / Germany

Use of modern control systems in compressor stations for underground gas storage

1 Abstract

The underground gas storage Epe (salt cavern storage) is a fully automatically operated facility including a system for failure avoidance.
Regarding the operation of a storage, the requirements for a flexible usage of the storage have gone up decisively.

The goal of the exchange of all electrical-, process-, measurement- and control-technology was to:

- achieve a central data management and a fully integrated system
- set up an outright asset management
- shorten the start-up and shut-down periods during injection and withdrawal procedures

Simultaneously operation modes and manners of driving the injection and withdrawal processes were simplified, supported by an effective operation and control of the process-involved compressors.

2 RWE Energy and WWE – short overview

- RWE Energy AG is the sales and net company for Continental Europe within RWE AG
- Supply of power, gas and water from one hand
- Total length of the gas grid: approx. 40.000 km in Germany
- Employees (in 2006): 28.418
- Sales revenue (in 2006): 28,1 billion €

- RWE WWE is a regional subsidiary of RWE Energy
- Employees (in 2006): 2.700
- Sales revenue (in 2006): 5,6 billion €
- WWE operates a cavern storage in Europe’s largest cavern storage field in Epe

3 Description of the cavern storage in Epe

- Epe is located at the German-Dutch border near Gronau.
- With 3 billion m³ storage capacity, Epe is Europe’s largest cavern storage field.
- WWE owns a storage capacity of 500 million m³ in Epe which is operated by remote control from the headquarters in Dortmund (Germany).

The necessary procedural equipment for the storage operating-mode can be found in figure 1.

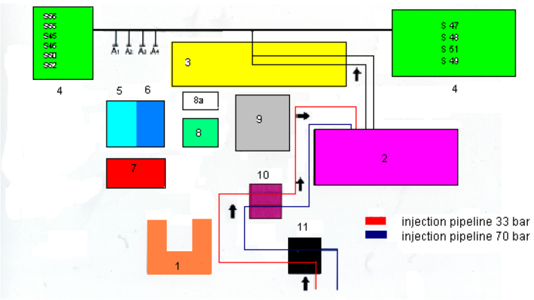

1: control room
3: cavern manifold
5: scrubber
7: heater
9: dehydration and regeneration
11: scrubber

2: compressor
4: cavern
6: heat exchangers
8: letdown stations
8a: vortex tube separator
10: metering station

Figure 1: scheme of the storage operating-mode

- By an entry filter and a gauging station, natural gas flows to the compressor station.
- Compression of the natural gas from 30 bar to 210 bar.
- Afterwards it is transported to the caverns over a manifold.

4 Technical data

All relevant technical data are summarized in figure 2:

Caverns

- Number =10
- Geometrical volume =3 million m³
- Working gas volume =500million m³
- Total volume =630million m³

Storage

- 5 gauging stations
- 3 two-staged piston compressors
- 28 – 211 bar
- 10.000 m³/h – 75.000 m³/h
- 3 synchronous electrical engines controlled by rotational frequency

Withdrawal

- 3 discharge lines with 140.000 m³/h
- 1 discharge line with 240.000 m³/h
- preheating of natural gas with 3 facilites:
  2 x 4,5 MW
  1 x 8,9 MW
- 3 absorbers with one regenerating facility for glycol respectively
  2 x 140.000 m³/h
  1 x 240.000 m³/h
- 1 x vortex tube separator 140.000 m³/h

Figure 2: Technical data

Basic data of the compressors:

Manufacturer:	BORSIG	BORSIG
Type:	BX 45-80/63/4S2	BX 45-80/63/4S2
Name:	V1+V2	V3
Year of manufacture:	1988	1990
No. of cylinders:	4	4
Stages:	2	2
Capacity:	20.000/80.000 Nm³/h	20.000/100.000 Nm³/h
Controller action:	Lifting of the suction valve	Lifting of the suction valve
Power:	3.700 kW	3.700 kW
Revolution speed:	200/370 min^{-1}	180/370 min^{-1}
Piston stroke:	270 mm	270 mm
Diameter of the piston rod:	130 mm	130 mm
Cylinder bore 1^{st}-stage:	365 mm	365 mm
Cylinder bore 2^{st}-stage:	265 mm	265 mm

Figure 3: basic data of the compressors

5 Development of the cavern storage in Epe

- Epe started operation in 1988 with conventional Electrical Instrumentation and Control-Technology (E/I&C) for fully automatic operation
- In the mid-90s PROFIBUS-technology was employed for further expansions
- A larger procedural facility with 10 SPS started operation in 1999
- In 2003 3 more caverns were put into operation. Asset management with DTM and EDD was enabled.
- Renewal of the total EMSR-equipment from December 2005 to December 2007

6 Specification of the new E/I&C-equipment

Criteria for the new E/I&C-equipment:

- Explicit structure
- Control of the automatic process flow
- Connection of safety technology according to IEC 61508/61511
- Unified build-up
- Remote dispatching
- Archival storage of all data in real-time
- Vertical and horizontal consistency of data as well as data consistency over all software tools
- Asset management of all electrical devices with FDT/DTM or EDD

Scope of the project in the planning phase:

- Approx. 2.100 sensors
- Approx. 600 actors
- 51 SPS S7-400
- approx. 30.000 data points

7 Solutions

- buildup of a bypass-line
- demounting of not required cross-connections and armatures
- pipe-rebuildings at compressors, rejections and blown out shot due to safety reasons
- implementation of an asset management

8 Time Schedule / Realisation

- Beginning of planning-procedure in 2005.
- Exchange of E/I&C-equipment during operation
- Main operation modes (according to season) were to be ensured
- By-stage approach with time-scheduled interim solutions

A rough time schedule can be found in figure 4:

Project phase	Activity / mile stone	Date	Scope
	Start of project	January 2006	
	Test 1	August 2006	Line 1 and compressor 1
	Test 2	March 2007	Line 2-4; Compressors 2-3, 3 caverns
Realisation			Impact on storage
Step 1	Start of construc-tion	April 2006	Outfall line 1 / operation A500
Step 2	Shutdown 1	since July 2006	Outfall 6 weeks/ outfall compressor 1
Step 3	Change-over compress-ors	since November 2006	Outfall compressors 2 and 3 / operation A500 / compressor 1 and line 1 with PC S7
Step 4	Change-over discharge lines and caverns	since April 2007	Outfall line 2-4 / operation A500 compressors 1-3 with PCS7
Step 5	Shutdown 2	since July 2007	Outfall 4 weeks
Step 6	Beginning of operation process control system	since August 2007	Beginning of operation / operation PCS7
Step 7	Test run CS Epe	since October 2007	Distance traffic CS Epe
	End of project	December 2007	Handover, final documentation

Figure 4: rough time schedule

9 Conclusion

Due to extensive tests before the beginning of operation, only few faults occurred. Safe operation was always guaranteed and after successful launching, the installed equipment fulfilled all requirements and demands.

Advantages are :

- Central data management
- Continuous system
- Complete asset management

Due to an explicit structure and standardisation, operational properties of the system have considerably increased. Additionally, defined interfaces have been established for the planned extension of the plant.

3D Acoustic modeling in PULSIM for high frequency dynamics

by:

Erik Slis

Leonard van Lier

Jan Smeulers

Flow & Structural Dynamics

TNO Science & Indusrty

Delft

The Netherlands

erik.slis@tno.nl

e.g. 6th Conference of the EFRC
October 28th / 29th, 2008, Dusseldorf

Abstract:

Current developments in compressor technology such as capacity control systems and high speed machinery lead to high frequent pulsations in compressor installations. Conventional tools, like PULSIM, frequently used for simulating generation and propagation of pulsations in compressor installations, are limited to 1D plane wave propagation. Whilst the 1D plane wave propagation method is valid for most parts of the systems, depending on the frequency content of pulsations, this method can be erroneous in case of large vessels like coolers, dampers, separators and sections of large diameter piping. In these parts of the system 3D acoustic modes are to be expected resulting in a response that deviates considerably from the 1D simulations.

3D acoustics can be modelled using finite element programs like ANSYS, Comsol, Sysnoise. However the modeling of a complete pipe system including all vessels with such a program is not practical because of the complexity of the model and the large computation times. Therefore a method has been developed to make a coupling between 1D and 3D models. In doing so, the fast simulation speed of a 1D simulation can be combined with a more complex 3D element when it is required, reducing the computation time of complete 3D simulations and increasing the accuracy of 1D simulations.

In this paper a method is described with which 1D PULSIM models can be extended with 3D elements.

1 Introduction

High speed compressors and capacity control systems are current trends in compressor technology that result in high frequent pulsations in compressor installations. This requires that a pulsation analysis should be extended to higher frequencies. This can be a problem, because the commonly used modelling tools, like PULSIM[2], use the plane wave or 1D approximation, which is valid for low frequencies. However, dealing with high frequencies, 3D acoustic modes can be expected in system parts such as large dampers, separators, coolers and large diameter pipe sections. 1D simulations may be erroneous for these parts resulting in wrong prediction of pulsation levels and frequencies.

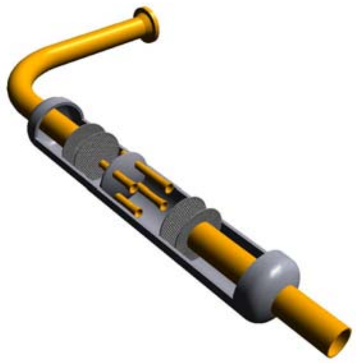

Figure 1: Complex damper in which 1D and 3D acoustics are important.

The plane wave propagation theory is valid for frequencies below the cut-off frequency (*fc*) for circular pipe cross sections given by [1]:

fc = 1.84c/πD,

with c the speed of sound [m/s] and D the pipe diameter [m]. This gives for a system with a speed of sound of c = 340 m/s a cut-off frequency of fc=1 kHz for pipe with a diameter of D = 0.2 m. However, a large vessel with a diameter of D = 2 m only has a cut-off frequency of 100 Hz.

In case of high speed compressors (1000 RPM) or other sources of high frequent pulsations the 1D solution is valid for the piping however, often not in separators, coolers, large dampers where the cut-off frequency could be in the order of the 6th harmonic of the compressor speed.

Running full 3D simulations of such systems is far too time consuming. Therefore a method has been developed that makes a coupling between a 1D model of the pipe system and special elements that model the 3D acoustics of large diameter equipment. In this way the best of both worlds is combined: fast computation time and a model that includes 3D effects where necessary. This is achieved by creating an element in PULSIM carrying the 3D characteristics of large elements by means of a transfer function.

The acoustic properties of system elements, such as piping and vessel, can be fully described by a scattering matrix (Figure 2), which describes the relation between the incoming and outgoing pressure waves.

$$\begin{pmatrix} p_1^- \\ p_2^+ \end{pmatrix} = S(\omega) \begin{pmatrix} p_1^+ \\ p_2^- \end{pmatrix}$$

Figure 2: Definition of scattering matrix (S). p+ and p- are the pressure of the up- and downstream travelling waves.

2 Determining 3D characteristics

The transfer or scattering matrix of the 3D elements can be determined both experimentally and numerically. Experimentally, this can be done by means of the "two load method"[1]. In this method two sets of acoustic measurement are required to obtain the full transfer matrix (figure 3). The transfer matrix is equivalent with the scattering matrix. The transfer matrix is written in terms of the acoustic pressure and velocity whereas the scattering matrix is written in terms of the travelling pressure waves.

$$\begin{pmatrix} p \\ Su \end{pmatrix}_{in} = \begin{bmatrix} A(f) & B(f) \\ C(f) & D(f) \end{bmatrix} \begin{pmatrix} p \\ Su \end{pmatrix}_{out}$$

Figure 3: Definition of transfer matrix. p is the acoustic pressure amplitude, u is the amplitude of the acoustic velocity, S is the pipe cross-sectional area and A, B, C and D are the frequency dependent matrix elements.

These two sets of measurements can be obtained by changing one of the acoustic boundaries for instance by changing a valve setting or by adding a section of pipe downstream. By applying upstream and downstream of system element multiple pressure transducers, the upstream and downstream travelling waves (p^{+}, p^{-}) using a multi-microphone method can be reconstructed as function of frequency. From these amplitudes the scattering and transfer matrices can be calculated.

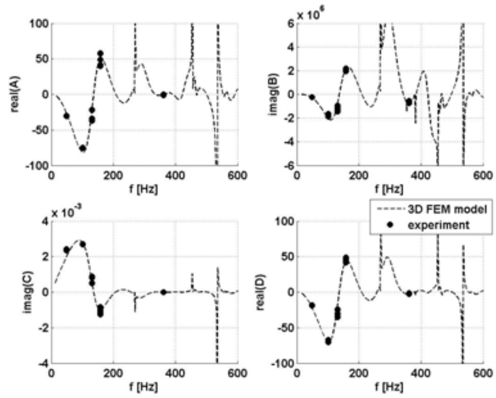

Figure 6: Comparison of the experimental and numerical results of the obtained transfer matrix elements

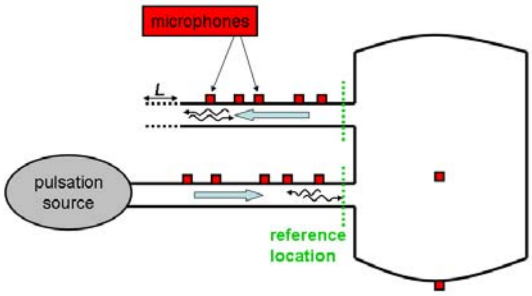

Figure 4: Experimental setup for validation "two load method"

Several software packages are available to analyse the 3D acoustics of complex systems. These include for example ANSYS, Sysnoise, and Comsol. Important in the numerical simulations is the inclusions of acoustic damping. Especially, in the case of dampers with chokes the influence of pressure drop due to the flow on the acoustic behaviour of such elements is very large. Therefore, the inclusion of damping in the 3D simulations is essential. To determine the transfer and scattering matrix using models, a similar numerical experiment must be done as a real life experiment. Two sets of simulations must be run with two different boundary conditions. The simulations must be done for the full frequency range of interest. The frequency steps in the simulations will determine the final accuracy in which the frequency dependent transfer matrix can be calculated.

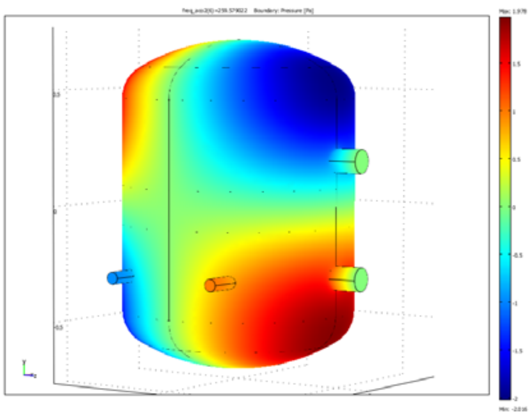

Figure 5: Calculated acoustic eigenmode at 260 Hz

Both methods were validated on a large vessel with a diameter of 0.99m and a height of 1.43m (figure 5). This vessel has a cutoff frequency of approximately 200Hz.. Both experiments and numerical simulations were done based on this vessel. In figure 6 the reconstructed transfer matrix elements are plotted for both the numerical and for the experimental results. The comparison between the experimental results and the 3D numerical simulations is very good.

3 1D – 3D coupling

Based on numerical simulations or based on experimental results the transfer or scattering matrix can be obtained for large diameter system elements.
The method we have developed uses the scattering matrix, which can be calculated easily from the transfer matrix. As PULSIM is based on the method of characteristics in the time domain, a conversion of the scattering matrix to the time domain must be made. This can be achieved by an Inverse Fourier Transformation (IFT) of the four elements of the scattering matrix, resulting in an *impulse response matrix (IRM)*. The IRM is used in the time domain simulation of PULSIM for calculating the reflected and transmitted waves by convolution of the incoming waves with the IRM elements.

Figure 7 schematically presents the procedure of the coupling between 1D and 3D acoustics after determining the transfer matrix of a large element. First the frequency dependent scattering matrix is calculated and translated into a time dependent Impulse Response Matrix (IRM). The steps to determine the IRM only need to be carried out once. (Figure 7 left part) After this the IRM is available as a simulation element in the PULSIM program and can be inserted at any location in the model of the complete system. (see Figure 8)

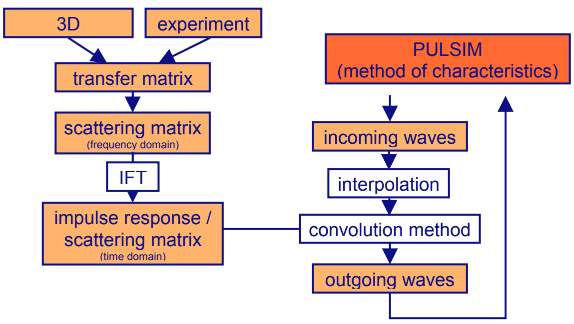

Figure 7: Procedure of the coupling between 1D and 3D acoustics[3].

During the execution of a simulation run each time step the convolution product of the IRM elements with the incoming waves are calculated. (Figure 7 right part). As the scattering matrix is known at discrete frequencies and thus the IRM is known for specific time steps an interpolation must be performed between the simulation (PULSIM) time steps and the IRM time steps.

The interpolation and calculation of the convolution products will increase computation time of a simulation run. This increase depends greatly on the frequency range of interest and the method of interpolation used during the convolution method. However, computation time is still much shorter than simulating a complete model in 3D.

4 Verification case

Figure 8 shows an actual damper model of a NEA hydrogen compressor. This model is used to compare an 1D case of a regular PULSIM simulation where the damper is modelled using only piping elements and with the damper replaced by the IRM convolution method. The system is such that the results should be comparable. For the IRM the scattering matrix was obtained by a model in Comsol.

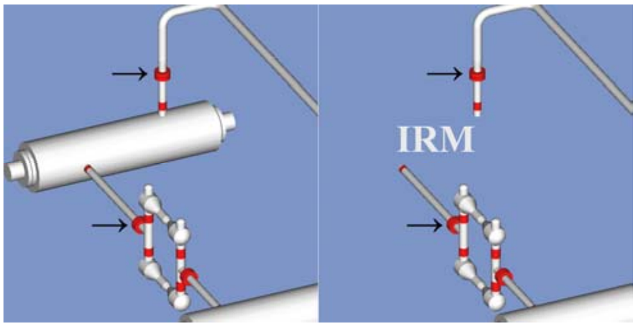

Figure 8 PULSIM model of pulsation damper modelled with piping elements (left) and replaced by an IRM node (right)

The simulation in PULSIM for both cases is done as it is normally performed by using a simulation range varying the velocity of sound between -20% and +20% of the nominal.

The orifices at the damper-cylinder connection and the damper-line connection are chosen as measurement points (indicated in Figure 7 by arrows).

Figure 9 and Figure 10 show the results of the pulsation levels of the 1st and 2nd harmonic of the compressor speed for both selected locations. The dashed line represents the results obtained by the regular PULSIM model using only piping elements. The straight line represents the results obtained using the IRM as a replacement of the damper.

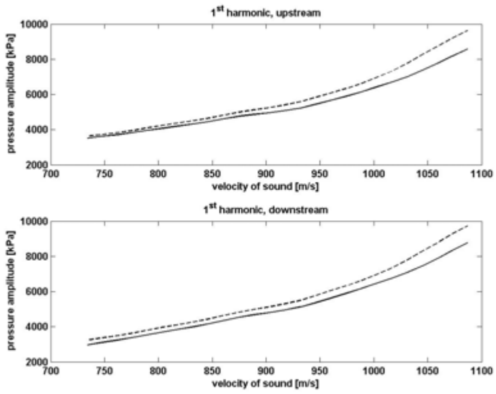

Figure 9 comparison of calculated pulsation levels of the 1st harmonic with (straight) and without the IRM (dashed).

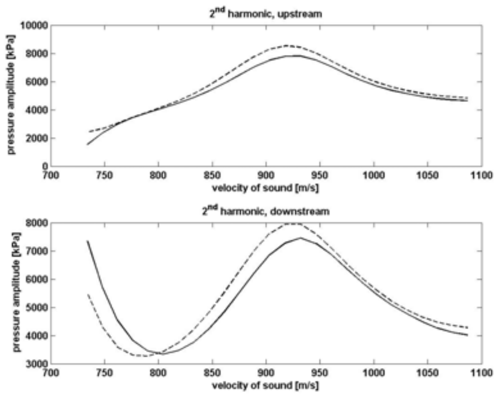

Figure 10 Comparison of calculated pulsation levels of the 2nd harmonic with (straight) and without the IRM (dashed).

It is clear that both simulations yield the same results showing only minor differences. The accuracy of the 3D simulation can be increased by reducing the frequency steps in the simulation and by increasing the modelling accuracy of the damping.

5 Conclusion

With the increased use of capacity control and high speed compressors, higher frequencies become important in the integrity analysis of installations. For some large diameter equipment a 1D wave propagation model may not be valid. To that end a special element has been developed with which equipment that shows 3D wave propagation can be included in PULSIM.

This element uses an impulse response matrix to calculate the transmission and reflection of incoming waves. The impulse matrix is based on an inverse Fourier transformation of a scattering matrix. The validity and accuracy of using a 3D element has been verified using a simple damper model for which the 1D approach would still be valid.

The scattering matrix can be obtained from experiments or from numerical simulations. Both methods have been validated on a large vessel including damping orifices.

The use of the 3D element allows including 3D effects only where required, which gives a large reduction of computation time in comparison to the computation times required for a complete 3D model.

6 Aknowledgements

The author would like to acknowledge the valuable help and assistance of G. de Groot who implemented most of the scheme in PULSIM as part of his graduation work.

References

[1] Lung & Doige, JASA 73(3), 1983, p.867-876

[2] Egas, G., PULSIM, a powerful tool for the control of vibrations in pipe systems", Proceedings of the 1st Conference on noise and vibration control in machinery and transportation, pp. 167 - 182, 3 – 5 July, Senlis, France

[3] G. de Groot e.a. "Application of convolution techniques for the modelling of boundary conditions in Pulsim", Graduation thesis Utrecht University (TNO report IMC-RPT-DTS-2007-01940)

Optimizing the Pulsation Control Solution

by:

Greenfield, Shelley

Beta Machinery Analysis

Calgary, Alberta

Canada

sgreenfield@BetaMachinery.com

6th Conference of the EFRC
October 28th / 29th, 2008, Düsseldorf

Abstract:

Reciprocating compressors require pulsation control to avoid large dynamic acoustical forces. A pulsation analysis (per API 618) will recommend a pulsation control solution based on the operating conditions, speed range, and other operating factors. Given these different issues, there are many possible solutions – each with a different result in terms of upfront and operating cost, pulsation reduction, and operating risk.

Owners and packagers are becoming more interested in an optimized pulsation design. This paper presents case studies and design ideas on how to optimize the pulsation control solution. These examples illustrate the significant cost savings and operational benefits available to the industry.

1 Introduction

The 5th Edition of API 618 (the Standard) was officially released in December 2007. A common theme through the new specification is energy conservation and optimization. The Standard specifies minimum design requirements. It does not require the compressor suppliers to utilize proven design techniques that improve efficiency and performance. To address this issue, the updated 5th Edition recommends **innovative approaches *"should be aggressively pursued by the manufacturer [packager] and end user [owner/ operator]"* during the compressor design and operation to reduce the total life costs and increase energy conservation.**

Improving efficiency and reducing the total life cost can be accomplished through different points of view. Three areas that can result in significant savings are:

1. Pulsation control devices introduce pressure drop into the system. Design modifications that result in lower "total pressure drop" through the system can realize a significant financial reward. Reducing pressure drop results in increased capacity, or reduced fuel costs. Increased capacity generates millions of dollars (per year) in incremental throughput. Fuel savings can generate hundreds of thousand dollars per year in savings.

2. Overly conservative pulsation control solutions may result in higher manufacturing cost for the packager/owner. For example, Beta recently saved a packager over $100,000 in manufacturing costs by optimizing the pulsation bottle design. An overly conservative design can have significant cost penalties. When a project includes multiple compressors, the cost penalty of a "conservative design" is multiplied, and directly affects overall capital costs and the packager's profit.

3. Over the life of a compressor, the field infrastructure may change the operating parameters of the unit (beyond what was anticipated during the initial design). This represents an opportunity to revisit the system design and optimize it where possible. Evaluating the system performance at current and future operating parameters will identify areas to improve capacity, reduce fuel costs, and assess the effectiveness of existing pulsation control devices. Depending on the original design and the degree to which the field parameters have changed, hundreds of thousands of dollars per year can be saved, even after factoring in the cost of modifying the system.

We term these points of view as "optimized design" efforts as some additional design work is required to determine the optimized solution. The return achieved from an optimized design easily justifies the additional design work.

The first step in optimizing a compressor design is to evaluate the "system performance." Once the system performance is understood, opportunities for optimization can be investigated.

Please note: the currency referenced throughout this document is US dollars.

2 System Performance

System performance includes capacity, efficiency, horsepower (HP), total pressure drop, and pulsations for all intended operating conditions. As shown in Figure 1, the "system" starts with the compressor inlet piping and includes the compressor, piping, vessels, pulsation bottles, orifice plates, scrubbers and coolers. The system typically ends where the discharge piping exits the skid (for performance optimization purposes, modelling on-skid components is usually sufficient).

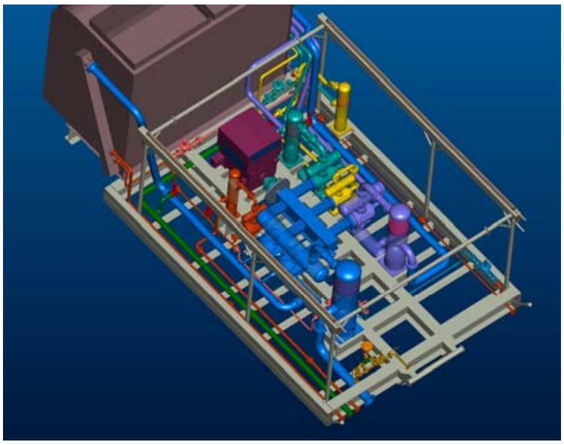

Figure 1: System performance includes all piping, vessels and pulsation bottles (typically skid edge to skid edge). Illustration courtesy of Exterran.

The system performance model is available once the proposed compressor design and pulsation solution are complete (see Figure 2). The pulsation solution provides the total static plus dynamic pressure drop results for each stage of the compressor and for each operating condition. Note that the pulsation analysis requires the use of Time Domain algorithms to produce the total pressure drop results. Older style pulsation analysis based on

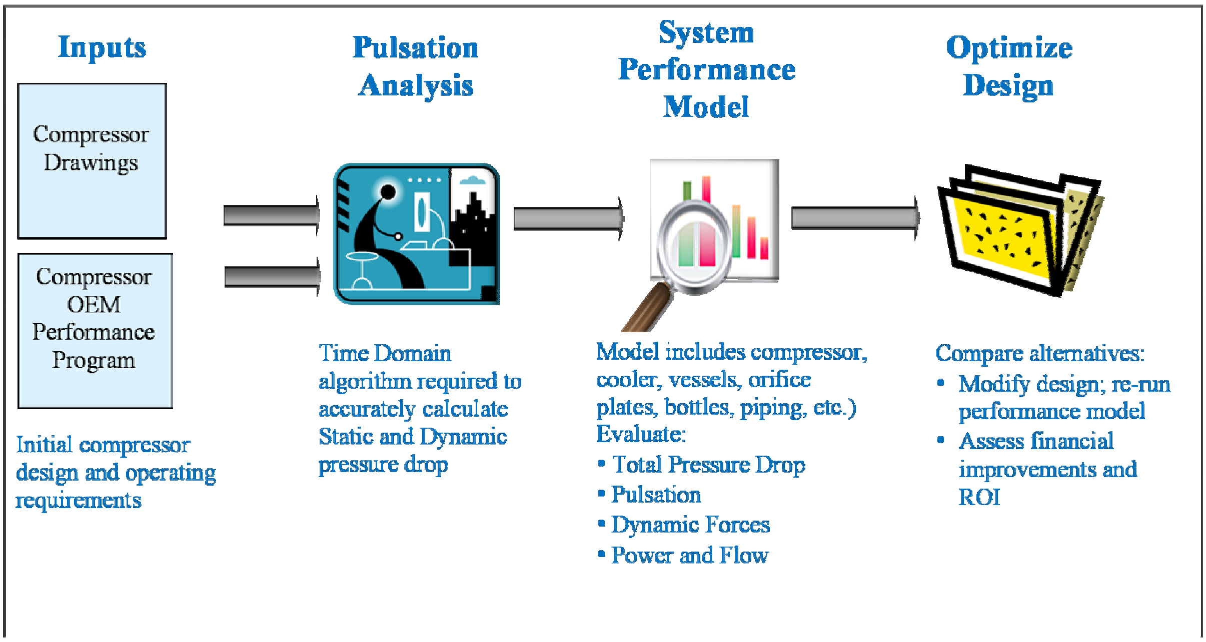

Figure 2: System Performance Model Enables Design Optimization

Frequency Domain algorithms do not accurately model total pressure drop and do not provide comprehensive results for system performance analysis.

The following two examples illustrate the importance of calculating and evaluating system performance models. In each case, the owner expected the compressor would deliver the required capacity based on assumptions used in the OEM performance program. However, the actual system performance is not known until the pulsation solution and final piping configuration is defined. Once the final configuration is defined, total pressure drop through the pulsation control devices, piping, coolers, scrubbers, etc., can be determined for each condition. The compressor performance is then re-evaluated using total system pressure drop (rather than assumed values used in the OEM program) for each condition. In each case the variance between actual system performance and "assumed" performance varies by up to 5% (blue line shown in Figures 3 and 4). This variance can have a significant impact to the owner's business plan.

- For a 4000 HP unit (single stage), the actual system performance is over \$10 million/yr higher than originally estimated (for conditions 10, 11, 13, 14 and 15). Figure 3 illustrates the variance percent and production value. Incidentally, the variance in fuel gas consumption varies by more than \$160,000 per year.

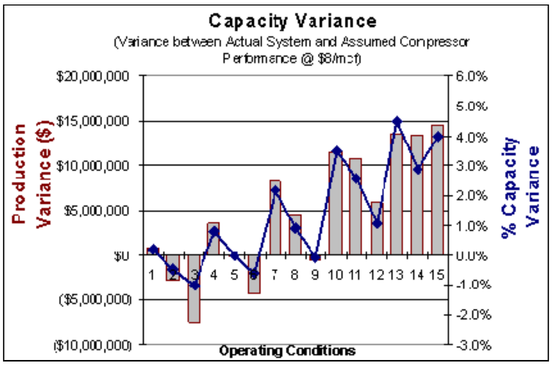

Figure 3: System Performance provides the most accurate picture of overall compressor design characteristics. Example is based on actual compressor installation (6 Throw; 1 Stage Compressor; 4000 HP; 105-245 MMSCFD)

- The second example is a much smaller unit (1600 HP), but in this case the actual system capacity is well below the assumed performance. The negative variance is over \$1million per year for conditions 1 and 2.

These two examples illustrate that variance can be either positive or negative. They also illustrate the importance of an accurate system performance model.

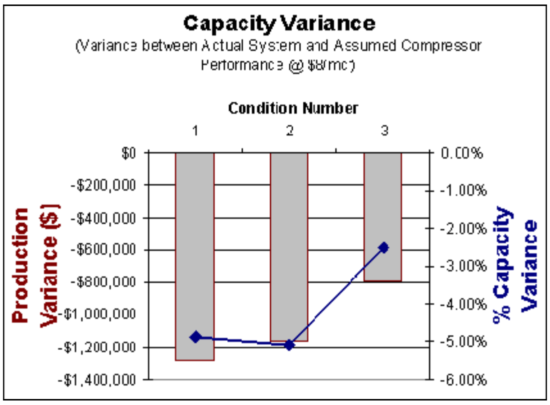

Figure 4: Actual system performance variance compared to planned performance (based on initial OEM performance runs, 1600 HP; 1200 RPM; 4 throw; 3 stage; 7-10MMSCFD; 3 operating conditions).

To optimize the design the recommended approach is to first develop the baseline system performance model. The baseline compressor design can be modified and optimized until a viable solution is found. The pulsation and performance software is rerun to identify the impact of changes in pressure drop and performance. A simple financial analysis of the incremental improvements (capacity and operating costs) is compared to the required capital costs. This process involves teamwork between the owner, packager and pulsation consultant.

3 Optimization Examples

3.1 Optimized Pulsation Control Design Increases Capacity

A 1400 HP reciprocating compressor in a gas gathering application was designed for a variety of operating conditions including flow rates between 7 and 19 MMSCFD.

During a field review, it was identified that the unit was experiencing high power losses. The analysis further indicated that the losses would prevent the unit from achieving maximum capacity – a key requirement for the owner.

An optimized pulsation analysis of the existing system identified an alternate approach to controlling pulsations. Modifications were made to bottles to include baffles and a choke tube. With these changes, the losses were reduced significantly. As shown in Figure 5, this optimization reduced HP losses between 90 HP and 150 HP for the key operating conditions under evaluation.

The owner was able to gain significant power by reconfiguring the vessels. The table in Figure 6 outlines the power savings for the key operating conditions.

The annual savings in fuel gas through the improvement is estimated at $75,000 per year – a reasonable gain.

The more interesting result is that the unit can deliver an additional 1.0 to 2.0 MMSCFD of throughput. Based on the customer's pricing situation, this translates to over $3.0 million of incremental production.

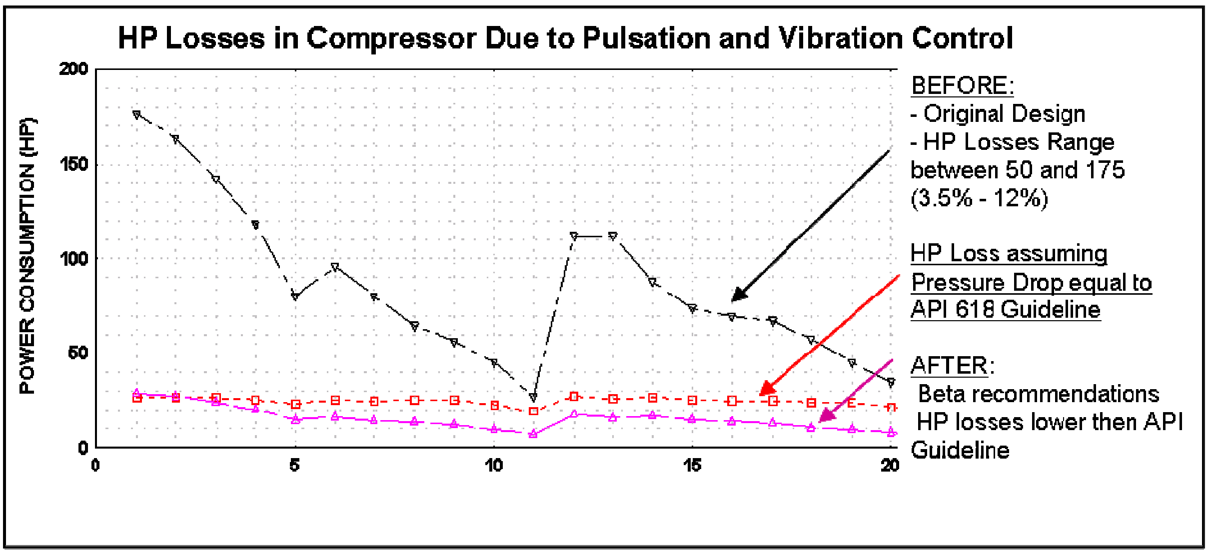

Figure 5: HP losses per condition (before & after)

Operating Condition #	1	2	3	4	12	13
HP Savings	150	137	118	100	95	100
HP/Q Ratio	72	75	83	92	92	92
Incremental Q (Capacity in MMSCFD)	2.08	1.83	1.42	1.09	1.03	1.09
Incremental Revenue (Annual)	$6.1 million	$5.3 million	$4.2 million	$3.2 million	$3.0 million	$3.2 million

Figure 6: Horsepower savings for key operating conditions

3.2 Optimized Pulsation Control Design Reduces Capital Cost

During a recent project, an initial pulsation solution recommended conservatively sized bottles for two 6 throw, 3 stage compressors. An alternative pulsation control solution involving smaller pulsation bottles was determined by evaluating the system model. See Figure 7. Smaller bottles were found to be acceptable for both pulsation and pressure drop criteria. The smaller bottle generated over $100,000 in savings, based on:

- two identical units in the project
- each unit realized $20,000 reduction in bottle costs; $20,000 reduction in skid costs (small bottles had a significant impact to the skid design); and approximately $20,000 reduction in factory overhead.

Many compressors would benefit from an optimized design. For each unit, the hidden capital cost per unit could easily be in the tens of thousands of dollars per package.

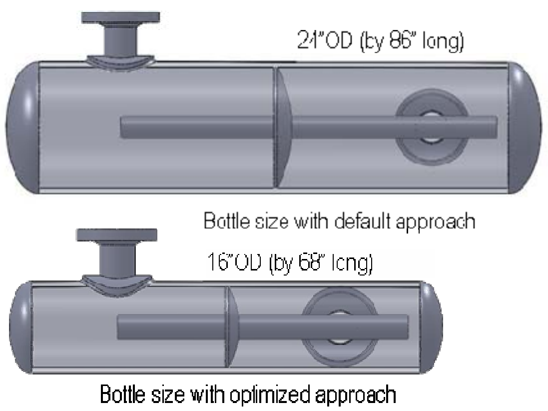

Figure 7: Optimized pulsation bottles saved over $100,000 for packager

3.3 System Performance Analysis Determines Maximum Capacity for Offshore Compressors

The operating parameters for two gas lift compressors located offshore had changed significantly since the units were originally installed. Recognizing that the changes were potentially significant, the owner of the units commissioned a system capacity audit to determine the maximum capacity that could be obtained under the new operating conditions.

Typically the units are assessed using OEM performance software and assumed pressure drops (usually a % of line pressure) to estimate maximum capacity for the new operating parameters. The recommended approach is to use Time Domain pulsation models to calculate the total system pressure drop for all operating conditions and then calculate the performance at the new conditions using the total system pressure drop, rather than assumed pressure drop, to determine the maximum capacity. As shown in Figure 8, the calculated capacity using total system pressure drop was between 5% and 7.5% lower than calculated using typical pressure drop assumptions.

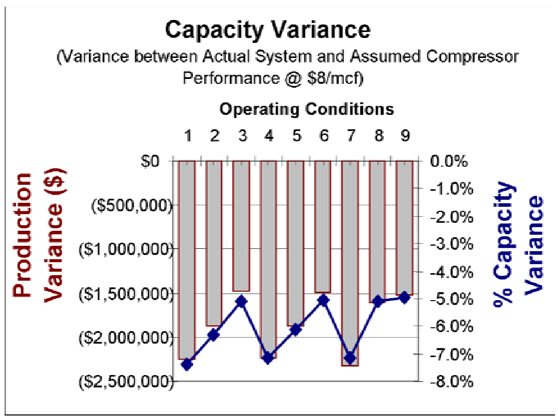

Figure 8: Estimated system pressure drop over predicts capacity

Investigation into the systems identified the suction control valve, several orifice plates and three of the four cooler sections as being the most significant contributors to high total system pressure drop. The pulsation models confirmed that these components could be resized without adversely affecting the pulsation and pulsation-induced unbalanced force levels in the installation. The capacity at the new operating conditions could be improved by between 2% - 4.5% with the redesigned components installed. This additional capacity would generate between $0.6 and $1.2 million dollars per year (based on $8/mcf). See Figure 9. Using this information, the end user can determine the payout on replacing the suction control valve, orifice plates and cooler sections.

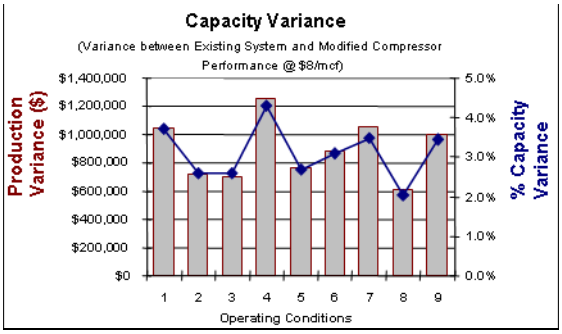

Figure 9: Reducing total system pressure drop increases capacity

While changing the orifice plates and increasing the size of the cooler tubes would reduce the pressure drop of the system, it would be imperative that the driver be fully loaded at all times to achieve the increased throughput rewards. It was recommended that the manually controlled variable volume pockets on the cylinders be replaced with automated load control to achieve maximum capacity.

The capacity audit also identified that the fourth stage compression ratio was low and had a low compression efficiency. Removing the fourth stage would dramatically increase the capacity of the compressor. However, pursuing removal of the fourth stage would create concerns regarding the maximum allowable working pressure (MAWP) of the third interstage equipment. Again, the increased capacity and revenue would have to be weighed against the cost of implementing the changes to determine payout.

5 Conclusion

Reciprocating compressors require pulsation control to avoid large dynamic acoustical forces. A pulsation analysis (per API 618) will recommend a pulsation control solution based on the operating conditions, speed range, and other operating factors. Given these different issues, there are many possible solutions – each with a different result in terms of upfront capital and long term operating cost, pulsation reduction, and operating risk. Innovative approaches are available to reduce the total life costs and increase energy conservation while addressing pulsation and vibration concerns.

To optimize the design, the recommended approach is to first develop the baseline system performance model using Time Domain algorithms. The baseline compressor design can then be modified and optimized until a viable solution is found. The pulsation software is rerun to identify the impact of pressure drop on system performance. A financial analysis of the incremental improvements (capacity and operating costs) is compared to the required capital costs. This process involves teamwork between the owner, packager and pulsation consultant.

Although the new API 618 specification recommends pulsation control should be designed to reduce total life costs and increase energy conservation, design optimization will not normally be pursued as part of a standard pulsation study. It is up to the packager or end user (owner/operator) to specify optimization requirements.

It is also up to the end user to identify when existing equipment may be operating outside the original operating parameters. These changes may introduce additional pressure drop, and create likely candidates for system performance optimization opportunities.

6 Acknowledgements

The author wishes to acknowledge the assistance of Brian Howes, Russ Barss, Kelly Eberle, and Jackie Walters, all of Beta Machinery Analysis, in the preparation of this paper.

Development of a Transient Fluid Dynamic Solver for Compression System Pulsation Analysis

By:

Brun, Klaus
Fluids Engineering
Southwest Research Institute®
San Antonio, Texas
United States
klaus.brun@swri.org

Edgar B. Bowles, Jr.
Fluids Engineering
Southwest Research Institute®
San Antonio, Texas
United States
ed.bowles@swri.org

Danny M. Deffenbaugh
Mechanical and Materials Engineering
Southwest Research Institute®
San Antonio, Texas
United States
danny.deffenbaugh@swri.org

6th Conference of the EFRC
October 28th / 29th, 2008, Dusseldorf

Abstract:

The Southwest Research Institute® (SwRI®) "Analog Computer" and the newer digital acoustic solver Interactive Pulsation and Performance Simulation (IPPS) have been successfully used in pulsation analysis for slow-speed compression system design for the last fifty years and more recently in the design of the new high-horsepower, high-speed compressor installations. The IPPS solver utilizes a solution algorithm of the transient acoustic wave equation in the frequency domain, which has been demonstrated to provide in most cases accurate results for compression system resonance frequencies and reasonable agreement for pulsation amplitudes. However, the mathematical assumptions associated with solving the acoustic linearized wave equations must lead to discrepancies in amplitude predictions as these equations are only a partial physical model of the actual transient fluid

dynamics. A full one-dimensional representation of the governing transient fluid dynamic equations (called the Navier-Stokes equations) can provide a more thorough solution for the pulsating flow field and can provide more accurate pulsation amplitude predictions. This is particularly critical in the design of variable high-speed compressor systems, as for these applications complete resonance avoidance is impossible. Thus, SwRI decided to develop a new one-dimensional time-domain Navier-Stokes solver to improve SwRI's prediction capabilities for transient compressor station manifold and piping systems. The resulting state-of-the-art piping pulsation analysis tool, called Transient Analysis Pipe Solver (TAPS), will lead to better design optimization capabilities for the pipeline industry. This paper describes the TAPS solver development and validation testing. TAPS code testing results showed:

- A transient one-dimensional solver of the Navier-Stokes equation can accurately predict frequencies and amplitudes of pulsations in a complex compression piping system.
- The non-linear terms of the governing (Navier-Stokes) equations have a significant influence on the solution of the pulsating flow field and must be considered in high speed compression system analysis.
- Transient and steady-state pressure drops can be accurately modeled using the TAPS solver.
- The TAPS solver predicts acoustic phase cancellation, phase interference, and amplification between compressor cylinders on a common header more accurately than previous analysis tools.

Thus, the new TAPS transient flow solver advances the state-of-the-art in compression system pulsation analysis and is an improvement over existing acoustic wave equation solver technology.

.

1. Background

Since 1952, the Mechanical and Materials Engineering Division of Southwest Research Institute® (SwRI®) has provided design analysis services to the gas transmission industry through the Gas Machinery Research Council (GMRC) Design Facility. The design analysis serves to reduce pulsations and vibrations at compressor station installations or, in some cases, predict the effects of proposed operational changes. Pulsation and performance analyses are performed as an essential part of the design service, for both existing compressor stations and new installations. In the early 1950s, SwRI engineers developed a simulation tool to model the dynamic operation of a gas compressor and the corresponding pulsations produced in the piping system. Based on acoustic wave theory, the simulation tool (referred to as the "Analog") utilized a scaled electrical model of the compressor manifold piping system and compressor station piping to simulate the physical characteristics of the gas compression process. The "Analog" simulation tool provided reasonably accurate predictions of the dynamic operational (pulsation) characteristics of the compressor station and adjacent piping.

SwRI used the electrical Analog simulation tool until the 1990s, at which time SwRI began developing digital computational algorithms. Digital algorithms offered the ability to more accurately estimate valve losses in the compressor cylinders and determine the effects of pulsation and dynamic pressure losses on system performance. The resulting digital design technology was named the Interactive Pulsation and Performance Simulation (IPPS) analysis package. By 2002, the IPPS simulation tool was used for approximately 80% of the compressor station design analyses performed by SwRI. Since then all compressor station designs have been performed using the digital design tool.

Development of the advanced digital model (IPPS) was motivated, in part, by changes in the U.S. gas transmission pipeline industry operating philosophy. The industry has transitioned to a broader use of high-horsepower (i.e., >2,000 horsepower), high-speed (i.e., >750 RPM) reciprocating compressors. This class of compressors presents an increasing challenge to the compressor station designer to meet both pressure pulsation and structural vibration limits, while not excessively restricting the compressor thermodynamic performance. Accuracy of the predictive model used in the design process has become increasingly important, as the new class of compressors has tightened the allowable design window.

2. Introduction

Pulsating flow compressor manifold and piping design involves optimum selection and use of primary volumes, choke tubes, and secondary volumes, as well as cylinder phase cancellation. These elements are used in designing pulsation filters that provide a sufficient volume for the high unsteady flow entering and leaving the compressor cylinders. While providing sufficient volume to filter the unsteady flow pulsations from the compressor, these filters must also be designed to avoid excitation of “acoustic” resonance inherent to the installation piping and in the compressor station filter system.

In the past, for low-speed gas compressors, acoustic (pressure) pulsation, and mechanical resonance avoidance was used to sufficiently control pulsation and vibration levels at a gas compressor station. Acoustic pass bands (i.e., frequencies of pressure pulsation amplification as shown in Figure 1 and mechanical resonances would typically be located between regions of possible operational excitation. This ability to optimally locate pulsation filter resonance frequencies for low-speed compressors is illustrated in Figure 1. In contrast, for high-horsepower, high-speed (particularly variable-speed) compressors, operational windows for placement of acoustic resonances are at least reduced and, oftentimes, eliminated above the third- or fourth-order of compressor running speed (Figure 2). Thus, the basic design philosophy has changed from one of resonance avoidance to one of resonance management. Resonance management involves balancing acoustic pulsation amplitudes with reductions in compressor thermal efficiency and controlling mechanical vibration levels and stresses in the manifold system. The mechanical stresses, thermal efficiency, and acoustic pulsations are interrelated through choices in the compressor manifold design.

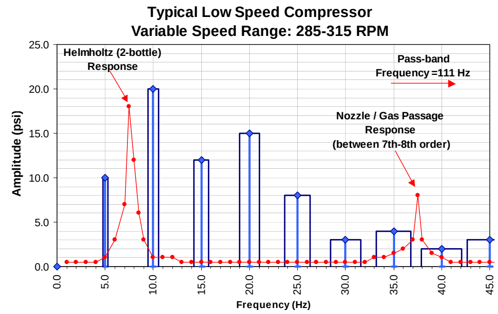

Figure 1: Typical Acoustic Response for Low Speed Compressor Manifold Design

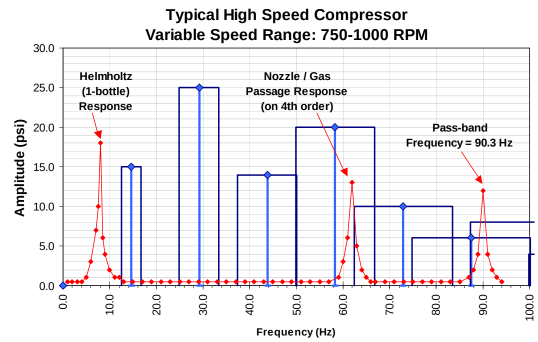

Figure 2: Typical Acoustic Response for High Speed Compressor Manifold Design

2.1 Motivation

The Analog simulation tool, developed in a cooperative effort between SwRI and industry, solved the linear acoustic wave equations by simulating circuits of resistors, capacitors, and inductors. The voltages developed in these networks represented pulsation levels in the compressor manifold and attached piping. The Analog simulator tool was continuously refined over a 40-year span to improve the cylinder models and damping estimates. In the mid-1990s, digital pulsation design analysis tools were developed. This software also solved the linear acoustic equations but calculations were made in the frequency domain.

The acoustic equations used in all modern digital acoustic design tools, including SwRI’s IPPS digital acoustic design tool, are accurate up to 140 to 150 dB (i.e., less than 1 PSI In general, pulsation amplitudes for a well designed manifold system are normally on the order of 5 to 10 PSI in the piping and up to 20 to 60 PSI nearer the compressor valves. For low-speed machines or fixed-speed, high-speed machines, where resonance avoidance is possible, the existing modeling tools have been sufficient. However, for variable-speed high-speed machines, where resonance management is required, accurate prediction of dynamic pressure levels is crucial. Frequency domain modeling codes assume that pressure waves at all frequencies travel at the same speed. However, non-linear fluid dynamic effects can cause these pressure waves to travel at different speeds, resulting in phase shifts that may be significant. Hence, a fully transient pipe flow analysis rather than an acoustic wave analysis will more accurately model the actual compressor dynamics.

The IPPS code has been used to design dozens of the new high-horsepower, high-speed compressor installations. However, the current IPPS model has predicted pulsation amplitude levels significantly below measured values in some of the design analyses. Furthermore, the pulsation level under-predictions produced with the IPPS code were also produced with the Analog simulation tool when both were used to model the same compressor installation. In particular, for 4,000 to 8,000 horsepower units running at speeds of 750 to 1,000 RPM, with six-throw, horizontally-opposed cylinders (i.e., three compressor cylinders on each side of the machine), actual (measured) pulsation levels on the first running order (12 to 17 Hz) have been shown to be two to four times greater than the levels predicted by the models. This under-prediction is of significant concern because these frequencies tend to align with mechanical resonance frequencies of the compressor yard piping and often lead to very high and potentially damaging vibration levels.

Numerical testing has indicated that very slight changes in cylinder-to-cylinder phasing can account for some of this under-prediction (due to loss of phase cancellation). However, the magnitude of the phase errors required to match field test data is unlikely associated with machine tolerances and fabrication errors. Thus, the assumptions associated with solving the acoustic wave equations are leading to the discrepancies in the predictions. Furthermore, inherently any acoustic wave model in the frequency domain can not accurately predict steady and transient pressure drops as no bulk flow is modeled. Thus, a full one-dimensional representation of the governing transient fluid dynamic equations (called the Navier-Stokes equations) of the compression system should provide a more thorough representation of for the pulsating flow field and possibly resolve these discrepancies.

3 Objectives

The principal objective of this research project was to develop a new one-dimensional time-domain Navier-Stokes flow solver to improve SwRI's prediction capabilities for transient compressor station manifold and piping systems. This model needed not only to properly predict the acoustic frequency response of the system, but also provide improved prediction technology for pressure pulsation, dynamic pressure drops, and steady-state pressure drops. The new code was exclusively developed for the analysis of highly pulsating flows in the complex piping systems found in reciprocating compressor stations and as such needed to include specialized features such as compressor cylinder models, valves, bottles, choke tubes, orifices, multiple-header manifolds, pipe transition pieces, infinite pipeline boundary conditions, end-pipe boundary conditions, etc. A literature review found that all currently commercially utilized models for compression station piping flow analysis either utilize the Method of Characteristics (MOC) or the transient wave equation solution, which are severe subsets of the full Navier Stokes equations. With the new model, SwRI can develop a better understanding of the transient fluid physics near the compressor manifolds, the cylinder valves, and within the acoustically-filtered regions of the system. Ultimately, this should lead to better design optimization capabilities for compressor station service work provided by SwRI to the pipeline industry. Thus, more specifically, the objectives of this research were as follows:

Develop a one-dimensional representation of the time-domain Navier-Stokes equations for any complex piping system.

Compare the predicted results of the new model with the linearized acoustic equations for standard compression station systems.

Compare pulsation amplitude levels for a key standardized manifold design using the full one-dimensional Navier-Stokes approach with the existing IPPS code. Use test data for the same system to determine the predictive accuracy of both models.

Thus, the ultimate aim of this project was to advance the state-of-the-art of compression station pulsation predictions from the existing frequency model of the simplified wave equation (which is a very basic subset of the equations of motion of a fluid) to a truer time-domain model of the fluid flow equations of motion (i.e., the Navier-Stokes equations).

4 Technical Approach

The approach was to develop a new time-domain one-dimensional solver of the actual fluid flow governing equations of gas dynamics, the transient Navier-Stokes equations, and embed it into a system analysis algorithm for an arbitrary number of interconnected pipes and inlet/outlet boundary conditions. Existing IPPS models and field data sets were available to verify the accuracy of this new model. Comprehensive new sets of test data were also acquired as part of this study in order to fully validate and compare the two models.

The existing frequency domain acoustic model (IPPS) and the new approach (TAPS) are briefly outlined below to highlight the difference in their method.

4.1 Existing Acoustic Pulsation Prediction Model

All pulsation analysis tools currently used in the industry are based on solutions to the linearized acoustic wave equation. They either solve the pseudo-transient wave equation in the time domain using the methods of characteristics or they solve the fully transient wave equation in the frequency domain using matrix solutions of linearized transfer equations. For example, in the existing SwRI IPPS pulsation model, an Acoustic Wave Element (AWE) procedure was used to describe the gas passage and piping acoustics. Using this approach, the piping was modeled as an assembly of acoustic elements (volumes, junctions, branches, and straight sections). This procedure readily translated the acoustic model schematic used by the designer to a mathematical description of the piping acoustics. The elements were assembled into a global matrix describing the acoustic characteristics of the system. The assembled global acoustic matrix was defined such that:

$$\left[G(f)\right]\left[wp(f)\right]=\left[\dot{m}(f)\right]$$

where: $\left[G\right]$ = Assembled global acoustic matrix

$\left[wp\right]$ = Column vector of acoustic wave amplitudes

$\left[\dot{m}\right]$ = Column vector of cylinder end mass flows

This equation was solved for the acoustic wave pair amplitudes, which yielded the response dynamic pressures as:

$$\left\{P(f)\right\}=\left[Z(f)\right]*\left[\dot{m}(f)\right]$$

where: $\left[Z\right]$ = Global impedance matrix (PSI/(lbs/sec)) = $\left[G\right]^{-1}$

Once the cylinder mass flows were determined, the second equation was used to simultaneously predict the dynamic pressures at all locations.

The cylinder pressures and flow rates were generated using a fundamental thermodynamic model of the cylinder, which incorporated a dynamic valve model with flow-squared losses. This model could be enhanced to any level of sophistication, including the simulation of valve stiction, non-linear spring forces, or other effects. Since the valve flow was a function of the difference between the cylinder pressure and the pressure behind the valve, estimation of the valve mass flow rates was an iterative process. When the process was complete, the full cylinder-to-cylinder and cylinder-to-piping interactive valve mass flows had been computed. The dynamic pressures throughout the piping system were then calculated in the frequency domain using the equation for *P(f)*.

4.2 New Time-Domain Fluid Flow Model

A full one-dimensional time-domain flow solver, named TAPS, applicable to any complex manifold and piping system was developed by SwRI. This transient flow solver included all terms of the governing equations including fluid inertia, diffusion, viscosity, and energy dissipation. The new solver model was then utilized to solve the pulsating flow in standardized compressor manifold and piping designs to determine whether through-flow and the non-linear terms of the Navier-Stokes equations had a significant influence on the solution of the pulsating flow field when compared to the conventional acoustic wave equation solution (IPPS). A number of factors were of particular interest in the new code development and the comparison to the existing code:

Does the new TAPS model accurately predict frequencies and amplitudes of pulsation in a complex piping system?

Is the TAPS solver adequately fast to be utilized as a service tool?

Does the TAPS model accurately predict transient and steady-state pressure drops in a compressor piping system?

Does the TAPS solver improve predictions of acoustic phase cancellation and resonance between compressor cylinders on a common header?

If the above questions can be answered affirmatively, then the new solver can be considered a significant improvement over existing pulsation solver technology.

4.2.1 Mathematical Model

The state of the gas in the compressor manifold and attached piping system is determined by two factors: (1) the kinematics of the compressor drive, which provides a forcing inlet boundary condition to the piping system, and (2) the fluid dynamic behavior (response) of the piping system and passive outlet boundary condition. The compressor cylinder boundary condition is determined from its piston position, $z(\varphi)$, which is given by:

$$z(\varphi) = \frac{V_s}{A_P} + r \times (1 - \cos\varphi) + \frac{r}{\lambda} \times \left(1 - \sqrt{1 - \lambda^2 \sin^2 \varphi}\right)$$

In order to calculate the velocity and the pressure at every point in time, the transient one-dimensional incompressible flow Navier-Stokes equations have to be solved:

$$\frac{\partial \rho}{\partial t} + \frac{\partial (\rho v_x)}{\partial x} = 0$$

$$\rho\left(\frac{\partial u}{\partial t} + u\frac{\partial u}{\partial x}\right) = -\frac{\partial P}{\partial x} + \mu_S \frac{\partial^2 u}{\partial x^2}$$

In the above momentum equation, the viscosity, μ_S, is the combined viscosity and turbulent eddy viscosity, where the turbulent eddy viscosity is usually determined using a second order Reynolds number based turbulence model. Note that the energy equation is not included here as it can be solved as a simple algebraic pressure loss equation.

The turbulence eddy viscosity is handled explicitly and is determined from a second order Reynolds number turbulence model. In pipe flow there are two terms in the momentum equation that include viscosity: a) The second partial derivative in the streamwise direction and b) the second partial derivative in the stream-normal direction. The b) term can be treated implicitly using a basic pipe friction loss coefficients and does not require viscosity directly (only within the context of Reynolds number). The a) term does require viscosity (and turbulence eddy viscosity) directly and must be handled explicitly. To properly capture the nonlinearity of this term, small time steps and fine grid spacing is required. However, this time step and grip spacing is not smaller than what is required to capture complex wave shapes of high frequency pulsating flow anyway, so this was not found to be a limitation.

4.2.2 Formulation of Equations for Transient Pipe Flow

The above described Navier Stokes equations can be rewritten into a more convenient form as:

$$\frac{\partial}{\partial t}\left(\frac{pA\gamma}{c^2}\right) + \frac{\partial}{\partial x}\left[\frac{pA\gamma u}{c^2}\right] = 0$$

$$\frac{\partial}{\partial t}\left[\frac{p\gamma u}{c^2}\right] + \frac{\partial}{\partial x}\left[p\gamma m^2 + p\right] = 0$$

Note that the viscosity term was eliminated in the above equations; i.e., these equations are effectively Euler equations. However, the viscosity and pressure (energy) loss terms are not neglected but rather are explicitly treated at every time step and used to correct pressures and velocities at all nodes. The momentum and continuity equations shown above can be expressed in the following form for the numerical approach:

$$\frac{\partial \vec{q}}{dt} + \frac{\partial \vec{F}}{\partial x} = 0$$

where ***q*** and ***F*** are vectors with the following designations:

$$q = \begin{bmatrix} \dfrac{pA\gamma}{c^2} \\ \dfrac{p\gamma u}{c^2} \end{bmatrix} \quad F = \begin{bmatrix} \dfrac{pA\gamma u}{c^2} \\ p\left(1 + m^2\gamma\right) \end{bmatrix}$$

In order to solve the discretized form of these equations second-order methods were utilized.[12]. As previously noted, here the energy equation and viscosity are decoupled and treated explicitly in between time steps to enhance computational efficiency. This results in a two-equation model with the requirement for relatively small time-steps but a time-space step dependency. The viscous energy loss terms can be divided into a pipe friction loss and a through-flow viscous energy dissipation; both terms are separately calculated and applied at all nodes. One should note that the viscous trough-flow energy dissipation represents the velocity gradient losses in the pipe flow direction which is usually very small for steady flow but can be significant for pulsating flows. The conventional pipe friction loss must also be included as it accounts for the normal flow gradient viscous losses which are primarily steady-state effects.

Within this project, a three-equation model (with the energy equation coupled) was also developed and compared to the two-equation model; as differences were found to be negligible, only the two-equation model was further advanced. One should note that the energy losses of the system are effectively pressure drops (and can be obtained from well established empirical pipe friction formulations[345] whereas the viscosity term results in an enthalpy reduction that must be converted to a pressure drop to be useful in the above model. Unless a cooler is utilized, measurements at many stations have shown that gas temperature drops between compressor discharge and station exit are less than 0.5 degree Celsius because of the dominant convection heat transfer from the process gas. Even at very low ambient conditions the gas temperatures throughout compressor stations tend to be constant and thus the influence of heat transfer on the pulsation can be neglected. Nonetheless, the model does allow for gas temperature changes but they are included in the model in the form of gas property changes from the real equation of state of the particular gas mixture (no ideal gas assumption) rather than heat transfer in the energy equation.

In a complex piping system, the above set of equations must be individually solved for all pipe segments with the appropriate inlet and outlet conditions updated at each time step. Within each pipe segment a simple central difference discretization and time-space forward marching solution was utilized. Pressure losses inside the pipe and at the interfaces are determined from friction loss models and viscosity losses are directly calculated from the discretized viscosity term of the momentum equation (in the flow direction); these two terms are applied at every time step at every applicable node. Pipe inlet and outlet conditions, which are also enforced at every time step, where either active inlet forced (sinusoid, square wave) or active un-forced functions (compressor), pipe intersections (branching nodes), or passive end conditions (infinite pipe, open- or closed end).

4.2.3 Pipe Boundary Conditions

Formulations must be provided to determine boundary conditions at multiple pipe interfaces such as pipe tee's or joints. The continuity equation may be applied to determine the resulting velocity in each pipe inlet and outlet. Pressure may be assumed to be equal at the intersection point and a weighted average function should be used to solve for the pressure at the intersection point. For example, Figure 3 shows a one-on-two pipe intersection.

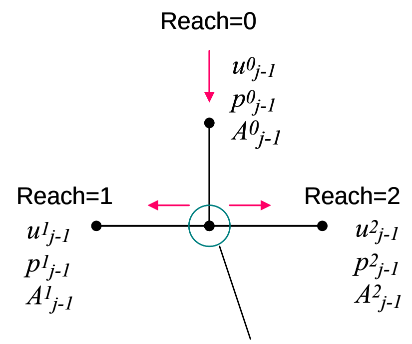

At intersection (j) node:

$$A^0_j(u^0_{int}) = A^1_j(u^1_{int}) + A^2_j(u^2_{int})$$

$$P = P_{int}$$

Figure 3: Branching Node Intersection (1 inlet / 2 outlets)

This model results in the volumetric flow rate in reach 0 and 2 from the continuity equation:

$$u^2_{\text{int}} = \frac{u^0_{\text{int}} \cdot A^0_j - u^1_{\text{int}} \cdot A^1_j}{A^2_j}$$

$$u^0_{\text{int}} = \frac{u^1_{\text{int}} \cdot A^1_j + u^2_{\text{int}} \cdot A^2_j}{A^0_j}$$

The pressure in each pipe interface node j and the j-1 is used to determine the weighted contribution towards the pressure at the intersection point is expressed as:

$$P_{\text{int}} = \frac{\sum_{n=1}^{3} (P^i_{j-1} \cdot A^i_{j-1})}{\sum_{n=1}^{3} (A^i_{j-1})}$$

Similar branching node equations can be derived for intersections of four of more pipe segments. As previously noted, these equations must be enforced at all pipe interfaces and inlet/outlets at each time step.

Boundary end-conditions, such as open ended pipe, closed pipe, or infinite pipe also must be defined but are relatively straight forwardly determined from basic physics. For example, at an open ended pipe the interface node pressure is set to ambient while velocity is conserved. Similarly, at a pipe closed end the velocity is set to zero and pressure maintained. Inlet conditions can be either forced with a hard boundary condition (sinusoids or square waves) or un-forced with a downstream dependent function (compressor cylinders). As compressor cylinders are varying-volume machines, boundary conditions based on velocity rather than pressure were found to be more practical (and physical) to implement.

5. Development and Verification

5.1 Code Development

The new unsteady one-dimensional Navier-Stokes model (TAPS) code was written for a complex system of pipes with multiple interfaces and has all standard boundary conditions, such as open ends, closed ends, a compressor cylinder, sine wave, and square waves, available. Interfaces between pipe segments can be one-on-one, two-on-one, one-on-two, one-one three, or three-on-one and include discrete pressure drops at the segment interfaces. Other boundary conditions are either passive (closed wall, open wall, infinite pipe) or active (compressor, sine wave, square wave). The pipe areas can change either gradually (transition piece) or abruptly (open end or bottles) within the pipes or at the interfaces of pipe segments. Models with up to 60 interconnected pipe segments were successfully tested. A very basic batch file pre-processor, windows graphical user interface, and graphical post-processor (for frequency and time domain data) were also implemented to allow for the software debugging and validation tasks. The post-processor interface includes a Hanning window function, a time domain, and an FFT output option.

This first version of the TAPS code was intended for the simulation of station compressor manifolds and lateral lines but terminated at the station header piping, as it is currently done in the piping system frequency-domain models. Two compressor cylinder boundary conditions were developed: (1) A basic volume based cylinder model that allows for quick frequency sweeps but does not provide accurate valve loss calculations, and (2) a complex model that solves the transient Navier-Stokes equations inside the cylinder and has a fully dynamic valve model which provides detailed compressor performance calculations and valve flutter predictions. Because of the complexity of the second cylinder model, it is recommended that piping design calculations are first performed with the basic model, and the complex model is only utilized for single point or limited range compressor performance checks. No significant differences in piping pulsation responses outside the cylinder could be seen between these different models when they were compared in parametric studies. Full frequency sweeps can be performed with all boundary conditions.

The solver model and code development focused on specific geometries instead of developing a general "user-friendly" model interface. However, the code was written open-ended so that a user-friendly pre-processor and post-processor are easy to implement. These pre- and post-processors are currently being implemented under a separate project.

5.2 Basic Model Validation

A first level model verification and debugging was performed using simplified piping geometries with small amplitude boundary condition inputs, which allowed standard linear acoustic applications and the current IPPS code to be used for reference and comparison. These basic validation tests included simple straight closed and open-ended pipe, Helmholz resonators, and two-on-one interface pulsation cancellation. Reporting on all of them is beyond the scope of this paper, however, as expected results were consistent with linear acoustic theory.

Some slightly more advanced models were used for frequency (but not amplitude) comparisons to assure that the new TAPS model properly predicts basic pipe and volume resonance frequencies. For example, Figure 4 shows the frequency response of pulsating flow downstream of a 5 m choke tube (area ratio 5:1) inside a 30 m wide open-ended pipe. A sine wave frequency sweep from 0 to 20 Hz was performed, and the results compared to calculations from the current IPPS acoustic model to identify any frequency discrepancies. As there was no bulk-flow applied for the sine wave case and the pulsation levels were low, identical frequency and amplitude results were expected. Figure 6 shows the calculated response from the IPPS code using a compressor sweep from 8–15 Hz and very close agreement for the basic case can be seen.

On the other hand, Figure 5 shows a compressor sweep (with through flow) using the TAPS code from 3–20 Hz to identify and compare higher harmonics with the IPPS results. Again, close frequency agreement can be seen, but the magnitude results are different from the IPPS results. As the TAPS compressor sweep has bulk flow, which is not modeled by the IPPS code, the results from the TAPS code are probably more accurate for pulsation amplitudes. Also, as the sweep on IPPS is over a smaller frequency range (8–15 Hz), not all higher harmonics are excited.

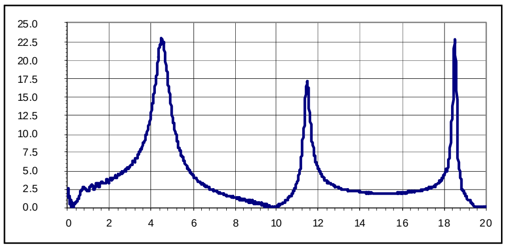

Figure 4: TAPS 0–20 Hz Sine Sweep in a Wide-Open Ended Pipe with a Choke Tube

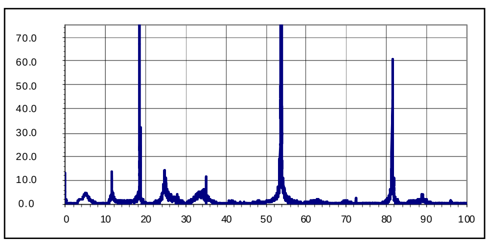

Figure 5: TAPS 3–20 Hz Compressor Sweep in a Wide-Open Ended Pipe with a Choke Tube

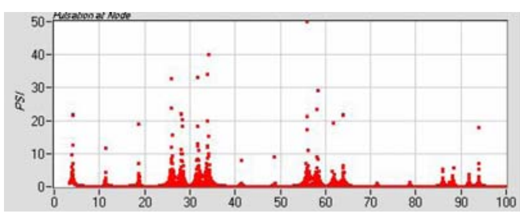

Figure 6: IPPS Compressor Frequency Sweep 8–15 Hz

5.3 Laboratory Data Validation

To validate the TAPS code, laboratory quality pulsation data in a piping system with actual flow and pressure drops was required. Thus, an experimental investigation of non-linear acoustics and dynamic pressure losses was undertaken. The testing was performed using a compressor in a closed pipe loop filled with Nitrogen, which was pressurized between 30 and 50 PSI. The loop through-flow was controlled using the positive displacement compressor between 0.2 and 0.5 kg/s. Pulsations were generated over a 5 to 40 Hz range of frequencies using a through-flow pulse generator (perforated flow interrupter). Figures 7 and 8 show the closed loop facility and the test section piping arrangement (including test locations for dynamic sensors), respectively. Fast response dynamic pressure transducers inside the loop were utilized to measure the transient flow field, and a flow meter was utilized to determine total volume flow through the loop. Measurement results were available both in the time domain and frequency domain using a FFT conversion.

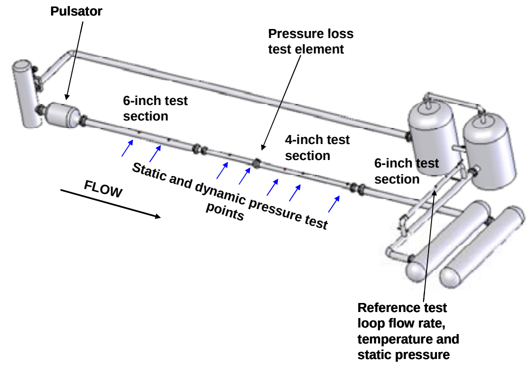

Figure 7: Experimental Test Loop Used for Both Phases of Laboratory Testing

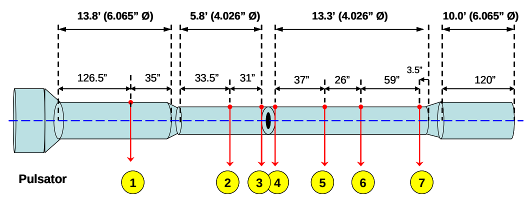

Figure 8: Experimental Dynamic Pressure Test Points Used in Laboratory Testing

The testing was divided into two phases: (1) a number of fixed frequency pulsations were applied to the closed loop system to measure pulsation reduction in a complex piping system, and (2) a set of frequency sweep tests to measure the system spectrum response over a wide range of frequencies were performed. Both test sets were performed over a range of gas pressures and through-flows to determine the effect of pressure drops on the measured acoustic response. A total of 20 different tests with varying pressure, flow, and, orifice plate beta ratios were completed and time domain and frequency data was acquired at all test points between 0 and 100 hz.

Total measurement uncertainties for this test series can be divided into uncertainty in frequency and amplitude. Frequency measurement uncertainties are primarily due to incomplete evacuation of the air prior to the Nitrogen fill of the loop (i.e., speed of sound uncertainty) and pipe length measurement uncertainties. This total frequency measurement uncertainty was estimated to be below 2%. On the other hand, uncertainty in measured pulsation amplitude can be due to many instrument, gas composition, and pulsation excitation related factors, such as sensor accuracy, sweep speed, resolution, pulsator installation, sensor installation, total flow measurement, flow stability, etc. Consequently, the total measurement uncertainty for pulsation amplitudes was much higher and estimated to be approximately 10% to 15%.

Results for all test cases were compared to TAPS predictions. For example, Figure 9 and Figure 10 show experimental test results from the closed loop versus TAPS prediction for a 1,050 RPM at 45 PSI, 5–40 Hz frequency sweep cases. Here Figure 9 presents the case without an orifice plate in the loop, while in Figure 10 results with a 0.45 beta ratio orifice plate are shown. For this comparison only the test point No. 5, downstream of the orifice plate, is presented. Clearly, the orifice plate provides pulsation damping and, thus, pressure magnitudes in the frequency spectrums are seen to be lower for this case. When comparing TAPS predictions to test results, close agreement in both frequency and amplitude content can be seen for both cases. These prediction results of both frequencies and amplitudes are clearly within the total measurement uncertainties (as discussed above) of the test. Similar results were obtained for the other test cases and measurement locations. Generally good agreement between TAPS predictions and measurement data was observed. However, a slightly high TAPS prediction in amplitude (10–15%) is apparent for some cases at low frequencies (below 20 Hz); i.e., TAPS appears to over-predict the first harmonic response frequencies. This needs to be further investigated, but it is likely caused by the simplified turbulence model (constant eddy viscosity) that is currently being utilized in the TAPS solver. This type of turbulence model tends to under-damp the transient terms and, thus, favors lower frequencies (highest pulsation velocities). A more sophisticated turbulence transport model, with a clearly defined Reynolds number dependency, will probably address this problem.

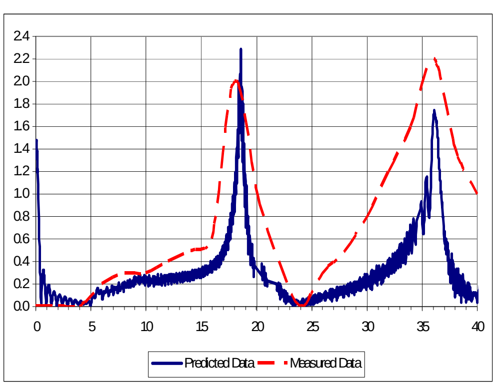

Figure 9: Test versus TAPS Predicted Results for Run No. 1 (No Orifice Plate)

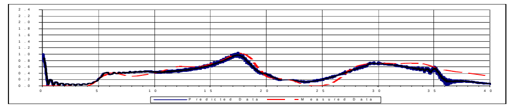

Figure 10: Test versus TAPS Predicted Results for Run No. 1 (with Orifice Plate)

6. Comparison of Prediction Methods with Actual Compressor Pulsation Data

In previous research projects, significant experimental test data was acquired on the 200 HP Arial reciprocating compressor that is located in the SwRI Metering Research Facility (MRF). This data collection included dynamic pressures, flows, temperatures, gas compositions, and total system performance of the compressor in the closed MRF natural gas loop. The data is ideal for comparative studies and validations of the TAPS solver as it represents realistic compression station testing that was performed in a laboratory type setting. Thus, a predictive model representation of this compression system unit was created for both the new TAPS code and the current IPPS software. A number of compressor operating cases, where highly reliable and accurate pulsation test data was available, were utilized for comparisons. TAPS predictions were validated with detailed data comparisons for frequency content, amplitude, and phase throughout the system. Agreement between the predictions of the TAPS code and test data in the order of 20–30% in amplitude were considered a significant improvement to the existing IPPS modeling.

Figure 11 shows the piping arrangement of the MRF compressor closed loop system. This piping and node system was input into the TAPS solver using physical dimensions and then compressor frequency sweeps from 5 to 15 Hz (300 to 900 rpm) were simulated. The loop gas was natural gas (speed of sound 444.4 m/s), and the operating pressures and temperatures were obtained from the test data. For these runs, the models were terminated at the bottles (using a wide open boundary condition) to reduce the overall complexity, and the basic (forced function) compressor model boundary condition was used for all frequency sweeps.

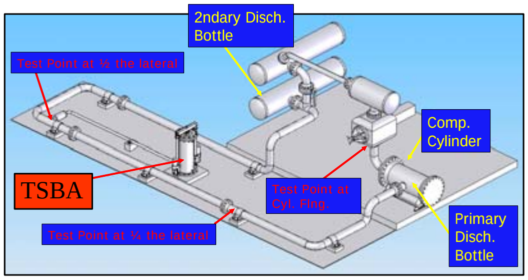

Figure 11: Closed Loop Compressor Set-Up for Real Compressor Tests at MRF Facility

TAPS predictions and test data were compared for four test locations and the 1.298 pressure ratio case. Figure 12 shows the measured pressure pulsation data in the frequency domain at the 25%, pipe No. 10 location for this case (shown in Figure 11 as Test Point). As a comparison, Figure 13 shows the TAPS output for the same case. Close agreement within the measurement uncertainties in both frequency content and overall pulsation amplitudes is seen. The only small discrepancy appears to be a small peak in the experimental data at 12 Hz that is not predicted by TAPS. This frequency is a pulsation inside the bottle that was not captured by TAPS as the numerical model was terminated at the last bottle inlet (with a wide open boundary condition). Similarly consistent results were obtained for other conditions and test locations. Thus, the new time domain TAPS solver is seen to accurately predict the frequencies and amplitudes of flow pressure pulsations in a realistic compression system.

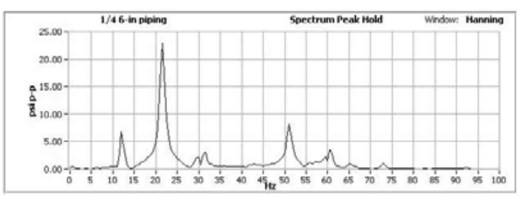

Figure 12: Test Results for the Dynamic Response of the MRF Compression System

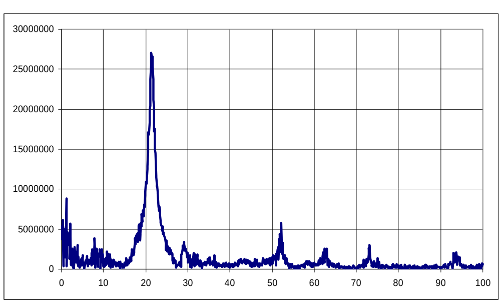

Figure 13: TAPS Output for Dynamic Response of the MRF Compression System to a 5–15 Hz Frequency Sweep Simulation

7. Summary and Conclusion

The mathematical assumptions associated with all conventional pulsation design tools (acoustic wave equation solvers) must lead to discrepancies in amplitude predictions as these equations are only a partial physical model of the actual transient fluid dynamics. A full one-dimensional representation of the governing transient fluid dynamic equations (called the Navier-Stokes equations) can provide a more thorough solution for the pulsating flow field and can provide more accurate pulsation amplitude predictions. This is particularly critical in the design of variable high-speed compressor systems, as for these applications complete resonance avoidance is impossible. SwRI developed a new one-dimensional time-domain Navier-Stokes solver, (TAPS) to improve SwRI's prediction capabilities for transient compressor station manifold and piping system design. When the new SwRI TAPS solver was applied to standard acoustic elements, laboratory test data, and actual compression system test data, the following observations were made:

A transient one-dimensional solver of the Navier-Stokes equation can accurately predict frequencies and amplitudes of pulsations in a complex compression piping system with area changes (expansions and reductions), pipe-tee's, bottles, choke-tubes, orifice plates, etc.

The non-linear terms of the governing (Navier-Stokes) equations have a significant influence on the solution of the pulsating flow field when compared to the conventional acoustic wave equation solution (IPPS). The primary influence of these terms is on pressure amplitudes, but due to frequency interference and pulsation cancellation, a non-linear model should also be more reliable in predicting frequency content.

The solution times for the new solver strongly depend on time step size and node spacing. These are limited by numerical stability requirements. In general, solution times of the new TAPS model were seen to be comparable or faster than the existing IPPS model.

Transient and steady-state pressure drops can be accurately modeled using the TAPS solver. However, as the TAPS solver utilizes a one-dimensional solver, it is critical to apply correct pressure drop coefficients at elbows, pipe tee's, orifices, and sudden cross sectional area changes.

Other code validation studies (not presented herein) showed that TAPS solver predicts acoustic phase cancellation, phase interference, and amplification between compressor cylinders on a common header. This is critical for the prediction of first order pulsations in compressor headers with multiple cylinders, as in many actual cases the valve piping, pressure drops, and individual header performance is not perfectly symmetric.

---

[1] Fletcher, C. A. J., 1988, **Computational Techniques for Fluid Dynamics, Volume I**, 2nd Edition, Springer-Verlag, London

[2] Machu, G., 2004, "Calculating Reliable Impact Valve Velocity by Mapping Instantaneous Flow in a Reciprocating Compressor," GMRC Gas Machinery Conference, Albuquerque, New Mexico.

[3] Miller, R. W., 1989, **Flow Measurement Engineering Handbook**, 2nd Edition, McGraw-Hill, New York, New York.

[4] Colebrook, C. F., 1938-1939, "Turbulent Flow in Pipes, with Particular Reference to the Transition Region Between the Smooth and Rough Pipe Laws," Journal of the Institution of Civil Engineers, London, **11**, pp. 133-156.

[5] Fox, R. W. and McDonald, A. T., 1992, **Introduction to Fluid Mechanics**, 4th Edition, John Wiley & Sons, Example Problem 8.8, pp. 366-367.

Reliable sealing technology for high pressure CO_2 applications

by:

Armin Gerland

Dr. Volker Peterseim

Freudenberg O-Ring GmbH u. Co KG

Georg Samland

MT Sealing Technology Inc.

Country

e.g. 6th Conference of the EFRC October 28th / 29th, 2008, Dusseldorf

Abstract:

CO_2 process gas compressors are a demanding application area regarding the use of O-Ring-seals. The paper presents the results of investigations and shows that it is possible to define an appropriate O-ring material. In a holistic approach for high pressure CO_2-applications all aspects concerning explosive decompression, lube oil compatibility und thermal loading were taken into consideration in order to achieve an extended lifetime. The chosen material shows an excellent resistance against explosive decompression effects and is now suitable for all stages of the high pressure CO_2-application. This approach eliminates down times and allows a reliable operation of the compressor.

1 Introduction

For the efficient operation of a CO_2 compressor, one of the important requirements is for high CO_2-pressures, which causes the CO_2 to be in its super-critical aggregate state. Moreover, as well as the high absolute pressures, in the three-stage CO_2 compressor considered here a significant pressure and temperature gradient occurs in the operation of the compressor, which is constantly and repeatedly changing in very short time intervals. If, for example, O-Ring seals made of elastomer materials are used for sealing the compressor, due to the constant pressure and temperature changes these must likewise absorb or re-emit CO_2 to maintain the respective thermodynamic equilibrium. As well as many other requirements these processes in particular place high demands on resistance to so-called explosive decompression. The diffusion processes into and out of the elastomer seal cannot take place at the same speed at which the thermodynamic equilibrium states in the compressor change. If a larger quantity of CO_2 is then dissolved in the O-Ring than is thermodynamically permissible, then due to this supersaturation of the seal with CO_2 a higher CO_2 pressure can build up inside the seal, which leads to the destruction of the polymer network of the seal. The extent of the destruction becomes visible in the form of cracks and bubbles in the sealing element concerned, and can in severe cases lead to the complete destruction of the entire sealing element.

If seals – O-Rings – made of elastomer materials are used which do not have the appropriate resistance against explosive decompression, then under the extreme demands present in a CO_2 compressor, the failure pattern described above consisting of cracks and bubbles leads to failure of the sealing property of the system. Even if no immediate leakage occurs, the damaged seals must be replaced every time the compressor is shut down. As well as the high degree of uncertainty in terms of increasing quality constraints demanded by current risk management strategies, this naturally has economic disadvantages as well. In addition to the increased demand for replacement seals, additional expense for maintenance costs must be budgeted for, mainly due to the extended down times of the compressor.

In this paper an integrated approach is presented with respect to the relevant properties of elastomer sealing materials, which is to be considered when selecting them for high-pressure CO_2 applications. The focus of the relevant particular experiments presented here is resistance against explosive decompression. At the same time however it will be shown that not every failure pattern found in a seal in a CO_2 compressor may be attributed automatically to the damage category covered by “explosive decompression”. In the analysis presented in the following, symptoms of damage can be clearly attributed to other, in part very complex interactions, which occur as a result of the start-up mode using air, and from the increased temperatures in the actual CO_2 operation itself. The damage mechanism postulated to occur is supported by laboratory experiments.

2 CO_2 resistant materials for high pressure applications

2.1 Requirement profile

In order to certify a sealing material for a CO_2 high-pressure CO_2 application, the standard tests used for elastomers – for example tensile elongation experiment or compression set – are not appropriate, or at least not sufficient as a sole decision criterion. Therefore, before selecting a suitable sealing material, the required characteristic profile for high-pressure CO_2 applications had to be provided using an appropriate test program, in order to define thereby relevant criteria for selection of materials. Fig. 1 sets out the three essential requirements of an elastomer material which certify it as resistant against CO_2 in the supercritical state:

- CO_2 resistant with regard to explosive decompression
- Low permeation of supercritical CO_2
- Resistance to lubricant used in CO2 compressor

The resistance against the lubricant used, given here as the third required property, does not have any direct relation to the “supercritical CO2” medium. But since an adequate oil resistance against the lubricant used in the compressor represents a central requirement and is often forgotten due to the “triviality” of the test provided for it, the aging of the oil cannot be discounted as a component of the triad of relevant requirements.

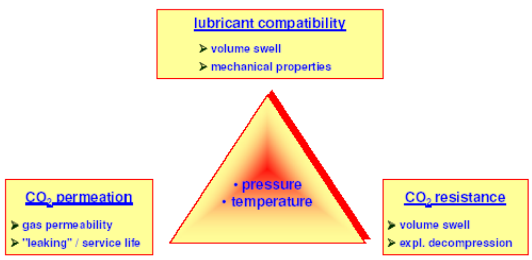

Figure 1: triad of requirements for CO_2 resistant elastomeric materials

In line with the central question addressed by this paper, the test for resistance against explosive decompression will be described again in further detail in the following sub-section.

2.2 Resistance against explosive decompression

2.2.1 Test procedure

The test for evaluating the resistance against explosive decompression must be carried out in an autoclave, in order to recreate appropriately high CO_2 pressure levels. In this process, each load spectrum of pressure and temperature is a separate test, which is set appropriately in the autoclave. Pressures up to 200bar and temperatures up to approx. 230°C can be implemented with the currently available autoclaves. Normally, the elastomer samples are exposed to the appropriate conditions of pressure and temperature overnight, in order to allow the samples to swell to their equilibrium. The absorption of supercritical CO_2 and the associated swelling can be very large, and in the case of elastomer samples with poor compatibility can reach levels significantly above 100%.

The actual demand placed on the elastomer material is ultimately set by the opening of the autoclave. Opening should take place as quickly as possible. This removal of the stress takes place independently of the chosen load spectrum in a time period of < 5 sec. This ensures that the pressure gradient between the CO_2 absorbed by the elastomer sample and the ambient pressure is as high as possible and therefore the failure pattern of explosive decompression can be induced. The more slowly the opening of the autoclave takes place, the more protective are the conditions for the embedded sample. The assessment of the resistance is carried out by a visual examination of the surface of the sample for bubbles, and by an assessment of the cut surface of the bulk material of the sample with regard to the formation of cracks. This is done using a microscope photograph. In most cases the presence of cracks or bubbles is already noticeable acoustically, in the form of a cracking sound.

2.2.2 Resistance against explosive decompression of fluorinated rubber -FKM

Seals made of fluorinated rubber –"FKM" – as well as of perfluorinated rubber – "FFKM" – display inadequate resistance against explosive decompression, such that the seals must be replaced each time after the compressor is shut down. Using the autoclave test this inadequate resistance of FKM can be attributed to the extremely high swelling of this material near to the critical point of CO_2 (31°C, 73.7bar). The swelling rates can be in the region of up to 100%, or depending on the overall material composition ("recipe"), even higher still. This means that in materials based on FKM or FFKM, every time the operating point of the CO_2 compressor even merely approaches the critical point, vast quantities of CO_2 are absorbed and then must be released again later at higher temperatures or pressures.

For sealing the CO_2 compressor therefore, on the basis of the autoclave experiments with the material 85 HNBR 230861 a material is selected which given an optimized recipe composition is not expected to exhibit explosive decompression in the load spectrum of pressure and temperature relevant to the CO_2 compressor. It should be noted however in this context that the choice of material for other specific cases at other pressures or temperatures can be different. In that case the most suitable material must be determined again under the relevant load spectrum in the autoclave experiment.

3 CO_2 gas compressor: simulation of start up mode (air) and CO_2 working conditions

The choice of material 85 HNBR 230861 using the autoclave experiments described under section 2 led as expected to a stable situation regarding the failure pattern of explosive decompression. All the O-Rings installed in the compressor are free of bubbles or cracks. Even under extreme loading at pressures right up to 235 bar the O-Rings remain free of defects with respect to this failure. However, a very marked deformation of the O-Ring is revealed in the third stage of the compressor, as is commonly known to occur as the failure pattern of thermal overload ("heat ageing"). This failure pattern however is not necessarily attributable to the load spectrum in the CO_2 compressor, since it is precisely the third stage of the CO_2 compressor that requires a lower thermal stress compared to stages 1 and 2. As a general rule a "heat ageing" pattern of damage requires contact of the elastomer with oxygen in the air or aggressive additives from lubricants at high temperatures. These conditions apply however neither in start-up mode nor in the actual CO_2 operating mode. The start-up mode is certainly driven with air, but the maximum temperatures of 70°C in the third stage of the compressor are very low. In the CO_2 operating mode the temperatures are certainly high enough in principle for an HNBR-material at up to 130°C, but with regard to a chemical attack CO_2 constitutes an inert gas and cannot therefore cause any damage due to thermal overload. In order to understand the cause of the thermal overload in the third stage of the CO_2 compressor, the autoclave experiment is extended in such a way that, in a two-stage process, firstly the start-up mode is simulated (pressure generated with air) and then the CO_2-mode (pressure generated with CO_2) is brought on-stream. The design of the experiment is shown schematically in Figure 2.

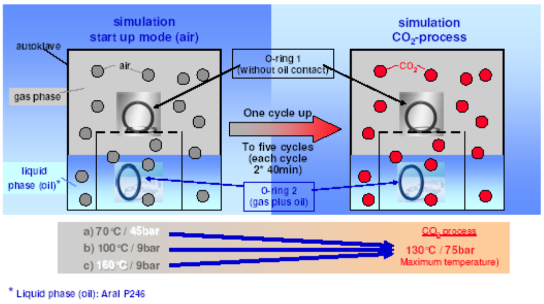

Figure. 2: autoclave test routine: simulation of start-up and CO2-modes of a compressor

The parameters varied in this experiment for the simulation of the start-up mode are both the temperature (70°C to 160°C according to the three pressure stages of the compressor) and also the associated air pressure (9bar to 45bar). For the simulation of the CO_2-mode, the maximum temperature of 130°C is chosen throughout at a CO_2-pressure of 75 bar. In both cases a further distinction is made depending on whether the O-Ring under the appropriate conditions additionally makes contact with the compressor oil, or exclusively comes into contact with air or CO2 as appropriate in the autoclave (see Figure 2).

3.1 Start-up mode: influence of temperature

The temperature during the simulation of the start-up mode is varied between 100°C and 160°C at constant pressure (9bar). As expected, the failure pattern increases with rising temperature. Noticeable damage is only detectable however when contact with the lubricant oil occurs at the same time.

The intensity of the temperature influence on the extent of the damage to the O-Ring is markedly less than that found on the damaged seals which had been removed from the CO_2 compressor at the third stage. Furthermore, the extent of the damage with increasing temperature is not comparable with that found in the case of pressure dependence (see 3.2).

3.2 Start-up mode: influence of pressure

For simulation of the start-up mode of the third stage of the CO_2 compressor, the load spectrum of 70°C and 45bar air pressure is set in the autoclave. The temperature thus lies clearly below that which has been described in section 3.1. for determining the temperature influence. Nevertheless the thermal damage is significantly more marked than at the two higher temperatures of 100°C and 160°C. The increased pattern of damage due to thermal ageing can therefore be attributed to the increased air pressure (45 bar compared to 9 bar).

As already established for the temperature influence, it is also true for the pressure dependence that severe damage occurs only under simultaneous contact with the lubricant oil Aral P246. The relationships between temperature and pressure effects are summarized in Figure 3 using the example of the change in the elongation of breaks.

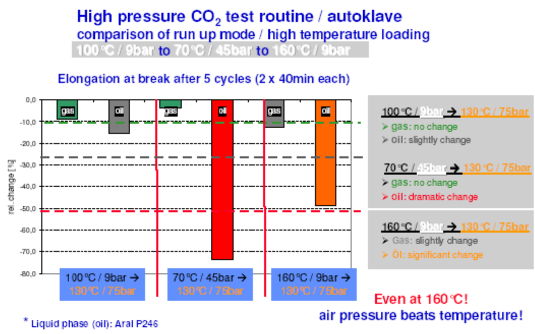

Figure. 3: change of elongation at break as a function of air pressure and temperature

3.3 Start-up mode: influence of lubricant

In sections 3.1 and 3.2 it has been shown that the increase in the pattern of damage to the elastomer seal with regard to thermal ageing as a function of (air-) pressure and temperature is only significant when there is simultaneous contact with the lubricant. In order to better understand this effect of a possible interaction between oxygen in the air and the lubricant on the ageing behavior, a follow-up experiment was carried out in which the elastomer sample of 85 HNBR 230861 is kept in the relevant Aral P246 lubricant. This is performed both with and without the additional inflow of air into the relevant lubricant, in which the elastomer sample is already being stored. The air is fed automatically via a pipette in the form of air bubbles (167ml/minute) into the syringe filled with lubricant. The test temperature is set at 130°C to match the temperature in the compressor during the CO_2-operating mode. The duration of the test is 336 hrs.

The influence of the oxygen in the air on the extent of the damage due to oil ageing is significant. While the contact with the Aral P246 lubricant after 336 hrs at 130°C does not on its own lead to noticeable damage to the elastomer sample, the damage is increased dramatically by the inflow of air under otherwise identical conditions. The damage to the 85 HNBR 230861 after 336 hrs has already progressed to the stage where it is almost as if there is no elastic restoring force left in the material. The elongation of the break in the material has for example declined by 97% (!) of the initial value. This change by comparison was only 11% using the identical experimental design but without the passage of air.

4 Root cause of damage

The experiments performed show that the cause of the large-scale occurrence of thermal damage to the O-Ring made of 85 HNBR 230861 in the third stage of the CO_2 compressor can be attributed to the loading spectrum during the start-up mode (air oxygen!). Essential in this context is that the intensity of the damage primarily increases with rising pressure during the start-up mode, and not with rising temperature.

It can also be concluded that a single start-up of the compressor is not sufficient to generate the degree of damage that is found. Only repeated start-ups alternating with CO_2 operation leads gradually to an ever increasing level of damage. The accumulation of the multiple start-up times to a – then longer – start-up cycle does not lead to an equally intensive level of damage (not shown in the presentation).

Damage mechanism: with higher pressure in the start-up mode, more air and consequently more oxygen is dissolved in the seal. The oxygen dissolved in the seal then leads, at the raised temperatures in the subsequent CO_2 mode (130°C), to the oxygen attacking the polymer chains of the HNBR polymer, but especially to an attack on the lubricant oil Aral P246. This causes the lubricant oil to be broken down and decomposition products to form. The decomposition products in turn attack the HNBR, which results in a markedly accelerated thermal ageing. This process requires a multiple start-up cycle, in order to progressively drive the breakdown process of the lubricant via the respective oxygen quantity dissolved in the seal. A single but correspondingly longer start-up mode does not have the same effect, since the solubility of air in the HNBR material 85 HNBR 230861 is limited and cannot be increased by an extended start-up process.

Possible preventative measures: On account of the excellent resistance of 85 HNBR 230861 against explosive decompression, and since the CO_2 operating mode is not primarily responsible for the observed failure pattern of thermal overload of the seal material, it should be useful to make a modification to the start-up mode of the CO_2 compressor as follows:
1) Low air pressure in the third stage of the compressor in the start-up mode would lead to a lower quantity of dissolved air oxygen in the seal. There is consequently less oxygen in the CO_2 mode at the temperatures occurring there to contribute to the cracking by the lubricant oil.
2) Use of an inert gas during the start-up mode (e.g. nitrogen), which is not capable of chemically attacking the lubricant.
3) Switching to another lubricant oil, providing improved oxidation resistance.

5 Conclusion

In the selection of an elastomer material as a seal for a high-pressure CO_2 application the three most essential criteria have been proposed that must be taken into account as a triad in the choice of a suitable seal material.

It has further been shown which type of analysis or experimental design can be used in laboratory tests prior to deployment to assess the quality of a seal material with regard to its resistance against explosive decompression. This form of the assessment has led to the conclusion that in the material 85 HNBR 230861 a seal material was successfully found which can seal the three-stage CO_2 compressor without failures occurring caused by explosive decompression faults. For other high-pressure CO2 applications with correspondingly different loading spectra in terms of pressure and temperature, or in the use of other lubricants, the selection of a completely different seal may be appropriate.

It has further been shown that not every failure pattern in a high-pressure CO_2 application may be automatically attributed to explosive decompression. It was therefore shown that the damaged seals from the third pressure stage based on the 85 HNBR 230861 can be clearly explained by the type of damage characteristic of a classical heat ageing process.

In order to understand the extent of the damage, the processes in the CO_2 compressor were simulated using autoclave experiments. These involved a distinction between a start-up mode using air and the actual CO_2 mode. An additional important factor has been shown to be the fact that the pattern of damage only occurs to its full intensity when air oxygen and Aral P246 lubricant act on the seal material at the same time. In this process the oxygen – dissolved in the seal – chemically attacks the Aral P246 lubricant at the increased temperatures in the CO_2 mode. The decomposition products of the oil in turn attack the seal in a second stage, which after repeated alternation between start-up mode and CO_2 mode leads to the pattern of damage found. A repeated alternation between start-up mode and CO_2 mode is therefore necessary in order to deliver the necessary quantity of oxygen to attack the lubricant oil. The quantity of oxygen transferred at each of these changes is limited by the solubility limit of the air in the HNBR seal at the pressure of 45 bar applying in the start-up mode.

BORSIG COMPRESSION ZM

The piston rod – an essential component on reciprocating compressors including crosshead – design, calculation and requirements concerning surface

Valve cages and covers – design and evaluation in respect of ease of maintenance

by:

Dipl.-Ing. Stefan Jarosch, Dipl.-Ing Steffen Schramm and
Dipl.-Ing. Marcus Zeibe
Design Department
BORSIG ZM Compression GmbH
Meerane
Germany
info@zm.borsig.de

e.g. 6th Conference of the EFRC
October 28th / 29th, 2008, Dusseldorf

Abstract:

In the first part of this article a general overview is given about the state of the art in piston rod technology and a summary of the requirements of API 618, design possibilities, calculation basics as well as design of the piston rod - an essential component of a reciprocating compressor - including crosshead.

One part of this paper will deal with the fixing of the crosshead and the connection with the piston. Experiences are presented in the design of the surfaces in the working area of the packings. This part was written in cooperation with the company WÜRSCHEM Oberflächentechnik GmbH in Moers profiting from its basic principles, experiences and knowledge.

In the second part of the paper ways of how to fasten valves in the cylinder are presented. A general overview is also given about the state of the art in this technology and the provisions in API 618. Additional presentations are made: design of valve covers and cages, design possibilities of the required gas proofing and evaluated especially with respect to ease of maintenance.

1. Piston rod

1.1 Function of a piston rod in a reciprocating compressor with crosshead

Picture 1 shows a piston rod including its 3 packings, the piston and the piston nut.

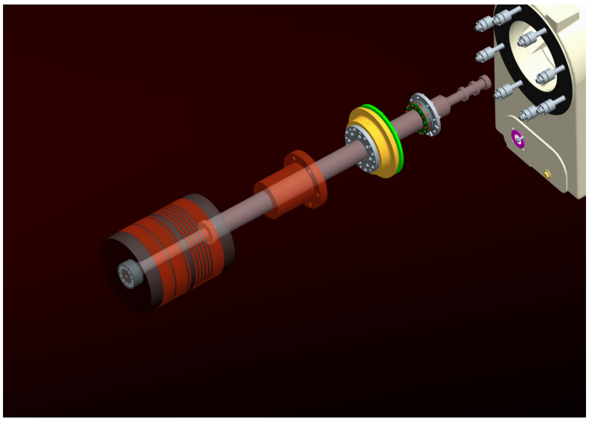

Picture 1: Assembly unit piston – piston rod

The piston rod is a component of the reciprocating compressor. It guides the piston in the cylinder and offers the technical possibility of sealing so that the crank-sided working chamber can be used by means of a compression gland. In addition, it establishes the connection to the crosshead.

At the same time a space is formed between crankcase and cylinder in order to:

- safely keep away the oil of the compressor frame from the cylinder or from the medium in the cylinder respectively

and

- achieve a medium-dependent supply and disposal and/or sealing of the chambers in the distance piece (both upper and lower chambers) by the packings.

A special case is the usage of an additional piston rod in the cover-sided working chamber, the so called "tail rod", which may only be used after written confirmation from the customer.

1.2 Requirements acc. to API 618, 5th edition, and changes compared to the 4th edition

API Standard 618 describes in paragraphs
- 6.10.1 "piston and piston rod assembly"
- 6.10.2 "piston rod and crosshead assembly"
- 6.10.4 "piston rods"
- Appendix G 6.-8.
the requirements on the piston rod component.

Extract from API 618, 4th edition [1]	**Extract from API 618, 5th edition [2]**
2.8.1 Piston that are removable from the rod shall be attached to the rod by a shoulder-and-locknut design or by a multi-through-bolt design. All nuts must be positively locked in place. Locking nuts attaching the piston rod to the piston and to the crosshead shall be tightened in accordance with the manufacturer's standard. <u>The rod shall be positively locked to the crosshead to prevent rotation.</u> As a minimum, the manufacturer's tightening procedure must assure a minimum thread-root pre-stress level of 1,5 times the rod's thread-root stress at maximum allowable continuous rod loading. Hydraulic or thermal methods are preferred for tightening piston-rod nuts when the rod diameter is 75 mm (3 inches) or larger. Use of slugging-type wrenches is unacceptable for this purpose.	**6.10.1 Connection of Piston to Piston rod** Pistons that are removable from the rod shall be attached to the rod by a shoulder and nuts(s) design or a multi-through-bolt design. Other proven attachment methods may be used, and in such cases they shall be noted in the proposal. Mechanical or hydraulic methods are acceptable for tightening piston nuts. Slugging (hammer) wrenches shall not be used for this procedure. … As a basic requirement, … a minimum pre-load in the connection of 1,5 times the maximum allowable continuous rod loading.

Table 1: Connection of piston to piston rod

Table 1 illustrates that in the 5th edition the requirement concerning the tightening pre-load is simplified compared with the 4th edition.

Table 2 shows that the necessity for an antirotation lock of the piston rod in the crosshead is strongly limited in the 5th edition.

Extract from API 618, 4th edition [1]	Extract from API 618, 5th edition [2]
	6.10.2 Connection of Piston rod to Crosshead 6.10.2.1 Piston rods shall be connected to the crosshead by a direct connection, where the rod is threaded into the Crosshead or an indirect connection, where the rod is not threaded into the crosshead. Positive locking of the rod shall be provided for direct connection methods. Other proven attachment methods may be used, and in such cases they shall be noted in the proposal. Mechanical or hydraulic methods are acceptable for tightening. Slugging wrenches … shall not be used. Where pre-load is achieved by hydraulic tensioning methods, which ensure proper pre-load, positive locking is not required. 6.10.2.2 The manufacture's tightening procedure shall assure a minimum preload in the connection equal to 1.5 times the maximum allowable continuous rod loading

Table 2: Connection of piston rod to crosshead

Extract from API 618, 4th edition [1]	Extract from API 618, 5th edition [2]
2.8.4 All piston rods, regardless of base material, shall be continuously coated from the piston-rod packing to the oil wiper packing travel areas with a wear resistant material.	**6.10.4 Piston rods** 6.10.4.1 Unless otherwise specified, all piston rods, regardless of base material, shall be coated with wear resistant material. The material and surface treatment of piston rods shall be chosen to maximize rod and pressure packing life and shall be proposed by the vendor at the time of purchase for the purchaser's acceptance. Coating shall comply with 6.10.4.2. Piston base material and coating for use in corrosive environment shall be suitable for the service and operating conditions specified. Alternatively, an uncoated piston rod may be proposed when the expected life equal or exceeds that a coated rod for the specified operating conditions. Uncoated piston rods shall be AISI 4120 or better and shall be surface hardened in the packing area to a hardness of at least Rockwell C50, and shall be inspected for cracking by magnetic particle examination. 6.10.4.2 When coatings are used, piston rods shall be continuously coated from the piston packing through the oil wiper travel areas. The coating material must be properly sealed to prevent corrosion of the base material at the interface of the coating, Fusion techniques that require temperatures high enough to permanently affect the mechanical characteristics of the base material shall not be used. High-velocity and high-impact thermal coating processes are acceptable for the coating of piston rods. Metal spray techniques requiring roughening of the surface of the base metal are not recommended because of the potentially

	destructives stress risers left in the surface. Use of sub-coating under the main coating is not recommended.

Table 3: Requirements on piston rod

Extract from API 618, 4th edition [1]	**Extract from API 618, 5th edition [2]**
2.8.4.1 Piston rods of AISI4140 steel used in sour gas service have a entire through-hardness not exceeding Rockwell C22.	6.10.4.3 The base material of piston rods used in H_2S service shall be in accordance with NACE MR0175. see 6.15.1.11 6.15.1.11 All materials exposed to H_2S gas service as defined by NACE MR0175 shall be in accordance with the requirements of that standard. *Ferrous material not covered by NACE MR0175 shall not have a yield strength exceeding 620 N/mm^2 (90,000 psi) or a hardness exceeding Rockwell C 22.* 6.10.4.4 Tolerances for finishing rods shall be 12,5 µm (9.0005 inch) for roundness and 25µm (0,001 inch) for diametral variation over the length of rod. The surface finish in the packing areas for lubricated and non lubricated services shall be 0.15 µm to 0.4 (6µinch … 16 µm)µm. 6.10.4.5 Piston rods with threads shall be furnished with rolled threads having a polished thread relief area. … An increase in hardness around thread surface due to thread rolling is acceptable as long as the base hardness meets NACE requirements.

Table 4: Material of piston rods

The most important findings of the above tables are:

All piston rods, regardless of base material, shall be coated with wear and corrosion resistant material. Alternatively, an uncoated piston rod may be proposed when the expected life equals or exceeds that of a coated rod for the specified operating conditions.
Uncoated piston rods shall be surface hardened to a hardness of at least Rockwell C50 and shall be of material AISI 4120 or better.

Piston rods shall be continuously coated from the piston packing through the oil wiper travel areas.

Metal spray techniques requiring of the surface of the base metal are not recommended.
The use of an additional sub-coating under the main coating is not recommended.

All materials exposed to H_2S gas service shall be in accordance with the requirements of NACE MR0175 standard, with a yield strength not exceeding 620 N/mm^{2}or a hardness not exceeding Rockwell C 22.

The manufactured piston rods normally have a universal, high quality of finish. Consequently, a good corrosion protection is obtained with respect to SCC (Stress Corrosion Cracking) and the exposure to H_2S service (SSC - Sulphide Stress Cracking).

Piston rods with threads shall be furnished with rolled threads having a polished thread relief area. An increase in hardness due to thread rolling is acceptable with sour gas applications as long as the base hardness meets NACE MR0175 requirements.

1.3 Suitable materials for piston rods

The general requirements of piston rods are sufficient strength, elasticity and a wear resistant surface.

BORSIG ZM uses following materials:

Material no.	Description	US standard	Tensile strength [N/mm^2]	Effective range of gasket	Surface hardness	Medium	Pressure range [bar]	Min. suction temperature
1.4021	X20Cr13 +QT800	ASTM A182 AISI 420	min. 750	surface hardening with 0.2% content of C still possible	min. 52HRC	non corrosive and corrosive gases	up to 250	-25℃
1.4120	X20CrMo13 +QT750		min. 750	surface hardening with 0.2% content of C still possible	min. 52HRC	non corrosive and corrosive gases	up to 250	-25℃
1.4021	X20Cr13 +QT700	ASTM A182 AISI 420	Min. 700 ...795 hardness max.22 HRC	surface hardening with 0.2% content of C still possible	min. 52HRC	Sour gas	up to 250	-25℃
1.8550	34CrAlNi 7		min. 800	nitrogen hardening	min. 58HRC	non corrosive gases	up to 100	-10℃
1.4542	X5CrNiCuNb 16 4	ASTM A705	min. 800	coating required	1500 ... 2000 HV30	acid gas	no limit	
1.7220	34CrMo4 +QT			surface hardening	min. 52HRC	every, not corrosive	up to 100	-60℃
1.6582	34CrNiMo6 + QT			surface hardening	min. 52HRC	Every, not corrosive	up to 100	-100℃

Table 5: Materials of piston rods used by BZM

1.4 Basic calculation approach

The following loads have influences on the calculation of this component:

- for the connection between piston rod - piston
  - ➔ the gas power being effective on the piston (differential pressure x piston area)
  - ➔ the frictional force of the piston rings
  - ➔ the effective mass forces (piston mass x acceleration)
- for the connection between piston rod and crosshead
  - ➔ the gas power being effective on the piston
  - ➔ he frictional force of the piston rings
  - ➔ the effective mass forces (mass piston + rod x acceleration)

- The surface pressures occurring have to be evaluated also at calculation temperature.

The task is a classical bolted connection calculation at both connections
- crosshead – piston rod and
- piston rod – piston

Therefore, guideline VDI2230 „Bolt calculation", for instance, may be applied.

The dimensioning of the nominal diameter of the piston rod depends upon the necessary stiffness for a reliable operation of the seal elements – packings as well as all piston rings. Calculation of the safety against buckling, according to Euler, results in a safety factor higher than 8. This, if ever, is only useful for extremely long piston rods.

The maximum load of a piston rod in operation must never exceed 80 %.

1.5 Mechanical designs

1.5.1 The connection between crosshead and piston rod

According to Appendix G-6…G-8 of API 618, 5^{th} edition this connection is classified as follows:

- direct rod connection (with thread at piston rod)
- indirect rod connection (with thread at piston rod)
- indirect clamped rod connection (without thread at piston rod)

Pictures 2 and 3 show an indirect clamped rod connection. The piston clearance is adjusted by means of a thread.

The pressure load is directly transmitted via the junction surface of crosshead and piston rod. The tensile loading is transmitted via flange and bolts. The piston clearance is adjusted by means of ground washers. The assembly is realized by 4 hydraulic clamping devices.

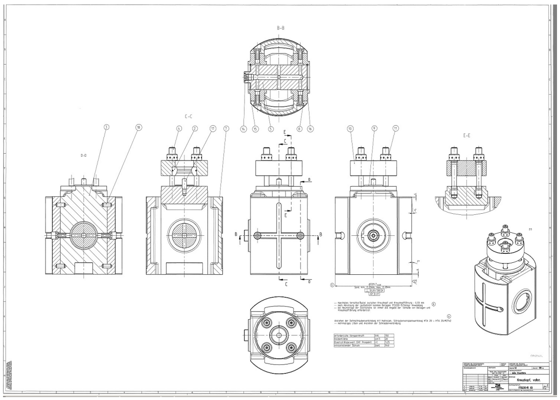

Picture 2: Drawing of crosshead component, indirect clamped, multi-bolt type

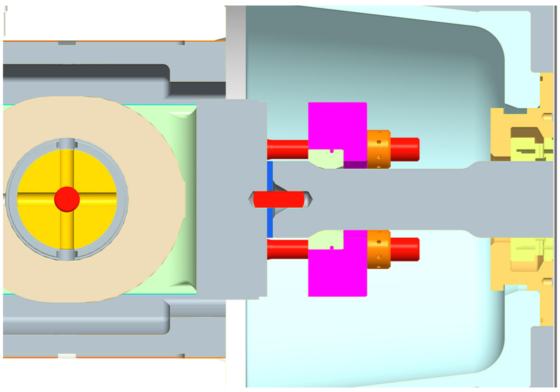

Picture 3: Crosshead, indirect clamped connection

This method is used with small compressors, in which the assembly of this connection may be realized by means of a torque wrench.

Pictures 4 and 5 show another example of an indirect clamped rod connection.

The assembly is realized by integrated clamping devices. The piston clearance is adjusted by means of a threaded ring.

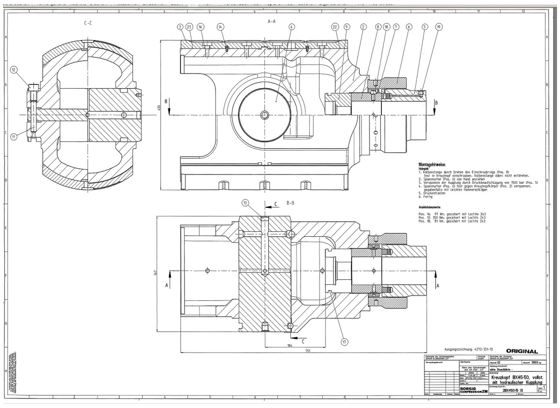

Picture 4:Drawing of crosshead, indirect clamped connection

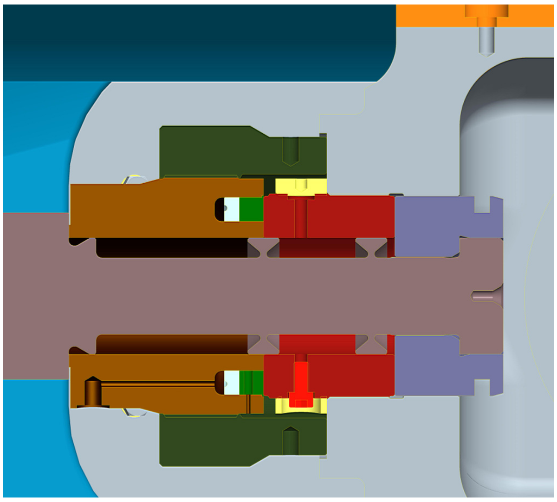

Picture 5: Crosshead

Picture 6 shows a direct clamped rod connection (year of manufacture 1959) with positive locking at the piston rod.

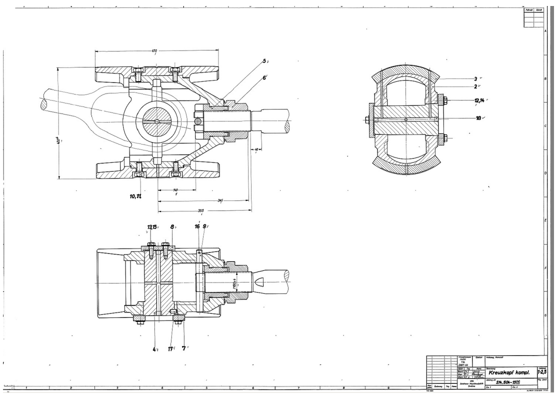

Picture 6: Crosshead assembly unit, direct clamped

1.5.2 The middle sector – scope for action of the packings

The necessary wear resistance of the piston rod may be reached by:

- surface hardening, resulting in a possible hardness of Rockwell C52,
- nitrogen hardening, resulting in a possible hardness of Rockwell C58…60,
- coating

Today the following two coating materials are mainly used for piston rods:

A.) Tungsten carbide (WC)
The chemical composition is 86 % tungsten carbide, 10 % cobalt and 4 % chrome

B.) Ceramic coating with chromic oxide
In this case the coating material consists of 99.9 % Cr_2O_3.
The following coating methods are most commonly used:
I.) High speed flame spraying (HVOF)
II.) Detonation coating
III.) Plasma metallizing coating

The costs may be roughly estimated as follows:
Ceramic coating is about 20 % more expensive than coating with tungsten carbide. Plasma coating is the cheapest coating method.

	Extract from the specification sheet of Würschem Oberflächentechnik GmbH **Tungsten carbide**	Extract from the specification sheet of Würschem Oberflächentechnik GmbH **Ceramic**
Coating material	WC Co Cr 86/10/4	Cr_2O_3 chromic oxide 99,9 % pure
Surface preparation	Blasting with high-grade corundum, without inclusion of ferritic particles	Blasting with high-grade corundum, without inclusion of ferritic particles
Coating method	High speed flame spraying	High speed flame spraying
Temperature of part	50 - 100 °C	50 - 100 °C
Coating hardness	approx. 1350 $HV_{0,3}$	approx. 1350 $HV_{0,3}$
Porosity attainable	< 1,0 % at optimum component geometry	< 1,0 % at optimum component geometry
Operation temperature	< 400 °C	< 250 °C
Quality of finish attainable	Ra 0,02 µm - 12 µm	Ra 0,03 µm - 10 µm
Bonding value	approx. 75 N/mm^2	approx. 55 N/mm^2

Table 6: Coating data

1.5.3 Connection between piston rod and piston

An often used method is the bracing of both components with a center-bolt connection (picture 7). In the following paragraph some solutions are presented.

With the first solution, which is certainly interesting, the piston rod is drilled and the assembly unit is connected with a tensioning bolt. This bolt is tightened into the crosshead and thus the piston rod and the piston are braced with a piston nut. The piston nut itself is fastened with a torque.
This solution is applicable to smaller dimensions.

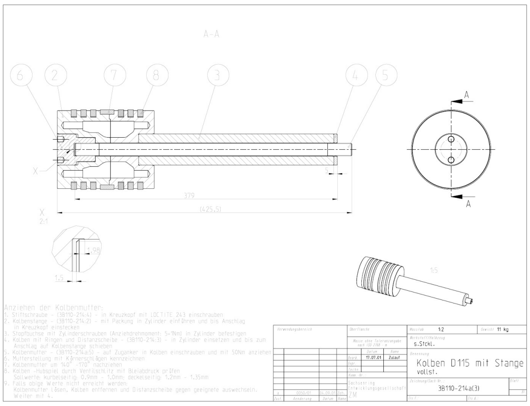

Picture 7: Drawing of center-bolt connection piston – piston rod

With the second simple solution (pictures 8 and 9) – in this case a piston rod with a diameter of 45 mm – the assembly moment is applied by a torque wrench. Taking into consideration the friction in the thread and on the supporting face of the nut, there is a smaller load factor at the connection. The piston nut itself is fastened twice by being driven home into a drill-hole in the piston. In this case a spanner space at the piston rod has to be provided for assembly. It is necessary with only one plain special tool.

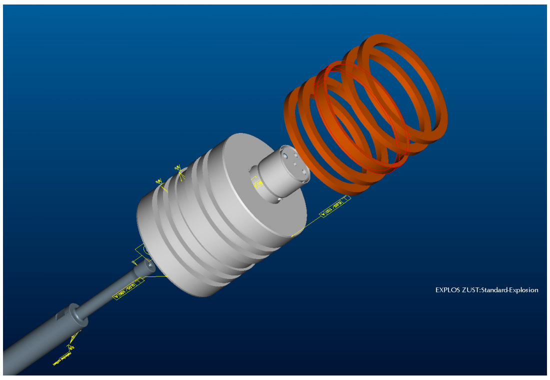

Picture 8: Piston and piston nut

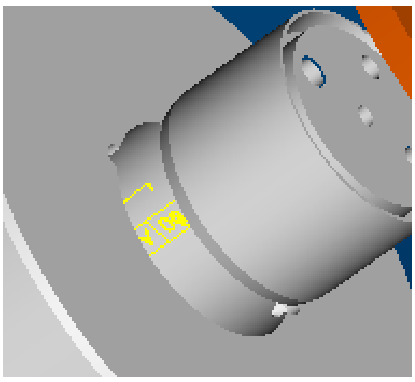

Picture 9: Piston nut

With the third solution (picture 10 – rod diameter 80 mm) the assembly moment is applied by a tensioning nut. In this case no spanner space at the piston rod has to be provided for assembly and the tensioning nut's mechanism of action regenerates low friction, which has to be taken into consideration for the calculation. This connection will therefore take a higher load. There is no need for special tools.

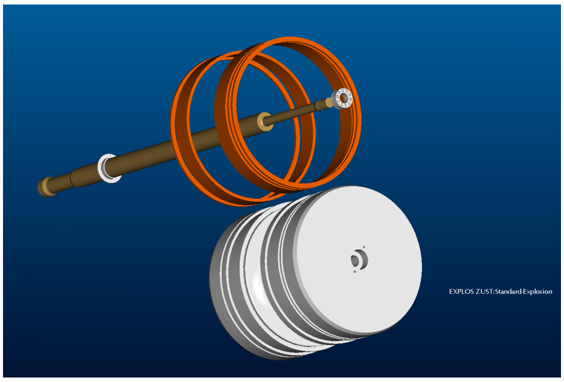

Picture 10: Piston nut

Further technical possibilities of bracing for big dimensions are as follows:

- Hydraulic method
  The advantages of this technique are a high load factor of the connection and high precision. Also in this case it is not necessary to take into consideration friction during the calculation.
  Special tools are needed.

- Thermic method
  Also in this case no friction has to be taken into consideration during the calculation. Special tools are needed.

Picture 11 demonstrates the principle of a compression joint.

This method may be used with big dimensions. In this special case as shown in picture 11 the cylinder diameter is 850 mm, the piston being of welded design, the piston rod diameter is 105 mm and the piston weight 552 kg. The positive locking metal sheets used (under the nuts) are not shown.

Taking into consideration the friction in the thread and on the supporting face of the nut, there is a smaller load factor. The use of special tools is not needed.

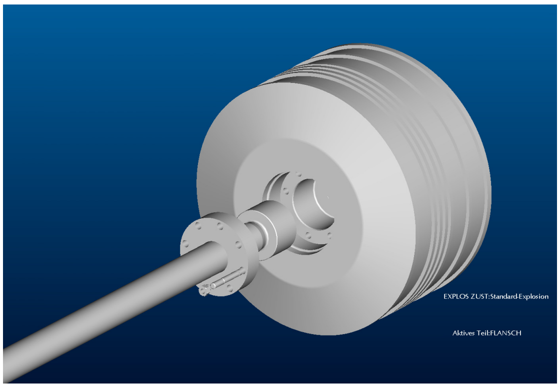

Picture 11: Compression joint

Picture 12 shows a design of former design engineers:
- including a lock against rotation of the piston rod at the crosshead and against rotation of the piston at the piston rod.
- the bracing of the piston is made by means of slugging (hammer) wrenches.

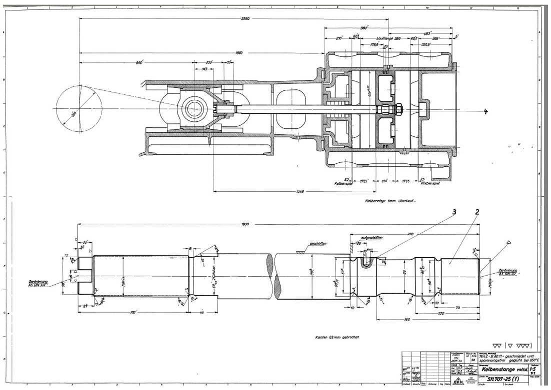

Picture 12: Assembly unit crosshead, rod, piston

1.6 Conclusion of part one

For the piston rod component propositions from API 618 have been summarized, changes pointed out in comparison with the 4^{th} edition and some technical design options presented without going too much into technical design details.

The most important and probably most difficult task is to find the right solution for each single case.

2 Valve fixing – valve cover and valve cage

Picture 13 shows a valve cover and a valve cage in front.

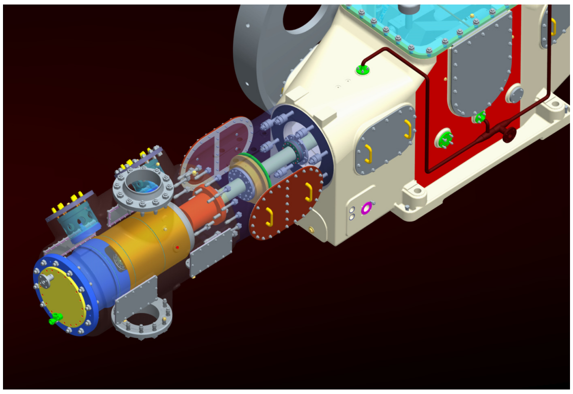

Picture 13: Assembly unit with valve cover and cage

2.1 Function and requirements

In every cylinder the compressor valves, responsible for gas control, has to stay reliably at the place of action and there must be easy access for required maintenance works.

In other words the valve must have a leakproof fit in the cylinder. The valve cover has the function of gasproofing to the outside and transferring emerging forces into the cylinder.

The functional characteristics for calculation - pressure, temperature and resistance – correspond with the data of the cylinder calculation.

The gas flows through the cross-section of the cage to the suction valve or away from the pressure valve outlet. The valve cage is subjected to compression stress.

Picture 14 shows a typical deformation of a valve cage under load. A rigid design is therefore necessary.

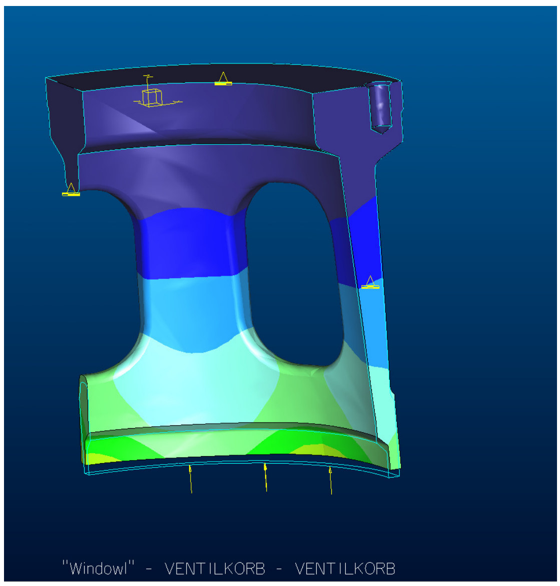

Picture 14: Valve cage – FEM results

2.2 Requirements according to API Standard 618

The few requirements to these components are listed in table 7.

Extract from API 618, 4th edition [1]	**Extract from API 618, 5th edition [2]**
2.6.2.7 Cylinder heads, stuffing boxes for pressure packing, clearance pockets, and valve covers shell be fastened with studs. …. Where captured o-ring valve covers are used, two extra long studs 180 degrees apart are to be provided for each cover to ensure the cover o-ring clears the cylinder valve port bore before the valve cover clears the stud. Extra long studs shall be capable of having a full-threaded nut when the o-ring is clear of cylinder valve-port sealing bore.	6.8.2.5 Where valve covers with radial captured o-rings are used … see 4th edition
2.6.2.8 Valve cage design shall be of the cylindrical type held in place by a circular contact cover. Center-bolt or other through-bolt designs shall not be furnished.	6.8.2.6 Valve cage designs shall be of the cylindrical type held in place by a circular contact cover. Center-bolt design shall not be furnished. Designs that utilize three or more through bolts acting on the circumference of the valve cage may be furnished with <u>purchaser approval</u>. If this design is furnished, the through bolts shall be self-retaining and shall be furnished with cap type nuts and gaskets to prevent gas leakage.
2.6.2.9 Valve port o-ring sealing surfaces shall not exceed an Ra of 1,8 µm (63 µinches). Valve ports using o-ring shall include an entering bevel for the o-ring.	6.8.2.7 The surface finish of valve port o-ring sealing surfaces shall not exceed an … Ra of 1,8 µm ... 6.8.2.8 Valve chamber and clearance pockets shall be designed to minimize trapping of liquid.

Table 7: Requirements to valve cover and cage

2.3 Suitable materials

Typical materials for these parts are grey cast iron, nodular cast iron and steel.

2.4 Basic calculation approach

The load to be calculated for the valve cage is composed of several parts.

One part of the effective load is the differential pressure on the closed compressor valve.
The differential pressure for the suction valve may be calculated as follows:

Discharge pressure in the working chamber of the cylinder minus the pressure in the gas passage of the suction side.

This differential pressure results in a pure pressure load for the outlet cage.

The differential pressure of the pressure valve may be derived from:

Suction pressure in the working chamber of the cylinder minus the pressure in the gas passage of the pressure side.

By way of calculation, the differential pressure does not result in a stress for the valve cage. The reaction force - caused by the gas flow or the change of gas direction - has to be taken into consideration in the calculation by means of allowances.

If, for example, a metallic flat gasket is used for sealing the valve seat, there has to be taken into consideration the required surface pressure at operating temperature.

The load to be calculated for the outlet top cover consists of the load just described and the outwards differential pressure via the component.

Thus the valve cover is loaded with a moment and a pressure.

2.5 Valve cage

This part represents the connection between valve top cover and the valve.

2.5.1 One-piece design

Picture 15 shows a one-piece design not yet machined.

The openings for the gas flow are cast and shall not be machined.

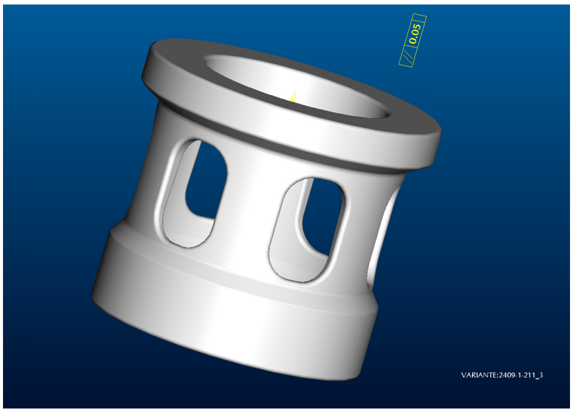

Picture 15: Casting valve cage

A one-piece already machined design is shown in pictures 16 and 17.

A cast bushing is used for semi-finished product. The openings for the gas flow can be designed according to the requirements.

This design is useful for small and medium-sized valves.

For dismantling two threads are provided on the top about 1mm clearance to the boring in the cylinder above (stain, contamination).

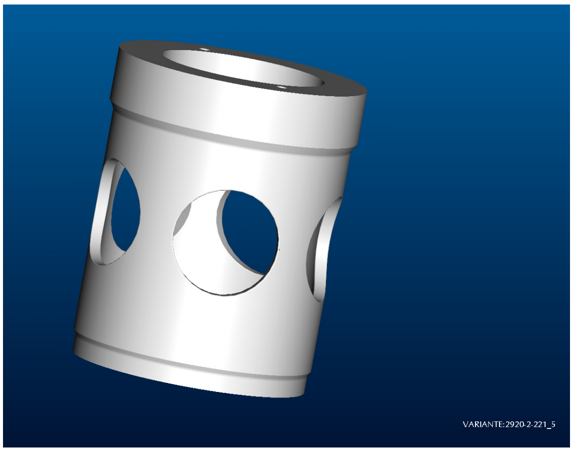

Picture 16: Valve cage – one-hole ring

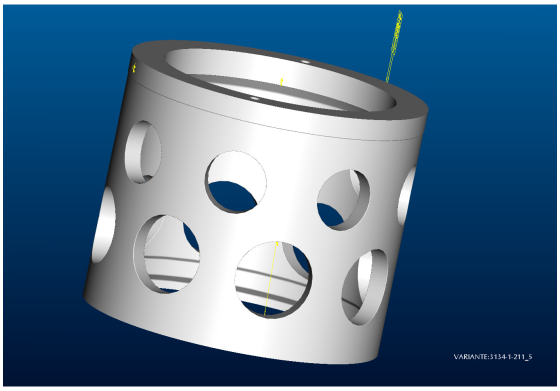

Picture 17: Valve cage – multi-hole ring

2.5.2 Complex fabricated cage

With a multiple-part design as shown in picture 18 large cross-sections are implementable.

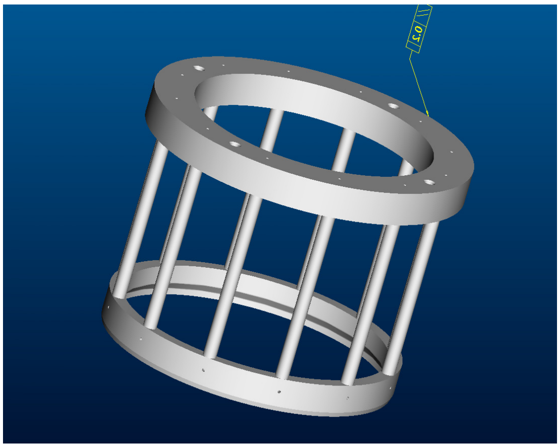

Picture 18: Fabricated cage

This design is used for large valves due to the low weights which are achievable.

2.6 Valve cover

2.6.1 Cover with pressure bolts

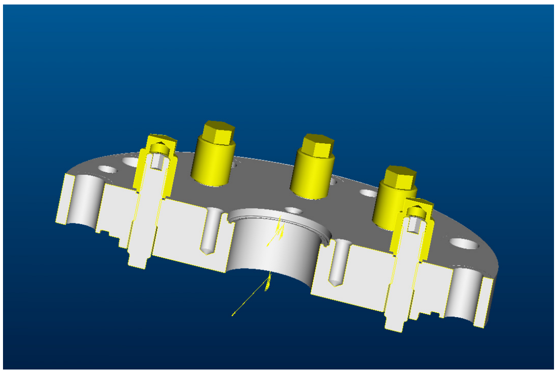

Picture 19: Valve cover assembly

Picture 19 demonstrates a suction valve cover with attachment for an actuator. The valve is fixed via the valve cage by the pressure bolts. The sealing is effected by an o-ring, which operates axially. No longer screws are required for assembly. Big dimensions will result in accordingly higher weights.
This is a common solution.

2.6.2 Valve cover without pressure screws

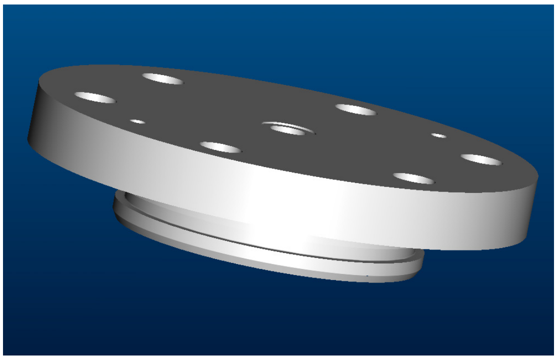

Picture 20: Valve cover without pressure bolts

The sealing is effected by means of a radially operating o-ring. In this case longer screws are needed for the assembly (o-ring). In addition, pressure test threadings and screws are required. The valve and its cage are stressed appropriately by pressure screws .

2.6.3 One-piece/ complex design

In this design (pictures 21 and 22) cage and cover are of the same body, cast or welded designs are possible. The sealing is effected by an o-ring.

It is a cost-effective option, however, there are limits of application with respect to pressure and weight.

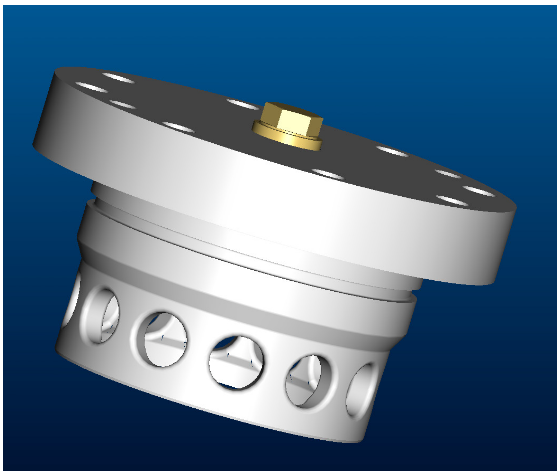

Picture 21: One-piece design – single-hole ring

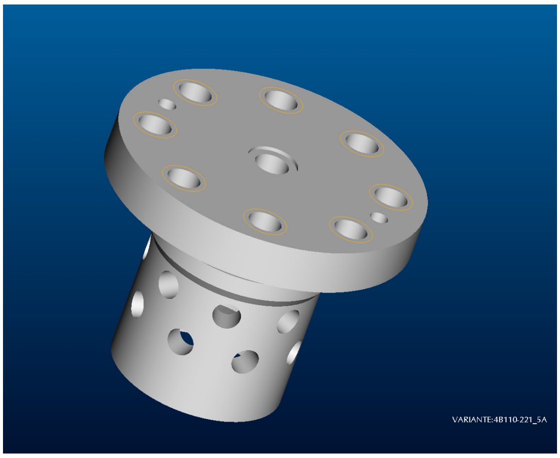

Picture 22: One-piece design – multi-hole ring

At BORSIG ZM this design is already used up to 275 bar with CNG compressors (pictures 23 and 24). Special attention has to be paid to prevent damage to the sealings during its depressurised assembly below the valve seat.

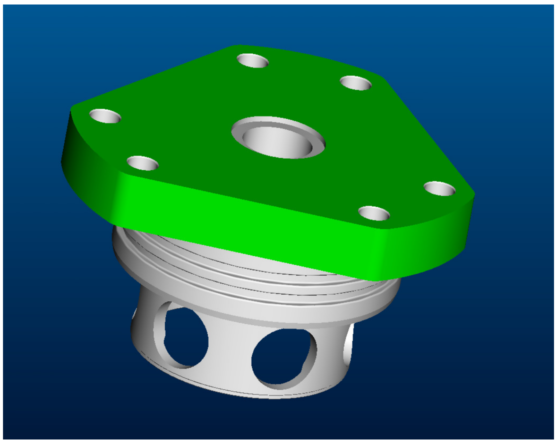

Picture 23: Reliable usage of this solution – CNG compressor, 1st stage up to 53bar

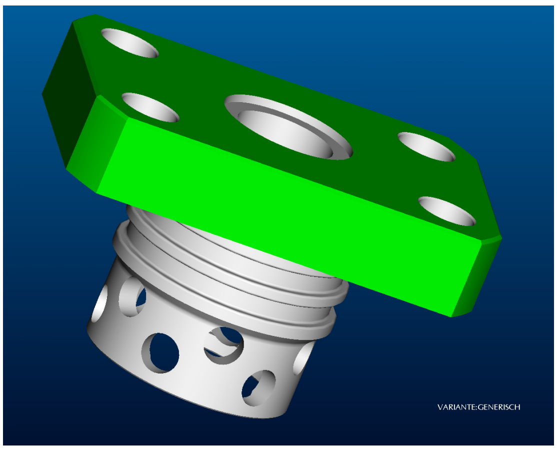

Picture 24: CNG compressor, 3rd stage 275bar

2.7 Conclusion of second part

We recommend application of the solutions presented, in particular with horizontal compressors according to table 8.

Design	Comments	Recommended application depending on valve weight
one-piece/ complex design	assembly together with valves installation device required	up to 15 kg including valve
valve cage one-piece design	fixing in cylinder during assembly necessary	up to 15kg
valve cage multiple-part design	fixing in cylinder during assembly necessary	from 15.1 kg

Table 8: Design solutions

For the determination of flow sections in the valve cage the following calculation approach is recommended:

➔ *Required flow section = min. 2.5 …3.5 x valve stroke cross-section*

➔ *the gap around the valve cage (formed by the cylinder wall and the outer diameter of the valve cage) has to amount to 25 mm as a minimum*

➔ Pressure limits for o-rings:
- up to 5 MPa without support ring
- up to 40 MPa with support ring
- up to 200 MPa with special support ring

➔ limits for hardness Shore A of o-rings
- up to 3.5 MPa 70...75
- up to 8.0 MPa 80... 85
- up from 8.1 MPa 90

In all these cases installation devices are required.
With the one-piece solution a connection is necessary (pin with threads) for the joint assembly of valve cage and valve.
With the two-piece design the valve cage has to be fixed in the cylinder by means of a pin or a tension spring.

There is a huge variety of designs for these two inconspicuous components. The task is to select the right solution for every particular application.

References

[1] API Standard 618, fourth edition, June 2005 Reciprocating Compressors for Petroleum, Chemical and Gas Industry Services

[2] API Standard 618, fifth edition, December 2007 Reciprocating Compressors for Petroleum, Chemical and Gas Industry Services

[3] M.I. Frenkel, „Kolbenverdichter - Theorie, Konstruktion und Projektierung“,VEB Verlag Technik Berlin

ATEX: from the perspective of a compressor manufacturer

by:

Krunoslav Hercigonja, Gerhard Braun
Technical department
Josef Mehrer GmbH & Co KG
Balingen
Germany
k.hercigonja@mehrer.de, g.braun@mehrer.de,

e.g. 6th Conference of the EFRC
October 28th / 29th, 2008, Dusseldorf

Abstract:

As long standing manufacturers of oil-free piston compressors for use in potentially explosive atmospheres and for hazardous gasses, such as natural gas, methane, fermentation gas, hydrogen, etc., we have become experts in this field. Problems related to ATEX often appear at the interface between the customer and sales person. They may be caused by communication issues or the superficial consideration of a both, customer specifications and technical details. Such problems could be easily avoided using a few principles. These can then be phrased into two main solvable queries, which could be discussed by the customer and the sales person.

Firstly, which classification applies to the installation site? Secondly, what is the exact chemical composition of the gas and what are its variables? Dealing with these queries will be the main concern of this presentation.

In addition, the relationship between the European ATEX Directive and the explosions directives in non-European countries will be considered. Particular focus will be placed on North America and China.

1 Introduction

Being manufacturers of „bare“ compressor blocks and complete compressor units, we are having the possibility to look at the implementation of Dirctive 94/9/EC [1] in practice from various points of view. Even before the introduction of Directive 94/9/EC [1] we built units according to „old Ex-regulations“ (ExVo, ElexV) for use in potentially explosive environments and, therefore, had the chance to sum-up our knowledge about explosion protection for many years. Today we can rely on broad knowledge of many years.

2 ATEX

2.1 History

The regulations are based on the European Community Foundation Contracts (Roman Contracts, 1957). These contracts stipulated in articles 100a and 118a, besides others, which common responsibilities had to be assumed by the European Community regarding safety of employees and environment protection, as well as harmonizing legal grounds for all members of the community. Upon signature of the Amsterdam Contracts in 1997, the renumbered version of the contract concerning the European Community and Contract about foundation of the European Community also became legally valid. The requirements originally listed in article 100a are since then found in article 95 (ATmosphère EXplosible 95), the requirements originally listed in article 118a are since then found in article 137 (ATmosphère EXplosible 137) and article 138.

2.2 More than just renaming

With introduction of ATEX 95 fundamental changes for manufacturers of equipments and protective systems resulted. Since July 1st, 2003 only equipments corresponding to these new regulations may be put into circulation. The former explosion protection applied to electrical equipments only. Upon introduction of the new regulations, non-electrical equipments and protective systems as well are concerned. Equipments and protective systems used in dusty environment have now been included as well. Furthermore, fundamental safety requirements for explosion-protected operational resources, a connection between ATEX-marking and CE-marking, as well as a quality assurance system, which is to be checked by defined parties, are now integrated into these new regulations, too.

Introduction of ATEX 137 is concerning plant operators. The aim for introduction of these new directive was improved protection of employees against risks in Ex-areas. The new directive is to be approached in the following only briefly.

Scope of the ATEX 137-regulations, which passed with Betriebssicherheitsverordnung (BetrSichV; Ordinance on Industrial Safety and Health) over to national law on 27.09.2002, is comprising – besides others – assessment of explosion risks, draw-up of an explosion protection document, classification of areas in which explosive atmosphere might arise, as well as the duty to coordinate all required tasks. The regulations are also giving minimum requirements for improvement of safety and health protection of employees who might be endangered by explosive atmospheres.

3 The Directive

3.1 ATEX 95

In Germany the European Directive 94/9/EC was transferred into national law by the Explosion Protection Decree (11.GPSGV, 12.12.1996). Already existing standards had been adopted or newly defined. Some harmonized standards important for compressor manufacturers are:

EN 1127-1 [2]

EN 13463-1 ff. [3]

EN 60079-0 ff. [4]

ATEX 95 is applied for equipments and protective systems, safety, control, and regulation devices used for safe operation of equipments and protective systems, as well as for components being built into equipments and protective systems. How is this to be interpreted, and how are the individual equipments, protective systems, and devices defined?

The regulation is defining ‘equipments’ [1] as "machines, apparatus, fixed or mobile devices, control components and instrumentation thereof and detection or prevention systems which, separately or jointly, are intended for the generation, transfer, storage, measurement, control and conversion of energy for the processing of material and which are capable of causing an explosion through their own potential sources of ignition.

‘Protective systems’ means design units which are intended to halt incipient explosions immediately and/or to limit the effective range of explosion flames and explosion pressures. Protective systems may be integrated into equipment or separately placed on the market for use as autonomous systems;

'Components' means any item essential to the safe functioning of equipment and protective systems but with no autonomous function.

What does this mean? Covered by ATEX are equipments, protective systems and components. A Component Assessment Procedure (Paragraph 3.5) for equipments, protective systems and components have to be done before putting in circulation in Europe. An ATEX-marking for each product has to be mounted. However a CE-marking can only be mounted on a self-actingly functioning machine, which can be used for conditioning energy. In cases of compressor manufacturers this means, that a compressor aggregate with electrical control box will get a CE-marking, because such a aggregate is a self-actingly functioning machine. More on this matter later.

3.1.1 Coverage of ATEX

ATEX is affecting all branches of industry. The ATEX-Directive is not applicable for the following special fields:-

- Medical equipments
- Equipments for explosives
- Personal protective systems
- Domestic areas
- Seagoing vessels
- Vehicles (except when used in an ex-area), and
- in military fields.

Further basic conditions for application range of ATEX are the ambient conditions. Even though ATEX is not defining them, values for the conditions can be gathered from the European Standards. For example EN 13463-1 for non-electrical equipments [3] is defining an "ambient temperature range from –20°C to +60°C" and an "ambient pressure range from 0.8 to 1.1 bar". Standard EN 60079-0 [4] for electrical apparatus is also defining the range of application of the standard as an „ambient temperature range from –20°C to 60°C", and an "ambient pressure range from 0.8 bar to 1.1 bar", and "ambient air having oxygen contents of 21% (V/V)". Consequently, the compression space in the compressor is exempted from ATEX, because the adiabatic temperatures during compression are often exceeding 60°C, and pressures usually are much higher than 1.1 bar.

3.1.2 Minimum requirements for an explosion

Besides the scope of application defined by ATEX, an explosion endangered area must be available, too. In case there is no explosion endangered area, ATEX does not apply. But: what does "explosion endangered area" mean?

Fig. 1:Explosion triangle with required explosion partners

Definition [5] states: „Area in which the atmosphere due to local and operational conditions can become explosive". As per definition [5] explosive atmosphere means "a mixture with air, under atmospheric conditions, of flammable substances in the form of gases, vapours, mists or dusts in which, after ignition has occurred, combustion spreads to the entire unburned mixture". Therefore, there are always three partners required to start an explosion. In case just one of the partners involved is removed there will be no explosion. That's the point where explosion protection starts.

In the following the explosion partners are listed together with possible protective measures:-

- *Ignition source* are avoided or the energy of the sparks is reduced to an nonhazardours level
- *Combustibles* are kept away from atmosphere, resp. the air-combustible-mixture is kept either too lean or too fat.
- Excluding *oxygen* can be done by inertising.

3.2 Correlation between category and zone

Depending on likelihood and extent of explosions, the two ATEX-guidelines are grouping differently.

German Ordinance on Industrial Safety and Health (BetrSichV) corresponds to ATEX 137, transferred into German Law. This ordinance is giving minimum requirements for operators/employers, who are putting working appliances at disposal of employees. Paragraph 3 of the BetrSichV [6] is laying down to „carry out a risk assessment". Same is comprising a "check of operational resources" concerning their "probability of ignition sources available", the "relative period of time of explosive atmosphere" and "the consequences expected in case of explosion" [6]. Based on this check, the workshop can be divided into so-called zones. These zones are graduated as per duration of explosive atmosphere available in the individual place. The explosion partners are as well differentiated. There are zone groupings for gases and for dusts. For gases there are zones 0, zone 1, and zone 2. Dusts are grouped into zone 20, zone 21, and zone 22. The relative periods of time of explosive atmospheres in zones 0 and 20, zones 1 and 21, resp. zones 2 and 22 are identical. Annex 3 of BetrSichV [6] is defining zone 0 as follows: "…it's place in which a hazardous explosive atmosphere consisting of a mixture with air of flammable substances in the form of gas, vapour or mist is present continuously or for long periods or frequently." Analogously zone 20 concerning combustible dusts is defined. Zone 1 is defined as a place, "in which a hazardous explosive atmosphere consisting of a mixture with air of flammable substances in the form of gas, vapour or mist is likely to occur in normal operation occasionally." Here as well, zone 21 is dealt with analogously. Finally zone 2, which is defined as a place, "in which a hazardous explosive atmosphere consisting of a mixture with air of flammable substances in the form of gas, vapour or mist is not likely to occur in normal operation but, if it does occur, will persist for a short period only." Analogously zone 22. When the operator during risk assessment is finding out that it cannot be excluded that dangerous explosive atmosphere can result in the process, he is obliged to make zone gradations. He must draw-up an explosion protection document (paragraph 6 [6]), where – besides others - he has to document the areas with relating zones and explosion risks, as well as the measures undertaken to prevent explosive atmospheres.

Since the directive took into account on national level into a general law – a law for non-electrical equipments and a law for electrical equipments – special standards according to needed application can be referred to. Unnecessary to say that the minimum requirements of the directive are contained in all laws. For manufacturers ATEX 95 is stipulating that equipments to be installed in explosion endangered areas are to be grouped into categories from 1 to 3, resp. groups I and II. Group I is relating to equipments used in underground mining. For these equipments the risk of explosion is usually originating from methane-air-mixtures. Equipments of group II can be used in all other ranges. In the following we are discussing equipments not being used in underground mining only, thus such falling into group II.

The equipment's categories are indicating the safety degree of a equipment regarding it's construction. Thereby the operator has to operate the equipment within the range stipulated by the manufacturer. Similar to definition of zones, with increasing category number the safety degree of categories is decreasing. Category 1-equipment is "intended for use in areas in which explosive atmospheres caused by mixtures of air and gases, vapours or mists or by air/dust mixtures are present continuously, for long periods or frequently. Equipment in this category must ensure the requisite level of protection, even in the event of rare incidents relating to equipment, and is characterized by means of protection" "either, in the event of failure of one means of protection, at least an independent second means provides the requisite level of protection, or the requisite level of protection is assured in the event of two faults occurring independently of each other" [1]. This means double protection in case of fault resp. no risk of explosion in case of two faults, independent from each other, at the equipments – very high safety degree. Category 2-equipment "is intended for use in areas in which explosive atmospheres caused by gases, vapours, mists or air/dust mixtures are likely to occur. The means of protection relating to equipment in this category ensure the requisite level of protection, even in the event of frequently occurring disturbances or equipment faults which normally have to be taken into account" [1]. This means simple protection in case of fault, resp. that faults may not result in explosion. Category 3-equipment "is intended for use in areas in which explosive atmospheres caused by gases, vapours, mists, or air/dust mixtures are unlikely to occur or, if they do occur, are likely to do so only infrequently and for a short period only. Equipment in this category ensures the requisite level of protection during normal operation" [1]. This means that any such equipment is safely running in normal operation only and will not cause any explosion, however, in case of fault ignition of an explosive atmosphere can result.

Zone grouping as well as category grouping is divided into three sub-groups. The individual categories are reflecting the requirements of the individual zones. In zone 0 equipments of category 1 are to be used only, in zone 1 equipments of categories 2 or 1, and in zone 2 only equipments of categories 3, 2, or 1.

Zone	Corresponding instrument category
0	1
1	2
2	3

Table 1: Relation of the individual explosion zones to the relating equipment categories

For manufacturers indication of the zone is a very important customer parameter. By this parameter it is decided at the manufacturer, whether the unit is to be designed in category 1, 2, or 3.

Since we cannot cover the conformity assessment procedure required for zone 0, we cannot produce compressors conforming to zone 0. More to this matter later.

In case the unit is designed for installation in zone 1, an increased number of monitoring instruments, controls and switches might be necessary, contrary to installations in zone 2. An risk assessment of ignition is additionally to be made for units as per ATEX.

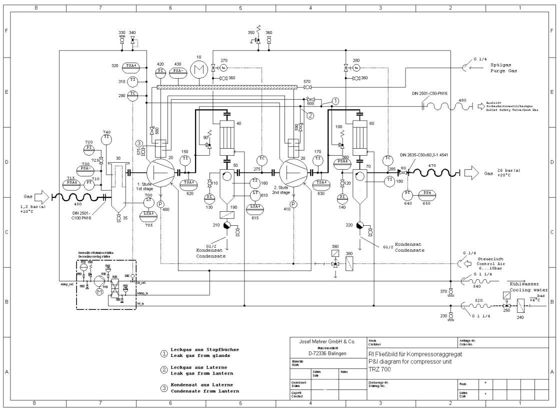

fig. 2: P&ID for an aggregate as per category 2, with many process monitoring devices

Furthermore, for units as per category 2 all technical documentation must be stored for 10 years at a notified body. These documents are:

- Operating and installation instructions, incl. dimensional drawing and P&ID
- All necessary certificates
- Risk assessment as per EN 1050 resp. EN 14121-1 [8] and EN 12100-1 [9], and risk assessment of ignition as per EN 13463-1 [3]
- Copy of conformity declaration
- Calculation sheets resp. design forms, indicating the max. adiabatic compression temperature
- Test report of compressor

Depending on the permissible surface temperatures additional temperature controls have to be integrated to the unit's control. Let's therefore have a closer look at the temperatures and relating conditions of units.

3.3 Temperature classes

Due to differing ignition temperatures of gas-air-mixtures, ATEX is describing different temperature ranges. The temperature ranges are graded into different temperature classes, from T1 up to T6. The temperature ranges are indicating the max. admissible surface temperature allowed for the unit. This temperature depends on the gas handled, and is to be indicated by the operator. For units of category 1 or 2, chapter 6.4 of EN 1127-1 [2] is stipulating the max. surface temperature to be 20% less than the max. admissible temperature of the temperature class applicable.

Temperature class	max. Surface Temperature	80% of max. admissible temperature
T1	450°C	360°C
T2	300°C	240°C
T3	200°C	160°C
T4	135°C	108°C
T5	100°C	80°C
T6	85°C	68°C

Table 2: Temperature classes with relating max. surface temperatures and corresponding 80%-temperatures

3.4 Marking

Contrary to CE-marking, which is to be marked on equipments and protective systems only, ATEX-marking is coercively necessary prior to putting equipments, protective systems, and components into circulation.

fig. 3: Manufacturer's name plate with separate plate for ATEX-marking

As generally applicable for marking purposes, name and address of manufacturer, type name, serial number and year of construction is shown. In the Ex-part of the tag – in this case a separate tag – next to the “epsilon kappa” in hexagon equipment group, category, and type of atmosphere must be shown in this sequence. The second part of the tag is showing kind of ignition protection, explosion group, and temperature class of the equipment, component, or of protective system.

Classification of the ATEX-plate shown in fig. 3 is as follows:

II	Equipment group 2, no mining
3	Equipment category 3, suitable for zone 2
G	for gases
EEx	ATEX-regulations are applied
c	Kind of ignition protection c „constructional safety“
II	Explosion group 2
T3	Temperature class T3, max. admitted surface temperature <200°C

3.5 Conformity Assessment Procedure

As already mentioned in chapter 3.2, Mehrer can produce units for installation in zones 2 and 1 only. Besides others, this depends on the conformity assessment procedure. Depending on future operation, directive 94/9/EG is describing in it’s annex, what kind of conformity procedure the manufacturer of an equipment, of a component, or of a safety device will have to apply. Generally, this procedure is always composed of assessment of construction and assurance of production quality.

If, for example, an equipment is to be installed in zone 0, an EC-Type Examination as per annex III [1] must be carried out. Having passed this Type Examination successfully, the manufacturer will receive a Type Examination Certificate. In order to assure that all equipments are fulfilling the same requirement than the certified equipment, a certified quality assurance system is to be installed, which is monitoring production, final inspection, and check of the equipment as per annex IV [1] and that is to be controlled by an notified body. Finally, the manufacturer has to carry out tests of his products as described in the EC-Type Examination Certificate, fulfilling the relevant directives; refer to annex V [1]. Such a conformity evaluation procedure, however, is only making sense for serial products. In case a manufacturer is producing only small batches or even individual pieces, he can have an individual test be carried out by a notified body, as per annex IX [1]. Both procedures are quite complex and expensive.

The evaluation procedure for equipments, components, and protective systems of categories 2 and 3 is much less complex and less expensive. For both the procedure of „internal control of production “ (annex VIII [1]) can be used. For this procedure the manufacturer has to file the documents listed in chapter 3.2 for at least 10 years. He furthermore has to take measures to assure the production procedure for matching the filed documents and the applicable requirements of the directive. For category 3-equipments the manufacturer can file the documents himself for a period of 10 years. For category 2-equipments all the technical documents have to be filed at a notified body. Instead of both these categories the manufacturer can apply for individual test as per annex IX [1].


JOSEF MEHRER GMBH & CO KG
MASCHINENFABRIK

Mehrer
KOMPRESSOREN

Declaration of Conformity
acc. to
Declaration 94/9/EC
(Explosion Protection Directive)

In accordance with EC-Directive 94/9/EG of 23.03.1994, together with legal regulations enacted for their application, the manufacturer:

Josef Mehrer GmbH & Co KG
Rosenfelder Str. 35
D – 72336 Balingen

declares, that the machine

Order No.

Compressor – Unit / - Plant Type

Compressor Type

Compressor No.

in design as supplied by us is fulfilling the basic safety and health requirements laid down in Directive 94/97EG for instruments and protective systems for use in explosion endangered areas as determined, and that same is complying to the following harmonized standards:

EN 13463-1
pr EN 13463-5

The machine can be used according to the following designation:

CE Ex II 3G
EEx c II T3

Balingen,

Josef Mehrer GmbH & Co KG
Maschinenfabrik

Jörg Peter Mehrer, Managing Director

JOSEF MEHRER GMBH&CO KG
Rosenfelder Str. 35
D - 72336 Balingen

Telefon (++49 - 07433) 2605-0
Telefax (++49 - 07433) 2605-41
WWW.Mehrer.de

CE Ex - II 3G EEx c II T3 . 2008 en.doc

fig. 4: Presentation of a Conformity Declaration for a compressor aggregate, category 3

All conformity assessment procedures have in common, in the end the manufacturer of an equipment, component, or protection system is issuing an EC-Conformity Declaration. The CE-marking is fixed to an equipment and to protection systems; components must not get a CE-marking.

4 Order procedure

Following we are describing the order procedure, from customer inquiry up to first on-site service from manufacturer's point of view. The individual stations and possibly upcoming problems as well as possible solutions are described.

4.1 Elaboration of offer

Even at planning stage the customer should save money. In most cases of dangerous, explosive atmospheres, zone 2 will be applicable. Upon placing an order for a compressor for zone 1, the operator should carefully check for correct grading of zone, and whether the installation site of the compressor might not be better at another location: a compressor for zone 2 is just more favourable than for zone 1. It is, however, up to the operator, to stipulate the zones in his company and for installation site.

The compressor manufacturer is manufacturing the compressor / the aggregate according to the zone indicated by the customer. Additionally to information regarding zone, the manufacturer is requiring some more project relating information. The more and the more detailed these data are, the more quickly and smooth the order process will be. Required data are:

- Ex-zone at installation site
- Type of gas and composition of same (traces of other components, in case these are know; most important in case of traces of H_2S, SO_2, NH_3, NO_x, HCl, Cl_2….)
- State variables of gas (temperature, pressure, rel. humidity)
- Ambient conditions (installation in production hall or outdoors; min./max. ambient temperatures to be expected)
- For water-cooled aggregates the quality, temperature, and pressure of the water will be decisive
- Peculiarities of the cooling water, i.e. radio-active, pH-value…..
- Control gas connection available? If so: pressure range
- Purge gas connection available? If so: pressure range
- Flow rate / Nm^3/h

Based on these data, the sales department can elaborate an offer. When the customer confirms the offer, a risk assessment as per Preliminary Hazard Analysis (pha-method) is made for the order – in our case by the Technical Department - considering EN 1050 [7], in future EN 14121-1 [8] and EN 12100-1 [9].

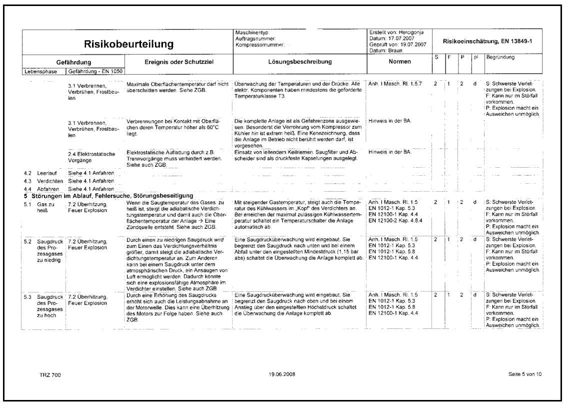

Risikobeurteilung

Maschinentyp:
Auftragsnummer:
Kompressornummer:

Erstellt von: Hercigonja
Datum: 17.07.2007
Geprüft von: 19.07.2007
Datum: Braun

Risikoeinschätzung, EN 13849-1

Gefährdung: Lebensphase	Gefährdung - EN 1050	Ereignis oder Schutzziel	Lösungsbeschreibung	Normen	S	F	P	pl	Begründung
	3.1 Verbrennen, Verbrühen, Frostbeulen	Maximale Oberflächentemperatur darf nicht überschritten werden. Siehe ZGB.	Überwachung der Temperaturen und der Drücke. Alle elektr. Komponenten haben mindestens die geforderte Temperaturklasse T3.	Anh. I Masch. Rl. 1.5.7	2	1	2	d	S: Schwerste Verletzungen bei Explosion. F: Kann nur im Störfall vorkommen. P: Explosion macht ein Ausweichen unmöglich.
	3.1 Verbrennen, Verbrühen, Frostbeulen	Verbrennungen bei Kontakt mit Oberflächen deren Temperatur höher als 60°C liegt.	Die komplette Anlage ist als Gefahrenzone ausgewiesen. Besonderst die Verrohrung vom Kompressor zum Kühler hin ist extrem heiß. Eine Kennzeichnung, dass die Anlage im Betrieb nicht berührt werden darf, ist vorgesehen.	Hinweis in der BA.					
	2.4 Elektrostatische Vorgänge	Elektrostatische Aufladung durch z.B. Trennvorgänge muss verhindert werden. Siehe auch ZGB.	Einsatz von leitendem Keilriemen. Saugfilter und Abscheider sind als druckfeste Kapselungen ausgelegt.	Hinweis in der BA.					
4.2 Leerlauf	Siehe 4.1 Anfahren								
4.3 Verdichten	Siehe 4.1 Anfahren								
4.4 Abfahren	Siehe 4.1 Anfahren								
5 Störungen im Ablauf, Fehlersuche, Störungsbeseitigung									
5.1 Gas zu heiß	7.2 Überhitzung, Feuer Explosion	Wenn die Saugtemperatur des Gases zu heiß ist, steigt die adiabatische Verdichtungstemperatur und damit auch die Oberflächentemperatur der Anlage → Eine Zündquelle entsteht. Siehe auch ZGB.	Mit steigender Gastemperatur, steigt auch die Temperatur des Kühlwassers im „Kopf" des Verdichters an. Bei erreichen der maximal zulässigen Kühlwassertemperatur schaltet ein Temperaturschalter die Anlage automatisch ab.	Anh. I Masch. Rl. 1.5 EN 1012-1 Kap. 5.3 EN 12100-1 Kap. 4.4 EN 12100-2 Kap. 4.8.4	2	1	2	d	S: Schwerste Verletzungen bei Explosion. F: Kann nur im Störfall vorkommen. P: Explosion macht ein Ausweichen unmöglich.
5.2 Saugdruck des Prozessgases zu niedrig	7.2 Überhitzung, Feuer Explosion	Durch einen zu niedrigen Saugdruck wird zum Einen das Verdichtungsverhältnis größer, damit steigt die adiabatische Verdichtungstemperatur an. Zum Anderen kann bei einem Saugdruck unter dem atmosphärischen Druck, ein Ansaugen von Luft ermöglicht werden. Dadurch könnte sich eine explosionsfähige Atmosphäre im Verdichter einstellen. Siehe auch ZGB.	Eine Saugdrucküberwachung wird eingebaut. Sie begrenzt den Saugdruck nach unten und bei einem Abfall unter den eingestellten Mindestdruck (1,15 bar abs) schaltet die Überwachung die Anlage komplett ab.	Anh. I Masch. Rl. 1.5 EN 1012-1 Kap. 5.3 EN 1012-1 Kap. 5.8 EN 12100-1 Kap. 4.4	2	1	2	d	S: Schwerste Verletzungen bei Explosion. F: Kann nur im Störfall vorkommen. P: Explosion macht ein Ausweichen unmöglich.
5.3 Saugdruck des Prozessgases zu hoch	7.2 Überhitzung, Feuer Explosion	Durch eine Erhöhung des Saugdrucks erhöht sich auch die Leistungsabnahme an der Motorwelle. Dies kann eine Überhitzung des Motors zur Folge haben. Siehe auch ZGB.	Eine Saugdrucküberwachung wird eingebaut. Sie begrenzt den Saugdruck nach oben und bei einem Anstieg über den eingestellten Höchstdruck schaltet die Überwachung die Anlage komplett ab.	Anh. I Masch. Rl. 1.5 EN 1012-1 Kap. 5.3 EN 1012-1 Kap. 5.8 EN 12100-1 Kap. 4.4	2	1	2	d	S: Schwerste Verletzungen bei Explosion. F: Kann nur im Störfall vorkommen. P: Explosion macht ein Ausweichen unmöglich.

TRZ 700 19.06.2008 Seite 5 von 10

fig. 5: Example page of a risk assessment as per PHA-method, assessing ‚pl' as per EN 13489-1

Risk assessment is done as per EN 13489-1 [3]. As a result of the assessment a performance level (pl) can be defined. This 'pl' is rendering information on reliability of used resp. required building components. Besides 'pl' there are other reliability parameters, like for example SIL (Safety Integrity Level as per EN 62061) or the former StK (Control category as per EN 954-1). A comparison of parameters is partially possible, and can be gathered from table 3.

pl EN 13849-1	SIL EN 62061	StK EN 954-1	Possibility of hazardous malfunction per hour
a	AM	B	$> 10^{-5}$ bis $> 10^{-4}$
b	1	1	$> 3 \times 10^{-6}$ bis $> 10^{-5}$
c		2	$> 10^{-6}$ bis $> 3 \times 10^{-6}$
d	2	3	$> 10^{-7}$ bis $> 10^{-6}$
e	3	4	$> 10^{-8}$ bis $> 10^{-7}$

Table 3: Comparison of reliability parameters pl, SIL, and StK with their relating malfunction possibility

Besides risk assessment an evaluation of ignition risk must be made for units in explosion endangered areas. Same is done as per EN 13463-1 [3] and is assessing the frequency of the individual ignition risks, possible to arise during operation. For every ignition risk, a protective measure must be taken care for. Afterwards, the frequency must be assessed once more, considering the protective measures.

	Zündgefahr		Bewertung der Häufigkeit des Auftretens *ohne* zusätzliche Schutzmaßnahmen					Angewandte Schutzmaßnahme			Häufigkeit des Auftretens *mit* zusätzlichen Schutzmaßnahmen					
lfd. Nr.	Potentielle Zündquelle	Ursache/Beschreibung (Unter welchen Umständen tritt die Zündgefahr auf?)	a im Normalbetrieb	b bei zu erwartender Störung	c bei seltener Störung	d nicht zu berücksichtigen	Begründung der Bewertung	Beschreibung der Schutzmaßnahme	Grundlage (Normen, technische Regeln, experimentelle Ergebnisse)	Nachweis	a im Normalbetrieb	b bei zu erwartender Störung	c bei seltener Störung	d nicht zu berücksichtigen	e Gerätekat. f. diese Zündq.	f notwendige Einschränkungen
9	Adiabatische Kompression	Durch das Verdichten des Gases im Verdichtungsraum steigt die Temperatur des Gases auf die adiabatische Verdichtungstemperatur. Bei überschreiten der zulässigen maximalen Oberflächentemperatur kann dadurch eine explosionsfähige Atmosphäre gezündet werden.	x				Der Verdichtungsprozess ist adiabat!	Eine Temperaturüberwachung des Prozessgases nach der ersten oder zweiten Verdichtungsstufe ist vorgesehen. Bei zu hohen Temperaturen schaltet die Überwachung die Anlage automatisch ab. Eine Temperaturüberwachung des Prozessgases ist bauseits vom Betreiber vorzusehen.	EN 13463-6	Baumusterprüfbescheinigung für die Überwachung.			x		2	
		Durch sinkenden Saugdruck vergrößert sich das Verdichtungsverhältnis. Mit steigendem Verhältnis steigt auch die adiabatische Verdichtungstemperatur an.		x			Schwankungen im Saugdruck sind anzunehmen.	Eine Saugdrucküberwachung schaltet bei abfallendem Saugdruck die komplette Anlage automatisch ab.	EN 13463-6	Baumusterprüfbescheinigung für die Überwachung.			x		2	

fig. 6: Example page risk assessment of ignition as per EN 13463-1

In case the new assessment is not within the equipment category intended, restrictions for use have to be stipulated. Prior to risk assessment of ignition, the compressor has to be dimensioned. The compressor's RPM, motor capacity, adiabatic compression temperature, and – for water cooled compressors – the cooling water quantity has partially to be considered for risk assessment of ignition.

After final risk assessment of ignition and risk assessment it might result that the control devices originally offered will not be sufficient, or that materials for gaskets, piston rings, gland, etc. will not be suitable for the order. Accordingly, the customer will receive a revised order confirmation.

4.2 Technical processing

Based on the results of risk assessment and risk assessment of ignition a P&ID and equipments list is drawn-up. Normally, same is sent to the customer for approval. At this stage, after checking by customer, amendments are often requested by the customer, which could have been avoided at earlier project stage, checking the specification more carefully. The new requirements will have to be integrated and a revised order confirmation is drawn-up.

After customer's approval of the P&ID, a dimensional drawing, showing all connections, is made. According to this drawing the aggregate is manufactured and built-up. The customer as well will receive this dimensional drawing. At this stage, customer amendments might again come up, i.e. when connections for media cannot be fitted regardless of the installation site, manometer panel is showing wrong direction, etc., restrictions which had not been given right in advance.

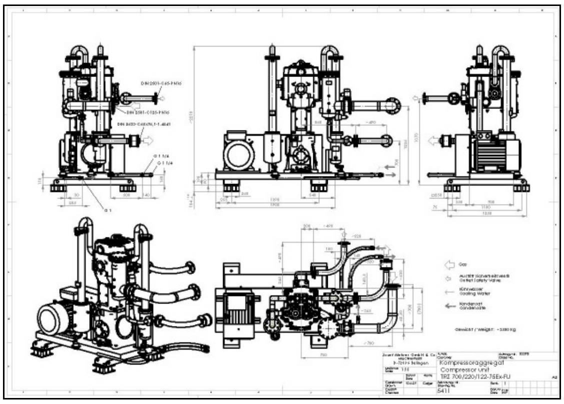

fig. 7: Dimensional drawing for a TRZ 700-aggregate for biogas compression

The project is then passed on to mechanical production, where parts are turned, milled, smoothed, and honed. Simultaneously orders for sub-suppliers parts are placed. After mechanical production pressure-bearing parts will be pressure tested with water. Thereafter the aggregate can be built-up. Electrical components to be used will be selected according to category and temperature class. Mostly components of ignition type "d", "e", "i", and "a" are used, resp. temperature class T4 or better, whereas ignition type "i" is not always accepted beyond Germany.

4.3 Documentation

The documentation is lodging all type examination certificates and conformity declarations for parts built-in, and is sent to the customer together with the operating instructions. The operating instructions are supplemented by several ATEX-notices. For combustible gases, for example, the compression chamber has to be purged by inert gas prior to taking into operation. Precautions for protection against static loading have to be undertaken. The compressor is to be operated by specially trained staff only. Service information, as well, have to be supplemented, i.e. spark-free tools only are to be used in some cases, or for combustible gases special precautions have to be undertaken avoiding process gas to catch fire upon opening of compressor. All the above is to be made by the documentation department, and means additional labour time and thus resulting higher costs.

4.4 Service

For service (maintenance and repair) of machines installed in explosion endangered areas special precautions has to be taken place. In case service is done by our own staff, our field engineers will have to know in what kind of environment the machine is installed, i.e.: is the machine installed in an environment asking for spark-free tools? In any such explosion endangered areas, they necessarily need to get a release note confirming that there will not be any danger for a certain period of time to service the machine. Inert gas has to be available resp. has to be taken along by our staff, to purge the unit prior to and after service.

In case service is done by operator's staff, these have to adhere to the above as well.

4.5 Summary

ATEX-units always mean extra expenditure. Each section/ department such a project is passing through will have to care for special ATEX-requirements, which are protracting the project and becoming more expensive. However, already at the start of a project later delays can be reduced or even completely avoided by good preliminary work (correct zone grading, exact information on process gas, states of the gas, ambient conditions, cooling water requirements, etc.).

Nevertheless, there will always be extra expenditure even for machines not installed in explosion endangered areas. This is resulting from increased number of controls depending on zone, use of special gas glands, special materials for piston rings and guide rings, pressure tests for pipelines to be carried out, etc. For documentation ATEX-units as well always means extra expenditure.

5 Comparison of the different standards for units installed in explosion endangered areas

ATEX is obliging for the European countries. Looking beyond Europe, there are regulations for units installed in explosion endangered areas, too. In the following we are briefly comparing the European ATEX with those explosion protection regulations of North America and China.

5.1 North America

In North America explosion protection regulations are applicable for electrical components only. In Canada these regulations are laid down in section 18, annex J of the Canadian Electrical Code (CEC) [10], in the USA in section 500 [11] and 505 [11] of the National Electrical Code (NEC). Depending on substance, there are three classes:

- Class I for gases, steams, or mists
- Class II for dusts
- Class III for fibres and fluffs

Depending on frequency of occurrence, there is a split-up into two Divisions:

- Division 1 for permanent or occasional endangering during normal operation
- Division 2 for unfrequent or no endangering during normal operation.

Furthermore, gases and dusts are divided into groups:

- Class I in A, B, C, D → whereas A is the most dangerous gas group
- Class II in E, F, G → whereas E is the most dangerous dust group.

For the temperature classes there are also some differences. In North America different limit temperatures are indicated depending on substance. For example besides temperature class T2, there are sub-divisions T2A, T2B, T2C, and T2D. The main grading, however, is identical to those defined by ATEX (T1 bis T6).

Besides the classical classification, NEC 505-7 [11] and CEC 18-006 [10] are defining classification for gases identical to ATEX, meaning 3 zones, 6 temperature classes, and 3 explosion groups.

5.2 China

Being member of the IEC (International Electrotechnical Commission), China is endeavouring to harmonize their national standards GB 3836 ff. [12] to those of the corresponding IEC-Standards. Even though this process is not yet finalized, it is said to be continued. In China there are explosion protection standards for electrical components only, like in North America.

In order to enter into the Chinese market, electrical apparatus need to be admitted by the national testing and certification society NEPSI (National Supervision and Inspection Centre for Explosion Protection and Safety of Instrumentation).

In Germany you can apply for admittance at the PTB (Physikalisch-Technische Bundesanstalt). PTB is having an agreement with SIPAI (Shanghai Institute of Process Automation Instrumentation) for mutual acceptance of tests and admittances, and since NEPSI is integrated to SIPAI, it will usually be sufficient to submit an EC-Type Examine Certificate from PTB and a complete set of documentation (description, drawings, data sheets) to receive the admittance for China.

References:

[1] Directive 94/9/EC of the European parliament and the council of 23 March 1994 on the approximation of the laws of the Member States concerning equipment and protective systems intended for use in potentially explosive atmospheres

[2] EN 1127-1 Explosive atmospheres - Explosion prevention and protection - Part 1: Basic concepts and methodology

[3] EN 13463-1 Non-electrical equipment for potentially explosive atmospheres - Part 1: Basic method and requirements

[4] EN 60079-0 Electrical apparatus for explosive gas atmospheres - Part 0: General requirements

[5] 11.GPSGV Elfte Verordnung zum Geräte- und Produktsicherheitsgesetz

[6] Betriebssicherheitsverordnung - Ordinance on Industrial Safety and Health (BetrSichV) Ordinance concerning the protection of safety and health in the provision of work equipment and its use at work, concerning safety when operating installations subject to monitoring and concerning the organization of industrial safety and health at work

[7] EN 1050 Safety of machinery - Risk assessment - Part 1: Principles (replaced by EN 14121-1)

[8] EN 14121-1 Safety of machinery - Risk assessment - Part 1: Principles

[9] EN 12100-1 Safety of machinery - Basic concepts, general principles for design - Part 1: Basic terminology, methodology

[10] 1998 Canadian Electrical Code, 18. redaction, Canadian Standards Association, Etobicoke, ON, Canada

[11] 1996 National Electrical Code Review and Application Guide, Killark Electric Manufacturing Company , St. Louis, MO, USA, 1998 Canadian Electrical Code Review and Application Guide, Hubbel Canada Inc. – Killark, Pickering, ON, Canada

[12] GB 3836 ff., Electrical apparatus for explosive gas atmospheres Part 1: General requirements

Taking the guesswork out of PTFE seals

by:
Stefan Tuma
Innovation and Technology
Hoerbiger
Vienna
Austria
Stefan.Tuma@hoerbiger.com

6^{th} Conference of the EFRC
October 28^{th} / 29^{th}, 2008, Dusseldorf

Abstract:

Compressor sealing topics that were not fully understood previously include the formation or destruction of so-called transfer layers on the surface of sealing materials, problems of heavy wear following a change in gas composition, and polishing of piston rods through contact with the packing. The precise interaction between the sealing material, the metal counter face and the gas appeared to be an impenetrable secret.

As a first step toward solving this tribological mystery a unique test rig to reproduce accurately the conditions found in real compressors was used. The tested specimens of metal and sealing materials were carefully analysed to determine the tribological system. Having established a reliable way to create wear and analyse the tribological process the results of this work led to new knowledge of the wear mechanisms in filled PTFE taking the guesswork out of PTFE seals.

1 Introduction

Hoerbiger's reputation as the world leader in compressor valves arises from a commitment to research and development. Valve design and dimensioning is based on a profound understanding of physics and thermodynamics taking place in a compressor.

In the field of rings and packings the knowledge was rather based on expert knowledge and experience. As a consequence there have always been topics that were not fully understood and thus it was decided to start a several year research project at Hoerbiger corporate R&D to bring "times of trial and error" to an end.

The results of this work are published in a very condensed way within this paper.

2 Test setup

2.1 Test equipment

Rings and packings of a compressor – the scope of this research work – are either located in places where no sensors can be positioned as e.g. in the groove of the oscillating piston. Or interesting values (or signals) like the frictional force of a piston ring when sliding on the liner or its actual wear rate are not accessible. Thus tribology with frictional force and wear rate as the primary measured values can not be monitored in a real compressor. The only viable way to analyse tribological phenomena in a compressor is to measure mass loss (or radial thickness) of its rings and packings on a large time scale

As a consequence test equipment for serious research work is needed. In order to get sound results from these tests by testing in the right way an in-depth knowledge of tribology is needed. As no test equipment ever will reflect the exact situation nor all the conditions of the aimed process an exact knowledge of the limitations of test results due to compromises in the test setup is imperative.

2.1.1 Some basic elements of tribology

Tribology, the branch of engineering that deals with the interaction of surfaces in relative motion, is determined by several mechanical processes and most often by chemical processes too. As a consequence any physical property, the topology of the surfaces and chemical reactivity between the tribological partners including the surrounding medium have to be taken into account. This makes tribology a vast field leading to misinterpretation sometimes as measured or calculated values though being defined in the same way differ completely if boundary or test conditions vary.

The coefficient of (kinetic) friction (μ) is defined as the ratio of the (kinetic) friction force (F) between the surfaces in contact to the normal force (N):

$$\mu = \frac{F}{N}$$

This simple definition could mislead to the assumption that this value is constant for a given pair of interacting surfaces. However it depends on many factors such as relative speed, contact area or shape of the surfaces and it even changes slightly along the surface as it is simply an approximation averaging microscopic effects to the macroscopic (measured) scale.

The wear rate is usually defined by the loss of volume (sometimes loss of mass) within a period of time. When referring to the tribological active surface the unit of the wear rate becomes µm/h or mm/year. The wear factor is defined as the ratio of the loss of thickness (lost volume divided by the tribological section: $\Delta l = \Delta V/A$) to the period of time (Δt), to the relative speed (v) and to the contact pressure ($p = N/A$)[1, 2]:

$$k = \frac{\Delta l}{p \cdot v \cdot \Delta t}$$

This relation too might imply a simple linear correlation of the different parameters to the wear factor. But as tribological systems depend on temperature it can easily be seen that the variation of the induced (specific) frictional power (being $p \cdot v$) will affect the temperature of the system depending on the thermal boundary conditions and thus it will affect the wear factor in a (sometimes highly) nonlinear way.

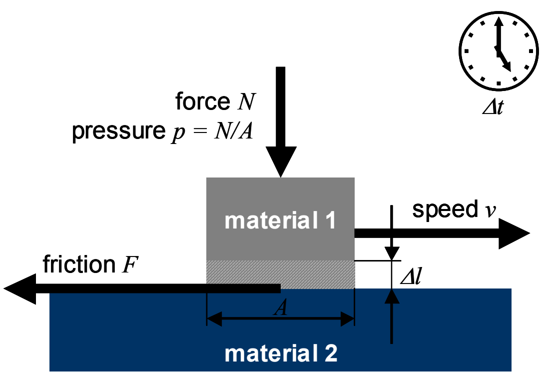

Figure 1: Definition of wear parameters

For a more profound understanding of tribology and especially of the non linearity of polymer tribology exceeding these mere basics please refer to the variety of literature that has been published in the past [3, 4].

2.1.2 Choice of tribometer used

When tribology has to be analysed and it comes to the choice of a tribometer (and the non linearity of tribology is neglected) frequently a pin on disc or a pin on ring tribometer is chosen. These test rigs are commonly used to test tribological behaviour but the kinematic of a compressor is not taken into account. As speed has an influence on test results the effect of a constantly reversing vector of velocity (an oscillating movement versus a linear) is much higher. As a consequence a test rig with an oscillating relative movement was chosen in order to get significant test results.

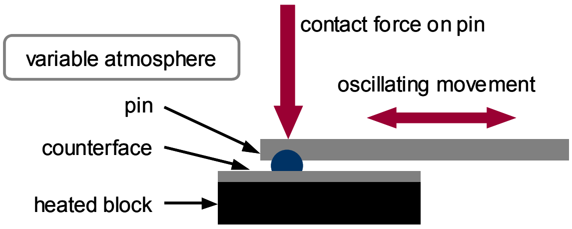

Figure 2: Working principle of the used test rig

To simulate as realistic conditions of a compressor as possible on the customized test rig temperature and atmosphere are controlled. Speed and the contact force are variable and the friction force as well as the wear rate (removal of material from the pin) are measured online.

2.2 Test conditions

As the conditions for the materials in the compressor vary with the application they have to be reflected in the test conditions. For example a PET compressor is running under oxidizing conditions, whereas a compressor for hydrocracking will be providing a reducing and dry atmosphere.

To obtain these different conditions a respective infrastructure for the test rig was built up. The atmosphere in the testing chamber can be air (oxidizing), nitrogen (inert) or hydrogen (reducing) and the water content can be varied between bone dry (dew point -40°C and below) and wet. The combination of these parameters gives nine possible different atmospheric conditions.

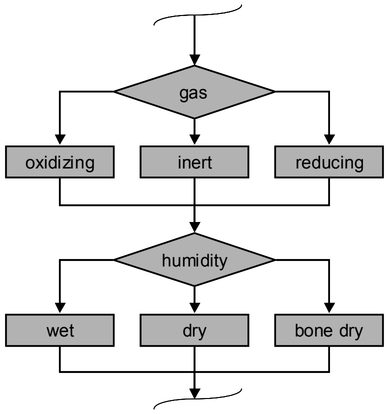

Figure 3: Different atmospheric conditions used

2.3 Choice of tribological material

Decades of experience have led to a large number of tribological materials in use today. To test all these materials in the different conditions would inevitably lead to a huge quantity of tests exceeding the given time frame. As a consequence representative materials which are specific for the different conditions in a compressor were chosen and entered into the test matrix.

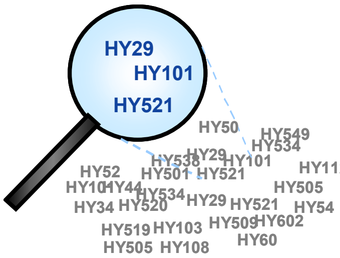

Figure 4: From the multitude of grades a few specific materials were selected.

Chosen materials range from conventional glass fibre filled grades to sophistically blended polymer filled materials to the well known bronze and MoS_2 filled type. These materials were submitted to different test conditions yielding test results (wear rate, friction coefficient) on one hand and samples for further investigations on the other hand.

3 Analysis

Apart from valuable wear data the tests on the tribometer yielded specimens tested at defined tribological conditions. These samples were taken for further investigations of the tribological material as well as of the corresponding counter faces.

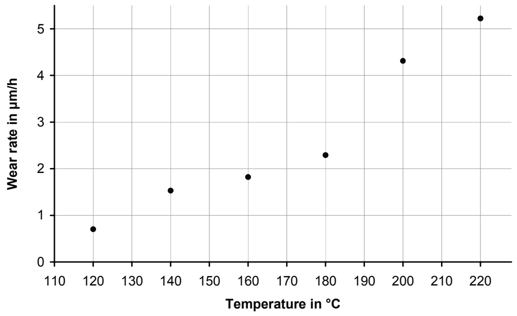

Figure 5: Example of tribological test results of a test series

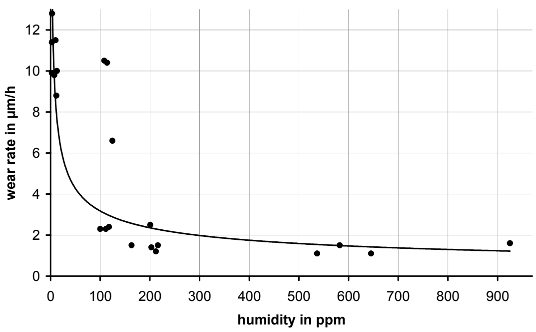

Figure 6: This diagram shows that the wear mechanism changes completely if the humidity drops below 100 ppm (bone dry) for a certain grade.

The results of the different methods of investigation are summarised in the following chapters.

3.1 Analysis of the surface

3.1.1 Scanning electron microscopy

Using a scanning electron microscope (SEM) has various advantages for this type of investigations as the magnification of imaging can be varied in a very large range and the chemical composition of the surface can be determined (if the microscope is equipped with the suitable detector).

Imaging – topographical analysis: The subsequent images show the same area in low to high magnification. Low magnification makes it possible to scan large areas for investigation, whereas with high resolution very small details can be analysed (while still having a very good depth of field):

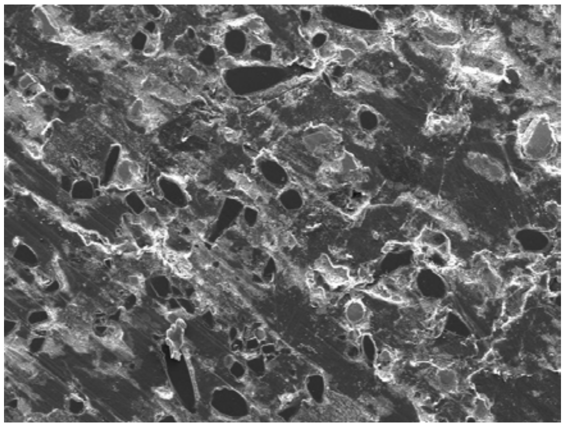

Figure 7: Surface of a tested pin at low magnification for a general view, filler distribution and special points of interest.

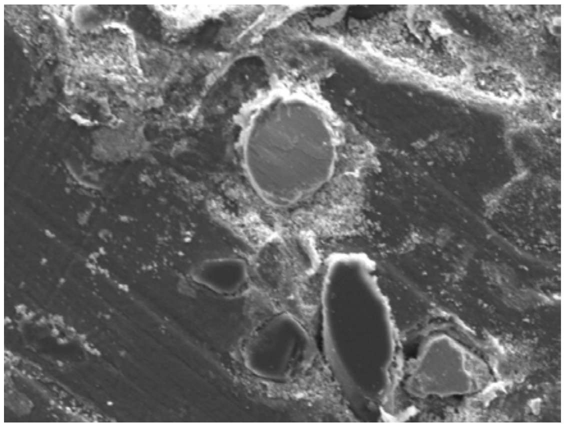

Figure 8: High magnification imaging is used for the analysis of tribochemical processes taking place at a very small scale.

This ability of wide zoom range makes it possible to analyse the same area at different instants of time of a tribological test. The next two images show such an analysis of the development of the transfer layer on the counterface of a glass filled grade.

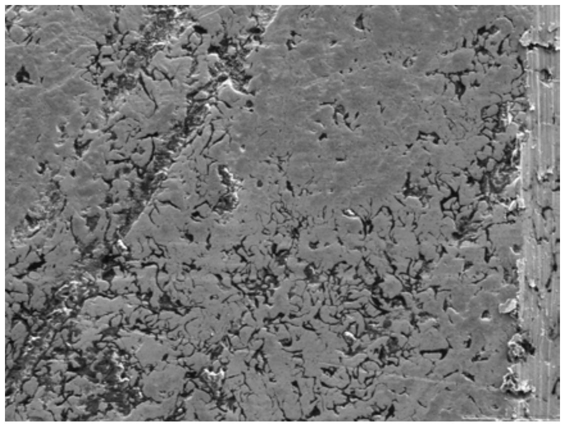

Figure 9: Surface of a cast iron counterface after 1h testing time: The original scratches of production and the grooves from the materials graphite lamellae are nearly untouched.

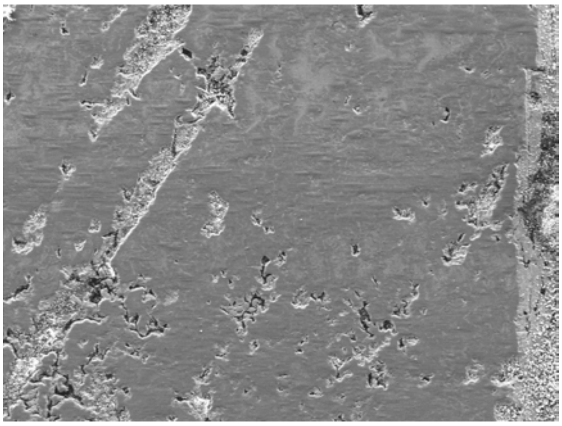

Figure 10: After 24h of running time the small grooves have been closed completely and the scratches are filled with very small particles of debris. In the upper half a transfer film has developed (sliding direction is horizontally).

Analysing many tests with the same material pairing but different atmospheric conditions in this way indicates the mode of development of the transfer film. As expected, humidity of the gas and the composition (whether oxidising, inert or reducing) are of major importance.

Chemical analysis: Using an EDX detector in a SEM the chemical composition of the surface can be determined by analysing the emitted X-ray spectrum provoked by the electron beam being focussed onto the surface.

By this means chemical elements in the surface can be detected and their ratio to the other elements present can be calculated by analysing the EDX spectrum. This reveals the composition of the transfer film on the counterface and the debris on the tribological material or in grooves of the counterface.

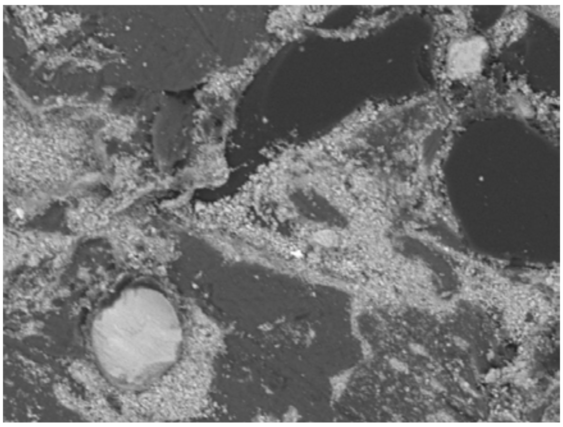

Figure 11: SEM image of the subsequent EDX spectra: dark spots are carbon fibres, the big bright spot is a glass fibre (whereas the many small bright spots are metallic debris). The matrix (grey) is PTFE.

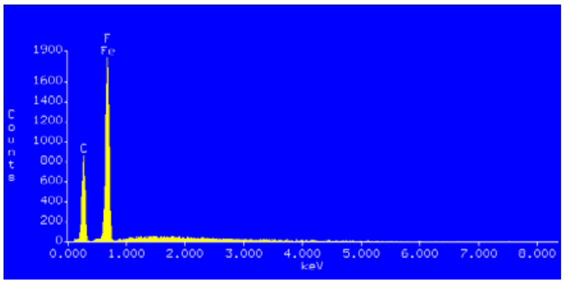

Figure 12: EDX spectrum of PTFE consisting of carbon (C) and fluorine (F). The peaks of fluorine and iron (Fe) are very close, but they can be distinguished

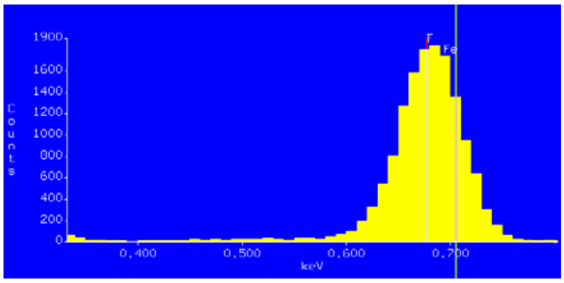

Figure 13: Zoom into the EDX spectrum of PTFE showing the presence of fluorine (F) and the absence of iron (Fe).

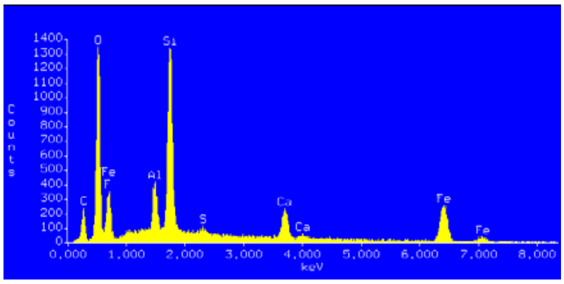

Figure 14: EDX spectrum of a glass fibre consisting of alumina (Al_2O_3), silica(SiO_2) and calcia (CaO). The peaks of iron (Fe), fluorine (F) and carbon (C) are noise of surrounding PTFE and cast iron debris.

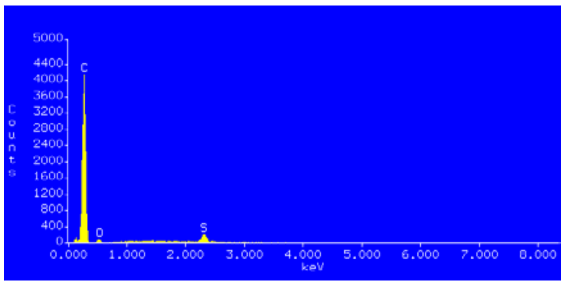

Figure 15: EDX spectrum of a carbon fibre being pure carbon (C). Oxygen (O) and sulphur (S) are noise of other polymeric fillers of this tribological material.

Another helpful tool for chemical analysis is imaging with backscattered electrons (BSE) instead of secondary electrons (SE), which are used commonly as they render a much sharper image of the topography of the specimen.

Images taken by a detector for backscattered electrons do not reveal the topography but the atomic weight of the elements on the surface. Dark shades of grey correspond to light elements such as carbon whereas bright shades indicate heavy elements (metals such as iron)

By this means the existence or the thickness of a transfer film on a metallic counterface can be detected easily. For an exact chemical analysis EDX spectroscopy will be used then.

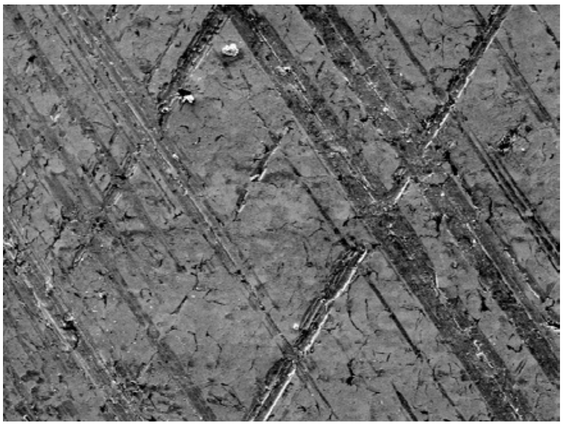

Figure 16: Image of a cast iron counterface taken with the detector for secondary electrons: loose particles, scratches and other topographic information is imaged precisely.

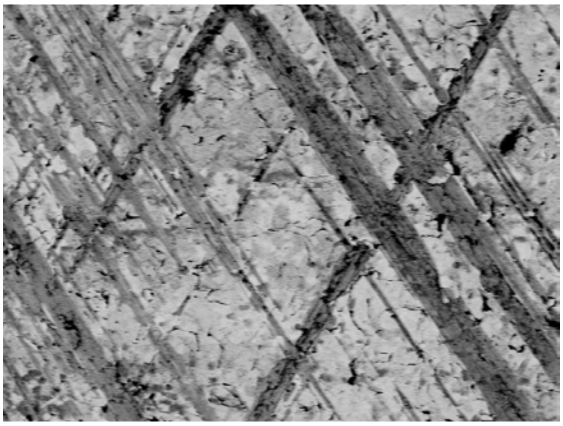

Figure 17: The same area as above taken with the detector for backscattered electrons: the grooves are filled with polymeric debris (light elements – dark shades) and a transfer film is developing in the top half of the image (indicated by a slightly darker shade of grey)

3.1.2 Other methods of surface characterisation

Other means of microscopy than the SEM that have been used within this work have been Auger electron microscopy (AES), secondary ion mass spectroscopy (SIMS) and infrared spectroscopy (attenuated total reflection – ATR).

These techniques are used for pure characterisation of the surface as the penetration depth is only a couple of nanometers depending on the method. As a consequence the gained results exceed the conclusions obtained by the SEM only slightly. They mainly prove or enhance the information about the transfer layer.

3.2 Analysis of sections

The key for understanding tribology in the given context and for the comprehension of the formation of the transfer layer is found in an in-depth analysis. As a consequence the methods described in the last subchapter provide only part of the full picture as they analyse the surface (and a couple of nanometres beneath) only.

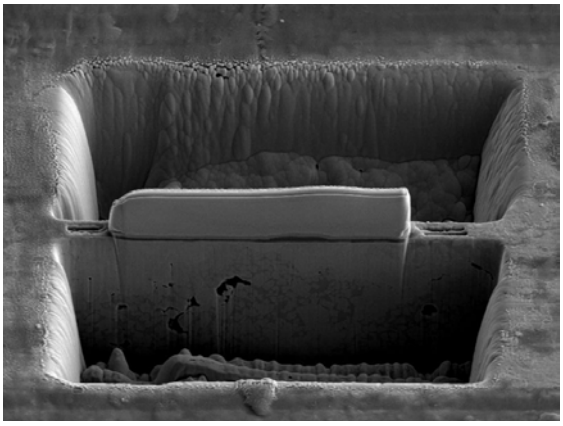

Figure 18: Two trenches leaving a thin ligament in between. To protect the transfer film a protective layer is sputtered before ion beam cutting.

When using an ion beam to cut into the depth of a sample, the transfer film is not damaged as it would be the case with mechanical cutting. Further it is possible to cut in a manner that a trench with a very distinct side is obtained. In order to analyse this face it has to be removed from the rest of the sample.

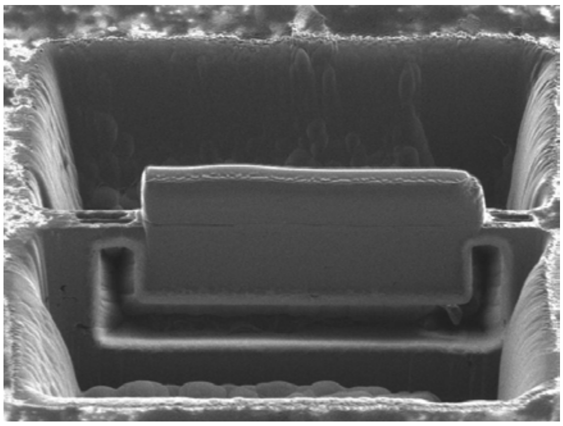

Figure 19: The ditch underneath the thin ligament leaves only two small bars holding the lamella to be removed easily.

By cutting a second trench in a way that only a very thin bar or partition wall is left over this ligament can be removed from the sample and be analysed separately.

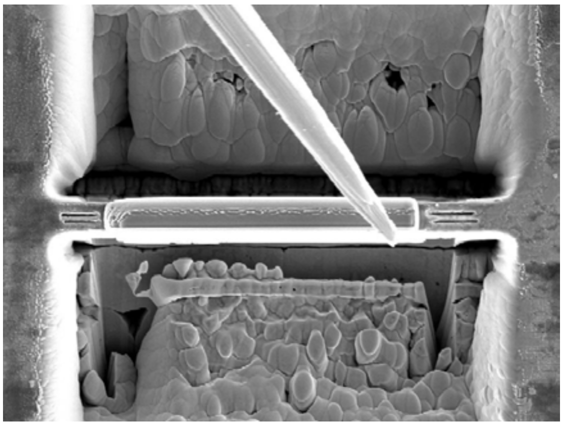

Figure 20: View onto the lamella when removing it from the rest of the sample.

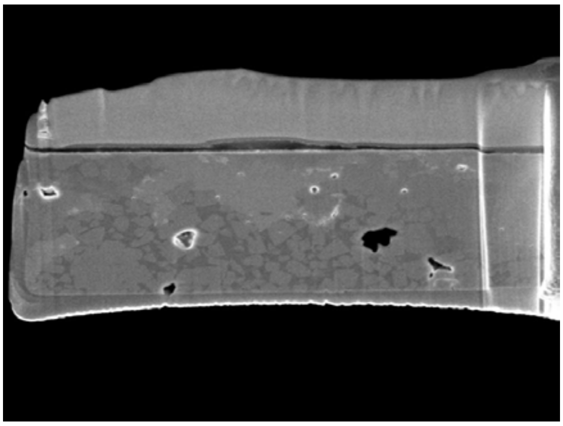

Figure 21: The lamella is fixed laterally ready for TEM examination. The bright top region is the protective layer with the transfer film beneath (dark). The bottom is the bulk (an inhomogeneous and porous WC coating).

The thickness of the lamella is so small that transmission electron microscopy (TEM) is possible. This type of microscopy has the same advantage as SEM, that not only imaging but chemical analysis is possible as well. In the case of TEM it is no x-ray spectroscopy (as EDX in a SEM) but an electron energy loss spectroscopy (EELS). By this method the presence of chemical elements is detected.

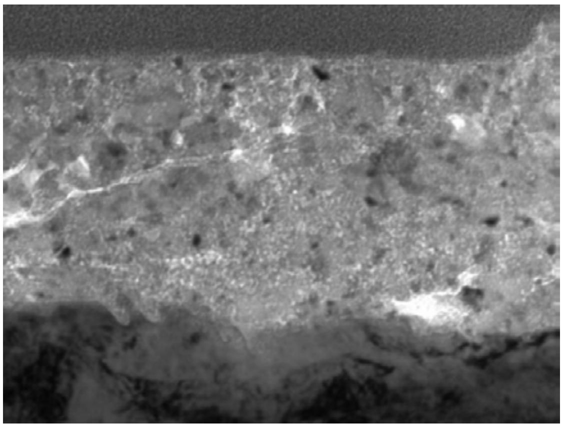

Figure 22: TEM image of a transfer film: Thickness at this position 300 nm.

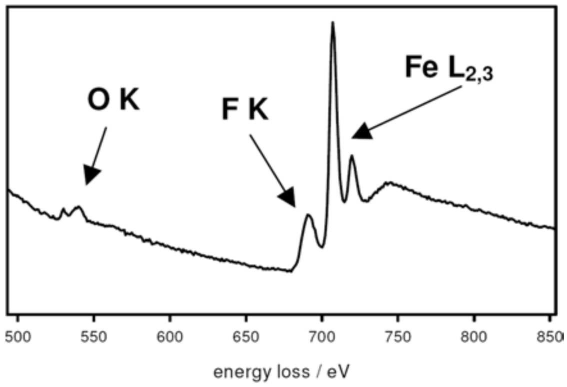

Figure 23: EELS spectrum of the transfer film showing the presence of oxygen (O), fluorine (F) and iron (Fe).

4 Results

4.1 The constitution of the transfer film

The transfer film is a quite inhomogeneous layer, depending mainly on the tribological history of that domain. It usually consists of iron fluoride (*FeF_2*) and iron oxide (*FeO*). Sometimes a carbon enriched ply can be found where PTFE has not decomposed completely.

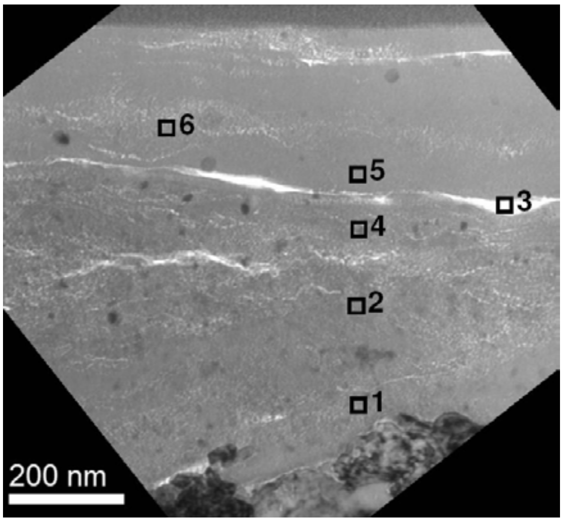

Figure 24: In this TEM image of a transfer film different positions of chemical EELS analysis are marked. On top the Pt protective layer can be seen, the bottom is the cast iron bulk of the counterface.

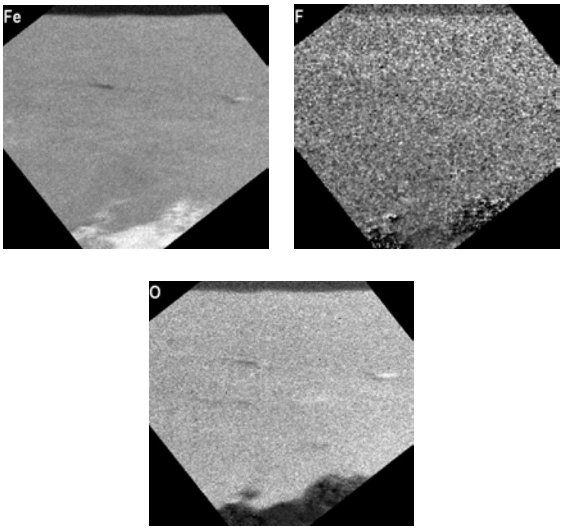

Figure 25: Element mapping of iron (Fe, top left), flurine (F, top right) and oxygen (O, bottom) onto the TEM image. The brightness corresponds to the ratio of the respective element present.

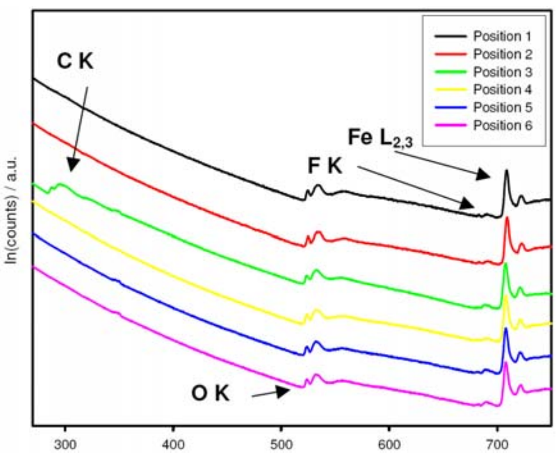

Figure 26: Superposed EELS spectra for the different positions in the TEM image above. Only at position 3 a carbon (C) peak can be found.

The thickness of the transfer film varies across the surface of the counterface. In some cases depending on the pairing of the tribological partners and surrounding conditions a multilayer structure is built up where a couple of distinct layers are superposed. They are usually confined by an oxygen rich ply. Fe

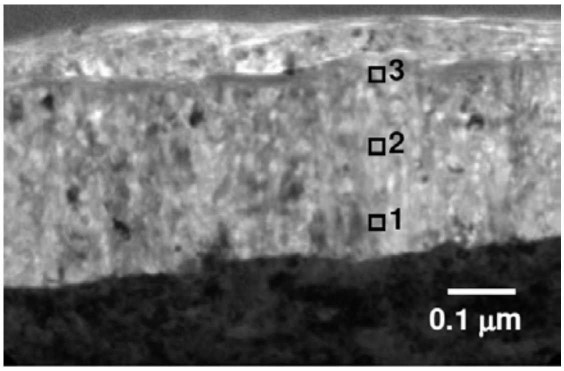

Figure 27: In this TEM image of a two layered transfer film different positions of chemical EELS analysis are marked.

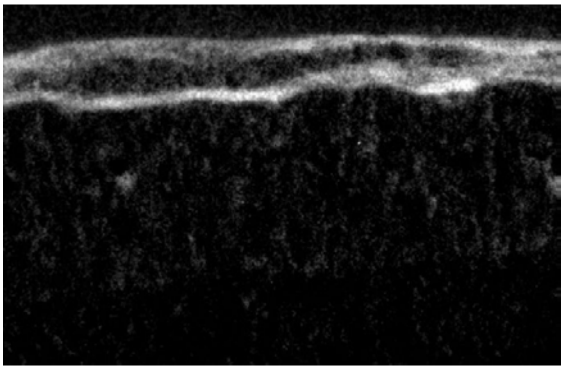

Figure 28: Element mapping of oxygen (O) onto the TEM image. The brightness corresponds to the ratio of oxygen present.

Summing up, it can be stated that the transfer film is consisting mainly of iron fluoride with a inhomogeneous cellular morphology which is due to the oscillating relative movement of the tribological partners. This iron fluoride layer is chemically bonded to the counterface acting as substrate. On top of the transfer film in the reactive zone fractions of PTFE (detected by ATR infrared spectroscopy) are found; they are a precursor for the fluoride of the transfer film, where PTFE has decomposed completely.

4.2 Wear modes and tribochemistry

As easily can be seen the chemical processes taking place in the reactive zone of the transfer layer depend strongly on the surrounding conditions as oxygen and especially the water-vapour content.

When PTFE is decomposed very reactive fluorine radicals form oxidising iron or fissioning water-vapour into hydrofluoric acid which would attack glass fibres in turn:

$$\underbrace{(CF_2)_n}_{\text{PTFE}} + H_2O \rightarrow HF + CO_2$$

The knowledge of these reactions and the essential conditions for them makes it possible to predict the suitability of a tribological material for a certain process.

Another astonishing chemical reaction was found taking place in the tribological system of the bronze (*CuZn*) and molybdenum disulfide (MoS_2) filled grade (HY52) in an air compressor. In this case the sulphur of the sulphide is needed to form a stable copper sulphate ($CuSO_4$):

$$\left.\begin{array}{ll} Cu & \text{from bronze} \\ S & \text{from } MoS_2 \\ O_2 & \text{from air} \end{array}\right\} \rightarrow CuSO_4$$

or in a chemically more correct way:

$$CuZn + MoS_2 + O_2 \rightarrow ZnO + MoO_2 + CuSO_4$$

This reaction could not take place without MoS_2 as a filler and shows that in this very special case MoS_2 does not only act as lubricant but it is an essential component for the tribochemical reaction too.

5 Conclusion

Based on tests on the custom designed test rig and by investigating with different microscopic analysis tools it was possible to identify the constitution and morphology of the transfer film. Furthermore based on the constituents of the tribological system to describe the chemical processes taking place in the reactive zone of the transfer film can be described.

Passing trough a large test matrix of different combinations of atmospheric conditions and tribological partners has led to a general understanding of the tribological processes taking place and of the suitability of a certain material for a given application.

The results were condensed into so-called "decision trees" making it possible to define optimal atmospheric conditions (and from that ideal applications) for the complete Hoerbiger material range.

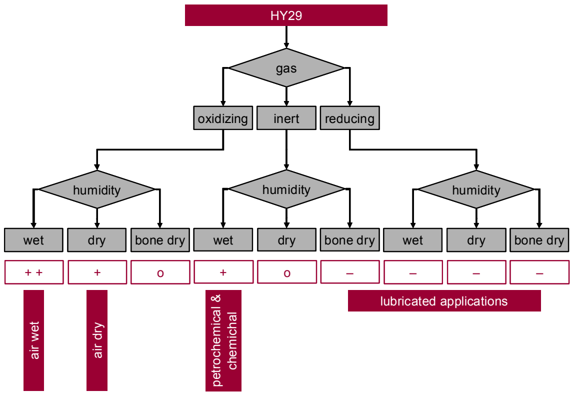

Figure 29: Example of a "decision tree" for the application of HY29, a glass fibre filled grade.

From these "decision trees" Hoerbiger engineers now are able to decide on a sound basis which material to choose for a given application. On the other hand the development of new grades is much easier with the scientific background at hand.

6 Acknowledgements

In commemoration of our colleague Andreas Dittmann who dedicated most of his time in the R&D group at Hoerbiger to this project.

This project was subsidised by the Federal Austrian Research Promotion.

References

[1] *Kriegl*, G. (1978). „Beitrag zur Berechnung des Radialverschleißes von Trockenlaufkolbenringen", Dissertation, Technische Universität Dresden, D

[2] *Feistl*, N. (2001). „Beitrag zum Betriebsverhalten trocken laufender Dichtsysteme zur Abdichtung der Arbeitsräume von Kolbenkompressoren", Dissertation, Technische Fakultät, Universität Erlangen-Nürnberg, D

[3] *Czichos*, H., *Habig*, K.H. (1992). „Tribologie Handbuch", Hanser, Wiesbaden, D

[4] *Tevrüz*, T. (1999). Wear **230**, 61

Efficiency Definition and Load Management for Reciprocation and Centrifugal Compressors

By:

Rainer Kurz, Ph.D.
Systems Engineering
Solar Turbines Incorporated
San Diego, CA
USA
kurz_rainer_x@solarturbines.com

Klaus Brun, Ph.D.
Fluids Engineering
Southwest Research Institute
San Antonio, TX
USA
klaus.brun@swri.org

6th Conference of the EFRC
October 28th / 29th, 2008, Dusseldorf

Abstract:

Reciprocating compressors and centrifugal compressors use different definition of compressor efficiency. This paper will provide guidelines for a true comparison, as well as a universal efficiency definition for both types of machines, based on the requirements the ultimate user is really interested in. Further, the impact of actual pipeline conditions on the change of efficiency at different loads, using different means of control, is evaluated .

1 Introduction

At first glance, efficiency calculation for any type of compression seems to be rather straight forward: We compare the work for some ideal process with the work that has to be expended for the actual compression process.

However, at this point we need to acknowledge, that these traditional efficiency definitions don't answer the operators main concern regarding the driver power required for the compression process. This means, that we also will have to discuss the mechanical losses (i.e friction in bearings, pistons etc.) in the compression system as well as the losses due to gas leakage. One of the key issues is the definition of appropriate system boundaries, that include the losses associated with the compression process and the treatment of instationary flows.

The other issue is the trends of efficiency if the compressor is operated at off-design conditions as they are imposed by typical pipeline operations.

2. Thermodynamics of Gas Compression

For a compressor which receives gas at a certain suction pressure and temperature, and delivers it at a certain higher output pressure, the isentropic head represents the energy input required by a reversible, adiabatic (thus isentropic) compression. The actual compressor will require a higher amount of energy input than needed for the ideal (isentropic) compression.

The actual head for the compression is given by:

$$\Delta h = h(p_2, T_2) - h(p_1, T_1) \qquad [1]$$

and the isentropic head is:

$$\Delta h_s = h(p_2, s_1) - h(p_1, T_1) \qquad [2]$$

where entropy of the gas at suction condition (s_1) is:

$$s_1 = s(p_1, T_1) \qquad [3]$$

The relationships described can be easily seen in a Mollier diagram (Figure 1)

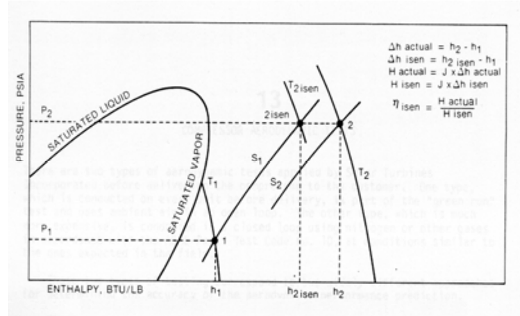

Figure 1: Compression Process in a Mollier (Pressure-Enthalpy) Diagram with Lines of Constant Temperature and Constant Entropy

The performance quality of a compressor can be assessed by comparing the actual with the head that the ideal, isentropic compression would require and define the isentropic efficiency as:

$$\eta_s = \frac{\Delta h_s}{\Delta h} \qquad [4]$$

If cooling is applied during the compression process (for example with intercoolers between two compressors in series), then the increase in entropy is smaller than for a process without inter-cooling. Therefore, the power requirement will be reduced. However, this process is no longer adiabatic (although it will consist of two adiabatic sub-processes)

3. Treatment of Unsteady Flow Conditions

Feeding a pipeline with a flow that fluctuates in its pressure around an average pressure will lead to a higher pressure drop in the pipeline than for a steady state flow at the average pressure. Fluctuations with sufficiently high amplitudes are usually low frequency fluctuations (below, say, 100Hz). The additional pressure drop is due to fact, that friction losses are proportional to the flow velocity squared. This means that the higher friction in the high velocity part of the fluctuation is not compensated by the lower friction at the low speed part.

Since the pressure loss in a pipe is

$$\Delta p = \xi \frac{\rho}{2} Q^2 \qquad [5]$$

a flow with a fluctuating component

$$Q = Q_0 + \tilde{Q} \cdot \sin \omega t \qquad [6]$$

will yield a higher pressure loss than a constant flow Q=const:

$$\Delta p = \xi \frac{\rho}{2T}\int_0^T (Q_0 + \widetilde{Q}\cdot \sin \omega t)^2\, dt =$$

$$\xi \frac{\rho}{2T}\int_0^T (Q_0^2 + 2Q_0\widetilde{Q}\cdot \sin \omega t + \widetilde{Q}^2 \cdot \sin^2 \omega t) dt \qquad [7]$$

$$= \xi \frac{\rho}{2T}\left(Q_0^2 T + \frac{\widetilde{Q}^2 T}{2}\right) = \xi \frac{\rho}{2}(Q^2 + \frac{\widetilde{Q}^2}{2})$$

$$\Delta p_{rel} = 1 + \frac{\widetilde{Q}^2}{2Q_0^2} \qquad [8]$$

4. Compression Equipment

The compression equipment used for pipelines involves either reciprocating compressors or centrifugal compressors.

Centrifugal compressors are driven by gas turbines, or, in some cases by electric motors. The gas turbines used are in general two shaft engines, and the electric motor drives use either variable speed motors, or variable speed gearboxes.

Reciprocating compressors are either low speed integral units, which combine the gas engine and the compressor in one crank casing, or separable "high-speed" units. The latter units operate in the 750 to 1200 rpm range and are generally driven by electric motors, or 4 stroke engines.

5. Efficiency Determination

The flow into and out of a *centrifugal compressor* can be considered as 'steady state'. Heat exchange with environment is usually negligible. System boundaries for the efficiency calculations are usually the suction and discharge nozzles. It needs to be assured that the system boundaries envelope all internal leakage paths, in particular recirculation paths from balance piston or division wall leakages. To determine the isentropic efficiency, based on total enthalpies, total pressures and temperatures at suction and discharge of the compressor are measured, and the isentropic efficiency then becomes

$$\eta_s = \frac{[\mathrm{h}(\mathrm{p}_{\mathrm{disch}}, s_{suct}) - h(p_{suct}, T_{suct})]}{[\mathrm{h}(\mathrm{p}_{\mathrm{disch}}, T_{disch}) - h(p_{suct}, T_{suct})]} \qquad [9]$$

and, with measuring the steady state flow, the absorbed shaft power is

$$\mathrm{P} = \frac{\dot{\mathrm{m}}}{\eta_{\mathrm{m}}}[\mathrm{h}(\mathrm{p}_{\mathrm{disch}}, T_{disch}) - h(p_{suct}, T_{suct})] \qquad [10]$$

The mechanical efficiency η_m, describing the friction losses in bearings and seals, is typically between 98 and 99%.

The theoretical (isentropic) power consumption (which is the lowest possible power consumption for an adiabatic system) follows from

$$\mathrm{P}_{\mathrm{theor}} = \dot{m}[\mathrm{h}(\mathrm{p}_{\mathrm{disch}}, s_{suct}) - h(p_{suct}, T_{suct})] \qquad [11]$$

Reciprocating compressors, by their very nature require extensive manifold systems to control pulsations and provide isolation from neighboring units (both reciprocating and centrifugal), as well as pipeline flow meters and yard piping. The design of manifold systems for either slow speed or high speed units uses a combination of volumes, piping lengths and pressure drop elements to create pulsation (acoustic) filters. These manifold systems (filters) cause a pressure drop, and thus must be considered in efficiency calculations. Heat transfer is usually neglected (just as in centrifugal compressors).

Theoretical gas horsepower for a reciprocating compressor is also given by equation 11, if suction and discharge pressure are the pressures up stream of the suction pulsation dampeners and downstream of the discharge pulsation dampeners. Potentially, additional pressure deductions from the suction pressure would have to made to include the effects of residual pulsations. In some instances, this equation is modified to:

$$\mathrm{P}_{\mathrm{theor}} = \dot{m}[\mathrm{h}(\mathrm{p}_{\mathrm{disch}}, T_{disch}) - h(p_{suct}, T_{suct})] \qquad [12]$$

i.e the discharge enthalpy is calculated based on the discharge temperature, which implies that the compression process by itself is isentropic and with the assumption that the suction and discharge pressures herein are the toe pressures (which neglects the pressure loss in the suction and discharge pulsation dampeners). The assumption of an isentropic compression process might be approximately true in low speed machines with relatively low piston velocities, but it is not true for high speed separable machines, or for machines with clearance pockets. P_{theor} represents the minimum power required at the compressor piston face for the given flow at suction and discharge pressures.

The actual gas power, or indicated power of the reciprocating compressor can be determined from a p-V where the integral depicts the area in the p-V diagram (Figure 2):

$$P_i = N \oint pdV \qquad [13]$$

Compressor efficiency is generally calculated by the ratio of Ptheor divided by the measured indicated power Pi:

$$\eta_s = \frac{P_{theor}}{P_i} \qquad [14]$$

P_i is estimated from the integration of cylinder pressure versus crank angle data.

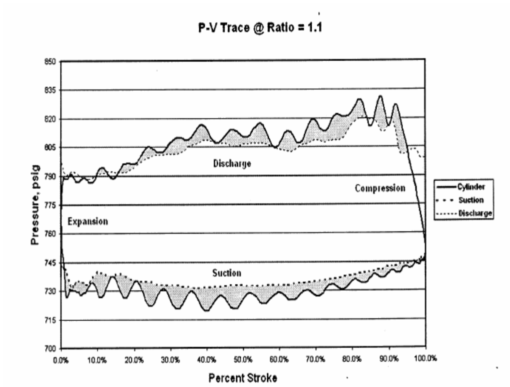

Figure 2: Typical Compressor P-V Diagram with Valve Losses shown as deviations from Ideal[1]. Percent stroke is directly related to the volume in the cylinder.

In general, compressor losses between indicated power and theoretical power are controlled by valve losses, pulsation driven effects on the cylinder pressure, and pressure drop losses through the suction and discharge manifolds, valves, tees and connected piping to the yard headers. Manifold pressure drop is generated in nozzle orifices, internal choke tubes, and all major area changes in the pulsation and piping system. Indicated power reflects the work required to move the gas from suction to discharge conditions, and will change based on the total pressure drop across the various elements in the manifold system. If ,as usually done, P_{theor} is simply calculated between cylinder toe suction and discharge pressures (Eq.12), it inherently limits the interpretation of the losses to in cylinder pulsation effects and valve losses, but does not account the pulsation, and pulsation dampening losses. Eq.11 is therefore the more appropriate approach.

Compressor indicated power is a traditional first measurement in efficiency determination and diagnostic analysis. For slow speed integrals this is a mature technology and measurement error correction methodologies accounting for the pressure measurements made at the end of the measurement channel have been well developed, validated, and built into the current generation of test equipment. For high speed compressors, measurement error can be significant, not easily corrected leading to a much higher level of uncertainty on actual HP estimates for the unit. Pressure drop through the manifold system is not easily measured or interpreted. Static pressure drop combined with mean flow estimates are not accurate representations of HP losses in highly pulsating environments with significant flow modulations. Flow modulations can significantly increase the HP cost of orifices, choke tubes and entrance and exit losses in the manifold design. Manifold installation losses can be assigned which are those power requirements associated with the design outside of the cylinder flanges, including nozzle orifices (if required).

The actual consumed power follows with the addition of the mechanical losses for n compression volumes (i.e number of cylinders for single acting and twice the number of cylinders for double acting machines) :

$$P = \frac{N}{\eta_m} \sum_{1}^{n} \oint pdV \qquad [15]$$

Mechanical efficiency in a compressor is generally considered the efficiency in which crankshaft power is applied to the piston face. The losses include rank pin bearings, wrist pin bearings, slider bearings, packing resistance, piston ring friction, and rider band friction. For pipeline users, these losses mainly represent a quantity to be accounted for when inferring crankshaft power (brake power) from indicated power, so that engine heat rate (brake specific fuel consumption) can be calculated as fuel energy consumption rate to brake horsepower. For integral machines, mechanical efficiency is generally taken as 95%. For separable machines a 97% mechanical efficiency is often used. These numbers seem to be somewhat optimistic, given the fact that a number of sources state that reciprocating engines incur between 8 and 15% mechanical losses[2] and reciprocating compressors between 6 and 12%[3]. It also would have to be assumed that the mechanical losses are largely independent of load, but strongly dependent on speed. That means that the mechanical efficiency drops if the compressor is operated at constant speed and reduced load.

6. Prime Mover Efficiency

The performance of the compressor drivers are generally categorized by the heat rate. Heat rate (brake specific fuel consumption, in BTU/HP-hr or kJ/kWh) is a measure of the conversion efficiency from fuel to shaft horsepower. A heat rate of 9000 BTU/HP-hr is a fuel conversion efficiency of just over 28 percent.
It is thus[1]:

$$HR = \frac{\dot{m}_{fuel} \cdot LHV}{P} = \frac{C_2}{\eta_{th,PM}} \qquad [16]$$

7. System Efficiency

To describe the appropriate system efficiency is conceptually simple (Figure 3): The useful work that is done to the mass flow of process gas is compared to the power contained in the fuel (this is basically the lower heating value of the fuel times the fuel mass flow). The useful work to the process gas is most easily described as the minimum amount of work to perform the compression duty in an adiabatic system: this is the isentropic head.

Issues are mainly in the definition of appropriate system boundaries. The system should contain all devices that are required to perform the compression process, and the flow across the system boundaries should be steady state. It is however important to define the boundaries of the efficiency description. As previously discussed, traditional compressor thermal efficiency only defines the ratio of the ideal work between compressor toe pressures and piston face indicated HP. It neglects the contribution to the losses of the manifold design. A more appropriate description of the overall system efficiency would include the losses associated with the manifold system and define system efficiency, thus describing useful work as the product of mass flow and enthalpy rise from suction lateral (upstream of the manifold) to discharge lateral (downstream of the manifold) locations.

The amount of fuel that is consumed to compress a certain amount of gas from a prescribed suction pressure to a prescribed discharge pressure is an important characteristic for the user. This can universally be described in terms of a package efficiency η_{global} in terms of the amount of fuel required to perform the compression duty with an isentropic compressor:

$$\eta_{global} = \frac{\dot{m} \cdot \Delta h_s}{\dot{m}_{fuel} \cdot LHV} = \frac{\dot{m} \cdot \left[h(p_{disch}, s_{suct}) - h(p_{suct}, T_{suct}) \right]}{\dot{m}_{fuel} \cdot LHV} \qquad [17]$$

If a centrifugal compressor and a reciprocating compressor are to be compared, the isentropic power per Eq. 11 must be used. The global efficiency can be approximated by

$$\eta_{global} \approx \eta_{s,compr} \cdot \eta_m \cdot \eta_{th,PM} \qquad [18]$$

The main difference between Eq.17 and Eq. 18 is the fact that Eq.18 does not consider the leakage flows. For pipeline applications, these leakages are usually negligible compared to the overall compressed flow. Compressor Isentropic Efficiency is obtained as the ratio isentropic enthalpy rise from lateral suction conditions to lateral line discharge condition to actual enthalpy rise between the same test point locations. It accounts for all pressure driven losses and compression irreversible losses but not heat loss effects from the manifold and attached piping.

Another interesting feature of this approach is (besides the fact that it allows direct comparison between reciprocating and centrifugal systems) is the fact that very little data is necessary (Eq.17):

- Fuel flow
- Gas Flow
- Gas composition (needed to calculate LHV, enthalpy and density)
- Suction temperature (Notably, discharge temperature is *not* needed)
- Suction and discharge pressures (suction lateral (upstream of the manifold) to discharge lateral (downstream of the manifold) locations)

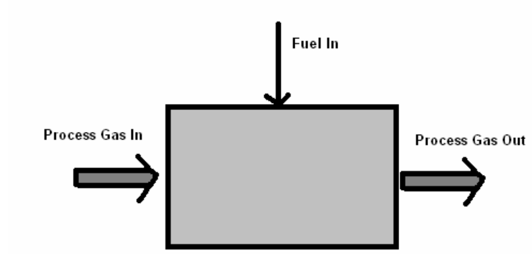

Figure 3: Compression System

.

Note that is the above approach, mechanical efficiency is not explicitly described nor is it

[1] Note that the constant C_2 is used for unit conversion. If the heat rate is in BTU/HPhr, C_2 = 2544; if the heat rate is in kJ/kWh, C_2=3600).

needed- a lower mechanical efficiency will automatically yield a higher fuel consumption for the same flow, and pressure ratio.

In this sense, the formulation in Eq. 17 lends itself to testing the units, while Eq. 18 might be more appropriate for the design phase, because individual losses of the driver, the compressor and compressor components can be captured more easily. That is, at design time losses can be assigned to compressor valves, and flow driven installation losses though the manifold and attached piping system can be predicted. Since this defines overall compressor efficiency as the ratio of piston face work to useful work (upstream and downstream of the manifold system), some assumption must be made toward mechanical efficiency if the overall system efficiency is to be estimated from published engine heat rates.

It needs to be further pointed out, that we have used the isentropic, rather than the polytropic efficiency and head definition. Eq. 17 strictly requires the use of the isentropic head, because the isentropic head is completely defined by station parameters (gas composition, suction temperature and pressure, and discharge pressure). The polytropic head is additionally a function of the compressor efficiency. The polytropic process is by no means a more accurate approximation of the true process than the isentropic process: Both are ideal and reversible. The isentropic process is additionally adiabatic, while the polytropic process is not adiabatic, but approximates the compression process by an infinity number of isentropic steps, each followed by a heat exchange (Therefore, the polytropic process yields the same discharge temperature as the real process. The heat generated in the real process by irreversible losses is generated by (reversible) heat transfer in the polytropic process).

8. System Integration and Station Operation

At the individual compressor station level, flow flexibility requirements translate into an increasing need for automation (remote start-up, shutdowns), reliability, and broader capacity control. Short-term contracts, combined with large price swings, have led to less use of "line pack" to store gas in the pipeline. Volume flow requirements are up to meet the increased demand, while less "line pack" results in lower pressure ratio requirements. Pipelines earn revenue only by transporting "other people's" gas. Increased efficiency directly affects fuel consumption, operating cost, emissions, and capacity, but contractual arrangements do not always motivate the most efficient compression solution. As part of the pipeline system, a compressor must manage these interacting factors: capacity control, pulsation control, and valves. System efficiency, smooth operation, and the resulting reliability are maximized at the system design point. Small departures from this design point have modest impacts on efficiency, smooth operations, and reliability. Major departures have significant adverse effects, but reciprocating compressors must increasingly operate over a wider range of conditions[4].

9. Operating conditions imposed by Pipeline Conditions

For a situation where a compressor operates in a system with pipe of the length L_u upstream and a pipe of the length L_d downstream, and further where the pressure at the beginning of the upstream pipe p_u and the end of the downstream pipe p_e are known and constant, we have a simple model of a compressor station operating in a pipeline system (Figure 4).

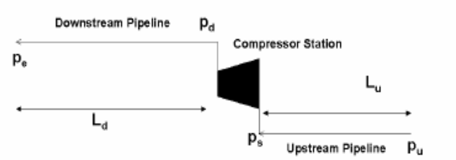

Figure 4 :Conceptual model of a pipeline segmen[5]t (Kurz and Lubomirsky [5])

The pressure gradient in the pipeline can be described by the Fanning equation

$$\frac{dp}{dx} = -32 f \left[\frac{\rho_{std} Q_{std}{}^2}{\pi^2 D^3} \right] \qquad [19]$$

which can be integrated. For a given, constant flow capacity Q_{std} , the pipeline will then impose a pressure p_s at the suction and p_d at the discharge side of the compressor. Kurz and Lubomirsky [5] show that for a given pipeline, the head–flow relationship at the compressor station can be approximated by

$$H^* = C_p T_s \left[\left(\sqrt{\frac{1}{1 - \frac{C_3 + C_4' \cdot Q^2}{p_d^2}}} \right)^{\frac{k-1}{k}} - 1 \right] \quad [20]$$

where C_3 and C_4 are constants (for a given pipeline geometry) describing the pressure at either ends of the pipeline, and the friction losses, respectively.

Equation 20 shows a direct relationship between the flow transported in the pipeline and the required head, assuming the pipeline losses are known., and the station discharge pressure is defined. This seems somewhat limiting, but one must consider that, in order to maximize flow in a pipeline system, the station discharge pressure will be at, or close to the maximum operating pressure of the pipeline.

Among other issues, this means that for a compressor station within a pipeline system, the head for a required flow is prescribed by the pipeline system (Figure 5). In particular, this characteristic requires the capability for the compressors to allow a reduction in head with reduced flow, and vice versa, in a prescribed fashion. The pipeline will therefore not require a change in flow at constant head (or pressure ratio).

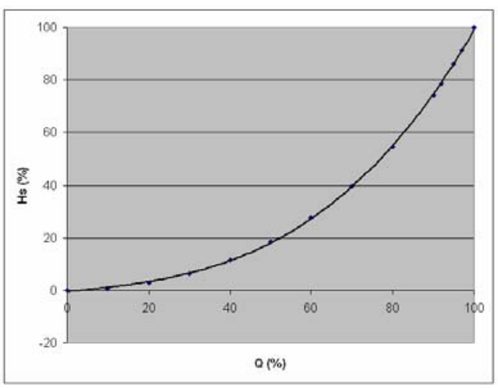

Figure 5: Station Head-Flow relationship based on Eq.20

10. Compressor Control

Based on the requirements above, the compressor output must be controlled to match the system demand. This system demand is characterized by a strong relationship between system flow and system head or pressure ratio. Given the large variations in operating conditions experienced by pipeline compressors, an important question is how to adjust the compressor to the varying conditions, and, in particular, how does this influence the efficiency.

*Centrifugal compressor*s tend to have rather flat head versus flow characteristic. This means that changes in pressure ratio have a significant effect on the actual flow through the machine[6] (Kurz [6]). For a centrifugal compressor operating at a constant speed, the head or pressure ratio is reduced with increasing flow.

Controlling the flow through the compressor can be accomplished by varying the operating speed of the compressor. This is the preferred method of controlling centrifugal compressors. Two shaft gas turbines and variable speed electric motors allow for speed variations over a wide range (usually from 40 or 50% to 100% of maximum speed or more). It should be noted, that the controlled value is usually not speed, but the speed is indirectly the result of balancing the power generated by the power turbine (which is controlled by the fuel flow into the gas turbine) and the absorbed power of the compressor.

Virtually any centrifugal compressor installed in the past 15 years in pipeline service is driven by variable speed drivers, usually a two-shaft gas turbine. Older installations and installations in other than pipeline services sometimes use single shaft gas turbines (which allow a speed variation from about 90 to 100% speed) and constant speed electric motors. In these installations, suction throttling or variable inlet guide vanes are used to provide means of control.

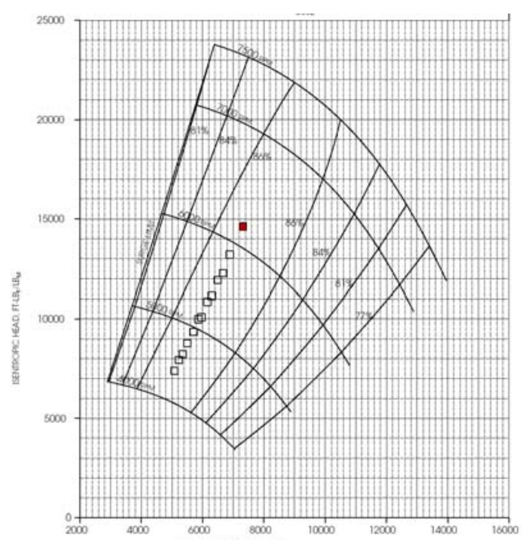

Figure 6 :Typical pipeline operating points plotted into a typical compressor performance map

The operating envelope of a centrifugal compressor is limited be the maximum allowable speed, the minimum allowable speed, the minimum flow (surge flow), and the maximum flow (choke or stonewall) (Figure 6). Another limiting factor may be the available driver power.

Only the minimum flow requires special attention, because it is defined by an aerodynamic stability limit of the compressor. Crossing this limit to lower flows will cause a flow reversal in the compressor, which can damage the compressor.. Therefore, modern control systems can prevent this situation by automatically opening a recycle valve. For this reason, virtually all modern compressor installations use a recycle line with control valve that allows to increase the flow through the compressor if it comes near the stability limit. Modern control systems constantly monitor the operating point of the compressor in relation to its surge line, and automatically open or close the recycle valve if necessary. For most applications, the operating mode with open, or partially open recycle valve is only used for start-up and shut-down, or for brief periods during upset operating conditions

Assuming the pipeline characteristic derived in Eq.20, the compressor impellers will be selected to operate at or near its best efficiency for the entire range of head and flow conditions imposed by the pipeline. This is possible with a speed controlled compressor, because the best efficiency points of a compressor are connected by a relationship that requires approximately (fan law)

$$H / N^2 = C_5 \qquad Q / N = C_6$$
$$H = Q^2 \cdot \frac{C_5}{C_6{}^2} \qquad 21]$$

For operating points that meet the above relationship, the absorbed gas power is (due to the fact that the efficiency stays approximately constant) :

$$P_g = C_7 \cdot H \cdot Q = \frac{C_5}{C_6{}^2} \cdot C_7 \cdot Q^3 = \qquad [22]$$
$$= C_5 \cdot C_6 \cdot C_7 \cdot N^3$$

As it is, this power-speed relationship allows the power turbine to operate at, or very close to its optimum speed for the entire range. The typical operating scenarios in pipelines therefore allow the compressor and the power turbine to operate at its best efficiency for most of the time. The gas producer of the gas turbine will, however, loose some thermal efficiency when operated in part load.

Figure 6 shows a typical real world example: Pipeline operating points for different flow requirements are plotted into the performance map of the speed controlled centrifugal compressor used in the compressor station.

Reciprocating compressors will automatically comply with the system pressure ratio demands, as long as no mechanical limits (rod load, power) are exceeded. Changes in system suction or discharge pressure will simply cause the valves to open earlier or later. The head is lowered automatically because the valves see lower pipeline pressures on the discharge side and/or higher pipeline pressures on the suction side. Therefore, without additional measures, the flow would stay roughly the same - except for the impact of changed volumetric efficiency which would increase, thus increasing the flow with reduced pressure ratio[7]. The control challenge lies in the adjustment of the flow to the system demands, because the without additional adjustments, the flow throughput of the compressor changes very little with changed pressure ratio

Capacity control is the method to vary the flow rate and engine load in response to end-user demand and pipeline required pressure ratio[4]. Historically, pipelines installed many small compressors and adjusted flow rate by changing the number of machines activated. This capacity and load could be fine-tuned by speed or by a number of small adjustments (load steps) made in the cylinder clearance of a single unit. As compressors have grown, the burden for capacity control has shifted to the individual compressors.

Load control is a critical component to compressor operation. From a pipeline operation perspective, variation in station flow is required to meet pipeline delivery commitments, as well as implement company strategies for optimal operation (i.e., line packing, load anticipation). From a unit perspective, load control involves reducing unit flow (through unloader or speed) to operate as close as possible to the design torque limit without overloading the compressor or driver. Critical limits on any load map curve are rod load limits and HP/torque limits for any given station suction and discharge pressure. Gas control generally will establish the units within a station that must be operated to achieve pipeline flow targets. Local unit control will establish load step or speed requirements to limit rod loads or achieve torque control.

The following equation for volume flow rate (suction conditions) helps illustrate available options[4]:

Flow = Swept Area × Stroke × Speed × Volumetric Efficiency
Volumetric Efficiency = f (Pressure Ratio, % Clearance) [23]

The common methods of changing flow rate are to change speed, change clearance, or de-activate a cylinder-end (hold the suction valve open). Another method is an "infinite-step unloader, which delays suction valve closure to reduce volumetric efficiency. Further, part of the flow can be recycled or the suction pressure can be throttled, thus reducing the mass flow while keeping the volumetric flow into the compressor approximately constant. As Table 1 shows, each method has advantages and disadvantages. Figure 7 is based on data for some of the control concepts described, and shows the impact of different control schemes on efficiency.

Capacity Control Method	Advantages	Disadvantages
Speed	Simple Control	Adverse Pulsation, impact on driver performance and emissions
Clearance Volume	Effective Control	Limited Range
Valve Unloader	Effective Control	Adverse Pulsation and Low Efficiency
Deactivate Cylinder	Effective Large Step	Adverse Pulsation and Low Efficiency
Recycle	Simple and Effective Control	Inefficient
Suction Throttling	Simple Control	Inefficient and limited Range

Table 1: Capacity Control Methods

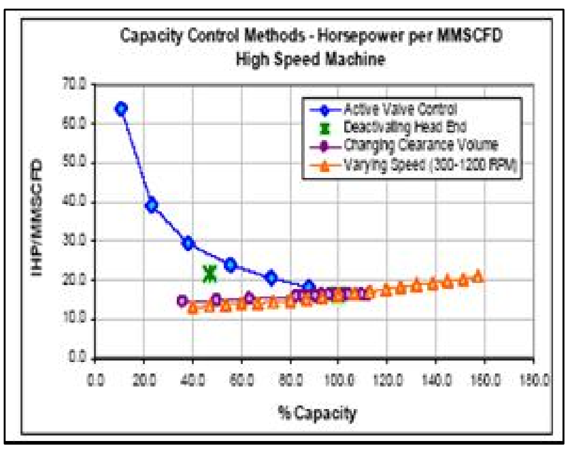

Figure 7: Compression efficiency impact of different capacity control methods[4]. Mechanical losses and losses due to pulsation control not included

Control strategies for compressors discussed in here have to be strategies that allow automation, and can be adjusted easily during the operation of the compressor. In particular, strategies that require design modifications to the compressor (for example: re-wheeling of a centrifugal compressor, or changing cylinder bore, or adding fixed clearances for a reciprocating compressor) will not be considered. It should be noted that with reciprocating compressors, a key control requirement is to not overload the driver or to exceed mechanical limits

Typically, the control strategy for a reciprocating compressor to move for the high flow high head operating point to the lower flow and lower head points would include the opening of pockets to reduce the flow. Clearance control is a frequently used controls method, as it is a very efficient method of varying the throughput (Figure 8). However, especially in low pressure ratio applications, the amount of range that can be achieved is limited (Figure 9[4]). On its way from the suction line into the compressor cylinder, or out of the cylinder into the discharge line, the gas encounters flow resistance not only in the valves but also in the valve pockets. These additional pressure drops are called pocket losses. Based on published laboratory measurements, these pocket losses can

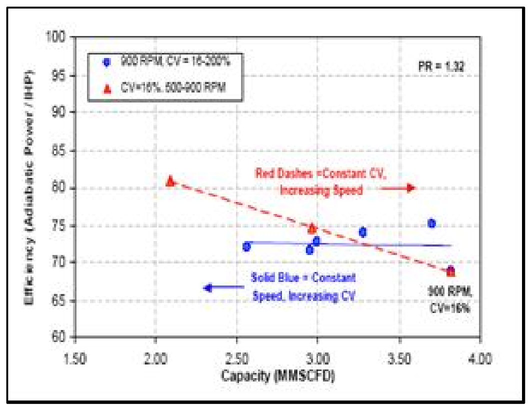

Figure 8: Measured Efficiency for Constant Clearance at variable speed and constant speed at variable clearance[4]

be quantified as long as flow areas in valves and valve pockets are constant. In reality, however, these flow areas are not constant but variable. This is easily understood in the case of a valve which opens, closes, and sometimes even flutters. With a pocket, this is less obvious, nevertheless its flow area may vary as a result of piston masking[8]. With modern short stroke high speed compressors, it may happen that the piston masks the pocket during 80% of its stroke. This may have a considerable impact on pocket losses.

Speed control (Figure 7and 8) can be used if the compressor is driven by an internal combustion engine, or a variable speed electric motor.

Reduction in speed will reduce mechanical losses and valve losses. Especially internal combustion engines, but also variable speed electric motors, produce less power if they operate at a speed different form their optimum speed. Internal combustion engines allow for speed control in the range of 70 to 100% of maximum speed. However, the requirement to meet lower emissions requirements often significantly reduces the allowable range of speeds. In general, the efficiency of a gas engine remains high, if it can be controlled to operate at 100% torque. In most applications, flow reduction is not initiated by a reduction in speed, due to concerns about driver flexibility (emissions and efficiency), and, in particular for high speed separable compressors, due to concerns about pulsation control[9] .

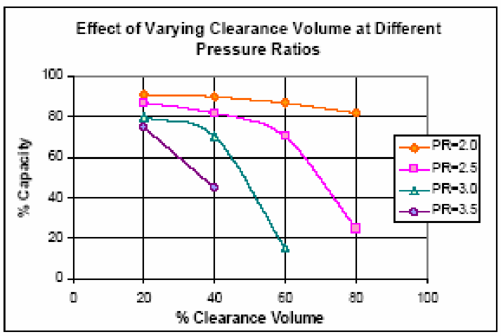

Figure 9: Effectiveness of Clearance Control for various pressure ratios[4]. The effectiveness improves with increased pressure ratio. For typical pressure ratios in pipeline applications (PR<2.0), the flow range that can be achieved is very limited.

Other control methods, such as external or internal bypass (Figure 10) or suction throttling allow to control flow very effectively, but will significantly reduce the efficiency of the compressor.

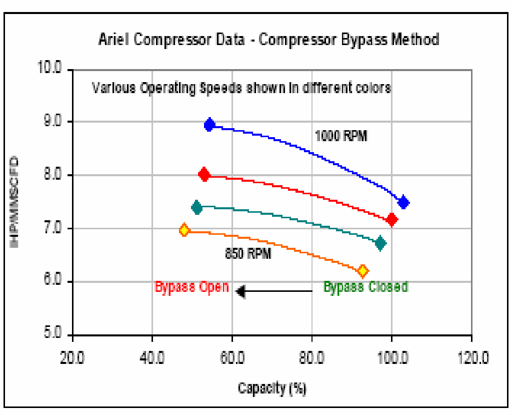

Figure 10 :Bypass control reduces efficiency (in Power per Standard Flow), but allows for a wide range of flow conditions[4].

Valve Unloaders are also quite effective controlling the flow through the machine. However, they basically still cause the same suction valve losses as in a loaded machine, i.e. the efficiency is reduced[9]. This is also true for infinite-step-unloaders, working with timed valve closing, because they keep the valve power losses about constant, while the work done by the compressor is reduced. Therefore, the compressor efficiency is reduced gradually with increased valve timing. Since the valve losses depend on flow and (to a lesser extent) density of the inlet and discharge flow respectively they would likely be reduced due to the lower volumetric flow. Ely et al.[10] present test data showing the effect of changes in pressure ratio and speed on reciprocating compressor efficiency (they did not evaluate the impact of unloaders and pockets on performance) or, to be more precise, on the portion of the valve losses on efficiency: If the pressure ratio is reduced from the design value, valve losses go up and therefore compressor efficiency is reduced. Similarly, as speed is reduced, the valve losses go down. If a given valve has a non-dimensional pressure loss coefficient ξ, then the power loss P loss due to this valve is

$$P_{loss} = const \cdot L_{stroke} \cdot A_{piston} \cdot N \cdot \xi \frac{\rho}{2} Q^2 \quad [24]$$

with L_{stroke} the compressor stroke, A_{piston} the area of the piston, N the compressor speed and Q the actual flow through the valve.

If the compressor has the capability for stepless clearance control, adjustment to any operating point on the curve is possible. If clearance control is in discrete steps, it may have to be combined with the capability to turn units on or off in a multiple unit station. In general, adjustment of the compressor to different flow conditions is possible, but it is in many cases done in a series of discrete, rather than continuous steps.

Different control devices are also distinguished by the smoothness of load changes they allow. End deactivation, but also the addition of fixed clearances, will allow only relatively large discrete load and flow changes. Variable clearance changes and infinite step unloaders allow smoother adjustments of load and flow.

Since valve performance is critical to compressor efficiency and reliability, pipeline companies have found it advantageous to invest in studies to determine which of the existing passive valve models perform most reliably. Noall and Couch[1] stated that a reciprocating gas compressor's efficiency is linked to the performance of the intake and discharge valves. The study investigated six different compressor valves from five manufacturers in order to determine valve efficiency, reliability, and cost of operation. The six-month investigation found that valve efficiencies were directly related to compressor ratios, where a decline in efficiency was attributed to valve leakage at low compression ratios. In addition, this study found that the losses through suction valves were approximately twice as great as the discharge valve losses. Figure 11 shows some of the results. The results don't indicate clearly whether the reduced valve efficiency is only due to the increased leakage, or whether other effects (such as increased volumetric flow even for constant mass flow) add to the losses.

Lastly, the mechanical losses of a reciprocating compressor are mostly speed dependent, and to a very limited amount load dependent. This means, that for constant speed, the mechanical power losses will stay more or less constant, which means that the mechanical efficiency will be reduced if the load is reduced at constant speed.

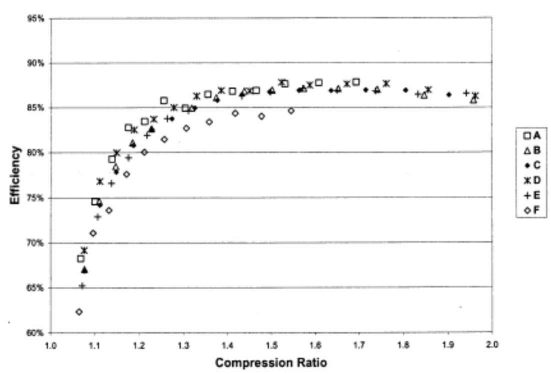

Figure 11: Valve efficiency for new valves (from 6 different manufacturers) as a function of compressor pressure ratio[1].

11. Conclusions

We have presented a universal method to describe the efficiency of a compressor station based on the definition of appropriate system boundaries. This allows to include the losses associated with the compression process.

Further, a methodology for appropriate treatment of losses due to unsteady flows has been outlined.

By describing the behavior of centrifugal compressors and reciprocating compressors at off-design conditions, in conjunction with the control concepts used, the reader gets an appreciation for the impact of these concepts on the operating efficiency. The off-design conditions are based on conditions as they are imposed by typical pipeline operations.

The ultimate goal of this paper is to serve as the basis of performance improvement on the station level, notwithstanding the type of compression equipment used. The accurate assessment of equipment efficiency is the basis for any improvement in performance. Understanding the impact of off-design operation further enhances operational efficiency. Today, operating equipment efficiency means more than reducing fuel cost and increasing the capacity of existing installation. It also means a reduction in CO_2 emissions for a given compression task.

12. Acknowledgements

The authors would like to acknowledge the contributions of Dr. Ralph Harris to this paper.

13. Nomenclature

A:	area
C_1-C_7:	constants
C_p:	specific heat capacity
D:	diameter
f:	friction coefficient
h:	enthalpy
k:	isentropic exponent
LHV:	lower heating value
$\dot{m}$:	mass flow
N:	speed (1/s)
p:	pressure
P:	power
PR:	pressure ratio
q:	heat
Q:	flow
s:	entropy
t:	time
T:	temperature
T:	time period
W_t:	work
V:	volume
x:	distance
η:	efficiency
ρ:	density
ξ:	loss coefficient
ω:	frequency

Superscripts

~:	amplitude

Subscripts

1:	inlet condition
2:	discharge condition
disch:	discharge
fuel:	fuel
g:	gas

i: indicated
m: mechanical
s: isentropic
suct: suction
std: at standard conditions
th,PM: thermal, prime mover
theor: theoretical

References

[1] Noall, M., Couch, W., "Performance and Endurance Tests of Six Mainline Compressor Valves in Natural Gas Compression Service," Gas Machinery Conference, Salt Lake City, Utah, 2003.

[2] Kuettner,K.H, Mollenhauer, K., 'Kolbenmaschinen' in 'Dubbel-Taschenbuch fuer den Maschinenbau', Springer, 1990

[3] Borsig GmbH, 'Borsig Pocket Book', Berlin, 1985

[4] Deffenbaugh,D.M., Smalley,A.J., Brun, K.,Broerman, E.L.,Harris, R.E., Hart, R.A., Harrell,J.P., Nored, M.G., McKee,R.J., Gernentz,R.S., Moore,J.J.,Siebenaler,S.P., Scedeman,S.J., 'Advanced Reciprocating Compression Technology - Final Report',SwRI, San Antonio, Tx, 2005.

[5] Kurz, R., Lubomirsky, M.,'Asymmetric Solution for Compressor Station Spare Capacity', ASME Paper 2006-90069, 2006.

[6] Kurz, R., 'The Physics of Centrifugal Compressor Performance', Pipeline Simulation Interest Group, Palm Springs, 2004.

[7] Gajjar, H., 'Natural Gas Reciprocating Compressor Sizing and Evaluation' , Gas Machinery Conference, Covington, KY, 2005.

[8] Machu,E.H., 1998, 'Problems with modern high speed short stroke reciprocating compressors: Increased power requirement due to pocket losses, piston masking and gas inertia, eccentric gas load on the piston', Gas Machinery Conference, 1998.

[9] Brahler,C., Shade,W.N., Hickman,D.A., Miller,E.J., 2005,'Performance Control of Reciprocating Compressors: Devices for managing Load and Flow', Gas Machinery Conference, Covington, KY, 2005.

[10] Ely,C.G, Anderson, R., Burdette,S., Couch,W.A., Harrington, T., Harrison,J., Howerton, B., Linn,C., Moosa, G., Noall,M., Stampka,S., 2005, 'Compressor Efficiency is Worth How Much?', Gas Machinery Conference, Covington,KY, 2005.

Development And Test Of An Electrical Valve Actuator For Reverse Flow Capacity Control Of Reciprocating Compressors

Herbert Kopecek, Helge Klockow, Michael Schmitz
Global Research
General Electric
Garching
Germany
Herbert.kopecek@ge.com

Simone Pratesi, Carlo Mazzali, Paolo Battagli
Oil and Gas
General Electric
Florence
Italy

6th Conference of the EFRC
October 28th / 29th, 2008, Düsseldorf

Abstract:

The amount of gas delivered by large reciprocating compressors is often controlled by forcing the inlet valves open over a certain time period. To achieve fast cycle by cycle control without the drawbacks of a hydraulic system, namely the high pressure hydraulic oil supply, a fully electrical valve actuation system was investigated that allows for fast inlet valve control. Prototypes of the actuation system have been theoretically and experimentally investigated with respect to their mechanical, dynamical and thermal behaviour.

1 Introduction

Large reciprocating compressors are often controlled by forcing the inlet valve open over a certain time period. This inlet valve control may be done by pneumatic or hydraulic means. Usually the pneumatic actuation allows for a relatively slow actuation speed, so the inlet valve is kept open for several piston strokes, meaning during the time of actuation, the cylinder delivers no flow to the discharge line, the cylinder idles. De-actuating the mechanism means the compressor operates back on full load. Hydraulic systems allow for a more sophisticated load control. These systems are fast enough to release the inlet valve at some portion of the compression stroke. This can be used for a so-called step less load control of the compressor.

To overcome several difficulties of a hydraulic system, namely the high pressure hydraulic oil supply and the electric current supply of the control valves of such systems, a fully electrical variable valve control system has been developed that allows for fast inlet valve control. The system comprises of an electromagnetic actuator that is able to provide the required force of 5kN to keep the valve open against the compression of the piston and that is fast enough to allow for compressor rotational speeds of 600 rpm. A highly adaptable control system has been developed that allows for step-less part load under operation over a wide range of flow rates. Prototypes of the actuation system have been theoretically and experimentally investigated with respect to their mechanical, dynamical and thermal behaviour.

2 Problem Background

Under full load operation, the inlet valve of large reciprocating compressors opens against the differential pressure between the cylinder and inlet during the suction stroke; analogous it closes during the compression stroke. For full load operation, no additional control, or mechanics is required; the valve opening is a passive event, controlled solely by the pressure differences at both sides of the valve plate or rings.

To control the output the inlet valve should be forced open over a certain percentage of the compression stroke. At a specified point, the force should be released and the valve plate closes the inlet valve again. From this time on, the rest of the compression stroke then delivers the flow to the discharge valve. The compressor operates at part load. Changing the release point means changing the part load point[1-5]. Figure 1 shows the principle of inlet valve actuation in the pressure-volume diagram.

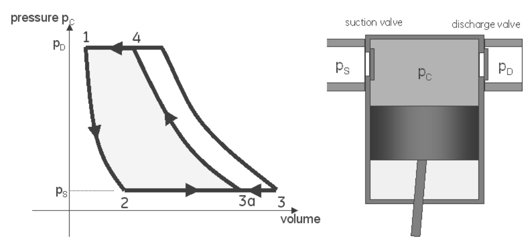

Figure 1: Pressure-volume diagram for part load operation

3 Actuation System Design

An electromagnetic solenoid was designed to actuate a single compressor valve. The actuator has to fulfil the following requirements:

- Holding force: 5000 N
- Lift: 4.6mm
- Max. switch on time: 24 ms
- Max. switch off time: 10 ms
- Repetition rate: 10 Hz (600 rpm)
- Max. surface temperature: 120 °C
- Max. core temperature: 180 °C
- Max. dimensions: 280 x 280 x 250 mm
- Max. weight: 30 kg

The design process was divided into the following steps:
1- Conceptual design of actuator and power electronics
2- Detailed design of the magnetic components (core plus coils) using finite element software to calculate magnetic field distribution
3- Dynamic modelling of the system to evaluate

transient behaviour of the actuator
4- Prototype manufacturing
5- Testing and validation of the prototype on a specially designed test rig

From a pool of different electromagnetic actuation concepts, a design for the solenoid was found to be the most suitable one for compressor applications, since it is of low complexity and can be built in a very robust fashion. However, the authors want to mention that there are also other different concepts for electromagnetic valve actuators like e.g. published by Haas[6]. The actuator type investigated in this study comprises a plunger connected to an anchor plate, which is attracted by a single magnetic core if current is applied through an electric coil. The plunger then pushes against a finger unloader which itself pushes against the valve plate or valve rings (see Fig. 2). At the same time an unloader spring and an actuator spring is compressed which leads to the counteracting force being necessary to return plunger plus unloader in case the current is turned off. Figure 3 shows the actuator prototype.

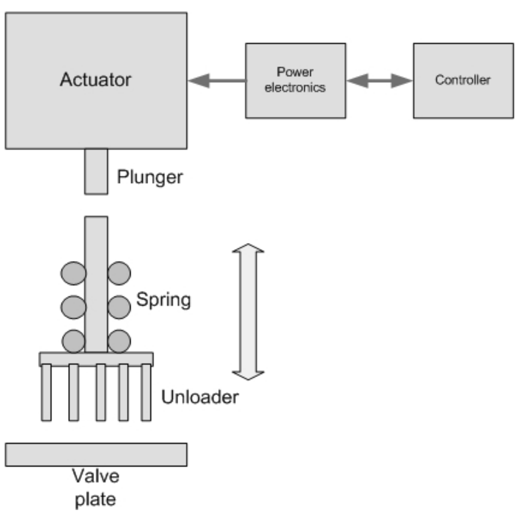

Figure. 2: Concept - Valve actuation system

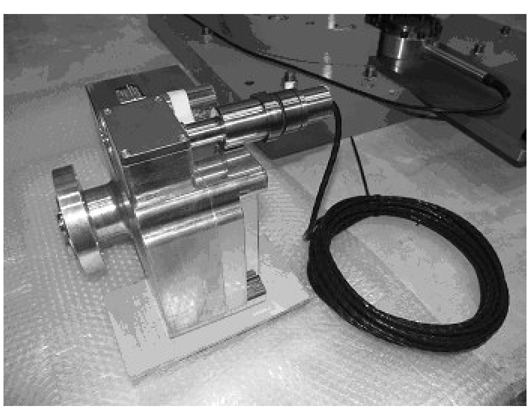

Figure. 3: Prototype of the electromagnetic valve actuator

The power electronics consist of a programmable frequency converter of proper electric power. The control algorithm was implemented on a rapid control prototyping platform, which sends the pulse width modulated (PWM) control signals to the converter. Closed loop control of the actuator current was implemented. The plunger position was predicted and the current was adapted during the stroke accordingly. This allows reducing the impact velocity when the unloader hits the valve plate without violating the maximum switch-ON time of 24ms.

4 Results

4.1 Dynamic Model

To evaluate the dynamic behaviour of the actuator, a transient model of the actuation system (actuator, unloader, springs) was developed. The model consists of a mechanical part, which contains the differential equations for the moving parts (plunger unloader and springs), the magnetic part, which calculates the time dependent magnetic flux and the current, and the control part, which involves the control loop of the actuator current.

Figure 4 shows the model concept for the mechanical part. The masses of unloader and plunger are connected via springs to the reference ground. The magnetic force is moving the masses of plunger and unloader in positive x directions. The springs are acting in negative x-direction if compressed. Equation 1 gives the mathematical expression for the moving masses. The friction term was set proportional to the square of the moving velocity of the plunger and a friction constant k. The spring constant c defines the return force of the spring for a specific length of compression. The model considers only one mass and one spring constant for both unloader and plunger, but change this mass according to the position of both. If the plunger does not touch the unloader the net moving mass is only the plunger mass and the spring constant is equal to the one of the actuator springs. If the plunger reaches the position where it touches the unloader, the net moving mass becomes equal to the sum of unloader and plunger mass, and the spring constants of both springs add up.

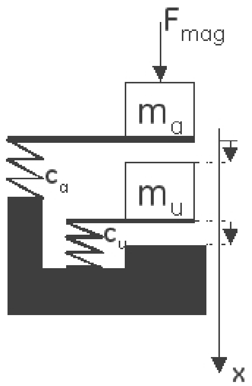

Figure. 4: Mechanic model of the actuation system; m_a…plunger mass, m_u…unloader mass, F_{mag}…magnetic force

$$m \cdot x'' + k(x')^2 + cx = F_{mag} \qquad (1)$$

The model also considers bouncing effects of the moving mass. This was implemented by considering the balance equation of momentum, which leads to the effect, that the velocity just changes it sign shortly after the impact[7].

The magnetic part of the model considers the relation between the magnetic flux inside the magnetic circuit and the current through the coils, the coil resistance, the relation between magnetic force, air gap, and current, and the properties of the magnetic materials. Magnetic hysteresis effects as well as leakage flux and eddy current effects were neglected.

The control part consists of a PID-closed control loop for the actuator current.

Upper left plot of Figure 5 depicts the simulation of desired- and real current during the switch-ON- and switch-OFF event. It can be clearly seen, that the controller is able to set the current to the desired value quite quickly. However, to reduce the switch-ON time, initially a higher current is applied for a short amount of time (10 ms). At the holding position, the current is reduced again to its nominal value to achieve the required holding force.

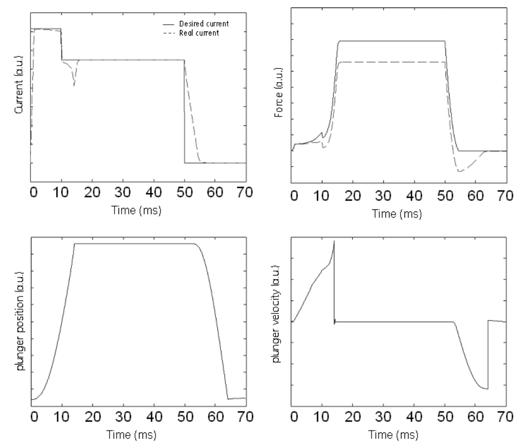

Figure. 5: Dynamic model results; upper left: Simulation of current (solid: desired current, dashed: real current), upper right: Simulation of actuation forces (solid: magnetic force of actuator; dashed: magnetic force minus spring forces of unloader and actuator springs, lower left: position of the plunger, lower right: plunger velocity

Upper right plot of Figure 5 illustrates the magnetic force induced by the current and the net actuation force, which is the magnetic force minus the spring forces. It shows, that with this design, the net actuator force, which acts on the valve plate, is above the required 5000 N. During the switch-OFF event, the spring forces are higher than the magnetic force, which leads to the desired negative net force and returns plunger and unloader to their OFF-position.

Lower left plot of Figure 5 shows the position of the plunger. The switch-ON time is found to be about 15 ms. In the velocity plots of figure 5, one can detect soft bouncing of the plunger at the end of the turn on event. Due to the type of solenoid, the shape of the velocity is much smoother during the turn off event than during the turn on event.

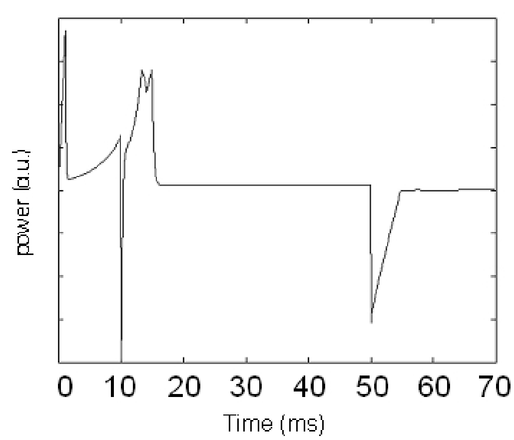

Figure. 6: Simulation of the electric power exchanged between actuator and AC/AC converter; Overall consumed power = average = 186 W

The electric power transferred between power electronics and actuator can be seen in figure 6. A positive value for the power means that energy is transferred from the capacitor of the power electronics to the actuator, a negative value means the opposite case. Although transferred peak powers can be in the kW range, the overall power consumption of the system is comparably low (less than 200W).

With help of the results and conclusions of the dynamic model, the detailed design of magnetic circuit, springs and power electronics could be finished.

4.2 Experiment

A special test rig was developed to experimentally verify functionality and specifications of the actuator prototype. With this test rig, it was possible to run the actuator up to the nominal repetition rate of 10 Hz. Time resolved positions of unloader and plunger were measured. by eddy current sensors. A specially designed load cell measured the actuator force, which was able to withstand 70 kN of dynamic force. Figure 7 depicts the scheme of the test rig.

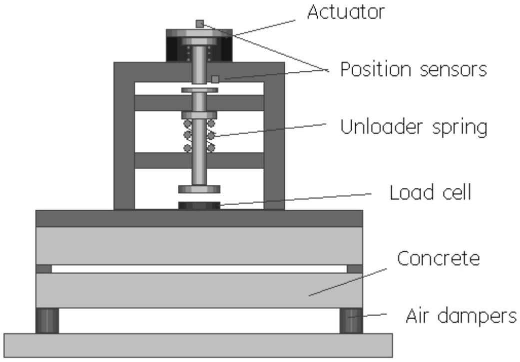

Figure. 7: Test rig conceptual design

The actuator mounted on the top moves its plunger towards the unloader, which itself moves towards the load cell. The return spring is compressed during that forward movement, which pushes both, unloader and plunger, back to initial position if the current is turned off. The whole setup is based on four air dampers to decouple it from the rest of the building. The overall weight was increased to 8 tons by blocks of concrete to avoid resonance effects. Figure 8 shows the test rig without the actuator (left) and with the actuator on top of the rig (right). The load cell was mounted on a skid to move it out for maintenance and disassembly.

Figure.8: Actuator test rig: left – without actuator, right: with actuator prototype on top

4.2.1 Static tests

Static tests were carried out to verify relation between currents, stroke and actuator force. Figure 9 illustrates the position of the plunger, Fig 10 the actuator force, both depending on current through the actuator coil. The numbers gives the sequence of the measurement:

Starting without current and the actuator being in initial position, the current was increased until the plunger starts to move and hits the unloader in 1. Significantly higher current is needed to overcome the spring force of the unloader spring to bring plunger and unloader to its final position in 2.

The current has to be reduced below some critical value to move both unloader and plunger back to their initial position in 3.

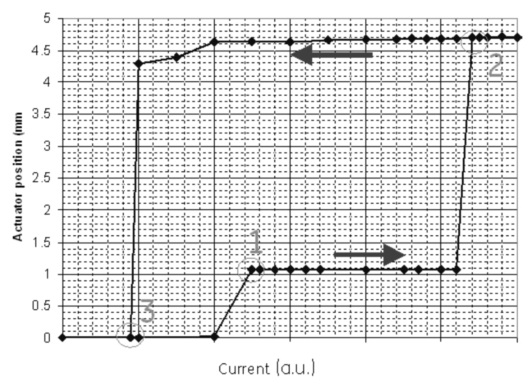

Figure. 9: Static measurements of actuator position vs. current; 1 – plunger hits unloader, 2 – unloader hits load cell, 3 – unloader and plunger moving back to initial position

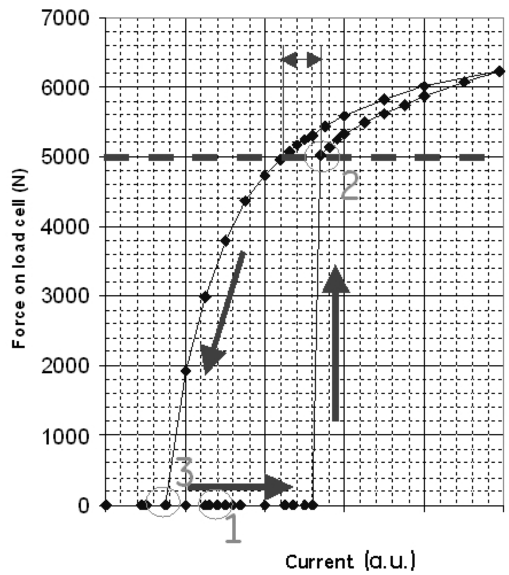

Figure. 10: Measurement of the static force on load cell depending on current; 1 – plunger hits unloader, 2 – unloader hits load cell, 3 – unloader and plunger moving back to initial position

The observed hysteresis is a consequence of magnetic hysteresis of the core material and sticking effects. The static tests also demonstrate the difference between switch-ON and switch-OFF behaviour of the actuator. This is based on the nonlinear relation between magnetic force and the air gap between anchor plate and magnetic core.

4.2.2 Dynamic tests

Figure 11 shows the measured force, current, unloader velocity and position during the switch-ON event (the velocity was calculated by differentiation of the position signal). At t=2ms the desired current is set from 0 A to its nominal value. Due to the coil inductance and the limited supply voltage, the maximum slope of the current is limited. At t=10ms the plunger starts to move, which leads to a reduced air gape between anchor plate and magnetic core, and, as a consequence, to an increased inductance. Since the controller is not able to compensate these quick change of the inductance, the current deviate from the desired one for a short time. At t=16 ms, the unloader hits the load cell and the controller is now able to reach the desired set point of the current. Bouncing effects can be detected out of the plots for force, velocity and position. This bouncing effects lead to increased wear and should be reduced as much as possible. Different control algorithm for soft landing can be implemented but they mostly lead to increased switch-ON times.

These measurements demonstrate that the actuator is able to stay below the maximum switch-on time of 24ms, which was required by specifications.

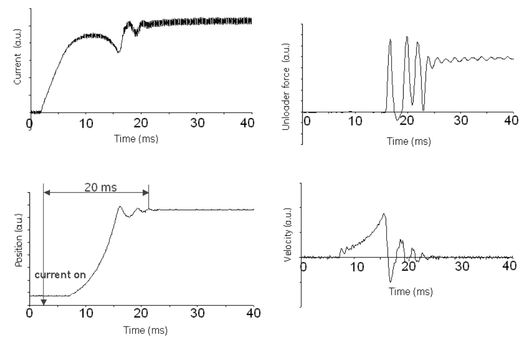

Figure. 11: Dynamic measurement during switch-on event; upper left: current, upper right: force on load cell, lower left: unloader position, lower right: unloader velocity

A typical turn-off event is illustrated in Figure 12. At t=14ms, the desired current is reduced from nominal value to 0A. Because of the induction voltage, the reduction of current is delayed. The position plot indicates again bouncing effects when the unloader reaches its initial position. The duration between the time when current is turned off and the time when the unloader reaches its final position is about 15ms in this case. If the delay of the reduction of the magnetic field is considered in the control strategy, the system is able to stay below the specified switch-OFF time of 10 ms. On a real compressor, drag forces would further accelerate the unloader and thus would lead to significantly shorter switch-OFF times. In this case, the specification for the switch-OFF time should be fulfilled anyway.

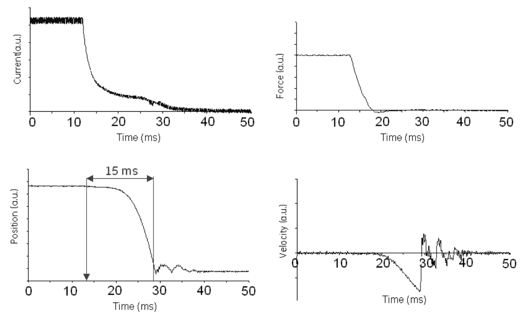

Figure. 12: Dynamic measurement during switch-off event; upper left: current, upper right: force on load cell, lower left: unloader position, lower right: unloader velocity

4.2.3 Thermal measurements

It is crucial for the application that the actuator surface- and core temperatures stay below the specified limits. The hot spot inside the actuator is the centre of the coil, which limits the maximum electric power consumed by the actuator. This hot spot is limited to 180 °C because of material issues of the insulation of the copper wire. The surface temperature of the actuator has to stay below 120°C to fulfil requirements of an explosion-sensitive environment. Therefore, both temperatures were measured during a mid-term test (see Fig. 13)

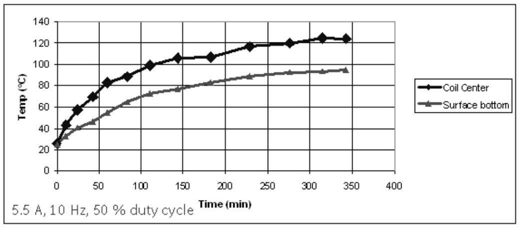

Figure. 13: Measured temperature development inside the coil and on the surface of the actuator

These measurements demonstrate, that the surface- as well as the core temperature stays below the required limits for the measured time period. It also indicates the characteristic heating time constant of the system to be in the range of ~ 100 minutes. However, for the compressor application it is necessary to do long term testing under more compressor-relevant conditions including surrounding flow, necessary containments and maximum possible ambient temperatures.

5 Conclusion and Outlook

A prototype of an electromagnetic actuator was developed to control the opening time of compressor valves. The prototype was tested on a specially designed test rig to verify specification limits. It could be demonstrated that the device is able to provide 5000 N of holding force as specified. The measured switch-ON time could be kept below the required upper limit of 24 ms. The switch-OFF time was 15 ms and thus slightly above the specification of 10ms. However, on the real compressor, gas forces will assist to push the unloader back to its initial position and hence will shorten the switch-OFF time significantly.

Surface- and core temperatures of the actuator stayed in between the given limits of 120 °C for the surface and 180°C for the core. However, thermal properties of the design and the materials used should be improved to make sure that the temperature limits are not reached even under more challenging conditions (i.e. ambient temperature up to 50 °C, thermally isolated containment, hot surrounding flows)

Next step should include optimization of the mechanic design, improvement of the thermal behaviour and tests on a compressor.

6 Acknowledgements

This work was partly sponsored by the Bavarian Ministry of Economics under the contract number 07 05/893 75/1096/05/3871/06.

References

[1] Costagliola M., “The Theory of Spring Loaded Valves for Reciprocating Compressors”, Journal of Applied Mechanics, Dec. (1950)

[2] Giacomelli E., Falciani F., Manetti S., “A New System to Simulate the Influence of Pressure Pulsation on Reciprocating Compressor Valve Behaviour”, Quaderni Pignone N. 46, (1988)

[3] Giacomelli E., Falciani F., Dini R., Giusti A., “Design and Service Engineering to Improve Reliability of Reciprocating Compressors”, NPRA 2001, Clean Fuels Challenge, Aug. 28-29, Houston TX, USA, National Petrochemical and Refiners Association, CFC-01-211, (2001)

[4] Mac Laren J.F.T., Tramscheck A.B., Pastrana O.F., “A Study of Boundary Conditions Encountered in Reciprocating Compressor Systems”, Proc. Compressor Technology Conference, University of Purdue, (1976)

[5] Traversari A., Lacitignola P, “Use and Calculation of Ring type Valves for Reciprocating Compressors”, Quaderni Pignone N.16

[6] Haas, “New technologies for reciprocating compressors based on combustion engine know how”, Compressors and their Systems, C591/038/2001, IMechE, (2001)

[7] Kaltenbach, Eick, Quendt, Ströhla, Feindt, "Elektromagnete", Stuttgart (2003)

Hydrodynamic calculation method for crosshead pin bearings especially under less rod load reversal loading

by:

Klaus Hoff

Egidius Steinbusch

Central Division of Technology

Neuman & Esser

Übach-Palenberg

Germany

klaus.hoff@neuman-esser.de

egidius.steinbusch@neuman-esser.de

6^{th} Conference of the EFRC

October 28^{th} / 29^{th}, 2008, Dusseldorf

Abstract:

Contrary to main and crank pin bearings of reciprocating compressors, the hydrodynamic working mechanisms of crosshead pin bearings are not fully understood so far. While for the rotating bearings the hydrodynamic pressure build-up both by tangential and radial movement of the journal takes place the crosshead pin bearing can only make use of the hydrodynamic pressure build-up by radial movement due to the lack of a real tangential movement. Since this pressure build-up needs a radial movement the API 618 e.g. demands a certain amount of rod load reversal.

Due to authors' experience the allowable loading of the crosshead pin bearing depends on the amount of rod load reversal. A bearing with a close to perfect rod load reversal loading can handle much more loading than the same bearing under a load with the same peak load but a marginal rod load reversal according to API 618 restrictions.

This paper explains by description of the theory and by some exemplary calculations the reason for the mechanism. Some influencing design parameters are given to improve or worsen the load capability. Generally, an optimum bearing design depends on the loading.

1 Introduction

The typical design of reciprocating compressor's plain bearings is done by defining a mean load value, which is the maximum rod load acting at the bearing divided by the projected area of the bearing. This design value mainly depends on the bearing material and the special bearing design concerning the oil supply grooves and/or holes. This value is, of course, the special know-how and secret of the compressor manufacturer. Mean load values up to 25 MPa are realized for modern tri-metal, aluminium or bronze bearings if the governing design parameter are properly chosen.

The assumption behind this design procedure is that the maximum hydrodynamic oil peak pressure and the minimum oil film thickness are directly connected with a mean load value. As long as the mean value doesn't exceed a critical value and the main design influences remain within certain limits this assumption is allowable and expresses the good experiences of manufacturers and users.

By the availability of modern designing tools, a general trend is visible to further increase also the load capability of plain bearings. This upgrading process, of course, is only possible if the real hydrodynamic bearing process is understood and taken into the consideration. The mean load design approach doesn't take important influencing factors into account, like the relative bearing clearance, the oil viscosity and the speed.

For bearings with no grooves or holes along the bearing circumference approximated procedures are available[1]. The description of the method, especially concerning the appropriate choice of the boundary conditions can be found in the literature[2,3]. These methods solve the Reynolds' differential equation numerically for both pressure build-up mechanisms, the pressure build-up by the rotation and by the radial movement of the journal, which take place in the bearings of reciprocating compressors. The numerical solution is summarized in a functional relation between the Sommerfeld number for rotation and radial displacement respectively on the one hand and the relative eccentricity and ratio of width to diameter of the bearing on the other hand. These functional relations are approximated by polynomial expressions. By applying these functional relations, it is not necessary to solve the Reynolds' differential equation again and again for each individual case which would be a time consuming procedure.

Various methods determine the displacement orbit of the journal in the bearing by applying these expressions. The basic idea is that the equilibrium must exist between the internal load by fluid pressure and external bearing load for each time step. The calculation procedure starts with a reasonable start condition and is repeated for each time step and some revolutions until convergence is reached, meaning no deviation in the displacement orbit. The various methods are described by Holland[4], Hahn[5] and Booker[6]. Knoll[7] and Waltermann[8] compare the different methods in order to assess the results which are not identical.

These methods are perfectly applicable for the main and crank pin bearing of a reciprocating compressor since they are very fast and the restricting conditions are fulfilled: The oil supply grooves are circumferentially arranged in the bearing centre or axially positioned in the unloaded area of the bearing and the bearing is always completely filled with oil by the rotary transport mechanism.

These methods are not applicable for crosshead pin bearings since for this type of bearings oil supply grooves are usually arranged also in the highly loaded area of the bearing. This design feature is necessary since the crosshead pin bearing needs a good refilling with fresh oil due to the lack of a real rotary movement. This is especially true for load scenarios with less rod load reversal. The other very important deviation from the theoretical assumption is that the bearing is always completely filled with oil at any location. For the crosshead pin bearing, the oil in the load area vaporizes when the load reverses. At this point in time, there is almost no physical mechanism creating the load equilibrium. The result is that the journal moves very fast to the other side of the bearing. This movement creates tension stresses in the former loaded oil film. Since liquids cannot transmit tension stresses the pressure falls below the vapour pressure and the vaporization takes place. This area needs to be refilled from the oil supply grooves during the time the journal is acting on the other bearing side. It is obvious that this refilling can be difficult for a load scenario with less rod load reversal. From these qualitative considerations, it is clear that the crosshead bearing design does not purely depend on the peak load but also on the rod load reversal.

This paper describes a hydrodynamic calculation method which accounts for all important features concerning the crosshead pin bearing design. The presented tool is able to predict the maximum oil peak pressure to assess a possible fatigue problem, the minimum oil film thickness to assess a possible wear problem and the refilling process to assess a possible wear problem due to lack of oil.

A by-product of this method is a very simple relationship between dimensionless load and dimensionless min oil film thickness.

2 The Hydrodynamic Algorithm

2.1 Definitions

For the algorithm some simplifications were assumed which are very common in the hydrodynamic bearing theory.

- Both the journal and the bearing are assumed to be absolutely rigid. Circles remain circles under the load.
- Bearing axis and journal axis are parallel.
- Surfaces are ideally plane.
- The oil is a Newtonian fluid. There is no dependency of the oil viscosity on the shear rate.
- Laminar flow is assumed.
- The temperature and, therefore, the viscosity of the oil within the bearing gap are constant.
- The pressure dependency of the oil viscosity is neglected.

2.2 Reynolds' Differential Equation for the Crosshead Pin Bearing

In **figure 1,** an arbitrary eccentric position of the journal within the bearing is given. The eccentricity is the distance between the journal centre and bearing centre.

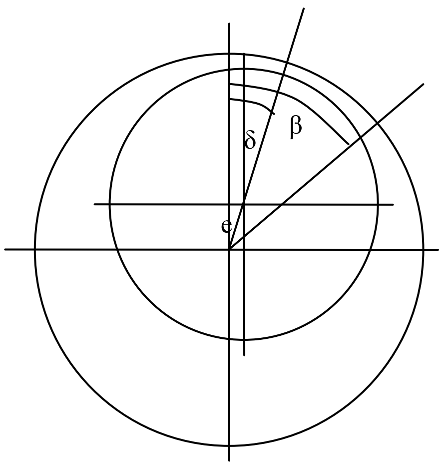

Figure 1: Geometrical definitions of the eccentric journal within the bearing shell

The angle δ denotes the angle between 12 o'clock position and the shortest distance between journal and shell (the minimum oil film thickness). The angle β is the independent variable the other values depend on.

The die gap can be described as a function of the relative eccentricity $\varepsilon = e/(R-r)$, the relative bearing clearance $\psi = (R-r)/r$, the journal radius r, the bearing radius R and the circumference angle β. Since ε(t) and δ(τ) is a function of the crank angle and therefore of the time t the die gap is dependent on time t and angle β:

$$h(\beta, t) = r\,\psi\,(1 - \varepsilon(t)\cos(\beta - \delta(t)))$$

The transient angular speed of the crosshead pin bearing is a function of the compressor speed ω and the connecting rod ratio λ:

$$\omega_K(t) = \frac{\lambda\cos(\omega t)\,\omega}{\sqrt{1 - \lambda^2\sin(\omega t)^2}}$$

The derivation of the general Reynolds' differential equation is extensively described by Lang[1]:

$$\left(\frac{\partial}{\partial x} h(x,t)^3 \left(\frac{\partial}{\partial x} p(x,z,t)\right)\right) + \left(\frac{\partial}{\partial z} h(x,t)^3 \left(\frac{\partial}{\partial z} p(x,z,t)\right)\right) = 6\,\eta\left(\omega_K(t)\,r\left(\frac{\partial}{\partial x} h(x,t)\right) + 2\left(\frac{\partial}{\partial t} h(x,t)\right)\right)$$

Herein, $x = r\cdot\beta$ denotes the circumference coordinate, z the axial coordinate, η the dynamic viscosity and p(x,z,t) the hydrodynamic pressure which, of course, is dependent on location and time.

The expressions for the die gap and the transient angular speed can be inserted in the general Reynolds' differential equation

$$\left(\frac{\partial}{\partial\beta}(1 - \varepsilon(t)\cos(\beta - \delta(t)))^3\left(\frac{\partial}{\partial\beta}\mathrm{So}(\beta, b, t)\right)\right) + \left[2\frac{r}{B}\right]^2\left(\frac{\partial}{\partial b}(1 - \varepsilon(t)\cos(\beta - \delta(t)))^3\left(\frac{\partial}{\partial b}\mathrm{So}(\beta, b, t)\right)\right) =$$

$$6\frac{\lambda\cos(\omega t)\left(\frac{\partial}{\partial\beta}(1 - \varepsilon(t)\cos(\beta - \delta(t)))\right)}{\sqrt{1 - \lambda^2\sin(\omega t)^2}} + \frac{12\left(\frac{\partial}{\partial t}(1 - \varepsilon(t)\cos(\beta - \delta(t)))\right)}{\omega}$$

In this equation, the pressure was replaced by the dimensionless Sommerfeld number.

$$\mathrm{So}(\beta, b, t) = \frac{p(\beta, b, t)\,\psi^2}{\eta\,\omega}$$

The axial coordinate z was replaced by the dimensionless coordinate $b = 2z/B$ where the axial width of the bearing is introduced with B. The differentiation can be done partly. Finally, one receives the ordinary partial differential equation for the unknown Sommerfeld numbers dependent on time and location and the relative eccentricity ε(t) and location of the minimum oil film thickness δ(t) which are time dependent.

$$3\,(1-\varepsilon(t)\cos(\beta-\delta(t)))^2\left(\frac{\partial}{\partial\beta}\mathrm{So}(\beta,b,t)\right)\varepsilon(t)\sin(\beta-\delta(t))$$
$$+\,(1-\varepsilon(t)\cos(\beta-\delta(t)))^3\left(\frac{\partial^2}{\partial\beta^2}\mathrm{So}(\beta,b,t)\right)$$
$$+\left[2\,\frac{r}{B}\right]^2(1-\varepsilon(t)\cos(\beta-\delta(t)))^3\left(\frac{\partial^2}{\partial b^2}\mathrm{So}(\beta,b,t)\right)=$$
$$-12\,\frac{\varepsilon(t)\sin(\beta-\delta(t))\left(\frac{\partial}{\partial t}\delta(t)\right)}{\omega}+\frac{6\,\lambda\cos(\omega\,t)\,\varepsilon(t)\sin(\beta-\delta(t))}{\sqrt{1-\lambda^2\sin(\omega\,t)^2}}$$
$$-\frac{12\left(\frac{\partial}{\partial t}\varepsilon(t)\right)\cos(\beta-\delta(t))}{\omega}$$

For the numeric solution, one can get rid of the axial coordinate by introducing a pressure distribution along this coordinate. In the thesis of Butenschön[2], a mathematical approach is given how to incorporate the pressure distribution along the axial coordinate without numerical differentiation of the Sommerfeld number along this axis.

2.3 Boundary Conditions

In order to close the partial differential equation of section 2.2 appropriate boundary conditions need to de defined. Since the differential equation is written in a coordinate system fixed with the bearing shell the external rod load F(t) acts only in one main direction. The dimensionless rod load must therefore be in equilibrium with the integrated Sommerfeld number along both directions for each time step:

$$\int_0^{2\pi}\int_{-1}^{1}\cos(\beta)\;So(\beta,b,t)\,\mathrm{d}b\,\mathrm{d}\beta=\frac{2\,F(t)\,\psi^2}{\eta\,\omega\,r\,B}$$

Consequently, the integrated Sommerfeld number perpendicular to this direction must disappear since no external load is acting in this direction:

$$\int_0^{2\pi}\int_{-1}^{1}\sin(\beta)\;So(\beta,b,t)\,\mathrm{d}b\,\mathrm{d}\beta=0$$

At the outer edge of the bearing, the Sommerfeld number is prescribed to zero since ambient pressure is acting there. The pressure in the oil grooves is given by the oil pressure p_{const} of the oil pressure system. Mathematically, this means:

$$So(\beta_i,t)=\frac{p_{const}\,\psi^2}{\eta\,\omega}$$

The angles β_i gives the geometrical location of the oil supply grooves.

2.4 Algorithm for Capturing the Evaporation Areas

In the introduction, it was qualitatively explained that the crosshead pin bearing will have areas under load where the oil evaporates due to the fast movement between the loaded areas. The algorithm has to take this effect into account. Vijayaraghavan[9] or Elrod[10] presented a theory how to handle this effect. They solve the Reynolds' equation for a compressible fluid in order to account for the changing overall density there. Theoretically, the density change only takes place in these bubbles of vaporized oil. Numerically, some adjustments are necessary to create a stable scheme. In this work, a modified approach was developed to overcome these numerical stability problems.

2.5 Discretization and Solution

The differential equation derived in section 2.2 is replaced by a set of discretized equations for the numerical solution. The circumference of the bearing is subdivided into discrete evaluation points. The derivatives with respect to location are centrally discretized with 2nd order exactness. In general notation:

$$\frac{\partial}{\partial x}\mathrm{f}(x_i)=\frac{1}{2}\,\frac{\mathrm{f}(x_{i+1})-\mathrm{f}(x_{i-1})}{\Delta\,x}$$

$$\frac{\partial^2}{\partial x^2}\mathrm{f}(x_i)=\frac{\mathrm{f}(x_{i+1})+\mathrm{f}(x_{i-1})-2\,\mathrm{f}(x_i)}{[\Delta\,x]^2}$$

Applied to this problem, f needs to be replaced by So and x by b or β. The discrete local positions are denominated with *i*. The derivatives with respect to time are unidirectional discretized with 1st order exactness. In general notation:

$$\frac{\partial}{\partial t}\mathrm{f}(t_i)=\frac{\mathrm{f}(t_{i+1})-\mathrm{f}(t_i)}{\Delta\,x}$$

Here, f needs to be replaced by δ or ε. The boundary conditions contain integrals which are discretized by sums:

$$\int_a^b\mathrm{f}(x)\,dx=\sum_i\mathrm{f}(x_i)\,\Delta\,x$$

The unknown Sommerfeld numbers at each location are a function of the neighbouring Sommerfeld numbers at the same time step. The unknown location of the journal relative to the bearing, given by ε and δ, is a function of the known location at the time step before.

After replacing the differential equation by a set of algebraic equations and collecting of all unknown variables on the left side and the known expressions on the right side one gets a set of linear equations for each time step in the form

$$A\,x = b$$

The coefficient matrix has the following structure:

$$A = \begin{bmatrix}
a_{1,1}, & a_{1,2}, & 0, & 0, & 0, & 0, & 0, & a_{1,n-2}, & a_{1,n-1}, & a_{1,n} \\
a_{2,1}, & a_{2,2}, & a_{2,3}, & 0, & 0, & 0, & 0, & 0, & a_{2,n-1}, & a_{2,n} \\
0, & a_{3,2}, & a_{3,3}, & a_{3,4}, & 0, & 0, & 0, & 0, & a_{3,n-1}, & a_{3,n} \\
0, & 0, & a_{i,i-1}, & a_{i,i}, & a_{i,i+1}, & 0, & 0, & 0, & a_{i,n-1}, & a_{i,n} \\
0, & 0, & 0, & a_{i,i-1}, & a_{i,i}, & a_{i,i+1}, & 0, & 0, & a_{i,n-1}, & a_{i,n} \\
0, & 0, & 0, & 0, & a_{i,i-1}, & a_{i,i}, & a_{i,i+1}, & 0, & a_{i,n-1}, & a_{i,n} \\
0, & 0, & 0, & 0, & 0, & a_{i,i-1}, & a_{i,i}, & a_{i,i+1}, & a_{i,n-1}, & a_{i,n} \\
a_{n-2,1}, & 0, & 0, & 0, & 0, & 0, & a_{n-2,i-1}, & a_{n-2,i}, & a_{n-2,n-1}, & a_{n-2,n} \\
a_{n-1,1}, & a_{n-1,2}, & a_{n-1,3}, & a_{n-1,i}, & a_{n-1,i}, & a_{n-1,i}, & a_{n-1,i}, & a_{n-1,i}, & 0, & 0 \\
a_{n,1}, & a_{n,2}, & a_{n,3}, & a_{n,i}, & a_{n,i}, & a_{n,i}, & a_{n,i}, & a_{n,i}, & 0, & 0
\end{bmatrix}$$

The last two rows describe the boundary condition concerning the equilibrium of the hydrodynamic pressure and the external rod load. The boundary condition concerning the fixed pressure in the oil supply grooves is introduced in the matrix by setting the value 1 on the main diagonal and the values 0 on the other elements of this row.

The elements $a_{1,n-2}$ and $a_{n-2,1}$ are created by the periodic coupling at the angle β = 0.

The vector b on the right side of the equation contains the information describing the pressure build-up by the pure rotation and the dimensionless external rod load due to the load boundary condition.

The vector x contains the unknown Sommerfeld numbers, starting with the position β = 0, at the discrete locations along the circumference of the bearing and the temporal changes of the relative eccentricity dε/dt and of the angle of the minimum oil film thickness dδ/dt.

The coefficients of the matrix A and the elements of the vector b are themselves functions of the unknown eccentricity and angle of the minimum oil film thickness. They need to be evaluated from the temporal changes of these values known from the time step before by unidirectional discretizing with 1st order exactness.

The solution of this set of linear equation makes use of the special structure of the matrix. Except for some deviations, one has a tridiagonal matrix structure meaning only the main diagonal and the elements right and left next to this main diagonal are filled with values different to 0. With this structure, a general Gauss algorithm is less effective since many operations would be done with zero elements which are not necessary. A modified Thomas algorithm was developed for this work which uses the tridiagonal structure, but incorporates the special characteristic of this matrix structure. Only the real necessary algebraic operations are done to receive a fast solver.

This equation needs to be solved for each time step and needs be repeated until a convergent solution is reached for one revolution.

3 Calculation Results

The influence of various oil supply groove distributions on the hydrodynamic behaviour of a crosshead pin bearing is explained at an example. The compressor application chosen for these calculations has a rod loading according to **figure 2**. This is a typical loading for a tandem piston configuration where two stages and a balance chamber are combined on one throw. This kind of configurations generally shows only a marginal rod load reversal and are, therefore, appropriate to explain the critical hydrodynamic effects.

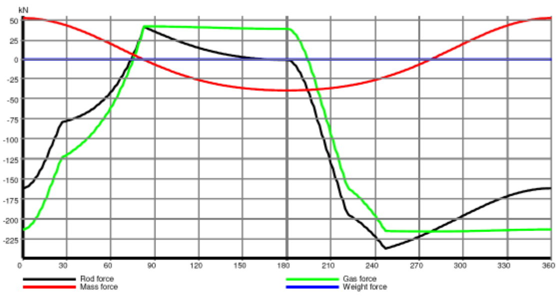

Figure 2: Rod loading chosen for the calculations

Besides the rod loading all bearing design parameters, which are the bearing dimensions, the oil viscosity, the clearance, the oil supply pressure and the compressor speed, are kept identical except for the oil groove distribution.

The pictures in the following figures show the cross-sectional positions of the journal (small inner circle) to a certain time step within the bearing (bigger outer circle). To visualize the movement of the journal the relative clearance is, of course, extremely amplified. The interruptions on the thick circular line of the bearing shell display the oil supply grooves. The central arrow in the journal gives the direction and, by its length, the magnitude of the external rod load. The circular arrow shows the rotational direction and, again by its lengths, the magnitude of rotational speed. The outer discontinuous line around the bearing shell visualizes the temporary oil filled or unfilled regions at the circumference of the bearing. The shaded parabolic curves between the oil supply grooves shows the local oil pressure related to the maximum oil pressure at the displayed time step. For the three test cases, the temporal visualization gives the hydrodynamic situation at five time steps starting with the situation immediately before the rod load reversal (crank angle position 165 degree in **figure 2**) and finishing with the maximum rod load (crank angle position 250 degree in **figure 2**).

Figure 3 is the result of the calculation for a groove configuration with a 14 degree distance between the grooves. Picture A1 shows the situation immediately before the rod load reversal. The important areas of the bearings are filled with oil. Only between 65 and 80 degree and 280 and 300 degree unfilled areas are visible. A2 gives the situation immediately after the rod load reversal. It is obvious that the oil is completely evaporated in the areas between the oil grooves on that side of the bearing. At time step A3 the journal is already close to the other bearing side due to the increasing rod load. The evaporated areas are partly refilled again by the oil pre-pressure in the grooves. At time step A4 the vaporized areas are completely filled with oil again. The pressure build-up on the load side of the bearing can be seen. At the maximum load in picture A5 the maximum pressure situation is reached. It is remarkable that almost only the central load area of the bearing bears the external load by its pressure build-up. The very important finding of this calculation is that the peak pressure for this bearing configuration is much higher than the mean design pressure which could explain a possible fatigue failure of the bearing. For this test case the mean pressure is only 5% of the peak pressure.

Figure 4 is the result of the calculation for a groove configuration with a 40 degree distance between the grooves. Picture B1 shows the situation immediately before the rod load reversal. It is visible that the area on the right side unloaded to this time step is not completely refilled with fresh oil yet. The time of the short load stroke between 75 and 165 degree in **Figure 2** is not sufficient to refill the long distance of this 40 degree design. B2 gives the situation immediately after the rod load reversal. Again, the oil is completely evaporated in the areas between the oil grooves on the left side of the bearing. On the right side an accelerated refilling of the unfilled areas takes place since the displacement effect by the fast movement of the journal against this side supports the refilling by the oil pre-pressure in the grooves. At time step B3, the refilling of the central load area is almost done.

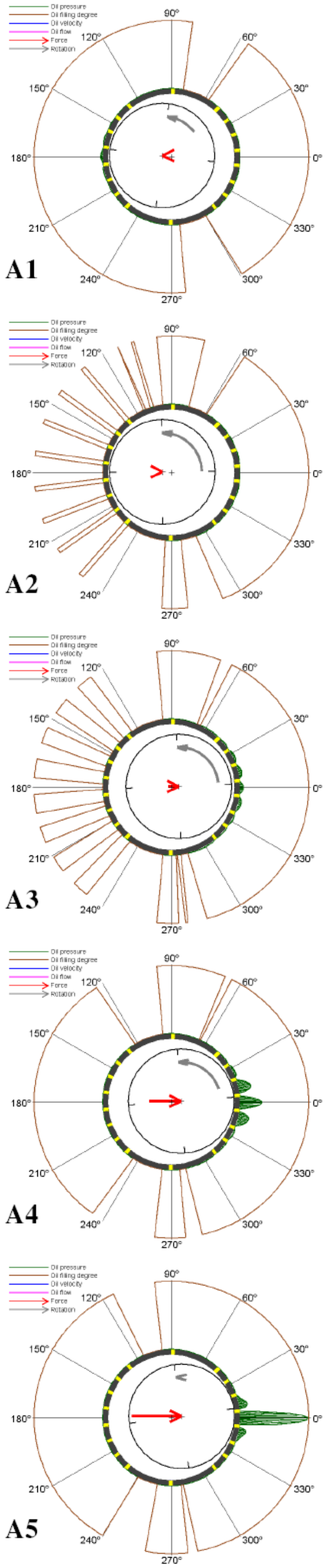

Figure 3: Test case with 14 degree groove distance

The rod load is comparatively small. A remarkable pressure build-up is not created yet. In picture B4, the loaded area is completely filled. A normal pressure build-up takes place. The unloaded area on the other side becomes refilled. Picture B5 represents the maximum load situation. Again, only the central load area is involved in the pressure build-up. The unloaded area is not refilled yet but there is enough time left to reach the refilling before the real load process starts on this bearing side. The ratio between the mean pressure and the peak pressure is improved to 14% compared to the bearing design of **figure 3**. A dramatic improvement concerning the minimum oil film thickness between these two bearing designs can also be identified (see table below). In accordance with the authors' experiences the 14 degree design would be critical for the given rod loading concerning the minimum oil film thickness, whereas the 40 degree design would be absolutely uncritical.

Figure 5 is the result of the calculation for a groove configuration with a 40 degree distance between the grooves. Instead of the bearing design of **figure 4** this design is equipped with a groove centrally arranged in the main load direction. Picture C1 shows the situation immediately before the rod load reversal. The refilling situation on the unloaded side is comparable to the former design (B). C2 gives the situation immediately after the rod load reversal which is pretty similar to B2. At time step C3, the refilling of the loaded right side is already done. The normal pressure build-up has already started. At time step C4, a further pressure build-up is visible according to the higher rod load. The refilling of the unloaded left side progresses, but is not finished yet. Time step C5 shows the situation at maximum rod load. Two pressure parabolas bear the external load. It is obvious that this bearing design C is a further improvement concerning the maximum peak pressure compared to B. The ratio between the mean pressure and the peak pressure is further improved to 20%. It is easy to understand this result since roughly two areas of 40 degree are loaded here (C) instead of one for design B. The disadvantage of the central groove design C (patent pending by NEA) is the worse minimum oil film thickness created by the central groove compared to design B.

The following table summarizes the relevant design results in comparison with the worst design A (multiplier to A):

Design	A	B	C
Peak pressure [-]	1	0.37	0.26
Min film thickness [-]	1	4.3	2,5

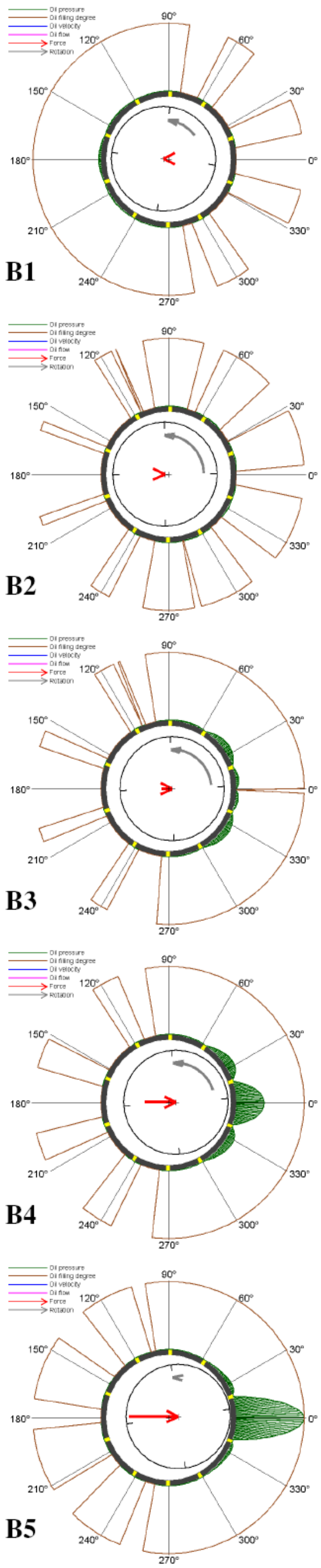

Figure 4: Test case with 40 degree groove distance

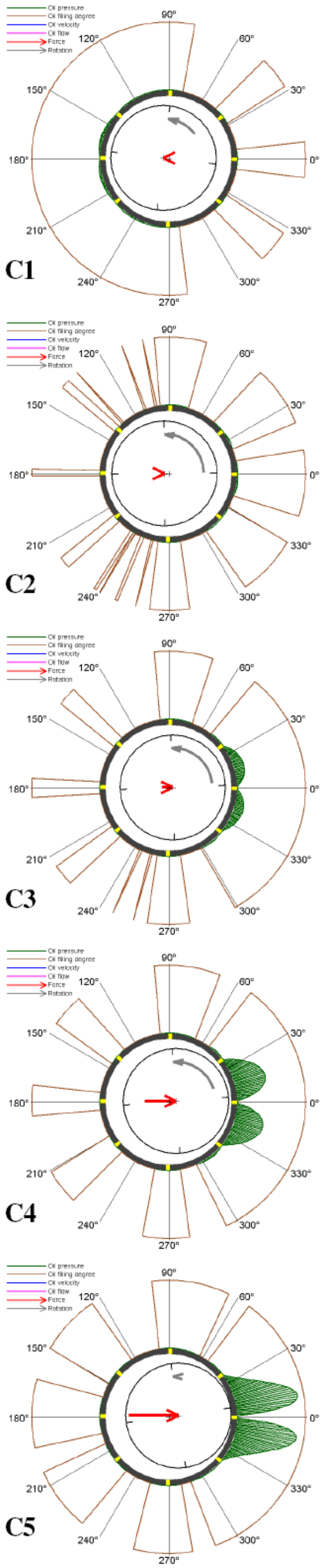

Figure 5: 40 degree groove distance/central groove

4 Design Approximations

This hydrodynamic design program was used to fulfil a parameter study with some compressor applications. By definition of a load characteristic in the following form

$$M = \frac{I \cdot \psi^2}{r^2 \cdot \eta}$$

a unique relation between this load characteristic and the maximum eccentricity ε, which corresponds to the minimum oil film thickness, can be given. The function I in the load characteristic is just a unique mathematical relation to the rod load distribution. The result of this parameter study is shown in **figure 6**. Both the load characteristic and the maximum eccentricity were related to their critical values. The critical values correspond to NEA's experience.

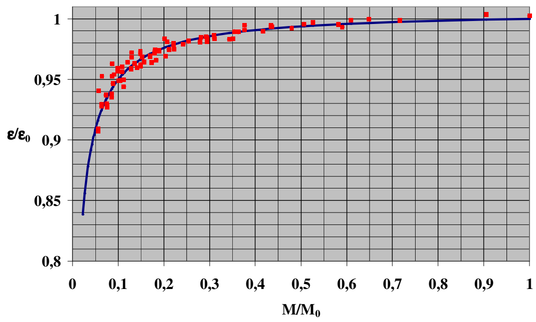

Figure 6: Load eccentricity relation

The calculation points in this graph can be approximated by a mathematical relation given by the continuous line. With this known relation for a given bearing design, the minimum oil film thickness can easily be calculated from the rod loading and the design parameters of the bearing without applying the hydrodynamic program. This value can be compared with the critical one.

The relation in **figure 6** is only valid as long as the refilling of the bearing is reached. To assess the refilling another relation should be applied:

$$\rho = \frac{p_{const} \cdot \psi^2 \cdot J}{\eta \cdot \omega}$$

The refilling characteristic ρ, again, is only a function of the rod load distribution given by another unique relation J and the bearing design parameters. The calculated value of a given load scenario and bearing design must exceed a critical limit which depends on the bearing design. This refilling characteristic is much more physical than the minimum rod load reversal criterion given in the API 618 for example. Defining only a minimum rod load reversal angle and a corresponding peak load can be either critical or conservative since these both parameters do not fully describe the refilling mechanism. The refilling characteristic ρ contains all variables influencing the refilling.

5 Conclusion

This paper presents a hydrodynamic calculation tool which is especially developed for the crosshead pin bearing design. Contrary to the main and crank pin bearings the hydrodynamics of the crosshead pin bearing is dominated by the radial displacement mechanism. Due to the small pivoting of this bearing the rotary displacement mechanism can be neglected. Because of this effect the so-called rod load reversal is essential for this type of bearing. Without this load reversal no real hydrodynamic mechanism is effective, a bearing failure due to lack of lubrication for modern highly loaded bearings is the result. Only moderately loaded bearings can survive without rod load reversal if the design is appropriate.

The test calculations in this paper show that a tremendous upgrade of a bearing with existing main dimensions can be reached just by rearranging the oil supply grooves. By doing this one critical phenomenon must be known and taken into account: The evaporation of the oil due to the fast movement of the journal between the load land areas of the bearing. These areas of evaporated oil need to be refilled with fresh oil from the oil supply grooves. This can become critical for load cases with a small angle of rod load reversal and relative big angle between the oil supply grooves. Then, the refilling cannot be accomplished and the bearing can fail due to lack of lubrication. The bearing failure pattern is similar to the pattern of a bearing failure resulting from a load without rod load reversal.

The presented method is able to predict the hydrodynamic oil pressure distribution, including the peak pressure, the journal eccentricity and, therefore, also the minimum oil film thickness on basis of the given assumptions. Besides these bearing design results a correct prediction of the evaporation and refilling process is included. With this tool a reliable crosshead bearing design is possible.

A parameter study done with this tool revealed that a unique relation between a load characteristic, defined from load distribution and bearing design parameters, and the maximum relative eccentricity can be derived. In addition, a refilling characteristic, also dependent on load distribution and design parameters, is introduced to assess the risk of a bearing damage due to lack of lubrication (refilling).

From this work three design criterions need to be taken into account for a reliable crosshead pin bearing design:

1. The hydrodynamic oil peak pressure must not exceed a critical value to avoid a bearing fatigue failure.

2. The hydrodynamic minimum oil film thickness must not fall below a critical value to avoid a bearing failure due to lack of lubrication.

3. The rod load reversal, defined by a new introduced refilling characteristic, must exceed a critical value to avoid a bearing damage due to lack of lubrication (refilling). Defining a limit for the reversal angle and the peak load can be risky.

Unfortunately, design measures improving the situation concerning the criterions 1 and 2 deteriorate the criterion 3. This can easily be verified by comparing the load characteristic with the refilling characteristic. The design task is to find the optimum compromise.

References

[1] Lang, O. R., Steinhilper, W.: Gleitlager. Springer, Berlin Heidelberg New York, 1978 [Pahl, G. (HRSG.): Konstruktionsbücher, Bd. 31]

[2] Butenschön, H-J.: Das hydrodynamische Radialgleitlager endlicher Breite unter instationärer Belastung. Diss., Universität Karlsruhe, 1976

[3] Sassenfeld, H., Walther, A.: Gleitlagerberechnungen. VDI-Forschungsheft 441, 1954

[4] Holland, J.: Beitrag zur Erfassung der Schmierverhältnisse in Verbrennungskraftmaschinen. VDI-Forschungsheft 475, 1959

[5] Hahn, H. W.: Das zylindrische Gleitlager endlicher Breite unter zeitlich veränderlicher Belastung. Diss., Universität Karlsruhe, 1957

[6] Booker, J. F.: Dynamically loaded journal bearings: mobility method of solution. Trans. ASME J. Basic Eng. 1965, 9: 537-546, 1965

[7] Knoll, G., Peeken, H., Waltermann, H.: Verfahren zur Verlagerungsbahnberechnung von Motorenlagern. VDI-Berichte 977: 121-148, 1992

[8] Waltermann, H.: Radiallager mit starren Gleitflächen. In: Tribo-Workshop „ Berechnungsverfahren zum Systemverhalten von Motorkomponenten mit hydrodynamischen Schmierfilmreaktionen“, Technische Hochschule Aachen, 1993, Vortag 3.1

[9] Vijayaraghavan, D., and Keith, T.G., 1989, “Development and Evaluation of a Cavitation Algorithm,” *STLE Tribology Transactions,* Vol. 32, pp. 225-233

[10] Elrod, H.G., 1981 “A Cavitation Algorithm,” ASME *Journal of Lubrication Technology,* Vol. 103, pp. 350-354

Simulation of reciprocating compressor start-up

by:

E. Huttar, V. Kacani, T.Heumesser
Leobersdorfer Maschinenfabrik GmbH & Co. KG
Vienna
Austria

Vasillaq.Kacani@LMF.at

6th Conference of the EFRC
October 28th / 29th, 2008, Dusseldorf

Abstract:

During the start-up phase of reciprocating compressors the components in the drive trains generally have the highest loads to bear. The modelling of the induction motor, coupling, crank shaft, damper, etc. is extremely important in simulating the start-up. The switching torque of the electrical motor and the instantaneous moment of inertia of the reciprocating compressor crank gear are equally important. The transient start-up process is described by using a non-linear differential equation system. Shaft torsional moments on the drive train and especially on the coupling, whether elastic or stiff, can then only be calculated using numerical simulation. This paper will describe some of the key elements in modelling and simulating the drive train start-up carried out on reciprocating compressor units, which are operating.

1. Introduction

During the start-up, the inductive motor develops a very high exciting torque, up to six times the rated torque of machine. The dominant frequency is the line frequency. (50Hz, 60Hz). The investigation of the expansion of this torque in the drive train is very important to determine the maximal load on several components of reciprocating compressors. The weakest component in drive train is generally the coupling. The coupling manufacturer provides the main data of the coupling such as stiffness, inertia, maximum torque witch occur during normal transient condition (start-up, passing through resonance) as well as the maximum allowable torque during any abnormal transient condition (short circuits). The goal of this paper is to determine the actual maximal torque on all shafts of the drive train, especially on the coupling and on the compressor shaft during the unloaded start-up of reciprocating compressors. The calculated torques can then be compared with allowable figures. Dependent on the number of spring-masses, the transient phenomena of the start-up is described by a set of nonlinear differential equation. The required torques on the shafts of drive train can be obtained from the numerical solution of differential equations [2), 3)]. First the torsional stiffness, inertia and damping coefficients must be calculated and the mathematical models of all components are required. Only a clear knowledge of the torsional parameters as well as a proper torsional model of reciprocating compressor components allows a safe dynamic design of drive train.

2. Nomenclature

C_1 C_2 C_3 C_4	stiffness, torsional model of four throw crank shafts
C_D	stiffness coefficient viscous damper
$C_{Crank\ shaft}$	torsional stiffness, crank shaft
C_{Web}	torsional stiffness, crank web
E_{kin}	kinetic energy of running gear
$f_{Crank\ shaft}$	1st NTF of crank shaft
J	Average constant inertia of running gear
$J(\phi)$	Equivalent variable inertia of running gear damper
J_1 J_2 J_3 J_4	rotating inertia, torsional model of four throw crank shafts
J_c	inertia, connecting rod
$J_{Crank\ shaft}$	crank shaft inertia
J_{DF}	inertia, flywheel viscous damper
J_{DH}	inertia, housing viscous damper
J_R	rotating inertia, throw
k_D	damping coefficient viscous damper
L	length connecting rod
m_{co}	osc. mass, connecting rod
m_p	piston mass
m_{osc}	sum of oscillating masses
M_c	mass, connecting rod
M_i	restoring torque, shaft i
M_{i+1}	restoring torque, shaft i+1
M_p	gas force torque
M_R	friction force torque
M_{Rated}	rated torque, induction motor
M_A	partial torque, induction motor
R	crank radius
T_0	time constant, induction motor
T_k	time constant, induction motor
T_{Web}	twist torque
X_c	CoG, connecting rod
Y_c	CoG connecting rod
ϕ_{DF}	angle flywheel, viscous damper
ϕ_{DH}	angle damper housing, viscous damper
$\Delta\phi_{Web}$	Twist angle, between journal centre and crank pin centre
β	angle, induction motor
γ	angle, connecting rod
λ	ratio R to L
ω_N	line angular frequency

3. Torsional model of drive train components

The accuracy of a simulation depends on the mathematical model of drive train components and the associated parameters. The main data to be specified are the torsional stiffness, mass moment of inertia, damping coefficient as well as the mathematical models.

3.1. Crank shaft

There are different types and design of crank shafts. Depending on the type of the reciprocating compressor there may be one or two throws between the journals. The crank pin usually drives the running gear: connecting rod, X-head, piston rod and piston. V-arrangement compressors have tow connecting rods at the same crank pin. W-arrangement compressors have generally three connecting rods at the same crank pin.

Torsional stiffness: The first approach calculation of torsional stiffness of the crank shaft can be performed with equations[1] developed by Carter, Ker Wilson, Jackson, Tuplin. The basic dimensions of the journals are needed as inputs, as well as the webs, crank pins, stroke and the shear modulus of shaft material. Generally these formulas are developed for engine crank shafts. The calculated torsional stiffnesses for the crank shafts of reciprocating compressors depend on the equation used. The torsinal stiffness value calculated with these equations may differ 100% or more from the actual value. In order to calculate the torsional stiffness, LMF has always used FEA. This can be done in two ways:

a) Calculation of the twist angle difference $\Delta\phi_{Web}$ between two sections in the journal centre and the crank pin centre of a crank shaft throw under an arbitrary applied torque T_{Web}. One end is symmetrically, rigidly fixed and the torque is applied across the other end of the crank shaft. SURF154[6]– elements are used for arbitrary applied moment. The ratio between torque and twist angle is then the corresponding stiffness of the crank web. The calculation can then be repeated for the intermediate crank web and for all possible web configuration of the crank shaft.

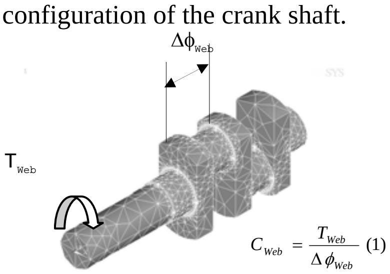

Figure 1: Web torsional stiffness

b) Calculation of the rotating inertia for each throw (crank web, crank pin,), and distribution of the shaft inertia parts to the corresponding throw. A FEA modal analysis has to be performed to determine the torsional eigenfrequencies and the corresponding mode shapes (eigenvectors). This data provides the necessarily required information to calculate the torsional stiffness. A solution of an algebraic system of equation must be performed[4], depending on the number of throw. For one cylinder compressor, the crank shaft is modelled as one spring-mass and the stiffness can be calculated explicitly according to equation (2).

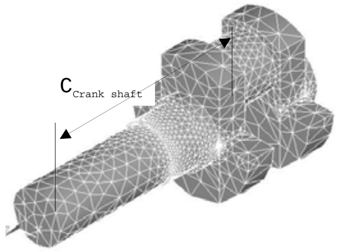

$$C_{Crankshaft} = 4 \cdot \pi^2 J_{Crankshaft} \cdot f^2_{Crankshaft} \quad (2)$$

Figure 2: Crank shaft torsional stiffness

3.2. Running gear

The inertia of the running gear (oscillating masses: connecting rod, cross head, piston and piston rod) varies during each crank shaft revolution (curves in Fig. 3). The equivalent inertia of the running gear can be approximated by adding half of the reciprocating mass multiplied by the crank radius squared to the rotating inertia (Lines in Fig. 3). For simulation of the start-up and the continuous[5] operation of the drive train the instantaneous moment of inertia must be considered. In Fig 3. a dominant amplitude of order two is noticeable for the inertia.

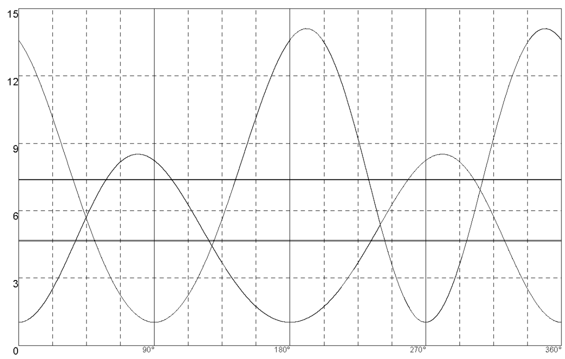

Figure 3: Equivalent mass moment of inertia J(ϕ) kgm² and average inertia (constant) versus crank angle for a four axis reciprocating compressor B254.

The equivalent inertia J(ϕ) of throw can be found by summing kinetic energy of all moving parts:

$$E_{kin} = \frac{1}{2} J(\phi) \cdot \dot{\phi}^2 = \frac{1}{2} J_R \cdot \dot{\phi}^2 + \frac{1}{2} J_C \dot{\gamma}^2 + \frac{1}{2} m_C (\dot{x}_C + \dot{y}_C) + \frac{1}{2} m_p \dot{x}_p \quad (3)$$

The equivalent variable inertia J=J(ϕ) is

$$J(\phi) = J_R + \frac{1}{\dot{\phi}^2}\left[J_C\dot{\gamma}^2 + m_C(\dot{x}_C + \dot{y}_C)\right] + \frac{1}{\dot{\phi}^2} m_p \dot{x}_p \qquad (4)$$

The classic average inertia J=constant is given by

$$J = const. = \frac{1}{2\pi}\int_0^{2\pi} J(\phi)d\phi \qquad (5)$$

Reducing the connecting rod (Fig. 5) in tow masses an oscillating mass m_{CO} and a rotating mass m_{CR} the above equation becomes a simplified form in ϕ as follows:

$$J(\phi) = J_0 + m_{OSC} R^2 \left[\sin\phi + \frac{\lambda \sin\phi \cos\phi}{\sqrt{1-(\lambda \sin\phi)}}\right]^2 \quad (6)$$

$$Where: \ \lambda = \frac{R}{L}, \ J_0 = J_R + m_{CR} \cdot R^2$$

$$m_{Osc} = m_p + m_{CO}$$

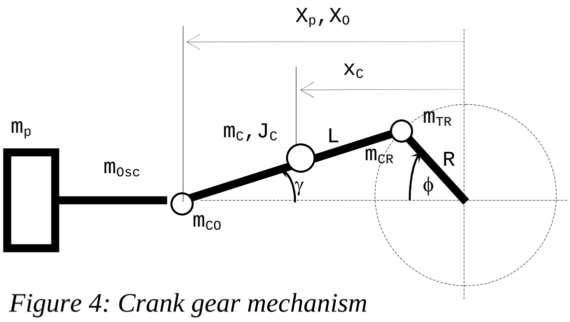

Figure 4: Crank gear mechanism

The next step is to develop the equation of motion for the crank throw. The equations of motion for the calculation of torsional forced vibration during start-up and continuous operation are described by the derivation of the variable inertia J(ϕ), external torque (gas force, friction force) as well as restoring torques and damping torques of the shafting system.

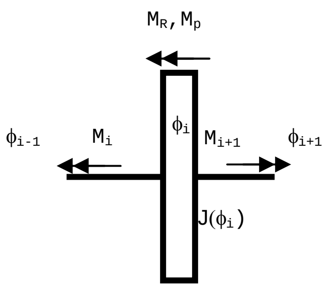

Figure 5: Running gear model

$$J(\phi_i)\cdot\ddot{\phi}_i + \frac{1}{2}\frac{dJ(\phi_i)}{d\phi_i}\cdot\dot{\phi}_i^2 + M_i(\phi) - M_{i+1}(\phi) + M_p(\phi) + M_R(\phi) = 0 \quad (7)$$

Where:

$$\frac{1}{2}\frac{dJ(\phi)}{d\phi} = m_{Osz} R^2 \left[\sin\phi + \frac{\lambda \sin\phi \cos\phi}{\sqrt{1-(\lambda \sin\phi)}}\right] \cdot \left[\cos\phi + \frac{\lambda \cos 2\phi + \lambda^2 \sin^4\phi}{\sqrt{\left[1-(\lambda \sin\phi)^2\right]^3}}\right] \quad (8)$$

M_p and M_R are the torque, due to the gas force and friction force. For the classical approach a set of linear differential equations is generated considering the average value of throw inertia, equation (5). With variable inertia, equation (4), (6) a system of nonlinear differential equations is generated.

3.3. Motor

Torsioanal stiffness and rotating inertia: Generally, the Motor manufacturers provide a torsional stiffness and inertia of rotor shaft including all other rotated parts mounted on shaft (fan,). The stiffness is then calculated from the end of the shaft (coupling side) to the middle of the rotor shaft. To get more accuracy a FEA is required. For single mass-spring system the 1st NTF and the total inertia of the 3D-model is calculated, Fig. 6. The equation (2) can be then used for the calculation of torsional stiffness.

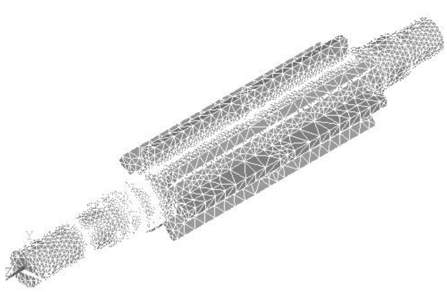

Fig. *6 3D-Model of rotor shaft of induction motor for 1.4 MW 375 rpm for a four axes horizontal balanced opposite reciprocating compressor B254.*

Switching torque: The air gap torque of induction motor is the main exciter of drive train during start-up. The maximum torque amplitude can reach values up to six times the rated torque of machine. The fundamental frequency is the line frequency

(50HZ or 60Hz). The torque is provided by the manufacturer based on basic equations developed in [7]. The torque is given by the following equation:

$$\frac{M}{M_{Rated}} = M_A + e^{-\frac{t}{T_K}} + \frac{M_A}{\sin\beta}\sin(\omega_N t - \beta)\cdot e^{-\frac{t}{T_K}} - \frac{M_A}{\sin\beta}\sin(\omega_N t + \beta)\cdot e^{\frac{t}{T_0}} \quad (9)$$

For the 1.4MW motor Fig 6. the coefficients in equation (9) are:

$$\begin{array}{ll}
Rated \quad Torque & : T_{Rated} = 35650 \quad Nm \\
Partial \quad Torque & : M_A = \dfrac{T_{Start}}{T_{Rated}} = 0.828 \\
Time \quad cons.: & T_0 = 1.22\ s,\ T_k = 0.0191\ s \\
Angle\ : & \beta = 0.163\ rad \\
Angular \quad Frequency & : \omega_N = 2\pi f_{netz} = 314\ s
\end{array}$$

Fig. 7 shows the torque, equation (9) over the acceleration time. The dominant amplitude of 1st order with a frequency of 50Hz (line frequency) is closed to six times the rated torque for this application.

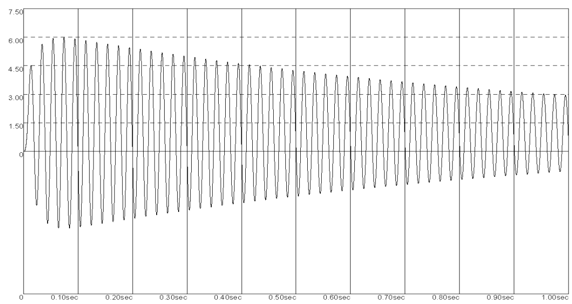

Fig.7. Ratio between the motor start torque and the rated torque versus time in s.

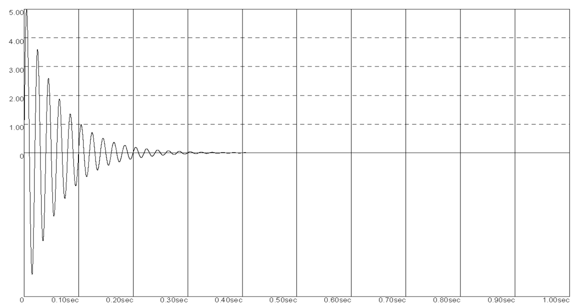

Fig.8. Ratio of motor short-circuit torque to the rated torque versus time in s.

3.4. Viscous damper

Viscous dampers are often used in reciprocating engines. Sometimes they are mounted in reciprocating compressors on the crank shaft end to reduce the dynamic torsional torque for resonance operation. A viscous damper consists of a flywheel (inertia J_{DF}) that rotates inside a housing (inertia J_{DH}) which contains a viscous fluid with stiffness C_D and damping coefficient k_D. The mathematical model, equation (10) of viscous dampers implied its mass moment of inertia, damping coefficient and stiffness. The damper manufacturer generally can provide all data required for the damper modelling.

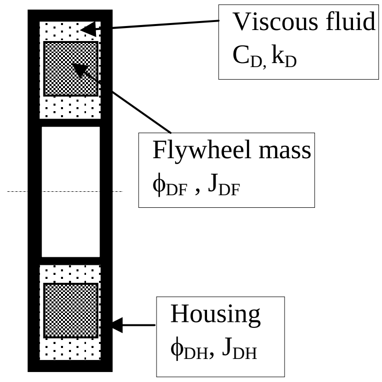

Figure 9: Damper model

$$J_{DF}\cdot\ddot{\phi}_{DF} - C_D\cdot(\phi_{DH}-\phi_{DF}) - k_D\cdot(\dot{\phi}_{DH}-\dot{\phi}_{DF}) = 0 \quad (10)$$

4. Start-up simulation and results

The mechanical system can be reduced Fig. 11 to an equivalent spring-mass system. A drive train with N components leads to a set of 2xN nonlinear differential equations. If a viscous damper is included, the number of equations is 2xN+2. The method of solving the nonlinear differential equation in time domain is described in [3)], [4)]. From the numerical solution, the angles and angular velocities of all masses are obtained. The dynamic torsional shaft torque is calculated from the difference of twist angles between tow masses multiplied by the corresponding torsional stiffness of the shaft.

Below, the use of the simulation method and the results of calculations on a 1.7MW LMF-B254 compressor will be explained. The drive train is composed of following components:

A) A four axis, four throw horizontal compressor. The crank shaft Fig. 10 is reduced to a torsional equivalent vibration system of four spring-masses. The inertias and stiffnesses are: C_1=18.7x10^6Nm/rad, C_2=31.3x10^6Nm/rad, C_3=20.4x10^6Nm/rad, C_4=31.3x10^6Nm/rad, J_1=6.52kgm²,J_2=6.53kgm²,J_3=6.53kgm², J_4=6.51kgm²

B) Flywheel with inertia J=1174kgm²

C) Highly flexible coupling: Stiffness C=5x10^5Nm/rad, relative damping ψ=0.8, max. allowable torque for normal transient conditions T_{Max}=150000Nm.

D) Induction motor: Inertia 709kgm², stiffness C=51.62x10^6Nm/rad. The starting torque short-circuit torque date is given above.

E) The running gear data is:

		Axis 1	Axis 2	Axis 3	Axis 4
Stroke	[mm]	250	250	250	250
Connecting Rod Length	[mm]	625.0	625.0	625.0	625.0
Cyl.Pos.from Vertical	[°]	270.0	90.0	270.0	90.0
Crank Angle to TDC 1	[°KW]	0	0	90.0	90.0
Axial Distance from CL	[mm]	-935.0	-665.0	665.0	935.0
Osc. Mass w/o Conn.Rod	[kg]	400.00	400.00	400.00	400.00
Osc. Mass Conn.Rod	[kg]	33.00	33.00	33.00	33.00
Rot. Mass Conn. Rod	[kg]	66.00	66.00	66.00	66.00
Rot. Mass Crankshaft	[kg]	38.59	38.59	38.59	38.59
Counterweight Mass	[kg]	0	0	0	0
Counterw. Rot. Radius	[mm]	0	0	0	0
Counterw. Axial Position	[mm]	0	0	0	0
Average gear function (w/O mRot,Kw)	[kgm²]	4.449	4.449	4.449	4.449

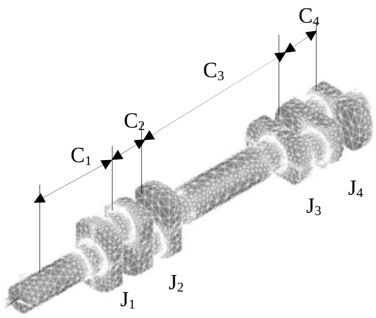

Fig. 10: Crank shaft of LMF-B254 compressor

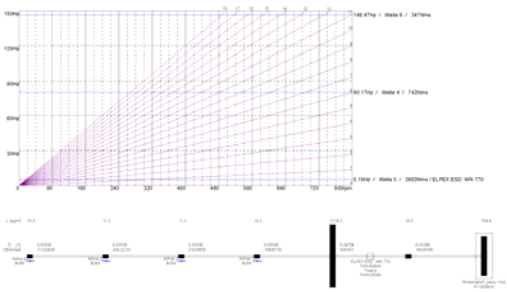

Fig. 11: Equivalent torsional model and Interference diagram of LMF-B254 drive train.

From the numerical simulation the maximal torque on the coupling 111637Nm is obtained. The allowable torque is 150000Nm. The dominant frequency of the coupling torque is NTF of the drive train and not the line frequency (50Hz).

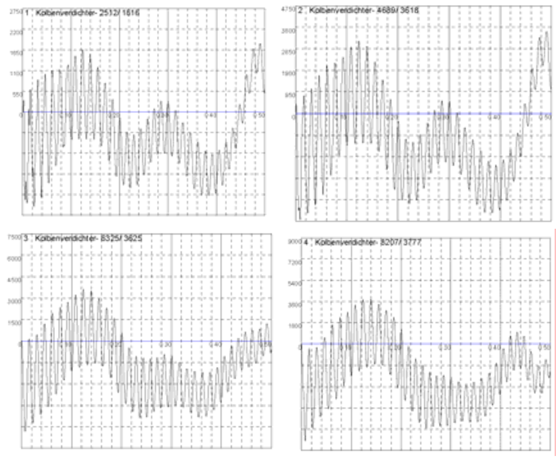

Fig.12 Dynamic torque at crank shaft versus starting time s

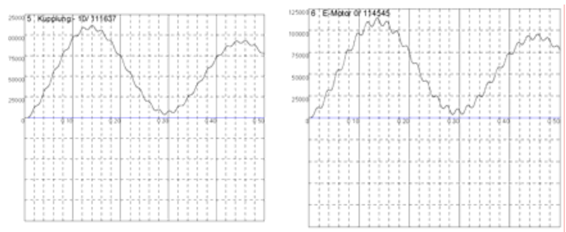

Fig.13 Dynamic torque at highly flexible coupling and E-motor

The next figures show the simulation results for a stiff coupling with fictive torsional stiffness of 2.9x10^7 Nm/rad

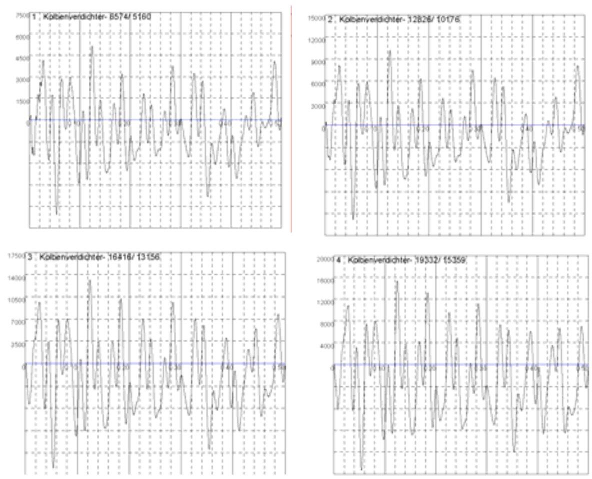

Fig. 14 Dynamic torque on the motor shaft, on the stiff coupling

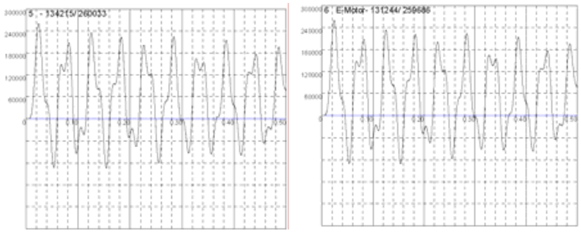

Fig.15: Dynamic torque at stiff coupling and E-motor shaft

With the stiff coupling solution the torques are much higher and the dominant frequencies are the NTF and the line frequency.

5. Conclusion

To ensure a safe design of drive train a start-up simulation is necessary. The torsional parameters of the crank shaft, induction motor as well as the mathematical model of the running gear are very important for the accuracy of the calculation. The torsional stiffness value of the crankshaft calculated by using classic methods may differ 100% and more from the actual value. The numerical solution of the nonlinear equations provides the shaft torques. The highly loaded component in drive train is always the coupling.

References

[1] Nestorides, E.J: A Handbook on Torsinal Vibration, B.I.C.E.R.A., cambrige

[2] Engeln –Müllgas G., Reuter F.: Formelsammlung zur nummerischen Mathematik mit Standard Fortran 77 Programmen. Biblographisches Institut Manheim/Wien/Zürich, B.I. Wissenschaftsverlag.

[3] Julien C.Sprott: Numerical recipes

[4] H.Dresig: Schwingungen mechanischer Antriebssysteme, Modellierung, Berechnung, Analyse, synthese

[5] Ernst Huttar, Vasillaq Kacani, Hans Stibi: Torsionsschwingungen in Kolben-verdichteranlagen, 1st EFRC conference, Dresden.

[6] ANSYS 11.

[7] Dieter Seifert, Thomas Strangmüller: Stoßmoment und stoßstrom der Asynchronmaschine. Wissenschaftliche Zeitschrift für Elektrotechnik und Automation. Sonderdruck aus Bd.11 (1989)

Virtual Prototyping technique applied to the design of a crankmechanism of a process reciprocating compressor

by:

Traversari Riccardo
Rotating Machinery Design Dpt.
Compression Service Technology
Florence
Italy
riccardo.traversari@cstfirenze.com

Faretra Marco -
Pellicciari Marcello
Mechanical & Civil Eng. Dpt.
University of Modena and Reggio
Modena
Italy
mf@barbanti-eng.it

6th Conference of the EFRC
October 28th / 29th, 2008, Dusseldorf

Abstract:

Virtual Prototyping (VP) is a novel computational approach that reproduces a complete mechanism to test it several times, as a scale 1:1 laboratory prototype. VP utilizes various CAE tools, such as 3D modelling, Structural FEA, Multibody Dynamic Analysis (MDA), Multiaxial fatigue analysis, in an integrated way.

The VP technique allows considering a realistic stepless loading pattern throughout the complete revolution and determining automatically the fatigue safety factors within the whole machine assembly.

This new approach was used to review the design of the crankmechanism of an existing reciprocating compressor. The loads (including inertia forces) were applied to the gudgeon pin and, by means of the MDA, to all the other components.

1 Introduction

Every design engineer knows very well that the design of almost whichever machine is often a rather difficult exercise because of the wide range of operating conditions that the machine will undergo which, in turn, will determine different loading conditions of the various machine components.

This variability of requirements has obliged in the past the designers to consider the "worst case" situation but this, due to the lack of highly refined computational tools, it often resulted to be too uselessly pessimistic and therefore irrealistic.

As we will see in this article, the availability and the integrated utilization of the most recent software tools allows the creation of Virtual Prototypes which help very much the designer to overcome the above mentioned problems.

2 A new design approach through "Virtual Prototyping"

During the last decades, the market competitiveness has grown and the same happened to the product complexity. In the meantime the "time to market" need was getting shorter and became a strategic factor. Pressure towards effectiveness is the logic answer to this situation.

To evaluate the effectiveness of a project one must have very clear in mind the following:

- When the money is committed
- When the money is spent
- When there are cost reduction opportunities.

These concepts [1, 2] are well explained in Figure 1 which reports a typical Life Cycle Cost (LCC) analysis. One can see that some 2/3's of the total LCC are fixed during project conception even though the real expenditure of funds will flow at a later time. One can see also that the chance to realize any cost reduction decreases with the development of the project.

Consequently the conception and design phases result to be largely the ones that determine the success of a project.

Furthermore, industrial products today must be optimized in terms of quality, performance, cost, delivery time, reliability and are therefore becoming more and more complex and requiring experimental investigation.

The advantage today is that machine design is supported by several so called CAE tools that help the designer to perform his duty. 3D modelling, structural FEA, Multybody Dynamic Analysis (MDA), Multiaxial fatigue evaluation, CFD modules, FSI modules, are the most important. However a great difference takes place whether the various software modules are utilized as separate tools or integrated ones.

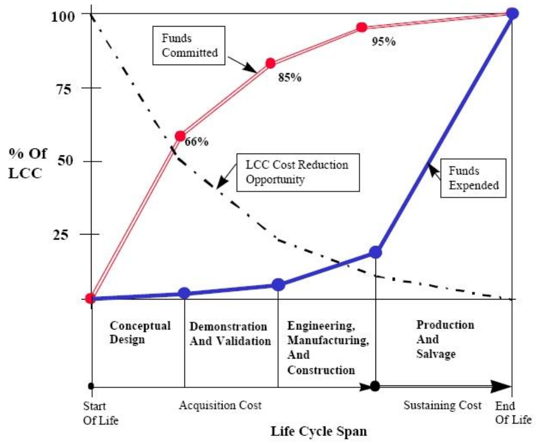

Figure 1: Funding trends by commitment and expenditure

2.1 Design process with separate individual CAE Tools

The different CAE software modules have been mostly utilized as separate tools. For instance, for the mechanical design of a machine subject to fluctuating loads, such as a reciprocating compressor, the normal process was the following:

- creation of the 3D model sizing the various components by means of the classic analytical equations;
- disaggregation of the machine assembly into the various separate components;
- definition of the loads that are transmitted from one component to the adjacent ones (this exercise normally requires a lot of simplifications);
- schematization of the shape of the component;
- FEA of the different components to find the equivalent stress in the most stressed areas;
- fatigue analysis, with the traditional methods (equivalent stress plus Goodman/Smith diagrams) in few areas that experience or the FEA have shown to be critical;
- construction of a physical prototype to validate the theoretical results.

The problem with this process is the simplifications required and the fact that if you want to change something you have to repeat the whole exercise.

The reason why the "galaxy" of software tools available is often utilized in an independent way, even if sometimes they have a fair degree of integration, is that, most frequently, in the same organization or project, they are utilized by different persons with different specialization.

2.2 CAE, 3D Modelling, Drafting, Design integration

Normally the selection of CAE systems is based mainly on some important aspects, such as the extension of the functions offered and the accuracy of results but not on the capability to be integrated or, better, native with 3D CAD Systems. In practice, a good analysis must start from a good model which must be complete, precise, and effective to represent the reality. This is particularly true when the passage must occur between a 3D CAD System and an analysis module, such as the FEA.

The possibility to utilize directly the 3D model on the CAE module, without any kind of translation, is very useful for time, cost and quality. This feature is at best when there is a native integration between the 3D CAD with the other CAE modules: in fact, in this case, the designer can make in real time, in an interactive way, the verification of shape and dimensions of the component he is working on, staying in the same ambient.

2.3 Verification vs. design

It is important to remind that all CAE modules are basically verification and not design tools. This means that, in the classic way of doing, one make a design of first approach by means of analogy, best practices, standards etc. and then one verify the correctness of the assumptions. More often through the CAE modules one searches possible weaknesses, even if a few of them have some optimization capability, more than finding the best solution.

The approach described in this article is a step in transforming these tools into a means of advanced design engineering.

2.4 Virtual prototyping

Virtual Prototyping is a technique by which one produces a model, the "Virtual Prototype" (VP), provided with all physical, mechanical, thermodynamic characteristics of the real component or assembly (starting from the material with all its characteristics) which is submitted to virtual constraints and loads that replicate the real ones and generate on the model the same stresses and interactions which will be generated on the real component or assembly in operation.

To have a good VP it is essential on one side to simulate effectively the interface with the constraints and on the other to apply to the model the loads corresponding to the real ones and not some conventional loads.

In the case of virtual prototypes of rotating machinery, the simulation includes also the actions due to the movement, f.i. the inertia forces, and all internal interactions between the various components.

The utilization of CAE techniques based on conventional loads and simplification of shape and constraints and separate investigation on the various parts of the machine (neglecting the real mutual actions) move the simulation away from the physical reality and consequently cannot be considered VP but only CAE analysis.

2.5 A test bench for simulating reality with no simplification

VPs are "tested" several times during the development of the project. During the tests one can evaluate the contribution of the various loads even better than what can be done with a real prototype. For instance, on a real prototype, it is very difficult to extract the effects of the inertia forces while on the virtual prototype this can be done easily and with the maximum precision.

This approach allows avoiding the execution of real prototypes of the single components, which are normally executed when proceeding in the classic way, so that the test on a real prototype is limited, in case it is judged necessary, only at the end of the development process and on the complete machine, getting the following advantages:

- time reduction
- cost reduction
- possibility to "see" things that on a real prototype could not be seen (in fact the virtual prototype is a device instrumented in all its points, which could never occur on a real prototype)
- real optimization of the solutions studied by having the possibility to run a great number of virtual experiments in a relatively short time.

2.5.1 Realistic stepless loading throughout the revolution and Multibody force transmission

Through the MBD module the behaviour of complex assemblies (typically rotating and reciprocating machinery) can be studied both in transient and steady conditions so that, in an integrated CAE system, the relevant results are fed to the other modules. In such a way the actions and reactions which are transmitted through the constraints and contact surfaces of the various parts of the VP represent very precisely the real ones, thus avoiding any simplification.

The inertia forces, which with traditional procedure are normally roughly estimated or simply neglected due to the complexity of the component shape, are instead taken carefully into account by the MBD module.

It is important to note that, by this method, the analysis of each component is not limited to one or few typical points of the revolution but to all the conditions that the component sees during the whole revolution.

As it will be treated in the following, this feature is very important, not only for an appropriate evaluation of all the conditions to which the component is subject during the revolution, but also for a correct evaluation of the fatigue cycle to which the material is subject.

2.5.2 Structural FEA

All data of the aforementioned simulations aimed at determining the loads, reactions and mutual interactions among the various components of the machine converge into the FEA module for stress and strain determination. This passage is automatic in case the CAE modules are integrated.

In case the method of point 2.5.1 is utilized, one can determine the load history to verify the fatigue conditions of every single component.

2.5.3 Modal Analysis

In the case of mechanical systems that are subject to excitations close to their natural frequencies, the VP can be tested also for an accurate modal analysis as a static analysis would not be sufficient.

2.6 Multiaxial full body stress and fatigue analysis

After having generated all the necessary information, one proceed to the determination of the stress and strain on the full body of the various components of the VP and then to the fatigue analysis with the relevant potential damage determination and localization of the critical points.

By appropriately putting together the various load histories, one can simulate on the VP tests with finite or infinite number of cycles, that, on real prototypes should require much longer times.

In case some problems occur, one can modify the VP and start again with the test which is a much less time consuming exercise than with a real prototype.

The execution of fatigue tests through VP has further advantages such as the possibility to define safety factors, according to one or more criteria, and to determine the most important stress raisers.

2.7 Validation through benchmarks

Extremely important in the virtual prototyping activity is the validation of the VP and of the virtual tests. This validation must be done with respect to sound experimental data or to reliable bibliographic information.

For instance, dealing with a problem of Hertzian contact, it is convenient to develop a VP simulating one or more cases whose solution is reported on documents of well reputed researchers, and verify the agreement of the results. One shall consider satisfactory the VP when, applying the same boundary conditions, the stress and strain differences between the VP and the reliable literature stay well within a few percent.

2.8 Easy repetition of the process prototype

A great advantage of the utilization of VPs is that one can modify the design, its parameters or testing conditions easily, quickly and cheaply, which makes this method a very flexible and practical tool.

2.9 A real scale 1:1 laboratory

Virtual prototyping, in case of machinery of large dimensions, has a further advantage in comparison with the classic experimental prototypes. In fact in this case, due to the large dimensions (costs, time, technology, test bench dimensions, etc.) it is often necessary to move towards scale models. To assure that the scale model represents carefully enough the original machinery, it is a rather complex activity, particularly when fluodynamic or lubrication aspects are concerned. Often, it is necessary to make compromises and then the correspondence between the scale model and the true machine is doubtful.

The experimentation of a VP shall not resort to these artifices, whichever the dimensions of the original machine are. The VP is always 1:1 scale and therefore the results of the virtual experiment are not affected by approximations and compromises.

Another advantage of virtual prototyping is the possibility to get information that would be impossible to obtain even from a real prototype, such as areas difficult to be reached or so small that could be hardly instrumented.

In other words, virtual prototyping is certainly more complex and expensive than the traditional utilization of CAE techniques, but it gives the same type of results that one could get from the construction of a sufficient number of real prototypes 1:1 scale instrumented and submitted, in a laboratory, to the real operating conditions.

VPs have also the advantage that while if on a real prototype one forget to install a strain gauge in a point that then appears to be critical it is impossible to have the information on that point, with the VP the experiment results can be reviewed anytime without any problem as the VP is, by definition, “whole body instrumented”.

2.10 A new design approach

Virtual prototyping can be the main pillar of a new advanced design approach that is based on the following steps:

a) first design set up with calculations according to traditional techniques (possibly by means of spreadsheets for guidance and speed);
b) determination of other variables not affordable through traditional calculation, i.e. those cases in which the De Saint Venant hypothesis are not applicable.
c) system drafting;
d) virtual prototyping (real load determination, definition of external and internal constraints, MDA, modal analysis) and verification calculation;
e) analysis of results and identification of critical points and of the necessary modifications;
f) iterative repetition of the steps a) through e) for a progressive fine tuning of design up to when one reach a completely satisfactory results (Figure 2);

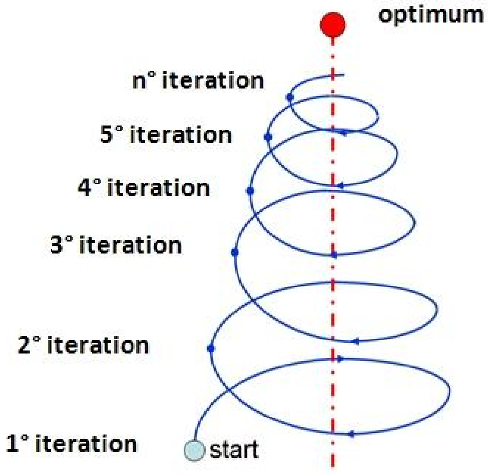

Figure 2: Iterative repetition of steps a) through e)

The two most important instruments of virtual prototyping are:

- MBD with rigid bodies
- FEA.

The MBD consists in defining the cinematic constraints of the mechanism assigning to each of them the relevant mechanical characteristics and giving to each individual component all dynamic properties (mass, stiffness, damping, etc). Once given the loads and the laws of motion (both in steady and transient conditions) the MBD allows to determine the resultants of the mutual interactions among the various components and between the components and the external constraints, inertia forces, energy parameters and everything that is related to the complete definition of the dynamic characteristics of the system.

Structural FEA is a well known software module designed to determine stresses and deformations of every component as a part of the system. But it is essential that the constraints assigned in the FEA are not intended as simple devices that limit the degrees of freedom of the mechanism, but are capable to simulate correctly the real interactions among the members of the mechanism in the contact areas, by generating a load distribution corresponding to that physically exercised by the real constraints.

The determination of the most appropriate simulation of the real interaction between constraints and components or between the load transmission system and the individual component is crucial to prepare a correct VP. In fact, in some cases, the simple utilization of standard FEA SW leads to results that are not accurate enough.

3 The design optimization of an existing reciprocating compressor crankmechanism

The new design method described above was utilized for the modernization of an existing typical 4 crank reciprocating compressor crankmechanism that was designed years ago with the traditional method. As a first design already existed, one started from point c) of Para 2.10 introducing the modifications that were deemed necessary for the modernization. Then a complete VP, including crankshaft, connecting rods and crossheads with the relevant bearings, was produced and tested according to points d), e) and f) of Para. 2.10.

3.1 The virtual prototype

As it is explained in the Introduction, the crankmechanism of a reciprocating compressor is typically subject to load patterns variable from one application to another and even within the same application from one operating condition to another. For the machine under examination, two extreme load patterns were selected for the single gudgeon pin load:

- perfect thrust reversal (Figure 3)
- no thrust reversal (Figure 4)

both at maximum allowable load.

As far as the external constraints, they are constituted by main journal bearings for the crankshaft and by cylindrical sliding connections for the crossheads, while the internal constraints are constituted by rotating joints between the crankpins/gudgeon pins and the relevant bearings.

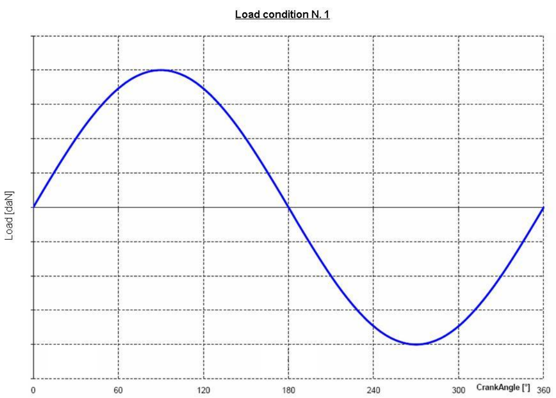

Figure 3: Perfect thrust reversal load pattern

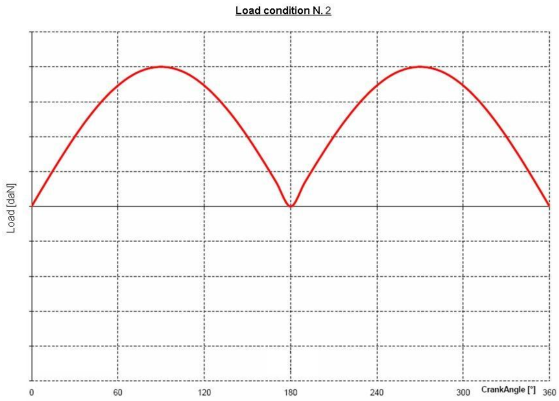

Figure 4:No thrust reversal load pattern

3.1.1 Models for the MDA

For the MDA, the following assumptions for the simulation were made:

- the main journal bearings are rotating joints that allow the rotation of the crankshaft, considered as a rigid body;
- the crosshead sliding connection is a cylindrical joint that allows linear translation and rotation around the translation axis;
- the constraint of the connecting rod to the crankshaft is a rotating joint that allows rotation around the crankpin only;
- the constraint of the small end of the connecting rod to the crosshead pin is a joint that allows the rotation around the pin itself and the translation along the same axis.

In this case no deformability of the constraints has been taken into account as the aim was just the determination of the resultants of the constraint reactions caused by the loads acting on the crossheads.

The load transferred from the pistons to the crossheads was simulated applying to them loads having the same axis of the piston rods and the value according to the assigned load profile.

The angular speed of the cinematic joint of the main journal and the relevant bearings was assumed to be equal to the maximum machine operating speed.

The MBD simulation supplied the diagram of various load components during the complete cycle on the interested members of the machine, including the inertial actions, for the two load conditions assigned. The development of the load components was then utilized to elaborate the fatigue analysis of the various pieces of the machine.

3.1.2 Models for the FEA

In order to perform with the necessary accuracy the FEA it is necessary to implement the mesh of the components in a way to minimize the error particularly in the most critical areas. This goal is reached by applying manually the mesh controls by means of an iterative process of optimization up to the point when every member results discretized in a manner to make the VP meeting the physical reality. The results are considered acceptable when a more refined mesh does not entrain meaningful variations of the stress results (asymptotic stresses trend).

It is also essential to lay down all the loads, coming from the MDA, and constraints in the most realistic way, so to represent the operation in the most accurate way, keeping the true degrees of freedom and avoiding to introduce stresses substantially different from the real ones.

An example of the special work done for the simulation of the bearing action can be understood comparing the different models utilized for the crankpin and the main journal bearings. As far as the crankpin, the actions of the connecting rod on it were simulated by means of a special feature of the software called “bearing load”, which is in a position to take account of the uneven pressure distribution of a hydrodynamic bearing. The same model could not be utilized for the main bearings as the bearing load model needs a predetermined direction of the load resultant which, for the connecting rod is known but it is not for the main bearings. Therefore for the main bearings a special model was created capable of simulating the way the main bearing reactions are transmitted to the crankshaft.

The behaviour of a hydrodynamic bearing (Figure 5) is such that it functions, within small elastic deformations, as a constraint which reacts with a certain stiffness to the only radial translation; i. e. it does not oppose any resistance to the shaft rotation either in the X-Z plane (around Y) or in the X-Y (around Z). In substance, the lubricant film, which supports the shaft, adapt its thickness in a manner to generate, in every instant, a pressure field capable of reacting to the resultant of the loads applied. In these conditions, point C of the shaft, which coincides with the geometric center of the bearing when the shaft in its ideal, unloaded and undeformed condition, once it is submitted to the loads, it moves to the C’ position where it finds a new equilibrium with an nominal eccentricity *«e»* (as it is measured in the average plane parallel to Y-Z of the bearing) having to components *«e_x»* and *«e_z»*.

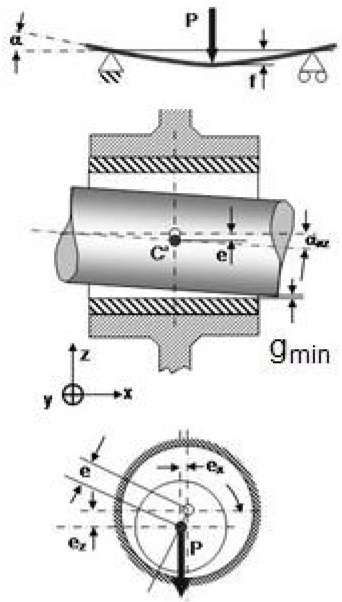

Figure 5: Behaviour of a hydrodynamic bearing

Besides, the deformations imposed to the shaft by the loads, indicated generically with P in Figure 4, modify the shaft position causing a rotation around point C’ of an angle *«α»* which, in turn, has two components *«α_{xz}»* e *«α_{xy}»* (the latter is not represented in Figure 4 for simplicity). The fluid film does not react appreciably to these rotations. This fact makes the verification of the minimum oil film thickness *«g_{min}»* in all operating conditions advisable.

So, for the case under examination, specific constraints with the suitable radial and rotation stiffness were modeled and validated through literature cases [3,4,5] .

Beside the statement of the constraints, for the FEA on complex assemblies, it is necessary to define the contact conditions among the various members in a manner to simulate conditions such as contact without penetration between elastic bodies with or without friction, union between two components, shrink fitting with or without friction and so on.

Once applied all the above basic statements on the various assemblies that represent the functional groups, such as crankshaft, connecting rod, crosshead, the static analysis for the structural verification were performed, loading every element with the loads corresponding to the worst case

At the end of the process a fatigue analysis was performed with the following steps:

- static analysis for all components of each stress;
- the stress state relevant to every reference static analysis was modulated in function of the development of the load curves elaborated through the MDA;
- determination of the amplitude of the equivalent alternate stress for each node;
- utilization, on a case by case basis, of the most suitable fatigue resistance criterion for infinite life.

For those areas of the VP that needed some optimization, an iterative method with progressive change of the relevant geometric and structural parameters was performed, up to when a satisfactory configuration was reached.

3.2 Crankshaft

3.2.1 Preliminary design review

Before starting with the creation of the VP the original design was reviewed and all necessary improvements introduced according to the most qualified literature [6, 7, 8]. Typically the modifications introduced were relevant to fillet radiuses between webs and pins, lube oil hole shape, dimensions and radiusing.

3.2.2 The mesh

A mesh with solid tetrahedric elements with Jacobian verification in 29 points was applied. A dimension of the base element of 47 mm was adopted. Several manual controls of the mesh were performed particularly in the following points:

- fillet radiuses between pins and webs with element size of 3 mm;
- lube oil holes with element size of 8 mm;
- edge radiuses between lube oil holes and the pin surfaces with element size of 4 mm.

Total number of degrees of freedom: 2'434'686.

3.2.3 Fatigue analysis and most stressed areas

After having obtained through the MBD the development of the components of the forces acting on the cranks as referred to a fixed reference system, the development of the same components as referred to a reference system solid with the rotating crankshaft was determined.

Then, 11 reference static analyses to be fed to the fatigue analysis were done:

- N. 8 analyses, one for each of the two components of the loads applied to the four cranks with a module equal to the maximum value reached during the cycle;
- N. 2 analyses relevant to the two components of the weight of the flywheel;
- N. 1 analysis relevant to the fitting of the flywheel on the crankshaft.

The fatigue evaluation was made matching the development of the loads, coming from the MDA, with every reference static analysis mentioned above. So doing, the stress state in every node is composed to take care of all load components in every moment of the cycle.

As usual, the most stressed areas resulted to be in correspondence of the fillets between the pins and the webs (Figure 6).

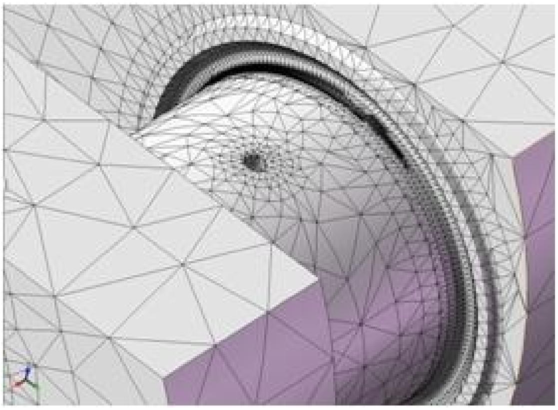

Figure 6: Stress concentration at the fillet radius between pin and web

However, the qualitative modifications introduced during the preliminary design review and fine tuned through the VP study brought the relevant fatigue safety factor well within acceptable limits. The analysis showed that also the other typically critical areas, the lube oil holes, after being cured, were fully acceptable from the fatigue point of view.

3.2.4 Corrections introduced

As stated above the dimensions of the radiuses were increased with subsequent attempts up to reaching the optimization of the fatigue safety factor.

3.2.5 Determination of constraint reaction of main frame supports

Only by means of a FEA one can determine, in an accurate way, the reaction of each main support during the cycle. In fact the crankmechanism is a highly redundant structure which can be solved only by considering the elastic deformability of the crankshaft and the supports.

In Figure 7 the development of the x and y components (as referred to a fixed reference system) of the reactions produced by the 5 crankcase supports are shown. They were obtained by compounding all the loads.

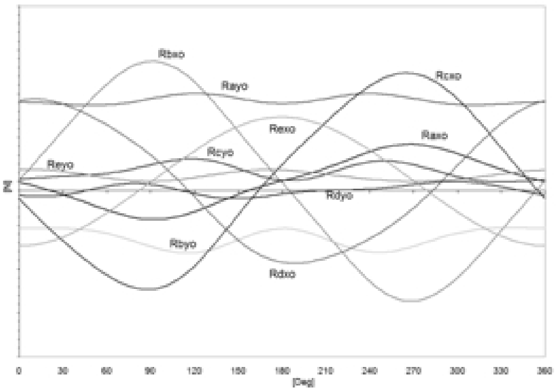

Figure 7: Development of the x and y components of the main bearing reactions

3.3 Connecting rod

The connecting rod was considered as an assembly composed by the shank, the hat, the connecting bolts with the relevant nuts, small end bushing and big end bearing.

The contacts among the different members of the assembly were modeled as follows:

- interference between small end bushing and conrod shank seat with the condition of maximum material;
- interference between big end bearing and conrod seat with maximum material;
- no penetration between hat and conrod shank;
- no penetration between bolt head and conrod shank;
- no penetration between nuts and conrod hat;
- no penetration between bolt shank and conrod shank and hat.

3.3.1 The mesh

A mesh with solid tetrahedric elements with Jacobian verification in 4 points was applied. A dimension of the base element of 15 mm was adopted. The manual controls of the mesh were performed particularly in the following points:

- fillet radiuses close to the contact areas between conrod shank and hat with the bolt head and nut with element size of 1,5 mm;
- contact areas between bearings and the relevant housings with element size of 10 mm;
- contact areas between conrod shank/hat with the bolt head and nut with element size of 5 mm;
- lube oil hole with element size of 8 mm;
- fillet radius on the bolt shank with element size of 2,5 mm;
- small end bushing with element size of 6 mm;
- nuts with element size of 5 mm;
- edge radius on the lube oil hole with element size of 1,5 mm;

Total number of degrees of freedom: 1'072'119.

3.3.2 Fatigue analysis and most stressed areas

The method utilized for the fatigue analysis was the same reported in Para 3.2.3 for the crankshaft. In the specific case, the following 7 reference static analysis were performed:

- N. 1 analysis relevant to the steady loads: interference fit of bearings and bolt preload;
- N. 1 analysis relevant to the typical compression load;
- N. 1 analysis relevant to the typical tension load;
- N. 4 analyses to take account of the translation and rotation inertia effect coming from the MDA.

In this case, the composition of the reference static analyses to perform the fatigue analysis was particularly complex as, for all the analyses, it required to combine stresses with different time pattern: the compression loads, which have a specific time law and the fitting and preloads which are steady.

The first results showed that the most stressed areas were the following:

- contact area between bolts and conrod shank;
- edge radius of the lube oil hole;

3.3.3 Corrections introduced

The following corrections were introduced following the iterative process:

- optimization of the edge radius of the lube oil hole;
- optimization of the bearing thickness in order to reduce the bolt preload taken by the bearing crash;

The above optimizations allowed reaching a completely satisfactory fatigue factor on all conrod components.

3.4 Crosshead

The same methodology applied to the connecting rod was utilized to verify the crosshead element of the VP. Also in this case the assembly was modelled without simplifications, in order to reach the necessary accuracy. To have a complete model, also the gudgeon pin was simulated.

3.4.1 The mesh

A mesh with solid tetrahedric elements with Jacobian verification in 4 points was applied. A dimension of the base element of 17 mm was adopted. The manual controls of the mesh were performed particularly in the following points:

- critical areas of the crosshead body and contact area with the gudgeon pin with element size of 8 mm;
- areas of contact of the flange with the crosshead body with element size of 4 mm;

Total number of degrees of freedom: 3'732'843.

3.4.2 Fatigue analysis and most stressed areas

The following 4 reference static analysis were performed:

- N. 1 analysis relevant to bolt preloading
- N. 1 analysis relevant to the typical compression load;
- N. 1 analysis relevant to the typical tension load;
- N. 1 analysis relevant to the transversal component (perpendicular to the crosshead sliding direction) of the load transmitted from the connecting rod to the crosshead.

Even in this case, the same comments made in Para 3.3.2 for the composition of steady and variable loads apply.
The most stressed area resulted to be the bolts connecting the flange to the crosshead body, but all components of the crosshead resulted to have satisfactory fatigue safety factors for infinite life.

4 Conclusions

Virtual Prototyping, when well set up and executed, is a fundamental pillar of a new advanced iterative design method which has the great advantage, in comparison with the traditional methods, to have a complete synoptic view of the system.

Notwithstanding the fact that it is based on verification techniques, it allows a progressive refining of the design on the basis of a series of contextual analyses which are possible in case of a deep integration of the CAE Tools.

This technique is a powerful integrated tool in the hands of design engineers and was utilized by the authors for many projects, including the modernization of an existing crankmechanism, which was reviewed working simultaneously on its main components.

The creation of Virtual Prototypes is useful also for subsequent utilizations of the machines designed with this method. In fact, in case of applications deviating from those considered in the original design, the VP can be easily brushed up and modified to suit the new conditions with great advantage for time and cost.

References

[1] H. Paul Barringer, P.E.; David P. Weber:
Life Cycle Cost Tutorial,
5th International Conference on Process Plant Reliability
Houston, Texas, October 2-4,1996

[2] E. Teicholz; J.N. Orr:
Computer integrated manufacturing Handobook;
McGraw-hill

[3] E. Funaioli; A. Maggiore; U.Meneghetti:
Lezioni di meccanica applicata alle macchine, Vol. 1, Editrice Patron Bologna

[4] R. Ghigliazza; A. Lucifredi; R. Michelini:
Lezioni di meccanica applicata alle macchine,
Editore Tolozzi Genova

[5] M.J. Neale:
Bearings - A tribology Handbook
Published by Society of Automotive Engeneers

[6] R. C. Juvinall; K.M. Marshek:
Fondamenti della progettazione dei componenti delle macchine,
Edizioni ETS

[7] Niemann; Winter:
Elementi di macchine, Vol.1
Edizioni EST-Springer

[8] W. Ker Wilson:
Practical solutions of torsional vibration problems, Volume 3, Chapman & Hall Ltd, London

Compressor Valves – How much do they contribute to operational Noise and Vibrations?

by

Harry Lankenau
Head of Technical Service and Engineering
Harry.Lankenau@NEAC.de
NEAC Compressor Service GmbH & Co. KG
Uebach-Palenberg, Germany

and

Roland Schuhmann
Manager Diagnostics and Monitoring
Roland.Schuhmann@BASF.com
BASF SE
Ludwigshafen, Germany

6th Conference of the EFRC
October 28th - 29th, 2008, Dusseldorf

Abstract:

During commissioning of three identical piston compressor lines for oil field gas lift service some vibration issues needed attention. In the run of investigations the suction pulsation vessels above all first stage cylinders became a particular focus point. High frequency vibrations drove the vessel and small bore nozzle vibration level up to unfavourable magnitude. The surprising factor was the also comparably high noise level in the vicinity of the first stage cylinders - and it was impossible to locate the source. The vibration issues were overcome – the noise remained.

Three years later - when all units had operated quite a number of hours - a routine vibration check was performed. At two of the three units the high sound level had disappeared whereas one unit was still as loud as in the past. The overall vibration level had also come down significantly. It turned out that first stage suction valves at the two silent machines had been replaced by a different design. The loud one, however, was still running with the original valve set.

Based on these findings the conclusion was that valve design and sizing must have a significant impact on compressor unit vibration and its sound level.

The paper outlines the path from the first observed phenomena through the conducted analyses to the results and the involved modifications.

1 Introduction

The subjects of this paper are three compressor lines for oil field gas lift service in the desert (figure 1). The medium to be handled is natural gas from the oil wells which is re-injected after conditioning and cleaning. The molecular weight of the processed gas is about 25 kMol/kg. Due to the origin of the gas it is saturated with hydrocarbons which require careful and reliable condensate drain.

(Figure 1.1: Desert Gas Lift Units)

The re-injection pressure of some 200 bar(g) is provided for by three Neuman & Esser reciprocating compressors of the type 3 SVL 320, three stages, four throws, frame size 320; double acting lubricated cylinders and spill back flow control (figure 1.2). The speed was selected to 353 rpm only (synchronous speed of 360 rpm). With a stroke of 315 mm the mean piston speed comes to 3.7 m/s which is considered being low for lubricated service. The sizing had been based on an overall conservative design.

(Figure 1.2: Neuman & Esser Compressor Units)

From the first day of operation in November 2003 a comparably high noise emission was noted in the vicinity of the two first stage cylinders which seemed to be generated by the first stage suction pulsation vessel. The noise level was very much the same at all three compressor units.

The major and more serious issue was, however, the mechanical vibrations at the pulsation vessels of all three units with characteristic frequencies above the 100 Hz range. Particularly some of the small bore nozzles of the vessels were suffering from the vibration induced loads and, thus, needed additional supports – at first by means of temporary provisional clamps and finally through adequate bracing.

The vibration issues were overcome – the noise remained. A link between both had never been recognized and is still today a kind of mystery.

Due to a common and proven design for the compressor valves their selection and sizing had initially not been subject to debate.

2 Vibration Issue

Figure 2.1 is showing the 1st stage side of the compressor unit. The lay-out is rather identical for all three of them. The suction line is entering the suction pulsation vessel 1st stage with two pipelines branching off to both 1st stages of the compressor.

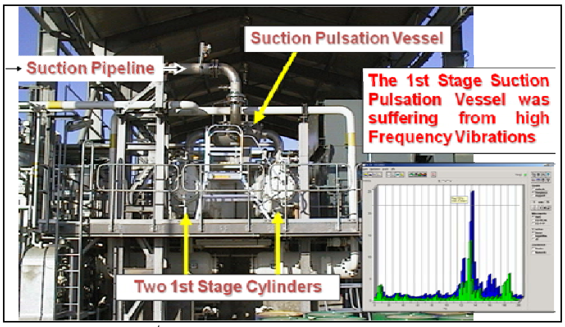

(Figure 2.1: 1st Stage Side of Compressor Unit)

The dominant vibration frequency of the small bore nozzles - for the installation of pressure gauges, vent valves, temperature wells and drain valves – was 132 Hz (small chart in figure 2.1).

The compressor speed of 353 rpm is in the range of a 1st order frequency of about 5.9 Hz. With a crank angle of 90° between both 1st stage throws and two double acting cylinders the characteristic pulsation frequency was supposed to be some 23.5 Hz.

Even considering higher orders - which may contribute to the vibration spectrum - a 132 Hz peak is surprisingly high and not common for such a conservative designed compressor unit.

It should, however, be noted that vibrations as well as gas pulsations in the high frequency range are occasionally encountered at reciprocating compressor units of various kinds.

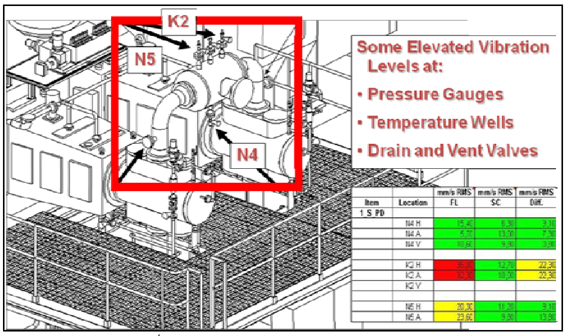

(Figure 2.2: 1st Stage Suction Pulsation Vessel)

The table in figure 2.2 represents an example of the typical vibration characteristic with values in the green (well acceptable) range but with certain points where the level had to be assessed as to be 'elevated' or even 'critical' with the potential risk of a nozzle crack. The black arrows depict the relevant nozzles being taken care of.

The mechanical vibrations had been detected during the commissioning phase. To enable continuous operation in a safe condition with minimum interruption through unscheduled shut-downs temporary provisional steel clamps were fitted to those nozzles which required reinforcement. The target of the clamps was to avoid individual nozzle movement and to increase the stability by the joint bracing (figure 2.3).

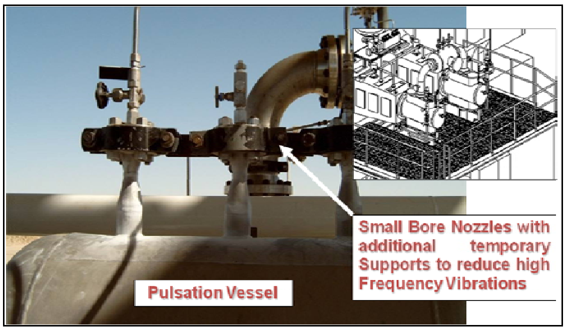

(Figure 2.3: Small Bore Nozzle Supports)

3 Noise Phenomenon

Everybody who approached the compressor units immediately noticed the comparably hard and loud noise in the vicinity of both 1st stage cylinders (figure 3.1) – next to the machines as well as downstairs on ground level.

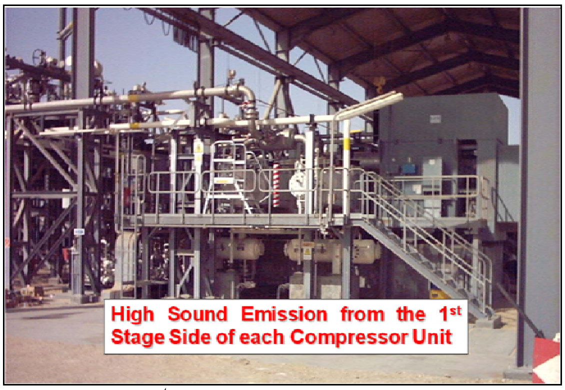

(Figure 3.1: 1st Stage Side of Compressor Unit)

From subjective perception it was the suction pulsation vessel which seemed to be the source of the noise emission – but it was impossible to reliably locate the point of origin.

Since sound emission is not really a key issue in the desert this subject was taken as given without serious attempt to fight this phenomenon.

Thoughts of potential sources concentrated on a couple of items.

Potential source no. 1 (figure 3.2):

The suction pulsation vessel (volume bottle)

- Sharp edges in the pulsation vessel
- Small bore nozzle connections
- Thermowell flow turbulence

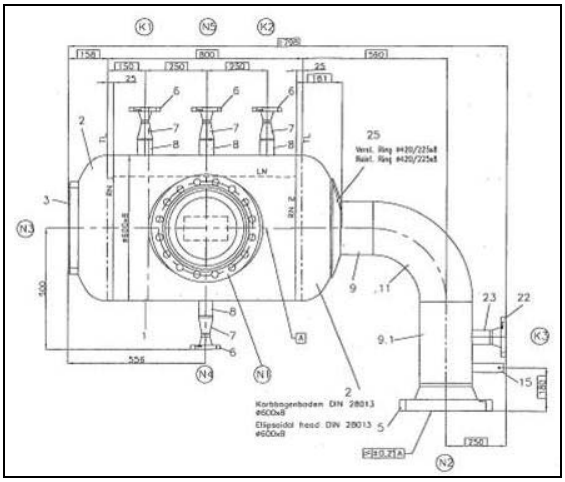

(Figure 3.2: Suction Pulsation Vessel Drawing)

Potential source no. 2 (figure 3.3):

The orifice in the suction line - being located close to the vessel inlet.

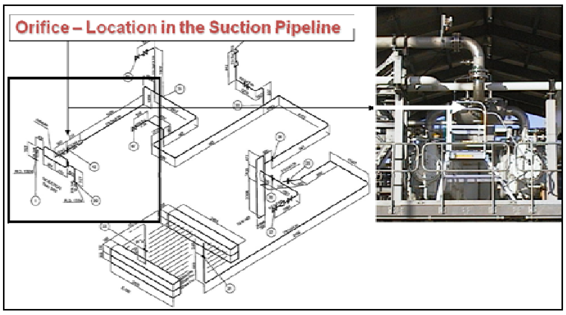

(Figure 3.3: Suction Pipeline Isometric)

Potential source no. 3 (figure 3.4):

The 1st stage cylinder gas passage.

- Sharp edges in the cylinder gas passage
- Valve cage flow turbulence
- Valve gas flow

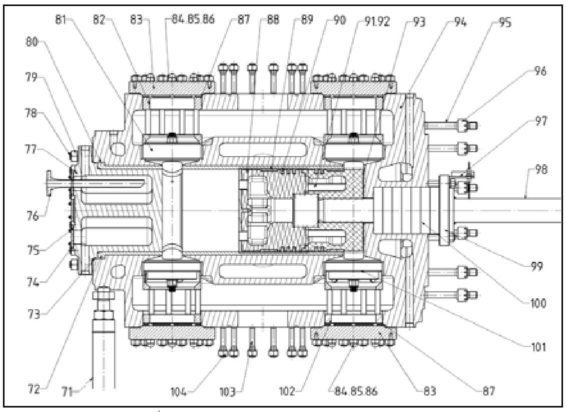
(Figure 3.4: 1st Stage Cylinder)

Investigation to identify the mechanism of the sound generation would have required intensive research and engineering which nobody was prepared to pay for. Consequently only little was done to fight the same.

Only some basic checks were conducted:

- The pulsation vessel – which is an empty volume bottle combining the suction side of both first stage cylinders – was opened and visually inspected. There was no evidence of anything which could be imagined to be the source of the sound emission.
- Based on a comprehensive acoustic study an orifice with moderately reduced inside diameter had been installed at the suction inlet flange. Removal for testing purposes resulted in higher pipeline vibrations – but the sound remained unchanged.

The cylinder internal had not been regarded in more detail because the noise – as mentioned before –appeared to be created somewhere in the pipeline or vessel.

A point of discussion is, however, also the fact that - comparable to an organ pipe - the sound generation point is not the location where the noise is loudest. A pulsation vessel can act as a sound resonator (like a violin resonator).

Apart from the above a lot more efforts were put into the analyses as mechanical vibrations can cause potential danger and therefore the full focus of all participating parties was required.

4 Investigations and Findings

Extensive pulsation and vibration measurements had been conducted to identify the root cause of the vibrations.


(Figure 4.1: Pressure Sensor in Nozzle)

Figure 4.1 shows the temperature nozzle of the suction side 1st stage with the dynamic pressure transducer installed.

The measurements in figure 4.2 show that the dominant frequency for the vibration of the flange is at 132 Hz. In the frequency spectrum of the gas the pulsation frequency of the pipeline can hardly be found. Out of this it can be concluded that the pulsation of the gas does not excite the mechanical vibration.

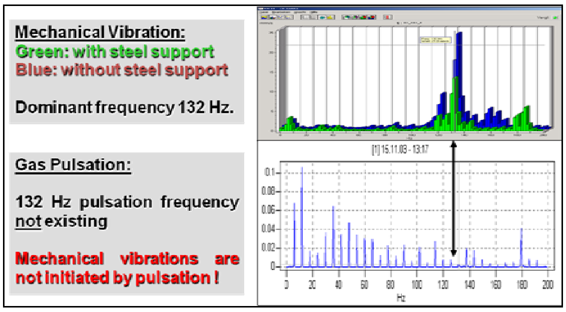

(Figure 4.2: Vibrations versus Gas Pulsations)

An operational deflected shape analyses was performed to get an idea about the mode shape of the vibration. With this information the right bracket was designed and applied to reduce the vibration amplitudes. The green bars in the frequency spectrum of the figure 4.2 shows that the amplitudes are reduced significantly.

Because the source of the vibration was still unknown, additional measurements were done. The cylinder pressures are shown in figure 4.3. The frequency spectrums of these signals also show no significant excitation at 132 Hz.

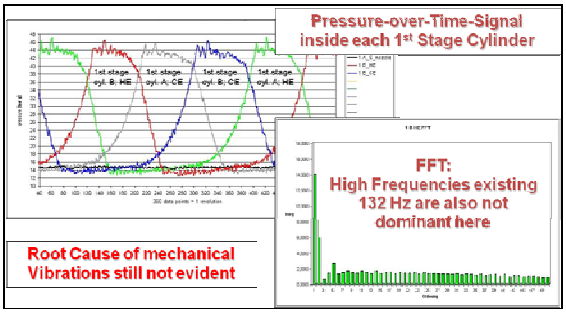

(Figure 4.3: Cylinder Pressure Signal and FFT)

5 Remedy for Vibrations

All investigations and measurements could not give a clear explanation about the root cause of the high frequency vibration. The temporary fixing of the nozzles reduced the vibration amplitudes significantly. Out of this experience final stiffening bracings for the nozzles were installed. Thiese nozzle bracings are shown in figure 5.1 to 5.3. Vibrations were reduced to a level that the compressors were suitable for a long term operation.

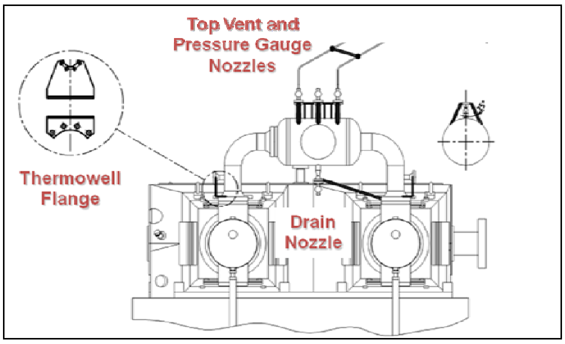

(Figure 5.1: Permanent Nozzle Bracing)

(Figure 5.2: Permanent Nozzle Bracing – PI and Vent)

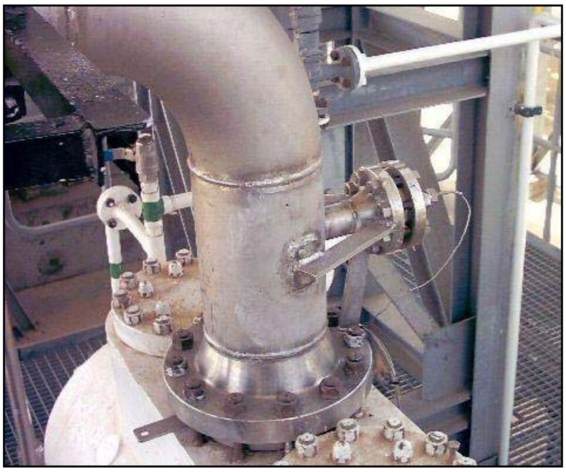

(Figure 5.3: Permanent Nozzle Bracing - TI)

6.1 Sound Check

About three years later after the start up of the compressors, a routine vibration check should verify that after these running hours no significant changes in vibration amplitudes are measurable and the compressor system is still in a good shape.

During these measurements it was noticed, that one of the compressor had a much higher noise level than the two others or in other words the noise of the other two ones was much lower than before, confirmed by dditional noise measurements.

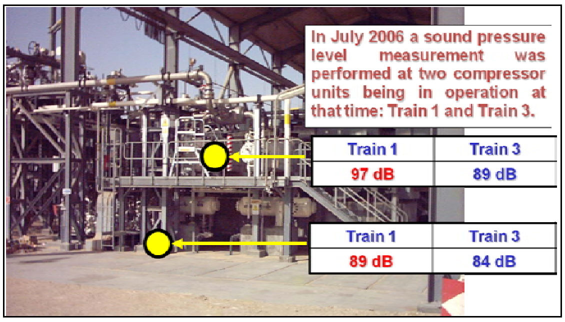

(Figure 6.1: Noise Measurement)

Figure 6.1 shows that there is a big difference in the noise level of about 8 dB between line 1 and line 3.

6.2 BASF Vibration Monitoring

After the commissioning a vibration monitoring system was installed at each line to monitor the mechanical behaviour of the compressor and give early warning in case of a mechanical defect. Because of the vibration problems at the suction side of the 1st stage, the accelerometer which was mounted originally at the crank case was moved to the pulsation damper 1st suction side to be aware of vibration changes.

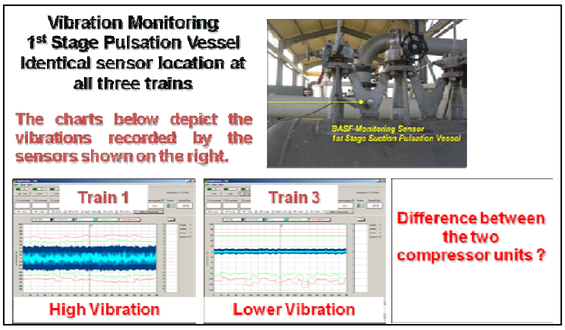

(Figure 6.2.1: BASF Vibration Monitoring)

The signals of these sensors coincided with the noise. Significant lower levels were observed at line 3 compared to line 1.

6.3 NEAC Mobile Vibration Meter Check

Two measurements – noise and online vibration measurement – clearly showed a significant difference between compressor 2 / 3 and compressor 1 at this time. Measurement with a mobile vibration meter showed that especially the high frequency components are lower at line 2 and 3 at this point.

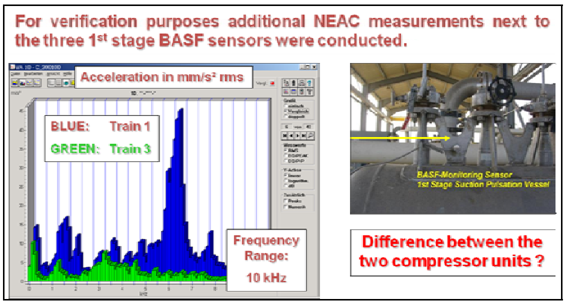

(Figure 6.3.1: NEAC Mobile Vibration Check)

Now what was the difference between line 2 / 3 and line 1?
Investigation of all the documents about maintenance indicated that the only difference was that line 1 had still the original valves installed at the suction side of 1st stage.

During operation some valve failures occurred and investigation showed that the valve guard had a week point at the outer diameter. Out of this the design was changed. These valves were already installed at line 2 and 3 but not at line 1.

7 Suction Valve Design

From the beginning a very common, standard ring type valve was used for all 3 lines, which is shown in figure 7.1 and 7.2.

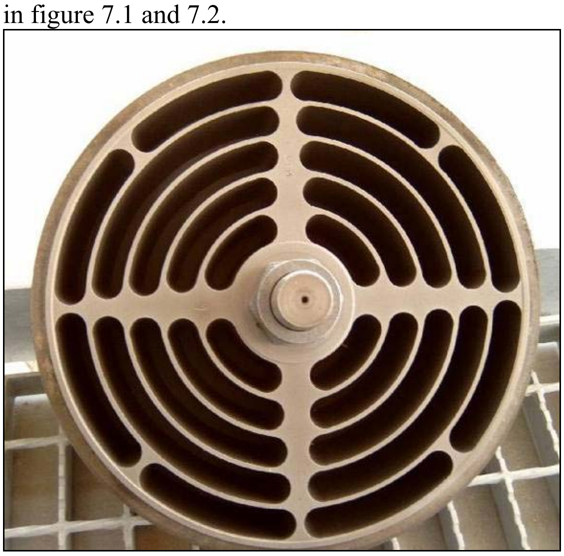

(Figure 7.1: Suction Valve – Original Design)

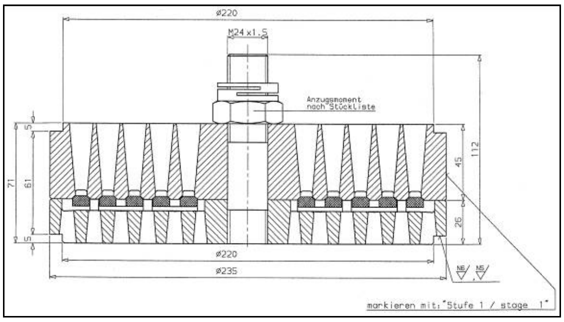

(Figure 7.2: Suction Valve – Original Design)

Due to a few valve failures during operation the valve design was reviewed by the valve manufacturer. The investigation showed high stresses at the outer diameter of the valve guard. Instead of grooves, the design was changed to holes at this area.

(Figure 7.3: Suction Valve – Modified Design)

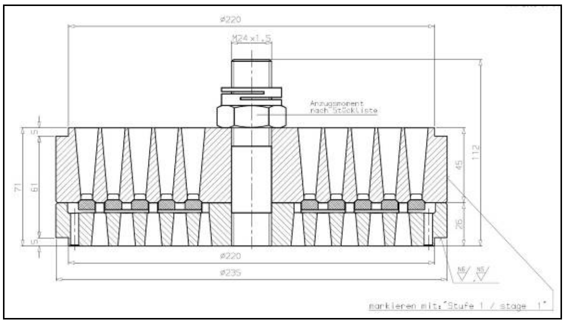

(Figure 7.4: Suction Valve – Modified Design)

Figures 7.3 and 7.4 show the modified valve. Except the holes at the outer diameter instead of the grooves nothing else (spring load, GAP) was changed.

8 Conclusion

During commissioning of the three compressor lines, high frequency vibration and a high noise level were observed, although a very conservative design (low speed) was chosen in respect of the operation in the desert.

Extensive investigations were done to find out the root cause of the high frequency vibrations. At least bracing of the nozzles was the only way to reduce the vibration amplitudes to an acceptable level to make the compressors fit for purpose.

Surprisingly three years later, after installing modified valves at the 1st stage suction side, the vibration amplitudes and noise level were reduced significantly.

It was evident that only the valves had changed between high and low noise level and nothing else.

Looking at the differences in the design of the original and modified valve nobody would expect a significant change in the acoustical behaviour.

The case history shows clearly the different impact of holes and grooves on vibrations and noise.

Now – at the end of this story – more questions than answers are left:

- What is the real root cause for the high frequency vibration?
- Which parameters have an impact on the occurrence of high frequency vibration and noise emission?
- How can we predict the acoustical behaviour of valves?

Additional investigations and studies have to be carried out to get a better understanding about the appearance of high frequency vibration.

The case history also shows that a "conservative design" is no guarantee for a smooth running and low noise and vibration of the compressor system but that also small differences of compressor components may have a big impact on the whole system.

Comparison of calculated and measured torsional vibration on recip cranks with evaluation of mechanical compressor efficiency.

by:

Dipl.Ing. Andreas Gottmer

Service Dept.

PROGNOST Systems GmbH,

Rheine, Germany

6^{th} Conference of the EFRC
October 28^{th} / 29^{th}, 2008, Dusseldorf

This briefing describes how the possibilities for implementing continuous torque measurement in an existing condition monitoring system have been explored in a degree dissertation. The work demonstrates the extent to which torque curve calculated from the dynamic pressure signals coincides with the directly measured torque curve.

In this regard, measured torques were compared to theoretical torques calculated using the dynamic pressures inside the cylinder. To do this, two horizontally opposed cylinder compressors being used for storing natural gas were considered. The torque was measured on the crankshaft of each reciprocating compressor.

1 Introduction: Superposition of the gas and mass forces

The crosshead force is composed, in the ideal case, of the gas force and the oscillating mass force. Frictional forces were ignored in this consideration.

This superposition creates compression and tension forces alternately in the piston rod. These forces act on the central point in the crosshead, the crosshead pin. Figure 1 shows the crosshead force curve of a cylinder with the corresponding pressure curves. This clearly shows that, when crossing the zero line, a tension/compression change occurs in which the contact surface of the crosshead pin in the crosshead eye changes. This is the important in ensuring optimal lubrication of the crosshead pin.

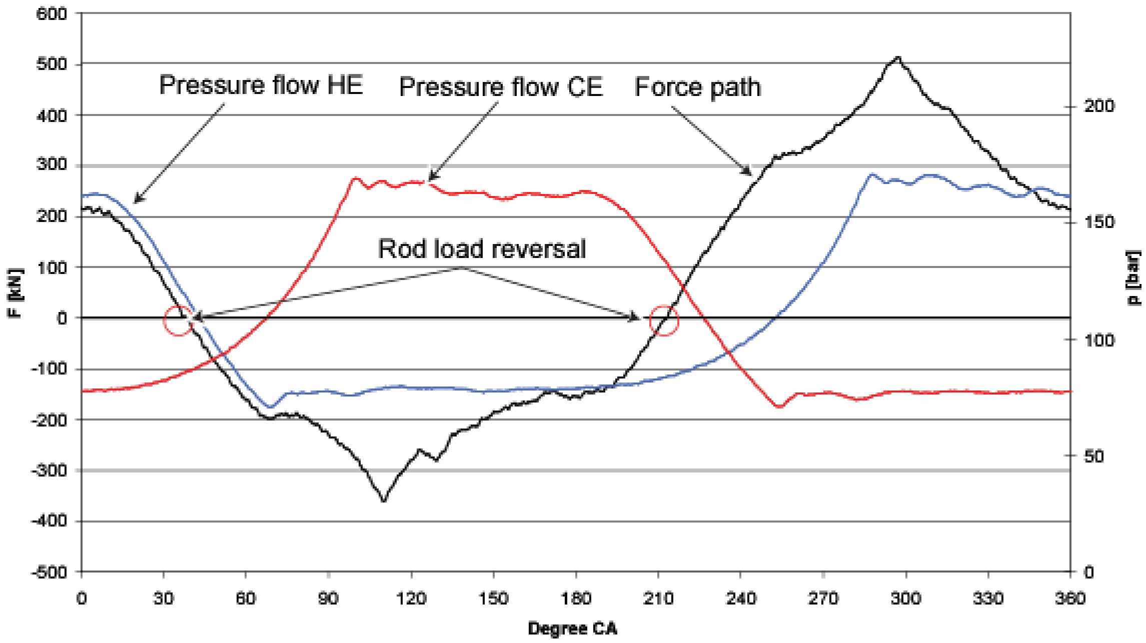

Figure 1: Pressure and force curves of a cylinder

Determining the torque

The equation for tangential force F_T is used to calculate the torque. For any compressor selected, the curves for the rotational force must be constructed individually for each crank and the values that apply for one crank position must then be added. To do this, the amplitudes are added in accordance with the existing crank angles, because the crankshaft is offset. In this regard, the beginning of the graph for a crank trailing by must be added to the value of the leading crank. The torque results from the sum of the individual tangential forces multiplied by the crank radius.

As the compressors considered here were already in operation, the only possibility for measuring the torque curve was the installation of a strain gauge on the crankshaft. In this way, changes to the structure were unnecessary.

Description of the compressor systems

Torque measurements were performed on two different reciprocating compressors. Both are reciprocating compressors with double-acting working chambers with opposed cylinder design, namely the Borsig BX 45-80/4S2 and the Ariel JGT/2. The most striking differences between these two machines were the masses they had to move and their power. In this respect, the Ariel compressor had a substantially lower mass to move than the Borsig compressor. Both machines were also speed-controlled.

Manufacturer:	**BORSIG**	***ARIEL***
Type:	BX 45-80/4S2	*JGT/2*
Designation:	V202	*V71300*
Model year:	1989	*2003*
Number of cylinders:	4	*2*
Stages:	2	*1*
Discharge flow:	10,000/100,000 Nm³/h	*4,000/16,000 Nm³/h*
Power:	3,700kW	*630 kW*
Rotation speed:	200/370 rpm	*750/1000 rpm*
Piston stroke:	270 mm	*114 mm*
Piston rod diameter:	130 mm	*50.8 mm*
Cylinder bore, stage 1:	365 mm	*171 mm*
Cylinder bore, stage 2:	265 mm	- / -

Table 1 Compressor technical data

Data acquisition using PROGNOST®-NT

PROGNOST®-NT, an already-existing condition monitoring system, was used to record the measured data provided by the amplifier. This ensures that the measured torque values are assigned a time. Consequently, the measured torque values can be analyzed in parallel with the other machine data, such as the dynamic pressure signals.

Operating conditions while performing the measurements

Borsig reciprocating compressor

Operating points during the measurements:

Two-stage operation			
Operating point	**Discharge flow [Nm³/h]**	**Suction pressure [bar a]**	**Discharge pressure [bar a]**
RF01	59000	33,5	162
RF04	46000	33,8	160
RF07	26000	33,2	160
RF10	16000	34,1	161

One-stage operation			
Operating point	**Discharge flow [Nm³/h]**	**Suction pressure [bar a]**	**Discharge pressure [bar a]**
RF01	68000	33,8	84,5
RF04	50000	33,6	84,3
RF07	35600	33,5	85,1
RF10	17600	33,1	84,2

Ariel reciprocating compressor

Operating points during the measurements:

One-stage operation			
HydroCOM regulation [%]	Suction pressure [bar a]	Discharge pressure [bar a]	Rotation speed [rpm]
100	60,3	80,6	720
100	60,4	80,5	989
80	60,3	81,1	982
70	60,6	80,4	989
64	60,4	81,2	986

2 Result of the torque measurement

Oscillating torque

The curve of the torque oscillated over the entire range of operation. An oscillating torque indicates that a changing torque component (dynamic component) is superimposed on a torque component that is constant over time or changing only slowly (average torque). The dynamic component may be periodic but need not be.

Figure 2 shows the oscillating torque. In this case, the average torque is constant and the dynamic component is periodic. Such a dynamic component that is at least semi-periodic is typical for reciprocating compressors. It is formed from the effects of the gas pressure forces and the mass forces of the crank drive system.

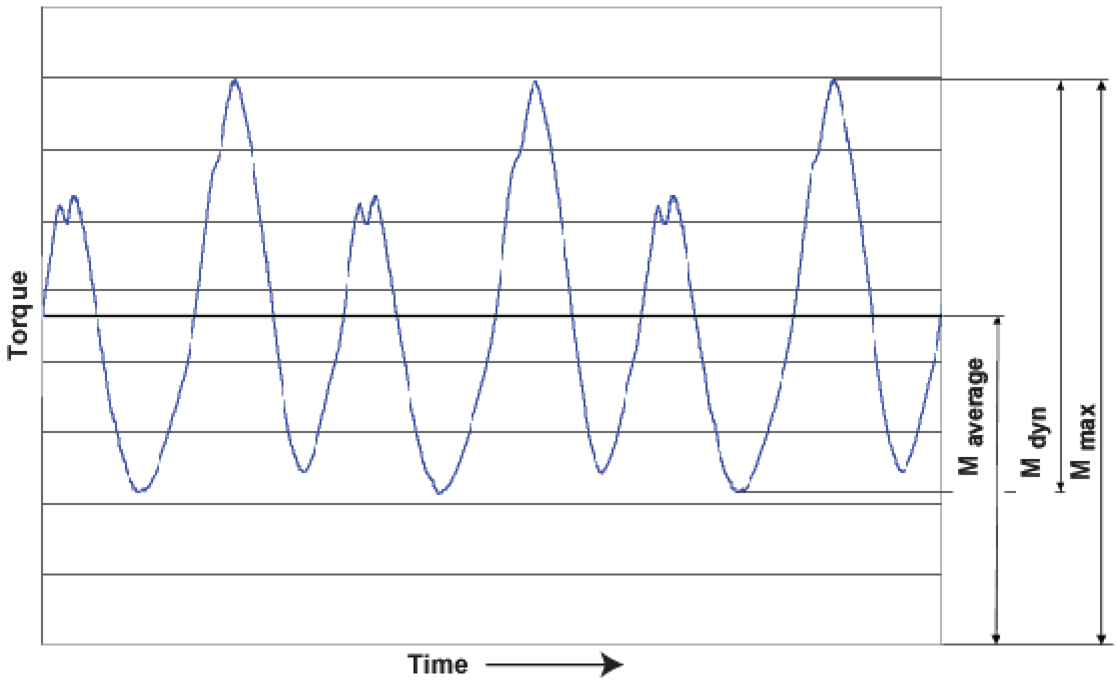

Figure 2: Superposition of the average torque and the dynamic torque component

The conversion of the rotation movement into the oscillating movement of the crossheads, pistons and connecting rods is considered the cause for the torque oscillation. The individual pressure curves of the compression chambers were considered for analyzing the torque.

Figure 3 shows the cylinder chamber pressures as a pt diagram, illustrating the pressure curve (p) versus time (t). As the time duration, the time for one crank shaft rotation (360°) was used.

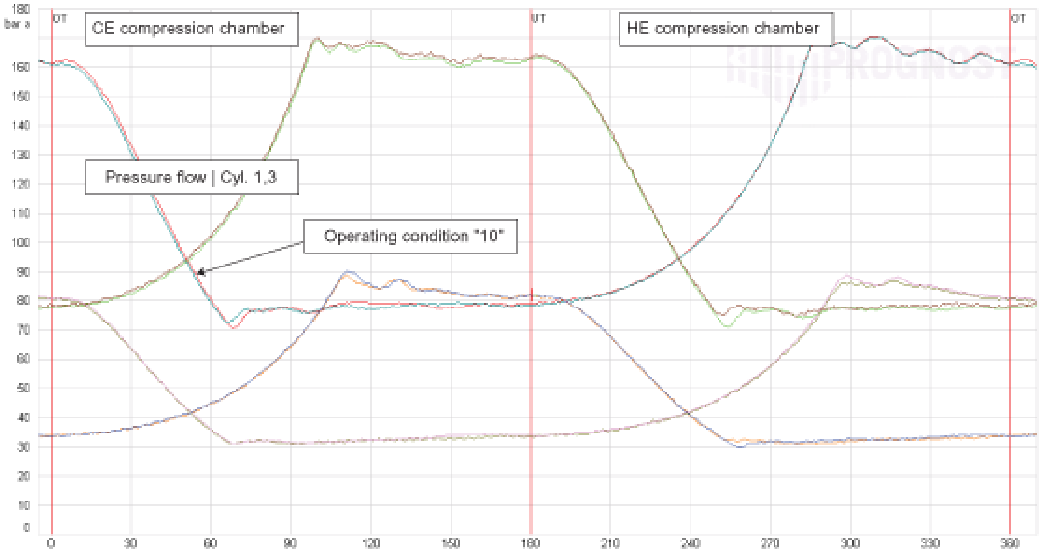

Figure 3: Cylinder pressure curves, crank end and head end, through one rotation for a two-stage operation in RF01, with 33 bar suction pressure and 160 bar discharge pressure.

The diagram shows the compression of the first stage (cylinders 2 and 4) of 33 bar suction pressure to 80 bar and the second stage (cylinders 1 and 3) to a discharge pressure of 160 bar.

In analyzing the individual operating conditions for the reciprocating compressor, it became clear that the suction valve capacity control was defective in the head end compression chamber of cylinder 1. This resulted in an increased alternating load placed on the crankshaft in the operating conditions RF04, RF07 and RF10.

Figure 4 shows four curves, each being assigned to one operating condition of the compressor.

The reciprocating compressor in two-stage operation had a suction pressure of 33 bar and a discharge pressure of 160 in this case, at a rotation speed of 350 rpm. This illustration clearly shows the different operating conditions in the torque curves. Especially The operating condition in RF10 (see the mark) results in particular in a high alternating load on the shaft, as the torque changes twice from positive to negative during one rotation. This corresponds to loads of 96.6 kNm to -27.6 kNm.

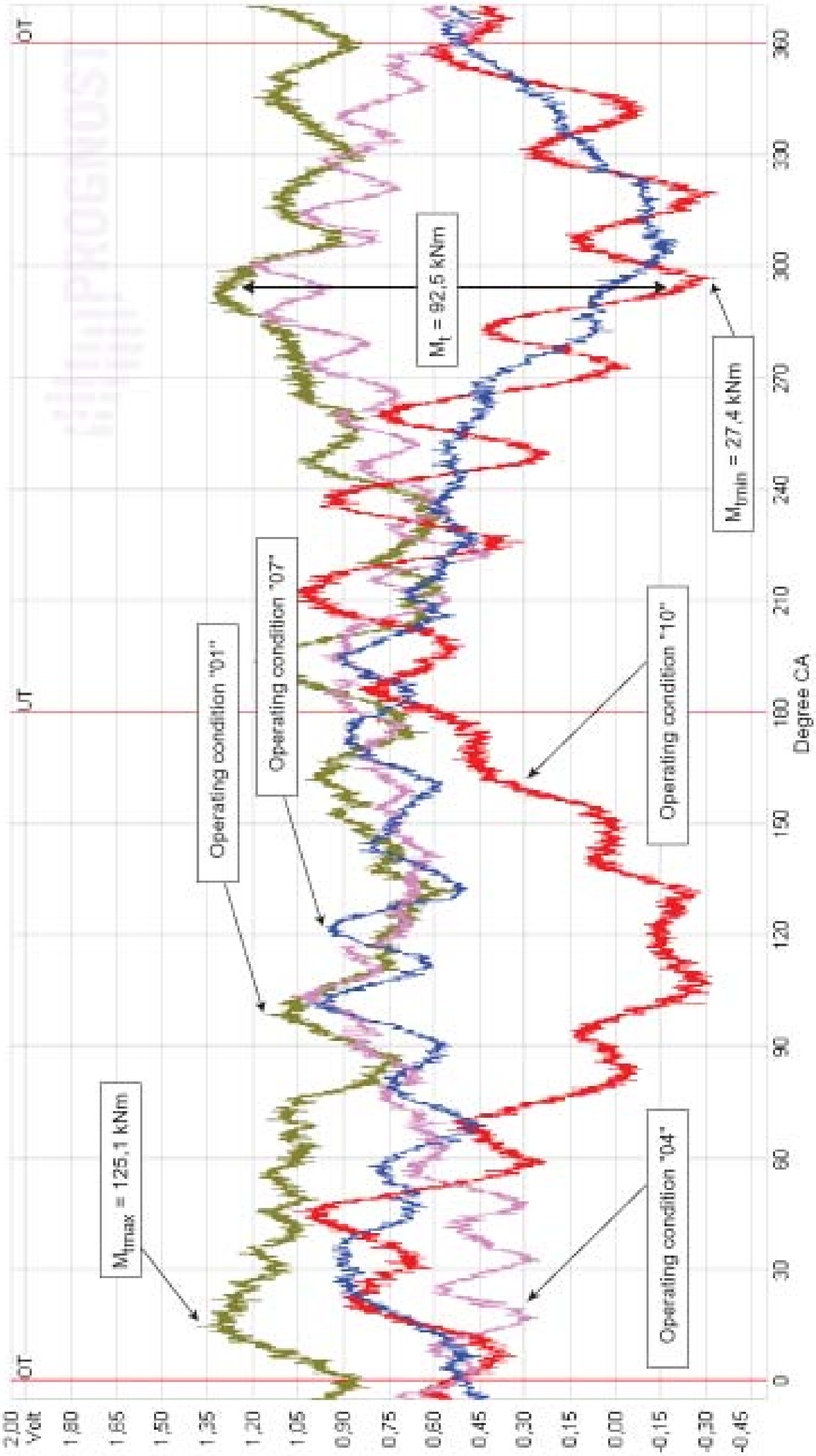

Figure 4: Torque curve through one rotation in two-stage operation from a suction pressure of 33 bar to a discharge pressure of 160 bar.

The curve of RF07 in which the crank end compression chambers are active, is particularly striking. The defect in the suction valve capacity control of the head end compression chamber of cylinder 1 also activates this. As a result, the torque is negative in the range from 280° CA to 320° CA. The compression on the head end (marked pressure curve) causes the torque to reach a value of -17,000 Nm at a crank angle of 300°.

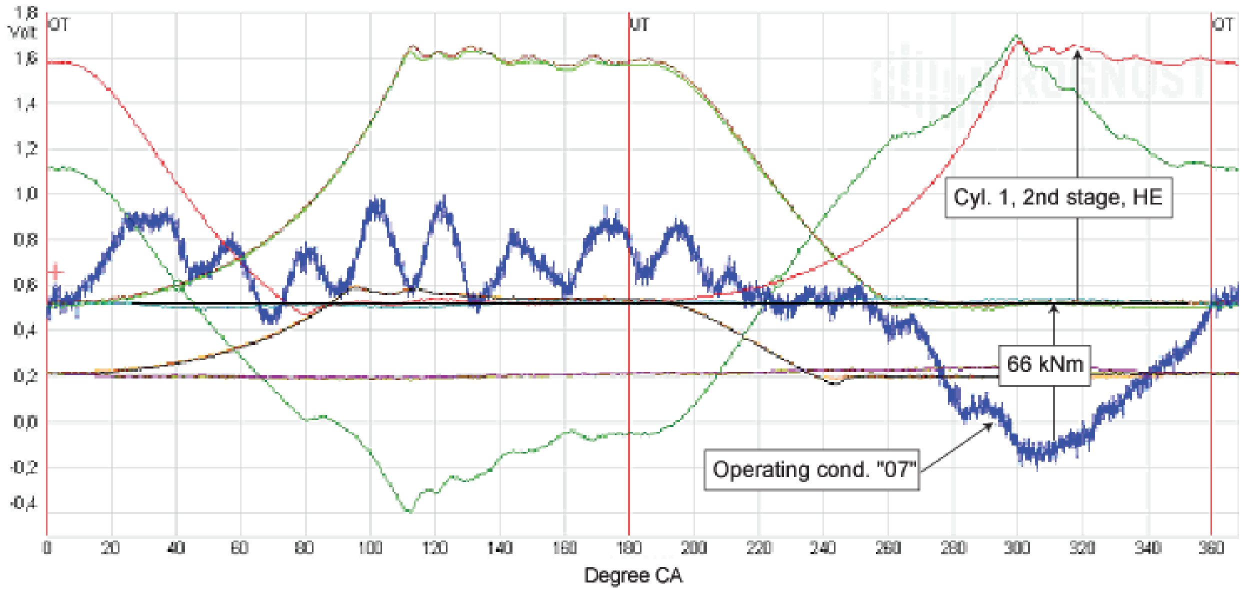

Figure 5: Torque curve in operating condition 07 with defective suction valve capacity control for cylinder 1, HE

Summary of the actual torque

Changes in the control elements of the compressor can be seen in the torque curve. If a torsion oscillation is superimposed on the torque, this can be recognized by displaying the torque in the frequency domain.

In general, information regarding the compressor can be recognized in the torque and this information can be used for condition monitoring. This can be obtained by installing a permanent torsion measurement system. As this permanent torsion measurement system leads to additional high costs for the machine operators, the next section examines whether the actual torque can be simulated using the cylinder chamber pressures. The cylinder pressure signals, which are measured using the PROGNOST® system, are to be used for this purpose.

Evaluation

To evaluate the torque from the cylinder pressure signals, the data from two different torque measurements was analyzed. These are the measurements on the reciprocating compressor from the Borsig Co., type BX 45-80/4S2, and on the reciprocating compressor from the Ariel Co., type JGT/2.

Results from the Borsig reciprocating compressor

The following four figures show the individual operating conditions of the reciprocating compressor. The figures show the torque over one crankshaft rotation.

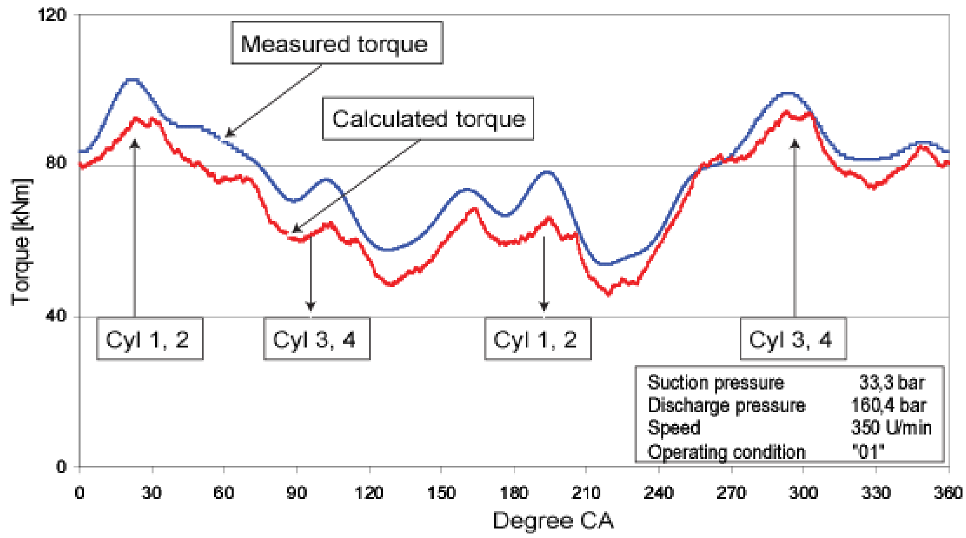

Figure 6: Torque curve of the reciprocating compressor (Borsig) over one rotation of the crankshaft in the operating condition 01.

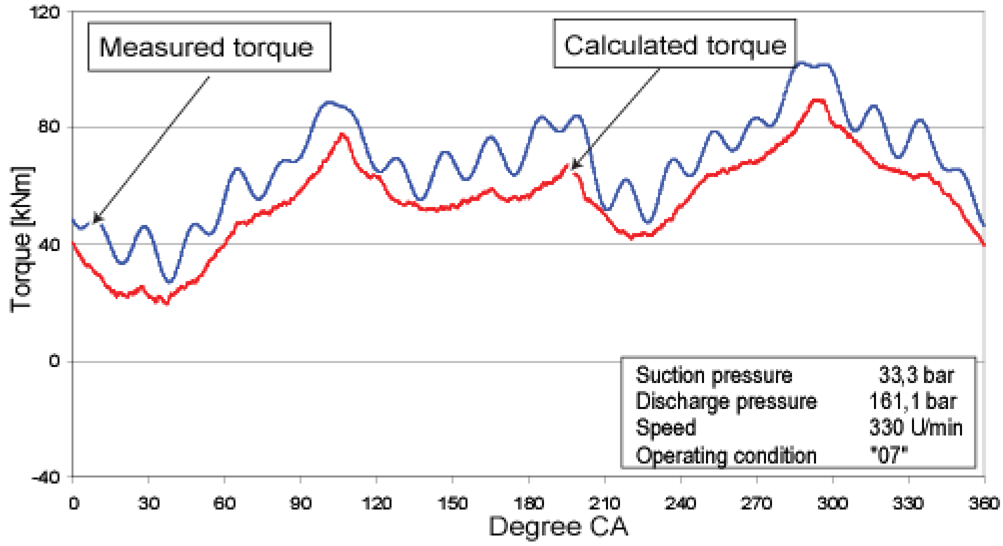

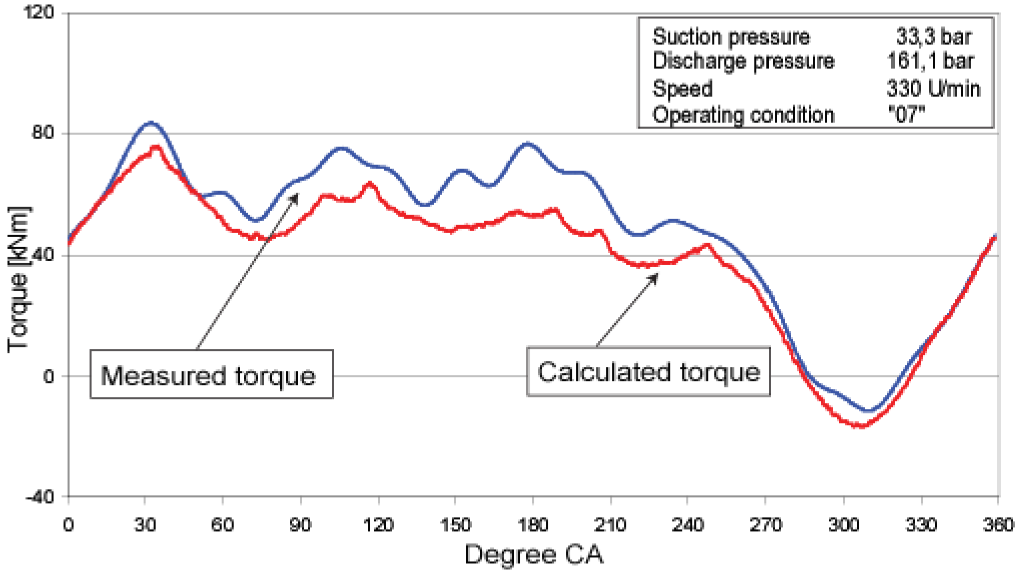

Figure 7: Torque curve of the reciprocating compressor (Borsig) over one rotation of the crankshaft in RF04 (top graph) and RF07 (bottom graph).

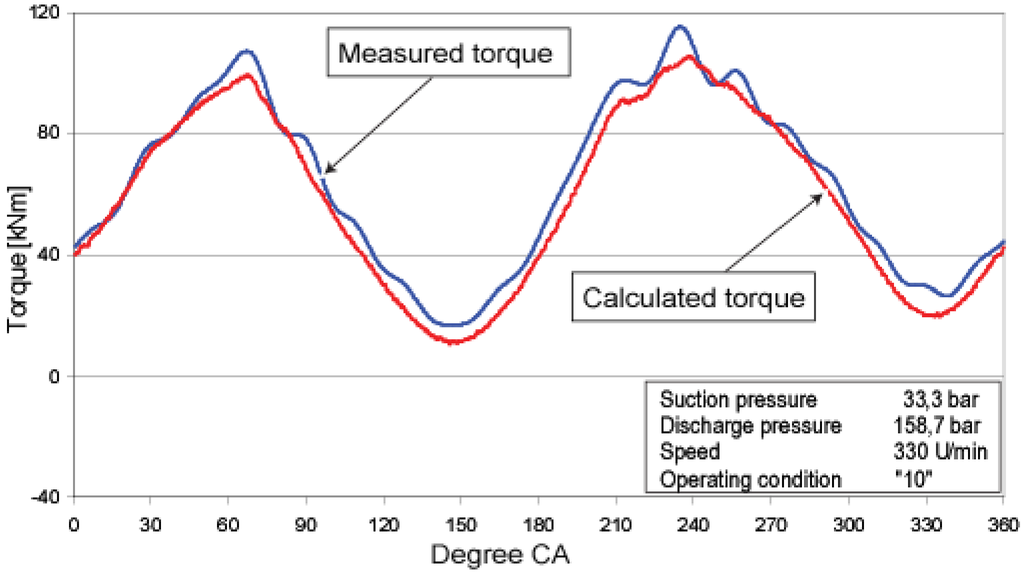

Figure 8: Torque curve of the reciprocating compressor (Borsig) over one rotation of the crankshaft in the operating condition RF10.

Based on these results, it can be seen that the curve of the calculated torque is identical to the actual torque over the entire range of operation of the reciprocating compressor. However, the oscillation present in operating condition 04 that is superimposed on the torque is not accurately reproduced. In conclusion, it can be stated that the torque can be reproduced quite well for this type of reciprocating compressor, using the cylinder chamber pressure signals.

Results of the Ariel reciprocating compressor

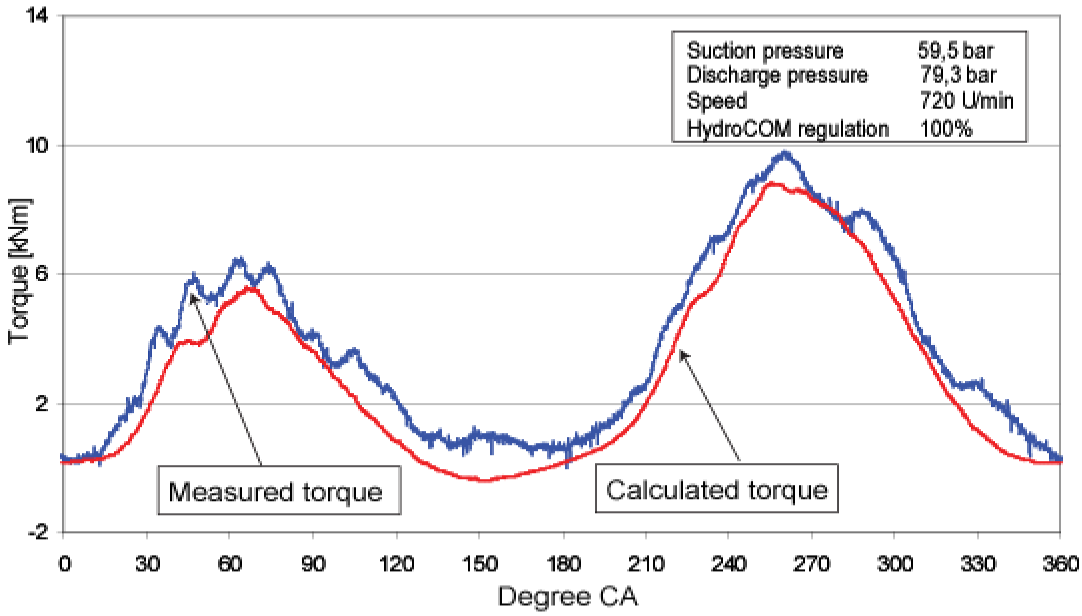

Figure 9: Torque curve of the reciprocating compressor (Ariel) at a 100% flow rate.

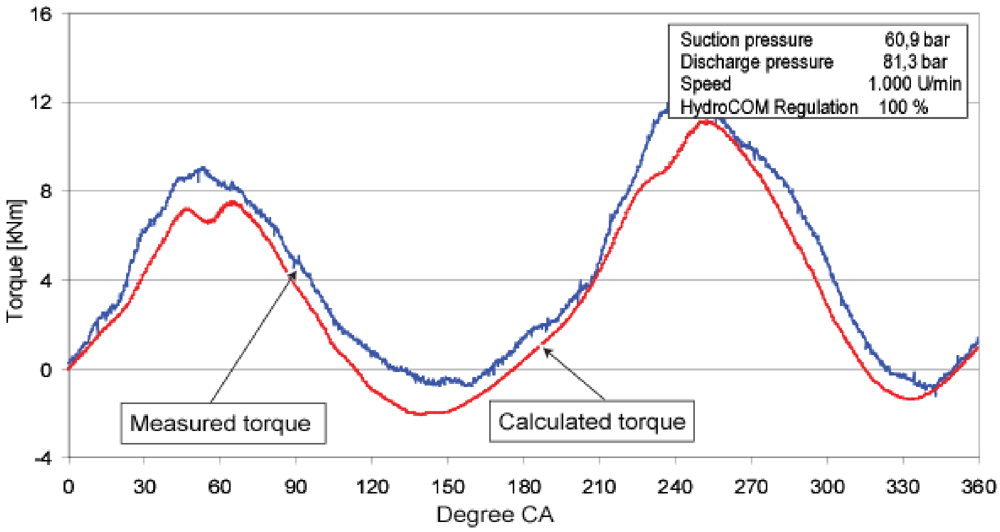

Figure 10: Torque curve of the reciprocating compressor (Ariel) at a 100% flow rate.

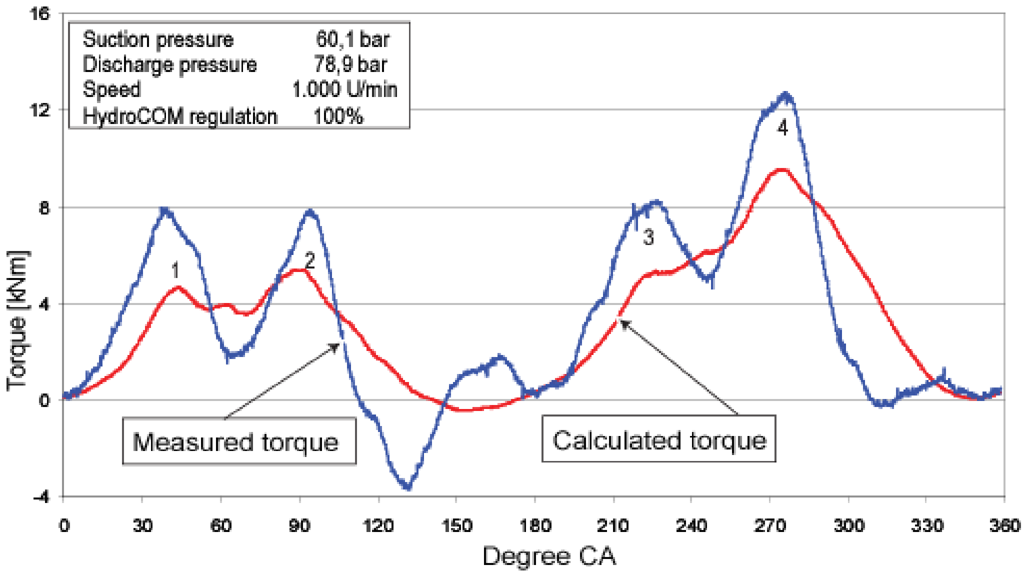

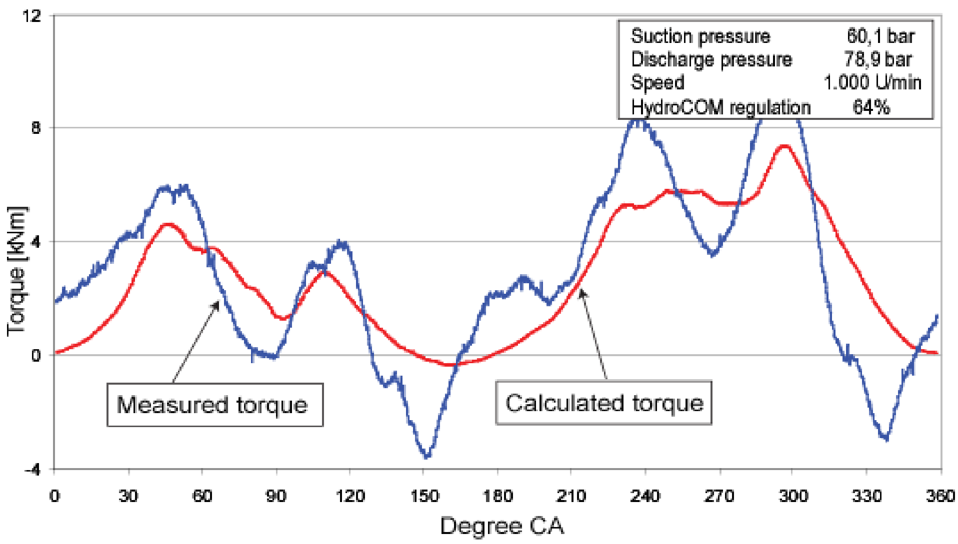

Figure 11: Torque curve of the reciprocating compressor (Ariel) at flow rates of 80% (top graph) and 64% (bottom graph).

In Figure 11, the discharge flow was regulated to 80% (top graph) and 64% (bottom graph) at a constant rotation speed (1000 rpm). Shifting the compression curves forms four positive amplitudes in the curve of one crankshaft rotation. At 64%, there is one clearly-pronounced negative amplitude, and at 80% there are two amplitudes, on the order of magnitude of -3,800 Nm. Consequently, this indicates a changing load on the crankshaft.

This torque curve can only be found in the torque curve calculated from the cylinder chamber pressure signals on a conditional basis. The calculated torque curve tends to be similar to the actual torque curve.

In conclusion, it can be seen in the results of the Ariel reciprocating compressor that very plausible information regarding the existing torque can be obtained from the pressure signals. In the operating range of a discharge rate of 100%, the calculated torque curve corresponds almost exactly to the actual torque curve, both at 720 rpm and at 1000 rpm.

In the operating range where the flow rate was reduced to 64% by the HydroCOM regulation of the suction valves, the calculated torque curve still tends to correspond to the actual torque curve.

The corresponding loads of the calculated torque tend to be somewhat lower than the actual (directly measured) values. It is assumed that friction losses that were ignored in the case of the calculated torque are chiefly responsible for this deviation.

Summary result of the evaluation

The results of both measurements show that the torque of the reciprocating compressor can be reproduced from the cylinder chamber pressure signals. However, none of the torsion vibrations superimposed on the actual torque can be detected in the calculated torque.

CONCLUSION / FUTURE

The results clearly show that information on the crankshaft torque can be obtained from the cylinder chamber pressure signals. The cylinder pressure signals can be used as an indicator for the existing torque. Absolute loads cannot be determined exactly from the calculated torque but the tendency of the torque curve can be reproduced. Critical load conditions on the crankshaft can be determined by this means.

Consequently, calculating the torque can be used to prevent damage to reciprocating compressors. Using the determined recordings regarding the OK condition of machines, limits can be set within which the measured values reproduce an acceptable condition of the machine.

For this reason, this method can be used as a comparison measurement to protect machines against damage.

Another interesting aspect in this connection could be the comparison of the calculated and the measured torque with regard to a compressor efficiency calculation. This would open the possibility of measuring the efficiency, excluding the influence of the driving machine. Against the background of increasing energy costs, the efficiency of compressor systems has increased in importance for many operators.

EFRC – the International Platform for Reciprocating Compressor Manufacturers and Users

Leonhard Keller Ph.D., Dr. Peter Steinrück
EFRC Board Members

Abstract:

The European Forum for Reciprocating Compressors has been founded to support users, manufacturers and researchers working with reciprocating compressors in terms of technology, exchange of experience, formation and enforcement of standards and pre-competitive research. Detailed information can be found EFRC's web site as well: http://www.recip.org

History

The European Forum for Reciprocating Compressors was founded in June 1999 as a communication platform to facilitate the interchange of information between European users, manufacturers and scientists working in the field of reciprocating compressors.

The Forum takes on the heritage of a long tradition of exchange among scientists researching at the TU Dresden and international experts, both groups working in the field of reciprocating compressors. The former "Kolbenkompressor – Kolloquium" initiated by Prof. Kleinert and hence kept alive by Prof. Will preceded the Forum. The initiative to form an association taking on the spirit of this rather academic venue and transforming it into a vivid forum incorporating the principles of commercial conferences as well as of an institution promoting the interest of compressor users and compressor industry has been initiated by two long term players acting in this industry: Burckhardt Compression and Hoerbiger.

The small crowd of 8 initial members meanwhile has grown to 21 in 2008. The Forum has become international: Language has changed from German to English and the geographical reach has grown from central Europe to entire Europe and recently to the US.

Background

The Forum has been formed in with the background that the increasing demand for economic plant operation has led to a critical discussion of the equipment as to selection, design, maintenance and automation. The well-known advantages of the reciprocating compressor - high efficiency in many different operating conditions, comparatively easy regulation possibilities, suitability for light gases, high compression ratios, and many more - have led to a renaissance of this type of machinery. Nevertheless there are still many reservations concerning the relatively complex mechanical design and the prejudice that reciprocating compressors involve high maintenance costs and that they are not reliable enough. It is one of the most prominent goals of the EFRC to overcome such prejudices.

Goals of the Forum

The goals of the Forum address this issues in particular

Exchange of Information and Experience

It is an essential goal of the Forum to create a platform where scientists and engineers engaged in the development of reciprocating compressors are given the opportunity to present the state of the art, to show that, because of progress in engineering, the reciprocating compressor has turned into a reliable machine not only being best in terms of efficiency and flexibility but also meeting the requirements of low maintenance cost and safe operation. Trends in design and operation of reciprocating compressors will be presented and a "forum of ideas" provide the opportunity to spread new ideas and/or to carry them out. The users in their turn can take the opportunity to report on their experience with such machines and to request the industry concerned for solutions to problems.

Improve the Image of Reciprocating Compressors

The Forum aims to show that reciprocating compressors meet all the requirements of modern machines and even create new possibilities. To In order to accomplish this goal related Research & Development projects are to be presented, and a platform for proposals for pre-competitive joint research shall be provided.

The EFRC Conference held about every second year is an ideal platform to foster such an exchange of information. The conferences help improving the images of the reciprocating compressor as well.

The EFRC Conferences held

1999 in Dresden
2001 in The Hague

2003 in Vienna
2005 in Antwerp
2007 in Prague

have shown a considerable growing number of participants. This fact is even more remarkably as the conferences have been organized by the members on a voluntarily basis.

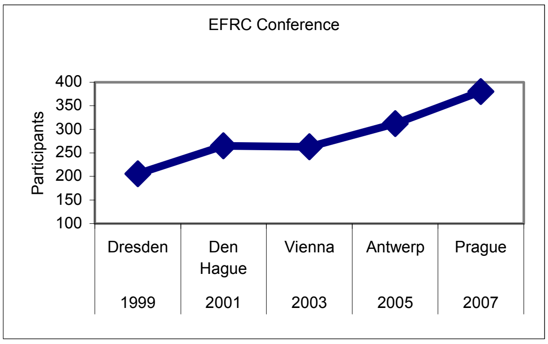

Figure 1: EFRC Conference- Growing number of participants

Improved Specifications and Standards

Up to now specifications and standards prescribed in tenders for reciprocating compressors have been mostly based on American recommendations such as API 618 and NACE, sometimes resulting in conservative executions. This is due to the fact that there are still no pertinent European regulations.

Therefore the forum also offers an opportunity for constructive criticism concerning the internationally used US standards. The aim should be to provide an interpretation and improvement of the above regulations adapting them to modern experience and specific European needs. Proposals based on scientific knowledge or practical experience will be presented and subsequently integrated into international use in tenders and final inspection.

Working Groups

These goals of the EFRC are supported by the activities of three working groups as well.

- Working Group for Pre-competitive Research
- Working Group for Improvement of International Standards
- Working Group for Promotion of "Recip"-Students

The working groups are presided over by a chairman appointed by the board of the association. EFRC members are invited to take part in the work of these groups by sending delegates who engage to take part in the meetings until revoked. The activities of the working groups are financed by EFRC membership fees unless otherwise defined; expenses incurred by the delegates are to be covered by themselves.

Working Group for Pre-competitive Research

Over more than 100 years reciprocating compressors have been the working horses boosting the pressure of gases in various consumer and industrial applications. Especially for the latter services most of the recips have been custom built, thus being individually engineered. Design work has been conducted by a number of competitive companies, thus duplicating engineering efforts. For obvious economic reasons comparably little amount of research has been attributed to these machines. Much of the design knowledge has been acquired by experience. Although in regard to plant availability recips have left behind an image of bad actors, it can be expected that better understanding of the basics will help to boost reliability and performance of these well proven machines. A solution to overcome the financial problems associated with economics of scale of the rather fragmented compressor industry is joint research funded by the manufactures and users of compressors.

Such research has been already conducted by the US pipeline industry improving the impressive fleet of more than 8000 natural gas compressors. However, no joint research addresses the problems of other type of recips, such as process gas, refrigeration, air compressors. Consequently there is only a very small scientific community dealing with recips subjects and well educated compressor engineers are scarce.

Organizing joint research on topics fundamental for the design and operation of reciprocating compressors is one of the most prominent objectives of the European Forum for Reciprocating Compressors - EFRC.

The combined knowledge and resources of

- Universities,
- Research institutes
- Manufactures
- Component manufactures and
- Users

are used to address research topics, which are basic to the industry but are beyond the commercial interest of a single party. It is intended to address national and international funds to support this work.

EFRC joint research program

Up to now the following subjects have been covered by EFRC R&D projects:

- Pulsation damper devices
- Failure diagnostics and failure identification
- Separator efficiency in a pulsating environment
- Effect of solid particles on compressors
- Rod load measurement
- Compressors for H2 refuelling stations
- Effect of in- cylinder pulsations on valve dynamics

- In-cylinder heat transfer
- Compressor noise
- Effect of cylinder flange misalignment on allowable nozzle loads
- Piston - & piston rod cooling
- Allowable vibration levels for reciprocating compressors

How to participate

EFRC joint research is handled by the R&D Working Group which has been set up in accordance with the provisions below:

(1) Membership in the R&D Working Group is open to all EFRC members.

(2) Membership registrations can be filed directly with the Chairman of the R&D Working Group.

(3) Registration for the R&D Working Group shall be binding on registering members for at least one work year of the R&D Working Group or longer if the registration indicates a longer period.

The working group decides upon:

- annual work program
- annual membership fee

Project results are available to the members of the R&D working group under the following provisions:

(1) The EFRC shall be entitled to all rights, in particular exploitation rights to the work results of the R&D Working Group, as well as incorporeal rights (rights to intellectual property) to the extent permitted in law.

(2) Members who have belonged to the R&D Working Group for the duration of a given project and who have rendered their contributions in full shall receive a documentation of the results and shall be granted the corresponding license rights free of charge.

(3) Members who have not belonged to the R&D Working Group for the duration of a given project shall have the opportunity to acquire these license rights the same as the members who have belonged to the R&D Working Group for the duration of a given project by rendering a mutually agreed upon monetary contribution or contribution in kind to EFRC.

(4) Licenses granted to the members in this way shall be non-transferable. The member shall therefore not be entitled without the written approval of EFRC to pass these licenses on in full or in part to third parties. No member has an automatic claim to receive such approval from EFRC.

Working Group for Improvement of International Standards

The task of this EFRC working group is, to promote and further improve the ISO 13707 so that it will become the world-wide accepted and specified document for reciprocating compressors in the petroleum and natural gas industries. In order to achieve this goal and to counterbalance the API Task Force, EFRC established this working group. It consists of experts from the following fields:

- end users and plant operators
- compressor manufacturers and
- engineering companies.

The respective EFRC working group has been actively participating in the API 618 5^{th} edition which has been published recently. The working group is lobbying a merger of API 618 and ISO 13707.

Quite recently the EFRC has started an initiative to develop a standard for allowable vibration levels for reciprocating compressors. Led by TNO compressor experts belonging to compressor manufacturers and compressor users have been reviewing an inventory of existing standards and recommendations prior complied by the EFRC working group. A guideline has been proposed and agreed. Hence the group has approached the ISO committee to integrate the outcome in ISO 10816-6. The rather promising results of this initiative will be presented at the 6th EFRC conference.

Working Group for Promotion of "Recip"-Students

In order to fulfil engineering tasks connected with manufacturing and operation of reciprocating compressors, the market also needs well trained and motivated university graduates.

To meet this requirement, the cooperation between the industry concerned and the educational institutions must be improved.

Practiced forms of cooperation are: commonly tutored theses for the diploma, special lectures by experts from the industry at universities, excursions, practical training, information on possible jobs for graduates and the recognition of excellence in studies or theses. Throughout the years it turned out that the EFRC student’s tour, an excursion open to students of technical universities interested in reciprocating compressor design, is an excellent tool to create interest for reciprocating compressor design and to initiate contacts between the industry and potential candidates for technical positions. Up to now such a tour has been completed four times involving in total more than 80 students.

EUROPEAN
FORUM
for
RECIPROCATING
COMPRESSORS

Educating reciprocating compressor engineers at the EFRC

by:

Dr.-Ing. Siegmund V. Cierniak
RWE Energy AG
Dortmund
Germany
Siegmund.Cierniak@RWE.com

Chairman of the EFRC Educating Committee

6th Conference of the EFRC

October 28 – 29, 2008, Dusseldorf / Germany

1 Why educate reciprocating compressor engineers?

The design, selection, operation and maintenance of reciprocating compressors makes the education and training of different types of engineers a must. Due to these facts all compressor manufacturers, packagers and end users have a need for highly qualified, educated and skilled engineers. Our branch need now and in the future, well educated and highly motivated graduates from the best universities and colleges.

The EUROPEAN FORUM for RECIPROCATING COMPRESSORS - EFRC is creating co-operation between the members of EFRC, other compressor makers, packagers, subsuppliers users and the well known universities, colleges, institutes and their students.

2 Some examples of these co-operative efforts:

- common supported thesises
- presentations – made by people from companies at the universities
- excursions to workshops and facilities in our branch
- practical work of students in firms
- information about jobs for graduates
- sponsoring of first class results of student's (thesis', etc.)
- realisation of workshops as platform for recent students and graduates
- publication of studies, theses, research work

3 What EFRC members are already doing:

- participating in EFRC promotion committee
- hosting of excursions
- organizing of internships
- sponsoring of events
- subsidizing highly qualified students and graduates

4 Advantages for EFRC members:

- access to qualified engineers
- influence on the education of students
- part time jobs of students

5 Important results of the EFRC activity „Educating reciprocating compressor engineers"

5.1 Autumn 2000: EFRC Workshop "The Netherlands and Belgium"

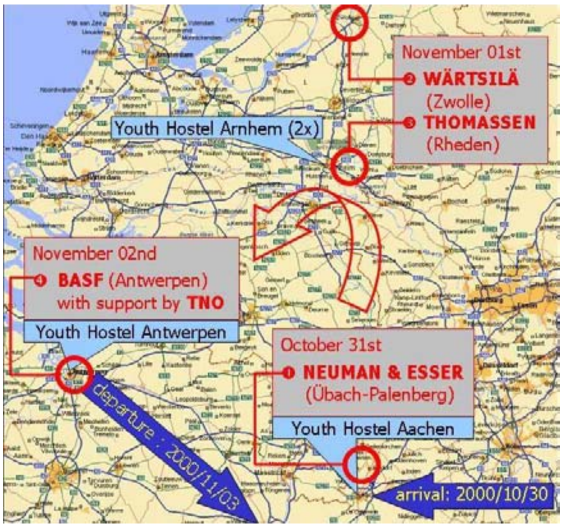

Picture 1: Students´ excursion 2000

Tour on the facilities of -

- NEUMAN & ESSER GmbH, Übach-Palenberg / Germany

- WÄRTSILÄ Nederland BV, Zwolle / The Netherlands

- THOMASSEN Intern. BV, Rheden / The Netherlands

- BASF AG, Antwerp / Belgium

- TNO Inst. of Applied Physics, Delft / The Netherlands

Picture 2: BASF AG, Antwerp / Belgium

5.2 Spring 2002: EFRC Workshop “Northern Germany”

- Natural Gas Underground Storage Kraak (near Schwerin / Germany)
  “HEINGAS Hamburger Gaswerke GmbH” / compressors “ARIEL / HGC”

- Natural Gas Underground Storage Hamburg-Reitbrook
  “HEINGAS Hamburger Gaswerke GmbH” / compressors “ARIEL / HGC”

Picture 3: Workshop participants at the Natural GasUnderground Storage Kraak Germany

Workshop’s tasks

A computerized simulation program „Reciprocating Compressors in Natural Gas Underground Storages“ > “Selection and sizing”

Picture 4: Tour on the facilities of the Tarnow site Poland

5.3 Spring 2004: EFRC Workshop “Poland”

Beginning of June 2004 the EFRC organized an event which was once again very successful.

Picture 5: Students in front of the lab of the Wroclaw University / Poland

App. 30 students from Austria, Czechia, Germany, Poland and the Netherlands travelled to Poland and visited the universities of Wroclaw and Krakow and its laboratories and also the compressor plants at the natural gas pipeline station of Tarnow and at the natural gas gathering station of Zanok. The participants had a very interesting training course reg. reciprocating compressor technology.

Picture 6: The group of students in front of the Krakow University / Poland

Workshop’s tasks

Diagnostics of leaking valves in reciprocating compressors.

5.4 Spring 2006: EFRC Workshop "Switzerland and Italy"

- Burckhardt Compression AG,
  Winterthur / Switzerland

- Polymeri Europa S.p.A.,
  Ferrara / Italy

- General Electrics Oil and Gas
  Nuovo Pignone S.p.A.,
  Firenze / Italy

Picture 7: Tour on the facilities of Burckhardt Compression AG Winterthur / Switzerland

Picture 8: Training of the students in the premises of General Electrics Oil and Gas Nuovo Pignone S.p.A. , Florence / Italy

One of the statutory tasks of EFRC is to educate young people to the design operation and management of reciprocating compressors.

In June 2006 EFRC organized the 4th workshop for students in reciprocating compressors sciences.

Picture 9: The group of students in the premises of General Electrics Oil and Gas Nuovo Pignone S.p.A. in Florence / Italy

5. 5 Spring 2008: EFRC Workshop "Vienna / Austria"

In May 2008 EFRC organized the 5th workshop for students in reciprocating compressors sciences.

The group of students guided by Dr. Siegmund Cierniak / RWE and Andre Eijk / TNO visited the following companies:

- LMF Leobersdorfer Maschinenfabrik AG
  Leobersdorf / Austria

- Hoerbiger Ventilwerke GmbH & Co KG
  Vienna / Austria

- BOREALIS Polyolefine GmbH
  Schwechat / Austria

- OMV Raffinerie AG
  Schwechat / Austria

Picture 10: The group of students in the premises of Leobersdorfer Maschinenfabrik AG Leobersdorf / Austria

At the end of the workshop the 25 students from seven different nations (Germany, Switzerland, India, Austria, Poland, England, The Netherlands) were assigned with a theoretical task to develop in the following 4 weeks with the understanding that the three best homework would be compensated with a prize.

Picture 11: The group of students, listening to a presentation in the premises of HOERBIGER Ventilwerke, Vienna / Austria

The goal for the participating students was to present a report (home work) to a committee of EFRC members and getting an award and once again very attractive prizes for the 3 best students:

1st prize	A free of charge compressor training course at Ariel's in Mount Vernon /Ohio/USA + a free of charge participating at 2008's EFRC conference in Dusseldorf / Germany
2nd prize	500,00 € cash + a free of charge participating at 2008's EFRC conference in Dusseldorf / Germany
3rd prize	a free of charge participating at 2007's EFRC conference in Dusseldorf / Germany

Evaluations of the individual works were made by the EFRC members Prof. Dr. Hans Quack, Institute for Energy Technology, Technical University of Dresden, Dresden, Germany, André Eijk, TNO, Delft, The Netherlands and Dr. Siegmund Cierniak, RWE Energy AG, Dortmund, Germany, supported by Christiane Hammer, Technical University of Dresden, Dresden, Germany.

6 Prize winners

1st prize

Matthias Kornfeld

e-mail:
matthias.kornfeld@direkt.at

Technische Universität Wien

VIENNA
AUSTRIA

2nd prize

Frank Franssen

e-mail:
fjf@thomassen.com

HAN University
Hogeschool van Arnhem en Nijmegen

ARNHEM / NIJMEGEN
THE NETHERLANDS

3rd prize

Dominik Höhner

e-mail:
dhoehner5@aol.com

Ruhr-Universität Bochum

BOCHUM
GERMANY

7 Next EFRC Workshop 2010

- Spring 2010 in the United Kingdom
- Details will be published in Fall 2009

8 Presentations, made during EFRC's workshops

Ariel Corporation, Katowice / PL	*Darek Rajtak*
ARLA, Kürten / D	*Dr. Andreas Laschet*
BASF AG, Antwerp / B	*Heinrich Ochs*
Burckhardt Comp., Winterthur / CH	*Dr. Leonhard Keller*
Burckhardt Comp., Winterthur / CH	*Dr. Georg Samland*
E.ON Hanse AG, Hamburg / D	*Dr. Ralf Luy*
E.ON Hanse AG, Hamburg / D	*Claus Pollok*
FEV, Aachen / D	*Dr. Martin Hopp*
FEV, Aachen / D	*Markus Graf*
GE O&G - Nuovo Pignone, Florence / I	*Stefano Giusti*
HGC GmbH Hamburg / D	*Dr. Siegmund Cierniak*
Hoerbiger Vienna / A	*Dr. Peter Steinrueck*
Hoerbiger Vienna / A	*Dr. Gunther Machu*
Hoerbiger Vienna / A	*Klaus Stachel*
Hoerbiger Vienna / A	*Andreas Horinek*
Hoerbiger Vienna / A	*Christian Prinz*
LMF Leobersdorf / A	*Dr. Ernst Huttar*
LMF Leobersdorf / A	*Dr. Vasillac Kacani*
LMF Leobersdorf / A	*Thomas Heumesser*
Neuman & Esser, Ü-Pa / D	*Dr. Klaus Hoff*
Prognost, Rheine / D	*Bernd Schmidt*
Prognost, Rheine / D	*Paul Bickmann*
RWE Energy AG, Dortmund / D	*Dr. Siegmund Cierniak*
THOMASSEN, Rheden / NL	*Hans Elferink*
TNO Delft Delft / NL	*Andre Eijk*
TNO Delft Delft / NL	*Dr. René Peters*
University of Crakow Cracow / PL	*Prof. Dr. Cyclis*
University of Dresden Dresden / D	*Matthias Huschenbett*
University of Dresden Dresden / D	*Prof. Dr. Gotthard Will*
University of Dresden Dresden / D	*Prof. Dr. Hans Quack*
University of Dresden Dresden / D	*Christiane Hammer*
University of Pisa Pisa / I	*Prof. Dr. Luigi Bertini*
University of Pisa Pisa / I	*Prof. Dr. Paolo Frendo*
University of Twente Hengelo / NL	*Remco Habing*
University of Wroclaw Wroclaw / PL	*Prof. Dr. Pietrowicz*
Wartsila-Nederland, Zwolle / NL	*Olavi Miinalainen*
Wartsila-Nederland, Zwolle / NL	*Dr. Siegmund Cierniak*

EFRC Guidelines for Vibrations in Reciprocating Compressor Systems

A. Eijk
TNO Science & Industry
Delft, The Netherlands

6th Conference of the EFRC
October 28-29th, 2008
Düsseldorf, Germany

Abstract

One of the disadvantages of a reciprocating compressor is that it generates pulsations and vibrations, which, without limitation and proper attention during design, manufacturing, installation and operation, can lead to fatigue failures, inefficiency, capacity limitations and unsafe situations.

To judge the integrity of the compressor system, vibration levels are normally evaluated and for this purpose several international standards (API, ISO and VDI) have been developed the last decade. Besides international standards, there is a wide variety of internal guidelines, which have been developed and are being applied by compressor manufacturers, packagers, engineering offices and operators. Most of these internal guidelines have been derived from international standards.

The lack in most of the international standards (and probably also the internal guidelines) is that they do not make a good distinction between recommended vibration levels for different parts of the compressor system, e.g. cylinder, crankcase, foundation, pulsation dampers, piping and/or different types/configurations of compressors e.g. horizontal/vertical, high/low speed, single/double distance piece, high/low power etc.
Within the R&D group of the EFRC a project was started to develop an EFRC guideline which takes into account recommended vibration levels for different parts of the reciprocating compressor system.
This paper will discuss the different international standards and the results of the EFRC project to develop EFRC Guidelines for vibrations in reciprocating compressor systems.

1. Introduction

The reciprocating compressor's flexibility to handle large capacity ranges, independent of density, makes it a vital component in today's energy markets. One of the disadvantages of a reciprocating compressor is that it generates pulsations and vibrations, which, without limitation and proper attention during design, manufacturing, installation and operation, can lead to fatigue failures, inefficiency, capacity limitations and unsafe situations.

The integrity of compressor systems is being judged by measuring vibration levels, and comparing those levels with limit levels from standards. Several international standards (ISO and VDI) have been developed during the past decade with vibration levels for reciprocating machinery. Besides several international standards, there is a wide variety of internal guidelines, which have been developed and are being used by compressor manufacturers, engineering offices and operators. Most of these internal guidelines have been derived from international standards.

Because there is an interaction between the different elements in a compressor installation, the compressor and pipe system should be treated as one integrated system, as indicated in figure 1.

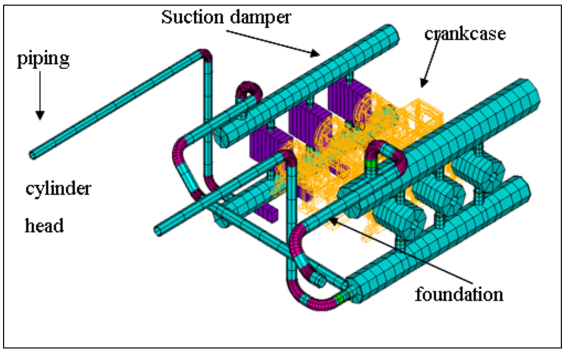

Fig.1 Different parts of a compressor system

However, most of the international standards do not make a good distinction between vibration levels for different parts of the compressor e.g. cylinder, crankcase, foundation and/or different types/configurations of compressors e.g. horizontal/vertical, high/low speed, single/double distance piece, high/low power, API 618/hyper.

For that reason an R&D EFRC project was started to develop an EFRC Guideline for vibrations in reciprocating compressor systems. The levels from the guideline should be used during a field survey to judge the safety, reliability and efficiency for the long term. It should be emphasized that the guideline is not intended for condition monitoring.

A spin-off of the project could be that the EFRC Guideline will be implemented into a future revision of an international standard e.g. ISO 10816[1,2], ISO-13707[3], API Standard 618[4].

The EFRC project has been divided into the following activities:

Activity 1
Literature survey (web, literature), study and evaluation of the most commonly used international standards and internally applied documents on vibrations of reciprocating machinery

Activity 2
Interviews with employees of several OEM's and operators to get insight into the application in practice of standards and/or internal guidelines,

Activity 3
Organising an international workshop on vibration levels in reciprocating compressor systems. The target of the workshop is to develop and achieve consensus on the EFRC Guideline for vibration levels in reciprocating compressor systems.

Activity 4
Developing new EFRC guidelines for vibrations in reciprocating compressor systems.

This paper will summarise the results of the different activities of the EFRC project.

2. Literature Survey

To get insight in the international standards that are being used for reciprocating compressors, a literature survey (web, literature), study and evaluation of the most commonly used international standards on vibrations of reciprocating machinery has been carried out. In the reference list a summary [1-18] has been given of the studied standards. It would lead too far to summarise all the studied standards. Therefore only a short summary of the following standards, which are applicable for reciprocating compressor systems and pipe systems, will be given:

- VDI 2056[5]
- VDI 2063[6]
- ISO 10816-6[2]
- VDI 3838[7]
- VDI 3842[8](piping)

VDI 2056[5] (1964)
This standard entitled: “Beurteilungsmassstäbe für mechanische schwingungen von Maschinen”, was one of the first international standards and has been applied frequently.
This standard defines allowable vibration levels for six different groups of machines: K, M, G, T, D, and S. Group G, for example,. is applicable for large machines with rotating masses that are mounted on high-tuned foundations. Group M is applicable for medium power machines such as electric motors with a power from 15-75 kW mounted on normal foundations.

Group D and S are intended for reciprocating compressors. However, the standard does not give vibration levels for these groups. This means in fact that only 4 groups are defined. Due to the fact that it is not clear which levels have to be applied for reciprocating compressors, different levels are being applied by different companies, which is rather confusing.

In table 1 a summary is given with vibration levels for different groups of machines. With this chart the integrity (good, usable, allowable or not allowable) of the machine can be judged with the highest measured vibration velocities in RMS (Root-Mean-Square, which is a measure for the energy content of a signal), also named severity grade value. The VDI 2056 has been applied for many years and proved to be useful for a number of different machine groups and some relevant international standards are based on it.
However, the VDI 2056 does not include guide values for the group of reciprocating piston machines. This is due to the fact that these machines differ from those with purely rotating masses in several aspects.
Typical features of reciprocating engines are the oscillating masses and irregular output or input torques which can cause considerable alternating forces and moments in the main supporting components and between the engine and foundation. This generally results in higher vibration levels on these engines, so the vibration levels from the VDI 2056 appear to be not suitable for piston type machines.

Table 1. Vibration levels for different groups of machines

Schwingstärke-Stufen		Äquivalente Amplituden an den Stufengrenzen		Beispiele der Beurteilungsstufen für einzelne Maschinengruppen *)			
Stufen-Bezeichng.	Effektive Schnelle v_{eff} in mm/s anden Stufengrenzen	Äquivalente Schnelle-Amplitude $\hat{v}_{äqu}$ in mm/s	Zu 50 Hz gehörige äquivalente Wegamplitude $\hat{s}_{50äqu}$ in µm	Gruppe K	Gruppe M	Gruppe G	Gruppe T
0,28	0,28	0,4	1,25	gut	gut	gut	gut
0,45	0,45	0,63	2				
0,71	0,71	1,0	3,15				
1,12	1,12	1,6	5	brauchbar			
1,8	1,8	2,5	8		brauchbar		
2,8	2,8	4,0	12,5	noch zulässig		brauchbar	
4,5	4,5	6,3	20		noch zulässig		brauchbar
7,1	7,1	10	31,5	unzulässig		noch zulässig	
11,2	11,2	16	50		unzulässig		noch zulässig
18	18	25	80			unzulässig	
28	28	40	125				unzulässig
45	45	63	200				
71							

VDI 2063[6] (1985)
This standard entitled: “Measurements and evaluation of mechanical vibrations of reciprocating piston engines and piston compressors”, is intended to include the reciprocating piston engines that were missing in the VDI 2056.
The guideline generally applies to reciprocating piston engines and piston compressors, mounted rigidly and resiliently, with a power output or input as from 100 kW and up to a speed of 3,000 rpm. Applicability of the guideline is restricted to the above-mentioned powers and speed ranges because only for these ranges measuring results were available at that time (1985) in support of permissible vibration limits.

The purpose of the guideline is the determination of a simple characteristic quantity in order to be able to compare similar or identical engines with each other.
The evaluation of vibration of reciprocating piston engines in this standard is based on the following:

- Ensuring trouble-free operation, in so far as engine-mounted components and connecting elements (pipelines, control equipment etc), may be damaged due to inadmissibly strong vibrations of the engine block
- Influence of vibrations on the vicinity (e.g. seating, foundation, ground, adjoining buildings)
- Stress on body and mind of people in the vicinity

The permissible vibration levels as a function of frequency are shown in the graph in picture 2. Direct application of the limiting line is possible only for the vibration velocity in case of sinusoidal vibrations. If the measurements show that the vibration consists of several harmonics, the RMS values should be used for evaluation. When determining the latter, any harmonic components with frequencies below 2 Hz and above 300 Hz are disregarded. This was done because vibrations of the frequency range below 2 Hz are to be considered as rigid-body movements, while harmonics above 300 Hz are considered to be local vibrations of the machine surface in the form of structure-borne noise; both kinds of vibrations are empirically known to be harmless. The composite vibrations are regarded permissible if the RMS vibration velocity level is less than 45 mm/s. If the composite vibrations contain harmonics components in the range of 2-10 Hz and/or 100-300 Hz the following additional conditions are to be considered for the vibration displacements and vibration accelerations:

- Total vibration displacement for composed signal s < 2 mm peak-to-peak
- Total vibration acceleration for composed signal a < 8 g peak-to-peak

All values are rather high and the standard gives only 2 grades: admissible and improvement.
The standard has not been applied frequently for reciprocating compressors due to the rather high vibration limits.

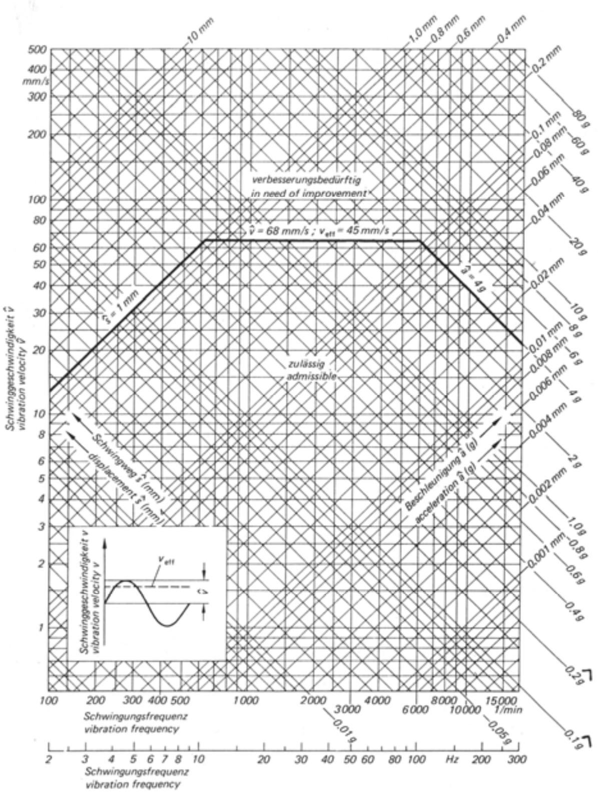

Fig.2 Limiting vibration levels for sinusoidal vibrations

ISO 10816-6[2] (1995)
This standard entitled: "Mechanical vibration-evaluation of machine vibration by measurements on non-rotating parts", is intended for reciprocating machines with power ratings above 100 kW. It is more or less an improvement and/or extension of VDI 2056 for reciprocating machines. The evaluation of the vibration of reciprocating piston machines is based on the measurement of the RMS value of:

- Vibration displacement
- Vibration velocity
- Vibration acceleration

The RMS value is defined as follows:

$$V_{r.m.s} = \sqrt{\frac{1}{T}\int_0^T v^2(t)dt}$$

In which:

- v(t) time dependent velocity,
- T sampling time

The classifications are based on the measurements of the overall values of vibration displacement, vibration velocity and vibration accelerations over a frequency range of 2 to 1000 Hz. It is recognised that the main excitation frequencies for reciprocating machines are generally found in the range from 2 Hz to 300 Hz. However, considering the complete machine including auxiliary equipment that is a functional part of the machine, a range of at least 2 Hz to 1000 Hz is required to characterize the vibration. For special purposes, a different range may be agreed between the manufacturer and customer. The standard is more or less identical to the VDI 2056. However, the ISO 10816-6 standard has 11 levels of severity instead of the 13 for VDI 2056. There are 7 groups of machines instead of 4 for the VDI 2056. The vibration classification numbers and guide values are shown in table 2. In this table, 4 different key zones are defined as follows:

- Zone A: Newly commissioned machines fall normally within this zone;
- Zone B: Machines with vibrations in this zone are normally considered acceptable for the long-term operation;
- Zone C: Machines with vibrations in this zone are normally considered unsatisfactory for long-term continuous operation. Generally, the machine may be operated for a limited period until a suitable opportunity arises for remedial action.
- Zone D: Vibrations in this zone are normally considered to be of such severity that the machine will be damaged.

Table 2 Vibration classification numbers and guide values

Vibration severity grade	Maximum values of overall vibration measured on the machine structure: Displacement µm (r.m.s.)	Velocity mm/s (r.m.s.)	Acceleration m/s² (r.m.s.)	Machine vibration classification number / Evaluation zones: 1	2	3	4	5	6	7
1,1	17,8	1,12	1,76	A/B	A/B	A/B	A/B	A/B	A/B	A/B
1,8	28,3	1,78	2,79	A/B	A/B	A/B	A/B	A/B	A/B	A/B
2,8	44,8	2,82	4,42	A/B	A/B	A/B	A/B	A/B	A/B	A/B
4,5	71,0	4,46	7,01	A/B	A/B	A/B	A/B	A/B	A/B	A/B
7,1	113	7,07	11,1	C	A/B	A/B	A/B	A/B	A/B	A/B
11	178	11,2	17,6	D	C	A/B	A/B	A/B	A/B	A/B
18	283	17,8	27,9	D	D	C	A/B	A/B	A/B	A/B
28	448	28,2	44,2	D	D	D	C	A/B	A/B	A/B
45	710	44,6	70,1	D	D	D	D	C	A/B	A/B
71	1125	70,7	111	D	D	D	D	D	C	A/B
112	1784	112	176	D	D	D	D	D	D	C
180				D	D	D	D	D	D	D

Vibration values for reciprocating machines may tend to be more constant over the life time of the machines than for rotating machines. Zone A and zone B are combined therefore in this table. If, in future, more experience is accumulated, guide values to differentiate between zone A and zone B may be provided.

The disadvantage of the ISO 10816-6 is that it has been developed mainly for reciprocating engines. This standard does not give a classification for reciprocating compressors and does not make a distinction between guide values for different parts of the compressor. It only gives a value for the locations as indicated in figure 3 and 4.

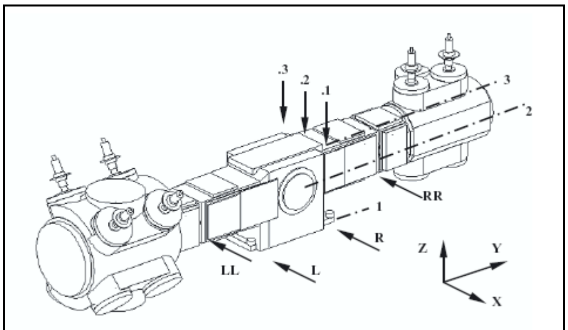

Fig.3 Measurement locations for a horizontal compressor

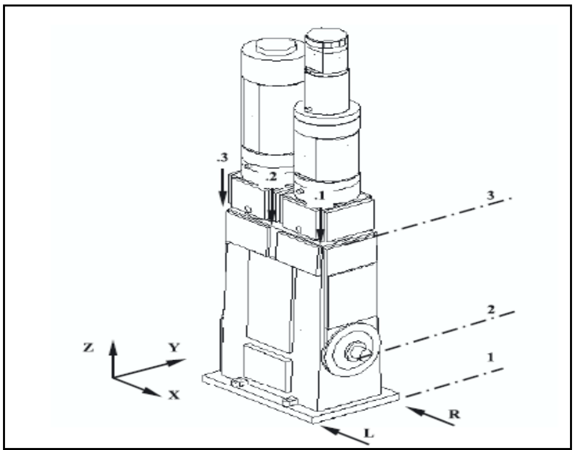

Fig.4 Measurement locations for a vertical compressor

VDI 3838[7] (2004)

This standard entitled: "Measurements and evaluation of mechanical vibrations of reciprocating piston engines and piston compressors with power rating above 100 kW", replaces the VDI 2063 and it supplements the ISO 10816-6. The standard is much easier to apply than the other standards.

The vibrations should be measured in a frequency range from 2 to 1000 Hz. In table 3 a summary is given of the guide values for the vibration levels. From this table it can be concluded that there is a difference in vibration level for high tuned (natural frequency of foundation 20% above the compressor speed) and low tuned (natural frequency of foundation 20% below the compressor speed) systems. From the table it can further be concluded that higher values are allowed for low-tuned systems. The values as given in the table are applicable for the positions of the compressor where the highest vibration levels have been measured. The standard does not make a distinction in vibration levels for different key zones e.g. safe, correction and danger as has been done in the ISO 10816-6.

Table 3 Guide vibration levels for reciprocating compressors

Foundation	Speed rpm	Displacement µm (rms)	Velocity mm/s (rms)	Acceleration m/s² (rms)
High-tuned	120-3000	280	18	28
Low-tuned	300-3000	450	28	44

VDI 3842[8] (2004)

As indicated in the introduction, the compressor system should be treated as one integral part. This means that also the vibrations of the pulsation dampers and the piping should be considered to judge the integrity of the complete system. Up to the year 2004 there were no international standards available for pipe systems with vibration levels. For that reason several vibration charts have been developed.

These charts have been derived from rotating equipment standards (e.g. VDI 2056) and field experience and have been widely used for many years. One of the most frequently used charts has been developed by SWRI and is shown in figure 5.

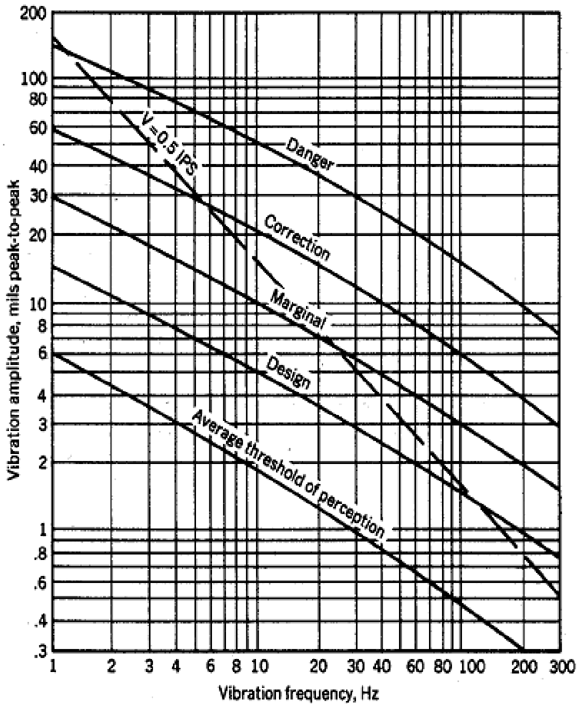

Fig.5 SWRI chart with vibration amplitude as a function of frequency

In the year 2004 the VDI 3842 standard titled: "Vibrations in pipe systems", became available. It is the only international standard for pipe vibrations at this moment. More important than vibration levels are the cyclic stress levels. If the cyclic stress level exceeds the endurance limit of the material, fatigue failure will occur. However, the cyclic stresses are difficult to measure. Cyclic stress levels are proportional with vibration velocity as indicated in the equation below. For that reason, the vibration levels can be used to judge the integrity of the pipe system.

$$\sigma_{\max} = f_w\ f_M f_\sigma f_\theta v_{\max} r_a \sqrt{Ew/I} \qquad (3)$$

f_w	correction factor for pipe contents and insulation
f_M	concentrated mass correction factor
$f\sigma$	stress concentration correction factor
$f\theta$	end correction factor (e.g. clamped-clamped, anchor)
Vmax	maximum transversal vibration velocity
Ra	pipe outer radius
E	modulus of elasticity
w	pipe mass per unit length
I	moment of inertia

In figure 6 a chart is given of the VDI 3842 with the vibration velocities as a function of frequency.
From this chart it can be concluded that higher vibration levels are allowed for higher frequencies. This is in contradiction with the common practice because at higher frequencies, higher mode shapes occur generally which means higher stresses. From the chart it can be further concluded that the vibration levels are rather high, especially for the high frequencies.

.

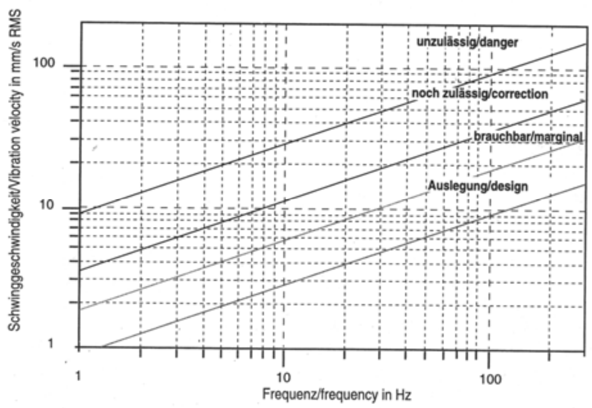

Fig.6 VDI 3842 chart with vibration velocities as a function of frequency

API 618

In the 5th edition of the API Standard 618[4], a chart has been included which is shown in figure 7. This chart is intended for design purpose only and cannot be used heck the integrity of the system during a field survey

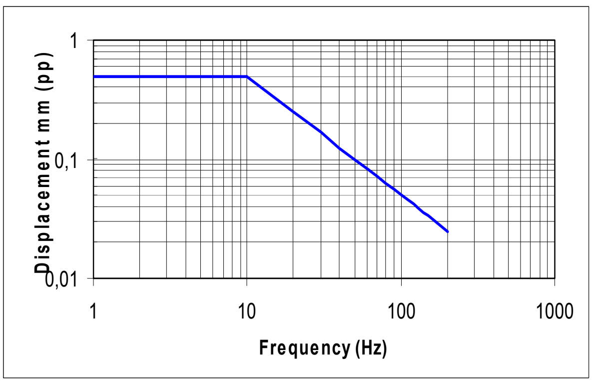

Fig.7 API Standard 5th edition chart with design values for vibration levels in pipe systems as a function of frequency

Further on it should be noted that fatigue failures frequently occur in small bore piping. For that purpose small bore piping needs special attention. In the API Standard 618 guidelines are given to avoid fatigue failure of these lines.

Summary literature survey

The summary of the literature survey is as follows:

- There is a lack of international standards with vibration levels for reciprocating compressor systems.
- None of the standards make a distinction between vibration levels for different parts of the compressor system
- Several standards give too high acceptable vibration levels.
- From all standards, the ISO 10816-6 gives the best guidelines for reciprocating compressors at this moment.
- Several standards do not give classification numbers for reciprocating compressors
- VDI 3842, the only standard for pipe systems at this moment, gives too high levels, especially for high frequencies.

3. Interviews

Introduction

To get insight in permissible vibration levels in reciprocating compressor systems, which are applied by different companies (OEM's and operators), a questionnaire was sent out. A distinction in results has been made between OEM's and Operators. The results have been obtained from 6 Operators and 9 OEM's, both EFRC and non EFRC members. The results of the interviews have been used to further develop the EFRC Guidelines.

Results

The detailed results of the interviews have been summarised in table 4. The results have been presented at the international workshop (see also next chapter) and the most important results can be summarised as follows:

1. The international standards that are applied most are ISO 10816-6 and VDI 3838
2. Most of the OEM's apply VDI 3842 for piping
3. OEM's have more internal guidelines than operators have.
4. There is a wide spread in applied levels e.g. for high tuned horizontal compressor systems:
   - Foundation: 1.1 - 2.5 mm/s RMS
   - Frame: 4.5 - 18 mm/s RMS
   - Cylinders: 7.0- 28 mm/s RMS
   - Piping: 4.5 - 18 mm/s RMS
   - Dampers: 15 - 22 mm/s RMS

The maximum level for the frame is 18 mm/s RMS which is rather high. This is caused by the fact that according to the VDI 3842 the levels are only measured on the frame and not on other parts of the system.

5. Generally: OEM's allow higher levels than operators:
   - Piping/dampers: OEM's apply 2 times the level of Operators;
   - Compressor: OEM's apply 2 times the level of Operators for cylinders and 3 for the frame.
6. General remark of most of the OEM's and operators: there is a strong need to have an easy-to-use guideline which takes into account most of the relevant items as discussed during the interviews.
7. A distinction between recommended levels for different parts of an installation is encouraged.
8. Most of the OEM's and operators do not make a distinction between vibration levels for the following:
   - High/low power;
   - High/low speed;
   - Horizontal/vertical;
   - Safety, reliability, efficiency, availability;
   - Temperature/pressure/gas type/ flow control.
9. From the interviews it appeared that the foundation is very critical in the design of the complete installation.

Table 4: Summary of questionnaire

Question	Score value OEM's	Score value End-users	General remarks
Which international standards are applied in the company	ISO 10816-6: 7 VDI 3838: 4 VDI 3842: 4 VDI 2063: 3 DIN 4024: 1 TNO values : 2 SWRI chart: 2	ISO 10816-6: 6 VDI 3838: 2 VDI 2063: 1	Most of the OEM's use classification no. 4 and 5 Most of the Operators use classification no. 2 and 3 Applied classes: A/B
Do you have internal guidelines	Yes: 8 NO: 1	Yes: 2 NO: 4	Most of them are derived from ISO 10816-6 and VDI 3838
Overall or frequency dependent levels	Overall: 6 Freq. dep: 3	Overall: 6 Freq. dep: 4	Frequency dependant OEM: piping (2) and compressor (1)
Resultant or 3 different directions	Resultant: 0 Different dir: 9	Resultant: 0 Different dir: 6	Nobody has the possibility of a tri-axial accelerometer
What kind of quantity do you measure	Strain: 1 Stress: 0 Displacement: 2 Velocity: 9 Acceleration: 3	Strain: 0 Stress: 0 Displacement: 2 Velocity: 5 Acceleration: 4	Strain only in USA
Cross over frequencies for displacement, velocity and acceleration (VDI 2063)	< 10 Hz: 2	< 10 Hz: 2	< 10 Hz only for displacement
What levels do you apply 0-peak, peak-to-peak, RMS	0-peak: 2 peak-peak: 1 RMS: 9	0-peak: 3 peak-peak: 2 RMS: 5	0-peak most for displacement RMS most for velocity
Up to what freqency do you measure	200, 300, 400, 10^{th}, 20^{th} and 40^{th} harmonic	10^{th} harm, 1000 Hz, High	Up to what freq. do you measure
Different levels for: foundation, Cylinder, DP, frame, dampers, piping	Yes: 8 No: 1	Yes: 4 No: 2	Most for foundation, frame, cylinder
Distinction high and low speed machines	Yes: 1 No: 8	Yes: 0 No: 6	For Yes of OEM: Directly coupled to speed
Distinction vertical and horizontal compressors	Yes: 2 No: 7	Yes: 0 No: 6	One OEM makes distinction for small power V-type machines
Distinction skid mounted , concrete, off-shore	Yes: 3 No: 6	Yes: 0 No: 6	
Distinction process refinery and hyper compressors	Yes: 1 No: 8	Yes: 0 No: 6	Only different levels for foundation (and also frame) are applied for hyper compressors
Distinction high and low power machines	Yes: 1 No: 8	Yes: 0 No: 6	For Yes of OEM: Directly coupled to power
Distinction w.r.t. safety, reliability, efficiency, availability	Yes: 0 No: 9	Yes: 1 No: 5	
Distinction w.r.t. gas, temp, Press, flow control	Yes: 1 No: 9	Yes: 0 No: 5	The yes of the OEM is for O2 compressors

4. International workshop

Introduction

On 24 and 25 April 2008 an international workshop on "EFRC Guidelines for Vibrations in Reciprocating Compressor Systems" was organised by TNO Science & Industry. The following companies had one or more representatives at the workshop: Total France, Shell Global Solutions, Neumann & Esser, Leobersdorfer Maschinenfabrik, SIAD, Burckhardt Compression, BASF, Ariel Corporation, Hoerbiger, GE Nuovo Pignone, Thomassen Compression Systems, SABIC and Technip. There was also an employee of AV Technology on the workshop, as a representative of the ISO 10816/TC108/SC5/WG8 (condition monitoring).

The target of the workshop was to achieve a consensus between OEM's and Operators on guidelines for vibrations in reciprocating compressor systems. The results of the workshop will be the basis for the EFRC Guideline and for the future target: include the results of the EFRC Guideline in future revisions of international standards of reciprocating compressor systems, e.g. API 618, API/RP 688, ISO 13707 and ISO 10816-6.

To be prepared well for the workshop the participants had to carry out some work to get consensus within the company on several topics e.g. vibration levels, differentiation in vibration levels for different parts of the system etc. The prepared material should serve as a good basis for the discussions during the workshop.

Results

The workshop was very constructive and there were a lot of interesting discussions. In general the final target of the workshop was reached: achieve consensus on the base vibration velocity levels and definition of the key to zones for the EFRC Guideline.

There are several items left which need to be worked out further into detail to finalise the EFRC Guidelines.

It was concluded unanimously that the EFRC Guideline should make a distinction between vibration levels for different parts of the system. Another question was if a further distinction should be made in vibration levels for different speeds, powers and foundation type. After ample discussions it appeared that no further distinction in vibration levels will be made for these parameters. The results of the workshop can be summarised as follows:

1. Hyper compressors will not yet be included because these compressors are a rather special type of compressors.
2. The Guideline is not to be used for condition monitoring. The guideline should focus on "field survey" and commissioning to assess the integrity and safety of the compressor system for the long term.
3. An annex will be included explaining the measurement procedures and data processing.
4. Limits for overall vibration displacements, vibration velocities and vibration accelerations will be in RMS (Root Mean Square)
5. A distinction will be made in allowable vibration levels for various parts of the compressor system. It has been decided that the following parts will be included:
   - Foundation (at compressor foundation bolts)
   - Compressor frame (top)
   - Compressor cylinder (rigid part of cylinder cover flange)
   - Suction and discharge pulsation dampers (inlet/outlet flange and head)
   - Piping
6. The measuring locations should be clearly described and indicated in pictures.
7. For bracing of small bore piping attached to piping and pulsation dampers, a reference will be made to the API Standard 618.
8. A note will be made for material used e.g. stainless steel or carbon steel as some materials are more susceptible to fatigue cracking.
9. Proposed measuring procedure is as follows:
   - Preferably use acceleration probes and detect overall vibration velocity levels in RMS
   - If frequencies below a certain value (to be determined later) are expected/observed, it is recommended to measure overall RMS vibration displacement.
   - If frequencies above a certain value (to be determined later) are expected/observed, it is recommended to measure overall RMS vibration acceleration.

10. All measured vibration levels: displacements, velocities and accelerations, must be within the specified vibration levels of the guideline.

Key to zones
In the ISO 10816-6 standard, zones A, B, C and D have been defined which will also be applied in the EFRC guideline. In table 5 an overview is been given of the relations between the different zones, vibration levels, qualification and the corresponding notes.

Table 5 Definition of different zones

Zone	Level	Qualification	Notes*
A	level < A/B	Good	1
B	A/B < level < C	Acceptable	2
C	C < Level < D	Marginal	3
D	Level >D	Unacceptable	4

*Notes:
1 Design
2 Field survey
3 Analysis and possible correction. Clarification between OEM and operator is necessary to ensure that the machine is suitable for the long term safe operation
4 Urgent correction or shutdown

Vibration velocity levels
It was decided to apply different vibration levels for different parts (foundation, crankcase, cylinder, dampers, and piping) of the compressor system. The gas (stretching) force in the cylinder is causing a vibration in the rod direction. In general the vibrations in the rod direction are higher than in the lateral direction. The vibrations in axial direction cause tensile and compressing stresses and is generally considered less harmful than the lateral vibrations which cause bending stresses. For that reason it was decided to allow higher vibration levels in the rod direction of the cylinder than in the lateral direction.

It has also been decided that for vertical compressors a higher level in lateral direction than in the rod direction of the cylinder is allowed due to the fact that the vertical compressor is more flexible in the lateral direction than a horizontal compressor.The finally agreed vibration velocity levels for the different zones are summarised in table 6 for the horizontal compressors and in table 7 for the vertical compressors.

Table 6 Vibration velocities for horizontal compressors

Part	Horizontal compressors mm/s RMS		
	A/B	C	D
Foundation	2.0	3.0	4.5
Frame (top)	5.3	8.0	12.0
Cylinder (lateral)	8.7	13.0	19.5
Cylinder (rod)	10.7	16.0	24.0
Dampers	12.7	19.0	28.5
Piping	12.7	19.0	28.5

Table 7 Vibration velocities for vertical compressors

Part	Vertical compressors mm/s RMS		
	A/B	C	D
Foundation	2.0	3.0	4.5
Frame (top)	5.3	8.0	12.0
Cylinder (lateral)	10.7	16.0	24.0
Cylinder (rod)	8.7	13.0	19.5
Dampers	12.7	19.0	28.5
Piping	12.7	19.0	28.5

Foundation:
Regarding the foundation of the compressor the following remark will be added: The vibration levels as indicated in tables 6 and 7 are valid for rigidly mounted compressor systems. This means that the compressor must be mounted directly to the concrete foundation.

If the compressor is mounted on a skid, the skid must be stiff enough and directly mounted to the concrete foundation. Isolated mounted foundations e.g. concrete block on springs and skids on anti vibration mounts (AVM's) are an exception and the vibration levels for such systems should be agreed upon with the customer.

Vibration displacements and vibration accelerations levels
During the workshop it was agreed that both the vibration displacements, vibration velocities and vibration accelerations should be measured and must be within the specified vibration levels of the guideline. The relations between the vibration velocity and displacement and between vibration velocity and vibration accelerations are as follows:

$$d = v / 2\pi f \qquad (2)$$
$$a = 2\pi v f \qquad (3)$$

In which:
d= displacement
v= velocity
a= acceleration
f= frequency

From these equations it can be concluded that the displacement and acceleration depend on the vibration velocity and frequency. If a frequency is chosen, the displacement and acceleration can be calculated for a given velocity. The chosen frequencies are also called "cross-over" frequencies. In the ISO 10816-6 the cross-over frequencies are respectively 10 Hz and 250 Hz for the displacements and accelerations.
If these frequencies are applied for the piping and pulsation dampers for the C key zone, the values for displacement and acceleration are respectively 0.3 mm RMS and 29.85 m/s^2 (3 g) RMS.
These values are already quite commonly applied nowadays. However, for other parts of the system, the displacements values will be too high if a frequency of 10 Hz is chosen.

A consensus was not reached during the workshop for the "corner frequencies". This needs to be investigated further into detail.
It should be mentioned that ISO will accept different cross-over frequencies for different parts of the system.

5. Summary and conclusions

Vibration levels are a good measure to judge the integrity of a compressor system for the long term. For that purpose several international standards have been developed. These standards have been developed mainly for reciprocating engines (gas and diesel engines) and not for reciprocating compressor systems.

There is a strong interaction between different parts in a compressor installation (foundation, frame, cylinder, piping, and damper). The different parts of a compressor system should be treated therefore as one integrated system.

The vibration levels from the existing standards are not suitable to be used for reciprocating compressors. Additionally, the shortcoming in all international standards is that they do not make a distinction between vibration levels for different parts of the compressor system, e.g. cylinder, crankcase, foundation. For this reason the R&D group of the EFRC has started a project to develop a vibration guideline especially for reciprocating compressor systems.

From interviews with several OEM's of reciprocating compressors and operators it appeared that they are already applying different vibration levels for different parts of the compressor, mainly for foundation, frame, cylinder, piping and dampers, to judge the integrity of the complete compressor system during a field survey. However, different levels are applied by OEM's and operators and there is a strong need to have an adequate vibration guideline for that purpose.

The results of a literature survey and the results of the interviews were used as a basis in an international workshop to get consensus on the vibration guideline. During the workshop a general consensus was reached of which the results have been summarised in this paper. There are still some items left which should be worked out to finalise the EFRC Guidelines for vibrations in reciprocating compressor systems.

A future target is that the results of the EFRC guidelines will be used in new revisions of international standards e.g. ISO 10816-6, API 618 or ISO 13707.

6. Acknowledgements

The author would like to thank the R&D sponsors of the EFRC for their permission for publishing the results of this project and all participants of the workshop for their active contribution.

References

1. ISO 10816-1: Mechanical vibration-Evaluation of machine vibration by measurements on non-rotating parts- Part 1: general guidelines. First edition 1995-12-15.
2. ISO 10816-6: Mechanical vibration-Evaluation of machine vibration by measurements on non-rotating parts- Part 6: Reciprocating machines with power ratings above 100 kW. First edition 1995-12-15.

3. ISO 13707: Petroleum and natural gas industries_ reciprocating compressors. First edition 2000-12-01
4. API Standard 618: Reciprocating compressors for petroleum, chemical and gas industry services, 4th edition June 1995.
5. VDI 2056: Beurteilungsmaβstäbe für mechanische Schwingungen von Maschinen. Oktober 1964
6. VDI 2063: Measurement and evaluation of mechanical vibrations of reciprocating piston engines and piston compressors. September 1985
7. VDI 3838: Measurement and evaluation of mechanical vibrations of reciprocating piston engines and piston compressors with power ratings above 100 kW. Addition to DIN ISO 10816-6. may 2004
8. VDI 3842: Vibrations in pipe systems. June 2004
9. ISO 2041: Vibration and shock-Vocabulary, 1990
10. ISO 2372-1974: Mechanical vibrations of machines with operating speeds from 10 to 200 rev/s-basis for specifying evaluation standards
11. ISO 2631-1: Mechanical vibration and shock- Evaluation of human exposure to whole-body vibration- Part 1: general requirements. Second edition 1997-05-01.
12. ISO 5348: Mechanical vibration and shock-Mechanical mounting of accelerometers. Second edition 1998-05-15
13. ISO 8528-9: Reciprocating internal combustion engine driven alternating current generating sets- part 9: measurement and evaluation of mechanical vibrations. First edition 1995-12-15
14. VDI 3839: Instructions on measuring and interpreting the vibrations of machines. Part 1- General principles. March 2001.
15. VDI 3839: Instructions on measuring and interpreting the vibrations of machines. Part 8- Typical vibration patterns with reciprocating machines. June 2004.
16. DIN 4024: Machine foundations. Part 1-Flexible structures that support machines with rotating elements. April 1988
17. DIN 4024: Machine foundations. Part 2-Rigid foundations for machinery subject to periodic vibration. April 1991
18. CEI-IEC 34-14: Rotating electrical machines-Part 14: Mechanical vibration of certain machines with shaft heights 56 mm and higher-Measurement, evaluation and limits for vibration. Second edition 1996-11

DEVELOPMENT OF ELASTOMERIC MATERIALS IN RECIPROCATING COMPRESSOR VALVES: AERODYNAMICS and SPRINGLESS VALVE DESIGNS

Kevin Durham
Director of Valve Engineering
&
Tom Dunn
Design Engineer

Cook Compression
Stafford, Texas
United States of America
kdurham@cookcompression.com

6th Conference of the EFRC
October 28 & 29, 2008 Dusseldorf

ABSTRACT: The history of valves in reciprocating gas compressors is dominated with the use of rigid materials from metal to advanced reinforced thermoplastic polymers. Research started in 1998 investigating the application of elastomeric materials has resulted in elastomeric valve designs that not only improve the sealing capabilities of the valve elements but also increase the durability and robustness of compressor valve performance. Specifically, compressor valves fail when the valve element loses its ability to form a gas tight seal. Solids entrained in the gas stream can damage the valve element-valve seat interface immediately upon contact or serve to erode the surfaces over time but in either case, once a leak path is formed local heating takes place, valve life is reduced and damage accumulates until the valve is replaced. The application of elastomeric materials is directed at improving the durability and damage tolerance of the seal at the valve element-valve seat interface.

In early elastomeric valve element designs, flexible materials were applied to rigid substrates for strength but this paper will present some of the advances in geometry and opportunities for not only reducing the pressure drop in reciprocating compressor valves but also improve the mean time between failures. In addition, some discussion will center on the how the use of elastomeric materials has resulted in valves being created and tested that operate without compressor valve springs and how this operating mode can further improve compressor valve reliability.

Introduction:

Looking forward, elastomeric valve technology has the potential to address two pressing issues 1) increasing the mean time between failures in compressor valves and 2) reducing the operating costs of reciprocating compressor valves by significantly reducing valve pressure drops through the use of aerodynamic shapes that are simply not possible, at least in any practical sense, with rigid thermoplastics. While rigid thermoplastics have outstanding properties and can be credited with dramatic improvements in compressor valve reliability, the inherent variability of their microstructure brought about by high sensitivity to manufacturing processes limits the precision with which the materials can be controlled and manipulated for improved performance. Incremental improvements are still possible but radical performance improvements with rigid thermoplastics will be increasing difficult to realize. We are approaching a limit imposed by the physics of the material. The detailing of these material limits is beyond the scope of this paper but it's clear that to meet the ever increasing demand for long life valve elements, material selection for valve element construction is going to require some radical thinking and novel approaches.

At the 5th EFRC in Prague, valve elements coated with elastomeric materials were introduced and the prototypes have outperformed their thermoplastic counterparts by a wide margin with all of the operating test valves running at least twice as long and in one instance, six years of continuous service has been recorded. In spite of these impressive results, more has been learned about the behavior of elastomeric materials and details have emerged about where and why they can be successful and in a few instances, unsuccessful. Whenever two materials are held together mechanically or chemically at a well defined interface, loads must be transferred across this interface and, more often than not, local shear forces develop. As elastomers deform, forces normal to the applied load appear as shear leads at the adhesive interface. Add cyclic loading and very quickly an environment is created that will break down the interface bond even though the normal loads are well within the limits for the adhesive and the elastomer. A better understanding of this process has resulted in a limit in the application envelope of coated parts to about 200 psi of total pressure and 150 psi of differential pressure. This limited operating window has still allowed very successful application on elastomer coated elements in flare gas service as well as in the first and second stages of gas gathering and fuel gas services.

Construction:

The mechanics at the interface between the elastomer and the rigid substrate are complex and difficult to control with great precision particularly since materials used in process environments must also be chemically inert in order to resist attack from aggressive constituents in the gas stream. Again there are too many variables and predictable performance evolves into a guess rather than well focused engineering. A new path has been selected to address these problems. The interface between two well defined materials is problematic. The aforementioned local shear forces are destructive, the adhesive itself is susceptible to chemical attack and manufacturing processes become more complicated as more effort is needed to ensure a good bond. If the adhesive interface could be removed the design becomes simpler and performance necessarily improves with simpler designs. All of this has been realized in prototype valves currently being operated. All is not well with the design since removing the substrate also removes the only material that contributed strength to the system. New problems must now be addressed.

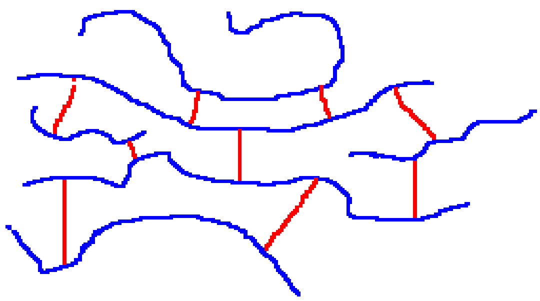

Crosslinked Polymer Chains

Elastomers have no inherent, useful strength. The long polymer chains are tangled and mechanically lock to impede (viscous) flow but the most significant contribution to the strength of an elastomer comes from the degree of crosslinking between polymer chains. The picture at the right shows a schematic of a material that has no polymer chain crosslinks and one that is heavily crosslinked. Sulphur bonds are the most common bonds that tie a collection of polymer chains together into a network that is "stronger" but still susceptible to strains of 300% or more with a disproportionately small amount of applied stress. As the degree of crosslinking increases, stiffness increases and the mechanical properties of the polymer approach those of more familiar rigid plastic. We don't want to lose the highly desirable sealing characteristics of a flexible elastomer but we can't have both. Or can we? Removing the rigid substrate leaving only a weak and flexible material appears to have been a bad idea.

The strength problem is not trivial but in these early applications it appears to be workable and predictable with the aid of non-linear FEA codes and variety of companies that specialize in elastomers with the complimentary expertise to blend recipes of highly engineered elastomers. Non-linear FEA tells us the mechanical properties needed for a given differential pressure and using this as a target, special polymers can be created to match the needs of the application window. With very good control over the mechanical properties the task then becomes to study and select an appropriate geometry that will more effectively carry pressure loads. Ported plate shapes for example must resist bending loads and thus these shapes would be poor candidates for elastomer construction but pyramidal and spherically derived geometries are much better selections because loads are applied in a manner that is more compressive and since elastomers are constant volume materials, they can be very strong in compression. Elastomer o-rings operate very well in this manner. So any shape that can be loaded in compression is a good choice and non-linear FEA can let us see the effects of the loads. This difficult problem is getting more manageable by effective modeling of the mechanical response of the materials and the system was made simpler by removing the troublesome adhesive interface.

Aerodynamics:

Elastomer shapes are typically compression molded and since molds can be created in almost any shape, it now becomes possible to consider aerodynamic shapes which, conveniently enough, lend themselves to being loaded in compression. The flexible nature of elastomeric materials means that machining tolerances and associated costs are no longer factors to be considered during valve design. One mold can make hundreds of thousands of parts and manufacturing complicated shapes becomes cost effective. So why are the shapes so important? Aerodynamics. The opportunity to design for efficient gas flow and reduced pressure drop has never been greater. Valves are operating at this moment that have a measured pressure drop that is four times LESS than the valves that they replaced while operating as a LOWER lift and WITHOUT springs. These performance features have never been combined in a single valve design that has operated for any remarkable length of time.

The valves in reciprocating compressors are aerodynamic devices. High velocity gas (and some solids) pass though them and the difficulty of the path taken by the gas determines, to a great extent, the pressure drop and subsequently the energy consumed. Energy is expensive and while solids in the gas are always undesirable, they are present in most gas streams but effectively managing the gas flow can keep the solids in transit and minimize the chance that they will drop out of the gas stream and into the valve where they can do more damage over time. Computational fluid dynamics, CFD, is a mathematical method used to solve partial differential equations that describe fluid flow through and over other objects. CFD is the tool of choice for evaluating solid shapes in a gas stream and the value of such computer to codes to permit the evaluation of different geometries cannot be overstated.

To this point we have a simplified valve element without an interface, flexible elastomeric materials designed for a particular application or group of applications and computer software capable of evaluating not only the mechanical response but also the aerodynamics of a valve element in the gas stream. The inherent variability of rigid thermoplastics has been substantially reduced by applying an array of analytical tools to elastomeric material more capable of being controlled during production of the parts. In addition, we can operate without springs as a result of the ability of elastomers to absorb and effectively dissipate impact energy. A compressor valve that embodies all of the aforementioned characteristics exists, is operating, proving to be reliable and is shown in the picture at the right.

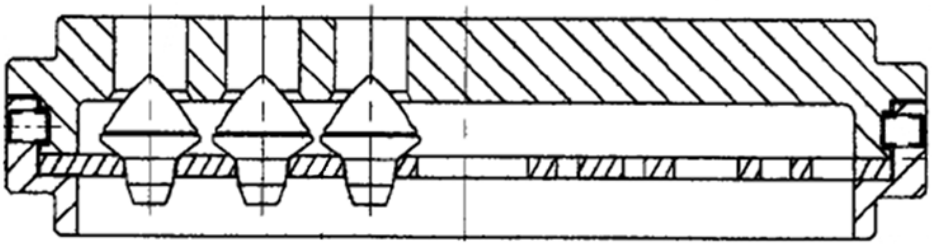

The simplicity of this valve is obvious from the picture above but it embodies concepts that are on the frontier of compressor valve design. The principle of operation is similar to the current state of the art. Gas pressure pushes the valve elements open, however it is the drag force that acts to close the valve elements when the process gas attempts to flow in the reverse direction. No springs are required. Sealing surfaces do not require lapping and fine surface finishes are not necessary. The valve elements are shaped in a way that permits very efficient gas flow, reduced pressure drops and before the gas reaches a valve guard that has generous flow areas. The valve guard, in fact, is little more than a web structure used to support and guide the valve elements. Without a need for springs or strength to resist differential pressures, the guard structure can be minimized resulting in thinner and less massive valve designs. As a consequence, all of the valve thickness can be placed in the seat (where it should be) to provide necessary strength.

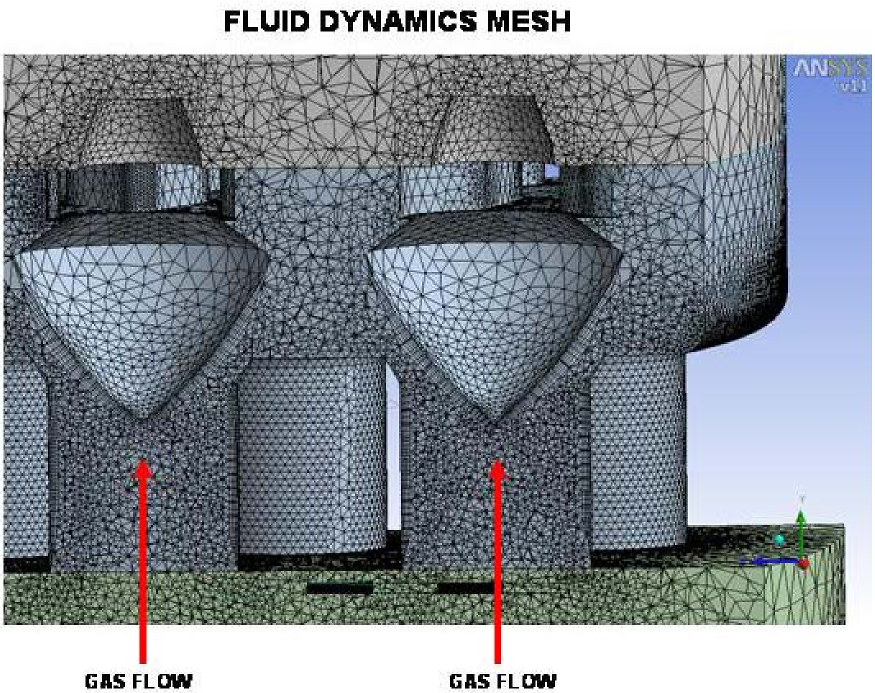

Determining the shape of the elastomeric valve elements requires a combination of computational fluid dynamic analysis and non-linear mechanical analysis to arrive at a shape that will provide necessary strength and aerodynamics. This is a level of effort well above what is required for current valve designs but the shapes have shown themselves to be scalable with pressure and most of the development will be front loaded to find attractive geometries. Elastomeric materials can be created with varying degrees of crosslinking for various pressure regimes.

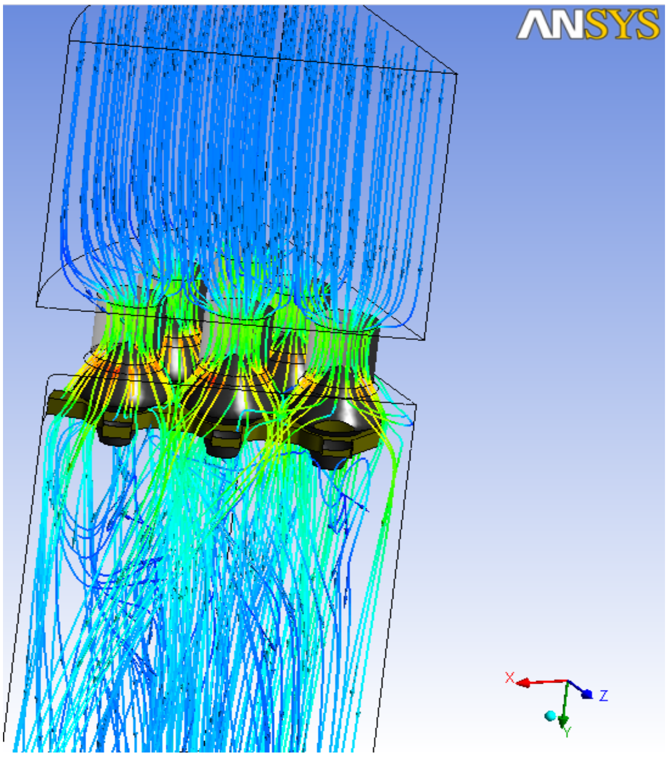

Presently, the valve is being operated at 700 RPM, in gas gathering service with a suction pressure of 4 psig and a discharge pressure of 70 psig with a volume flow of 2.2 MMSCFD. More tests are scheduled for subsequent designs and the operating envelope is being expanded.

The CFD result shown at the right shows a smooth flow path through the valve and very little interference from the guard. Continued shaping of the seat flow hole geometry will lead to more improved flow patterns.

Conclusion:

Operating compressor valves without springs is a dangerous proposition. Valve elements close late and with high velocity resulting in plate fracture or recession in the sealing region of the valve elements of the valve seats. The generally accepted position of valve manufacturers is that once the spring system is lost, valve failure is imminent. Clean, dry conditions in a reciprocating compressor are the exception rather than the rule.

Advanced valve designs like the one described in this paper are compelling because many of the failure modes that plague the current state of the art are eliminated or minimized. Springs in compressor valves can break into multiple pieces or escape the valve completely and once free, they can move about in the valve or compressor and cause secondary damage. Plastic or metal valve plates can also cause substantial secondary damage but elastomeric materials offer an option that is far more forgiving. Without springs to close the valve elements before top dead center, the possibility exists for some reverse flow to occur. The severity of this inefficiency is dependent on the severity and duration of the reverse flow. Field tests to date have shown that that while some reverse flow exists, it is small in magnitude and offset by lower pressure drop through the valve, lower clearance in the cylinder due the thin design and superior sealing ability of elastomeric elements.

Electromechanical Actuator for Reciprocating Compressor Stepless Control

by:

M.Schiavone, A.Raggi

Dott.Ing.Mario COZZANI S.r.l.

Arcola (SP)

Italy

info@cozzani.com

6th Conference of the EFRC
October 28th / 29th, 2008, Düsseldorf

Abstract:

Flow control systems represent one of the main topic of research and analysis for valve and reciprocating compressor makers. Among the methods already in use, the reverse flow one needs advanced electronic systems able to control the suction valve shutter position in a quick, reliable and accurate way.

Unlike the current systems, the new one developed by Dott. Ing. Mario Cozzani s.r.l. is characterized by the use of electromechanical actuators. The control algorithm definition has been made by using model-based and rapid prototyping techniques. This paper shows the results of the theoretical and experimental studies that the Cozzani company has carried out on the new stepless control system, considering also the energy saving.

1 Introduction

The increasing request from end-users to reduce energy consumption and to raise the machine reliability, involves a greater and greater effort in the designing and development of the reciprocating compressors and their components.

Since the cylinder valves directly influence machine performances and reliability, they have always been one of the most important components.

In this effort of improvement, the capacity control systems play a major role.

Nowadays, the research activity on the capacity control systems has been facilitated by the continuous technological evolutions, like the advanced calculation systems, new materials, electronic components, etc.

2 Capacity control

Thanks to the capacity control of the compressor, the process pressure or the process flow can be kept constant or can be adjusted to the process requirements. This kind of control can be realized through different kind of devices. Generally they can be divided in two different groups, the devices external to the compressor and the compressor own devices.

The main devices used for this kind of application are:

among the devices external to the compressor are: on/off operation, compressor motor speed variation, by-pass between discharge and suction side and the suction throttling.

among the compressor own devices are: cylinder unloading, volumetric control by fixed or variable clearance pocket and the reverse capacity control.

Presently the most widespread capacity control system is the cylinder unloading. It is made up by using actuators (usually pneumatic) which act on the suction valve shutters through finger unloaders keeping them in an opening position.

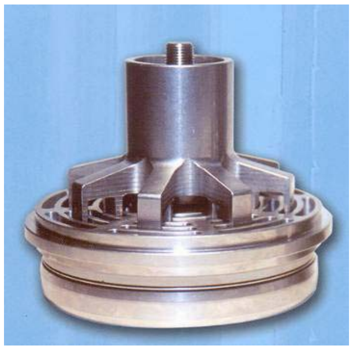

Figure 1: Suction valve with finger unloader

In a double acting cylinder, one single end or both ends can be unloaded determining approximately a 50% or 100% reduced flow. In multi-cylinder arrangements which operate in parallel more regulation steps are possible, for example, in a configuration of two double acting cylinders operating in parallel the flow can be reduced by 25%, 50%, 75% and 100%.

The cylinder unloading is often combined to the fixed clearance pocket system which allows an additional increase of the capacity control steps.

During recent years, thanks to the evolution in technology, electronics and software, stepless capacity control devices could satisfy the demand for energy saving. They are:

Variable speed drivers (VSD). The capacity control is realized by speed variation of the compressor motor. The large use of this system has been possible due to inverter improvements and cut in price.

Reverse flow capacity control systems. The reverse capacity control is realized by devices keeping the suction valve open over the bottom dead centre (BDC). In this way the gas that comes in the cylinder flows back through the suction valve as long as it remains opened. Till now these devices are hydraulic type.

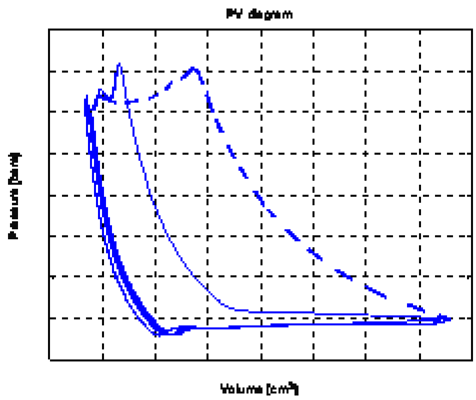

Figure 2: PV Cycle - Comparison between full load operation and reverse flow operation

Since the valve position control is very complex, it is necessary to introduce electronic control systems which are able to activate the valves and guarantee the required precision and repeatability.

The use of such electronic systems requires advanced calculation technologies in order to develop the appropriate algorithms for the control.

A mechatronic approach is expected in order to reach the technical targets.

Obviously the choice of a capacity control system involves economical and engineering analysis as well as preliminary studies.

Since this choice plays a key role in running the compressor, it should be analyzed by tight collaboration with the machine manufacturer.

3 The new capacity control system by Cozzani

The new capacity control system developed and patented by Cozzani, is mainly made up by the following components:

1. electric actuators installed on suction valve covers to control the position of their shutters;

2. System Control Unit (SCU);

3. Actuator Control Units (ACUs);

4. sensors for the measurements required by the system;

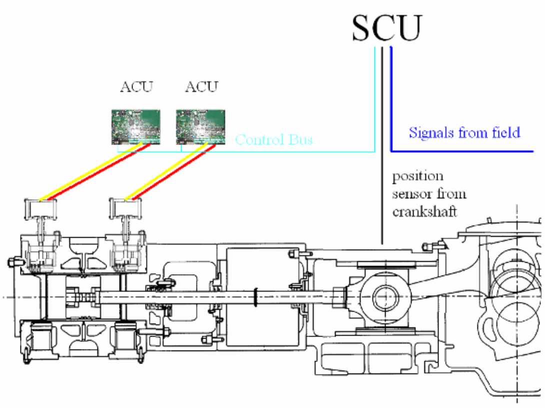

Figure 3: Electronic control scheme

The diagram of the suction valves actuator control can be represented like in fig 4:

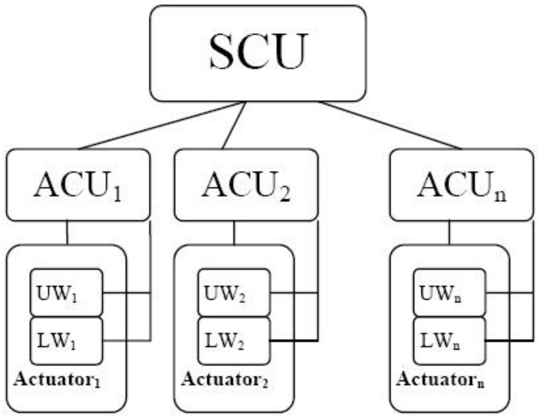

Figure 4: Diagram of the capacity control system

The System Control Unit (SCU) is used to interface the compressor with the actuator control units (ACUs).

The SCU receives digital signals from the compressor system (mainly the position signal of the crankshaft), in order to know the exact position of the piston during each cycle and the input signal used for the capacity control. This information is used to set the actuator control parameters.

Therefore SCU is able to control the suction valves and consequently the entire working compressor cycle. Obviously the development of this unit required the development of a customized software able to manage all the compressor working phases, from start up to full load working, during capacity control, up to switch off.

The ACUs are the actuator control units. They receive information from the SCU on the valve opening instant and its holding time.

The ACUs convert the above information in voltages across the magnetic windings which determine the positioning of the actuators. Every ACU is made up by two main parts, the control part which includes all the components for managing the signals and the communication interfaces, and the power part where the components for the voltage control of the two windings and for the measure of the currents are assembled.

Further details on the actuator are explained in the next chapter.

4 The electromechanical actuator

The new actuator, conceptually innovative~~,~~ as completely electric, has been entirely designed by Cozzani.

This actuator, shown in fig.5, has a central sliding part, called “armature”, two electromagnets, located at the opposite sides of the armature, with the aim to move it linearly and to move the lower rod that acts on the finger, and two springs located at the opposite sides of the armature in order to accelerate and decelerate the actuator moving parts.

The gaskets and the recycle gas connections are inserted in the lower part, while the connectors and the sensor used to measure the rod position are located in the upper part.

The new device has a high dynamic performance able to respond positively to the strict times required by the various phases of the compressor cycle.

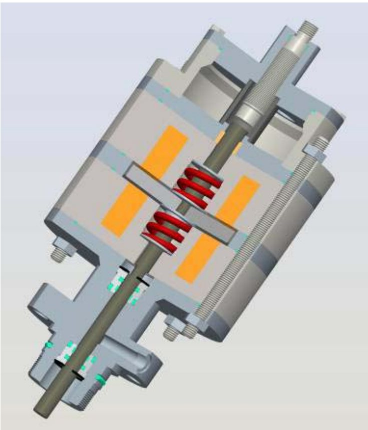

Figure 5: 3D model of the suction valve actuator

Without saturation, the force produced by the two electromagnets is proportional to the square of the current but decreases with the air-gap between the armature and the electromagnet.

A typical actuator working cycle begins by supplying the upper electromagnet. The force generated moves the armature upwards. The displacement creates a difference between the spring forces that in turn accelerates the armature when the voltage across the upper winding is reduced to zero. In the meantime the lower electromagnet is supplied in order to establish the flux necessary to attract the armature down. As soon as the armature moves closer to the lower electromagnet, it is caught and kept in position for the desired time. Also in this phase a difference in the spring forces is produced allowing an upward movement.

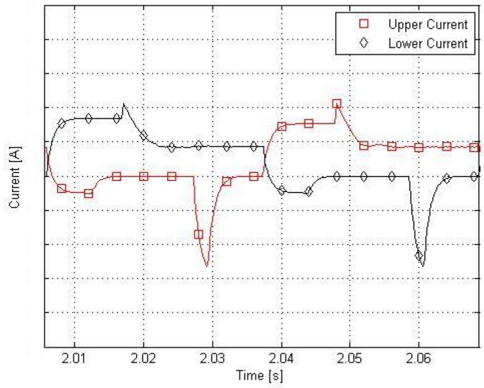

Figure 6: Current vs.time in a standard transition

It is important to highlight the role played by the springs since they provide the large inertial power to accelerate the armature at the beginning of its stroke and then to absorb the inertial power to decelerate when it approaches the electromagnet. Since the potential energy is stored in the springs instead of being dissipated, the inertial power is regenerative.

Another characteristic of this system is the non linearity of the force-displacement relation. For this reason the current required to hold the armature in contact with the electromagnet is low.

Since this system is unstable in the equilibrium positions close to the electromagnets, special control methodologies are required to:

a) limit the armature impact velocity during the landing phase. High velocities would produce unacceptable noise level.

b) ensure a transition time between the upper and the lower position compatible with the performance demands.

c) guarantee a high holding force when the air gap is equal to zero (forces necessary to keep the suction valve open during the reverse flow phase).

These requirements are in conflict with each other. For this reason Cozzani has developed and patented a sophisticated control algorithm.

The algorithm development has also dealt with non linearities in the magnetic force and with variation of the gas force which depends on the different running condition of the reciprocating compressor.

5 Research activity

The development of the new system has required the following activities by Cozzani R&D department:

- Actuator Mechatronic Design and prototype realization
- Development of mathematical models for analysis of theoretical system behavior.
- Design and realization of a customized control board.
- Experimental tests on the actuator through a dedicated test bench.
- Development of an algorithm for the positioning control of the actuator moving parts.
- Tests on a mono-stage single acting compressor.
- Tests on a two-stage double acting compressor.

5.1 Development of control algorithm

A scheme of test bench used for the actuator experimental tests is shown in fig 7.

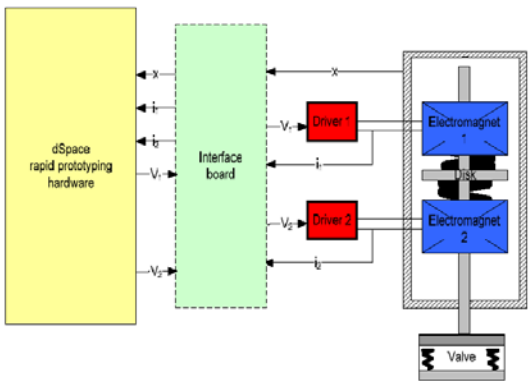

Figure 7: Experimental Setup for actuator control

The test bench is made up by an actuator housing that simulates the valve cover, two DC drivers, which provide the voltage required by the two windings, an interface board for the input and output signals conditioning and a rapid prototyping system dSPACE. The test bench is also designed to house a suction valve in order to evaluate its influence on the actuator functioning.

Figure 8: Actuator test bench

The force generated by each electromagnet depends on the winding geometrical features and on the material ferromagnetic properties.

A dynamometer has been used to determine the forces produced by the electromagnets. This enabled to obtain for different current values the air-gap / force chart shown in fig 9.

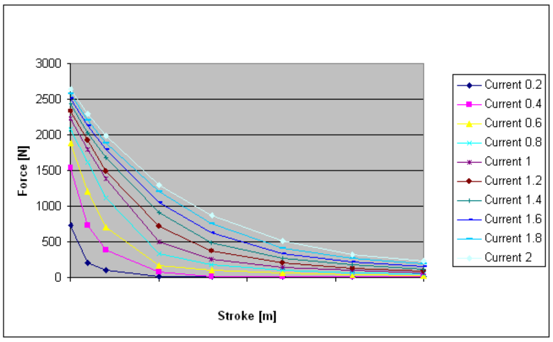

Figure 9 Air-gap vs force for different current values

The tests have been done by using different electromagnets characterized by different geometric dimensions, in order to determine the relationship between dimension and force.

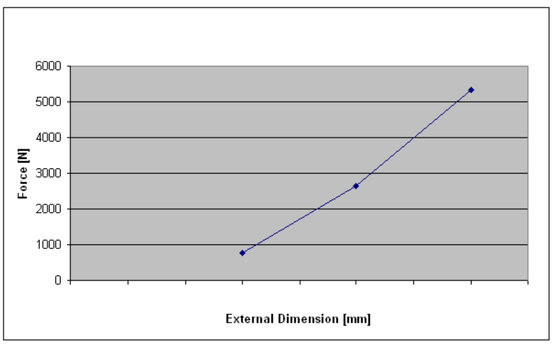

Figure 10: Maximum forces for different electromagnet dimensions

This first test phase has been fundamental for the development of the actuator algorithm control. It allowed to optimize the parameters, reduce the impact velocity, synchronize the reference trajectories with the measured armature position and to assure the system repeatability.

The use of advanced rapid prototyping system dSPACE integrated by Matlab/Simulink, enabled to develop the control algorithm in an efficient way, to monitor the values of all the variables and to modify the behavior by acting on its parameters.

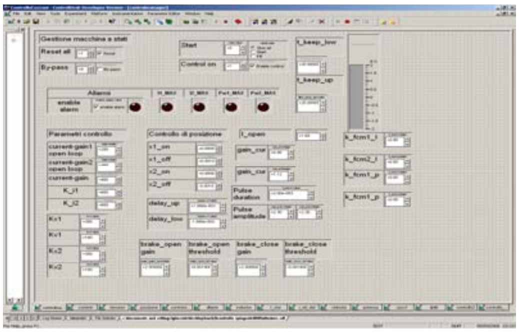

Figure 11: Control interface

After the development of a control algorithm, an actuator control board (ACU) has been realized. In order to make the control system operative, the algorithm has been implemented in an ACU board, provided by digital I/O, analogical I/O and field bus.

5.2 Test on the compressor

In order to verify the ACU functionality, the new regulation system by Cozzani has been installed on a mono stage single acting compressor. This first testing phase has allowed to obtain the first results on the capacity control and on the power consumption.

Afterwards the capacity control system has been installed on a two stage double acting reciprocating compressor.

The tests have been carried out by using air at the atmospheric suction pressure and at 10 bar for discharge pressure.

Figure 12: Compressor installed with the new capacity control system

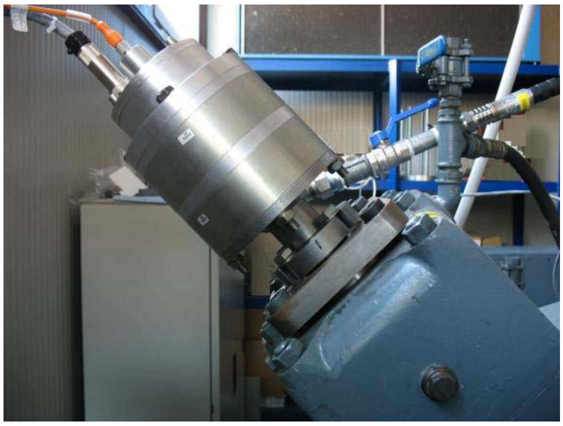

Figure 13: Actuator installed on the 2nd stage

Unlike the previous tests done on a single actuator, the new tests have been carried out on a more complex system constituted by one SCU and four ACUs, in order to control the actuators and the suction valves. The different units, SCU and ACUs, and the respective protection devices have been connected in a switch board (fig 13).

Figure 14: ACUs

The compressor has been equipped with an inverter, in order to test the system at different running speeds.

A proximity sensor has been installed on the compressor to determinate the Top Dead Center (TDC) as reference to make SCU generate the starting signals for the ACUs, depending on the compressor geometrical data.

Two pressure sensors, one in the inter-stage piping and another one in the vessel, let the SCU determine the holding time for the different valves. In order to do this, a closed-loop pressure controller has been implemented in the SCU. External controller can be interfaced with the SCU.

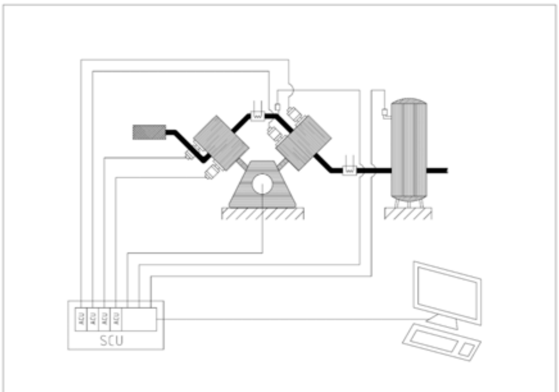

Figure 15: Diagram of the plant under test

A multi-channel data acquisition system records the pressure vs time diagram of the head acting cylinder and of the suction and discharge volumes.

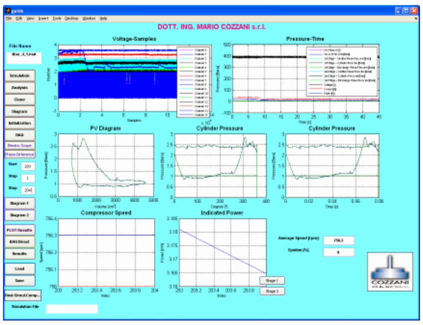

Figure 16: Acquisition data Software developed by Cozzani

The tests show the SCU capability to control the compressor capacity adapting it to the plant requirements. Fig.17 shows the pressure vessel vs time diagram from the loading phase until reaching the set-point pressure of 6 bar.

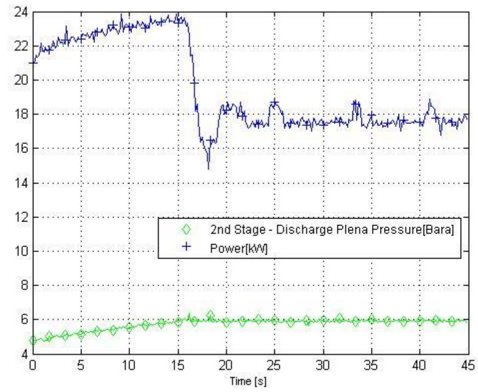

Figure 17: Vessel pressure and power consumption vs time

Fig 18 shows the data recorded by the acquisition system and the increasing in suction valve holding time during the control.

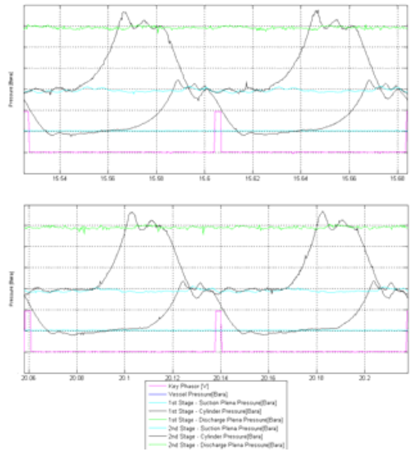

Figure 18: Pressure vs time during the reverse flow operation

Tests with different flow rates values have been carried out, fig 19 shows the decrease of the power consumption with the decreasing of required load.

The new system is able to vary the suction valve opening time to adapt the compressor capacity to the one required by the plant, therefore it enables to have the entire possible energy saving obtainable from the reverse flow regulation systems.

Regarding the actuators, acting on the suction valves at every compressor cycle, the extreme precision of the position control ensures a high versatility in the compressor control (capacity control with constant discharge pressure, suction or inter-stage pressure control, etc.).

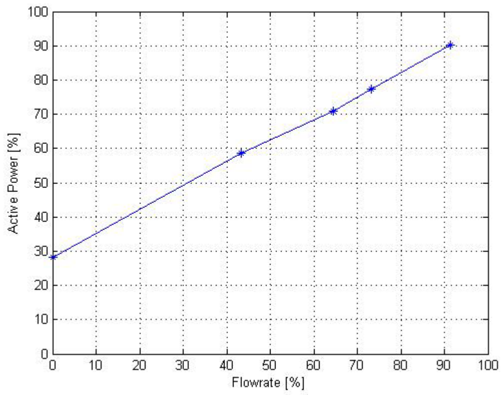

Figure 19: Power consumption vs flow rate using the capacity control system

Anyway, as previously explained, engineering and economical analysis are needed to establish the advantages of a capacity control system in comparison with another one, since it depends on the plant type and on the required operation.

6 Conclusions

The compressor capacity control, required to keep constant the process pressure or process flow or to adjust it to the process requirements, can be carried out with different devices.

This paper shows the new reverse flow capacity control system developed and patented by Cozzani.

The control of the position of the suction valve shutters has been carried out by using a new actuator characterized by two electromagnets. This new device has a high dynamic performance and enables to grant the strict times necessary in the different phases of the compressor cycle.

The realization of a dedicated test bench allowed the development of a control algorithm to control the position of the moving parts of the actuator. In order to evaluate the influence of pressure forces on the shutter, further analysis are needed.

Experimental tests carried out on compressors have given positive results about the capability of the new system to change the opening suction valve time adapting the compressor capacity to the plant requirement.

Activities for the certification of the system for use in potentially explosive atmospheres are in progress. This will allow to supply a system version in compliance with ATEX rules.

References

1 – API Standard 618 “Reciprocating Compressors for Petroleum, Chemical and Gas Industry Services”
2 – Workshop “ Compressor Control", 5th EFRC-Conference 2007 Prague
3 – A.Bianchi, M.Schiavone, "New rotary valve Actuated by Electronic Control", 2nd EFRC-Conference 2001 Den Haag.
4 – Matlab User’s Guide
5 – A. Isidori, Nonlinear Control Systems, Third Edition, Springer Verlag
6 – G. Marro, Controlli Automatici,Zanichelli
7 – H. K. Khalil, Nonlinear Systems, Third Edition, Pearson Education International Inc.

HOERBIGER

Material Design for Valve Applications

by:

B. Spiegl, T. Kriechbaum, P. Steinrueck

Innovation & Technology
HOERBIGER KT Holding
Vienna
Austria
bernhard.spiegl@hoerbiger.com

6th Conference of the EFRC
October 28th - 29th, 2008, Dusseldorf

Abstract:

Since the introduction of non metallic materials to the compressor market decades ago the valve suppliers constantly have tried to increase the reliability and lifetime of valve sealing elements. Nevertheless the improvement potential soon gets to the limitations of commercially available materials and production processes installed. All valve materials in use today were developed for general applications like automotive, consumer products,… and have not been designed to match the needed properties in compressors. The load on valve sealing elements is quite unique due to the combination of dynamic impact loads, high temperature and gas exposure and the more or less static load by the differential pressures. The specific overall load combination requires purpose designed material.

The basis to generate guidelines for new materials is the fundamental understanding of the loads occurring during operation and the micro mechanics involved during crack initiation and advancement.

Different new purpose built high performance materials with tailored structure, reinforcement and surface have already proven their outstanding properties in a high number of field tests in critical installations all over the world in a five years' field test.

1 Introduction

In the recent years short fibre reinforced thermoplastic (SFRTP) polymer compressor valve plates have attained a leading position in many application areas [1,2,9]. Much knowledge about processing and the typical behaviour of these fibre reinforced materials is necessary to make the great potential of these polymers in respect to an improvement of efficiency and reliability available.

The behaviour of SFRTP parts and in special valve plates machined out of centre gated injection moulded discs is determined by the properties of the fibre, the matrix, the fibre/matrix bonding and the orientation of reinforcement. Injection moulded fibre reinforced components exhibit a typical, three layer structure with two skin layers and a core layer. In the skin layers an orientation of the fibres in melt flow direction (MFD) can be observed. The core is defined by an orientation of the reinforcement perpendicular to MFD. This leads to anisotropic stiffness, thermal behaviour and – depending on the process parameters during moulding – more or less residual stresses by cooling down from the processing temperature.

The aim of finite element (FE) calculations is to get knowledge about the occurring stresses and to explain premature failure of valve plates. It is obvious that the results of FE calculation strongly depend on the given material data and thereby, only under consideration of the anisotropic character of SFRTP reasonable results can be achieved.

This paper deals with the determination of the stresses in valve plates impacting against a valve seat. The non-isotropic material behaviour is taken into account. The basis to generate guidelines for new materials is the fundamental understanding of the loads occurring during operation and the micro mechanics involved during crack initiation and advancement.

2 Material properties

In SFRTP the fibres get aligned during the mould filling process, leading to orientation dependent material properties. This anisotropy shows strong influence on the overall component behaviour. In the direction of the fibre alignment the material is e.g. up to a factor of three stiffer and the thermal expansion is lower compared to the off-fibre direction.

2.1 Fibre orientation fundamentals and measurements

Shear and elongational flow-conditions are responsible for the orientation of the fibres. Shear-flow aligns the fibres in flow direction, elongational flow in the direction of the main elongation.

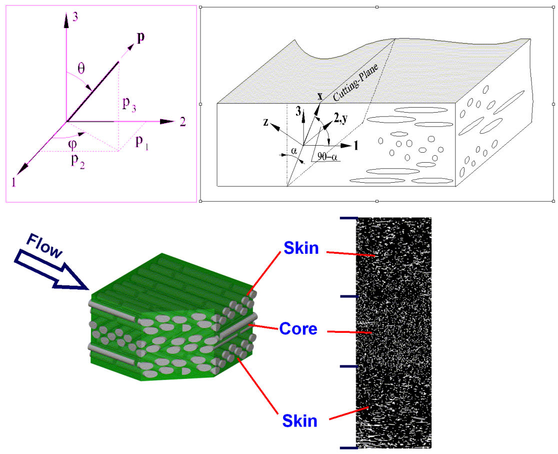

Figure 1: Orientation angle of single fibre in space (left). SFRTP sample with inclined cutting surface [3]. Typical fibre orientation in centre gated valve plates (right).

For a reliable judgement of the fibre orientation and as an input-parameter for the micromechanical modelling described in section 2.2 it is necessary to know the fibre orientation quantitatively. The most universal means of describing the fibre-orientation is an orientation function ψ, which describes the probability for a fibre being orientated between the space angles (Fig. 1) θ_1 and ($\theta_1+d\theta$) and φ_1 and ($\varphi_1+d\varphi$). ψ is defined through:

$$P(\theta_1 \le \theta \le \theta_1 + d\theta, \varphi_1 \le \varphi \le \varphi_1 + d\varphi) = \psi\,(\theta_1, \varphi_1)\sin\theta_1 d\theta d\varphi \,. \qquad (1)$$

Instead of using a spherical co-ordinate system with the sphere co-ordinates θ and φ a description of the probability function with the help of a unit co-ordinate vector can be done, $\psi(\theta, \varphi) = \psi(\underline{p})$. In this form the orientation in space is given by the co-ordinates of the unit vector, which are connected to the spherical co-ordinates in the following way (Fig. 1):

$$\underline{p} = \underline{p}(\theta,\varphi) = \begin{bmatrix} p_1 \\ p_2 \\ p_3 \end{bmatrix}, \text{ with } \begin{cases} p_1 = \sin\theta\,\cos\varphi \\ p_2 = \sin\theta\,\sin\varphi \\ p_3 = \cos\theta \end{cases} . \qquad (2)$$

As ψ is the density of a probability function, a normalisation condition can be given

$$\int_{\theta=0}^{\pi}\int_{\varphi=0}^{2\pi}\psi(\theta,\phi)\sin\theta\,d\theta\,d\varphi = \oint \psi\,d\underline{p} = 1 . \tag{3}$$

Although the orientation distribution function ψ is the most universal description form, in practical use it is difficult to handle and interpret. Therefore, it is common to calculate parameters, which characterise the fibre orientation state. Besides many other possibilities, so-called orientation tensors [4] can be used. They allow the representation of the whole, three dimensional distribution function. The quality of the description is given by the rank of the tensors. Orientation tensors are defined as the moments of the orientation distribution function. The second and fourth rank tensors are given through

$$\underline{\underline{a}} = a_{ij} = \oint p_i p_j \psi(\underline{p})\; d\underline{p} , \tag{4}$$

$$\underline{\underline{\underline{\underline{a}}}} = a_{ijkl} = \oint p_i p_j p_k p_l \psi(\underline{p})\; d\underline{p} . \tag{5}$$

From these definitions the full symmetry of the tensors is evident. Furthermore the normalisation condition (3) requires, that the sum of the main diagonal components is equal one.

For the second order tensor we see, that the main diagonal components describe the amount of orientation in the directions of the used reference frame. The off-diagonal components show the rotation of the main orientation axis with respect to the used co-ordinate system.

To determine the orientation tensors polished cross-sections are examined [3]. If a circular cross-section is assumed for the fibres, they are pictured as ellipses on the intercepting plane. The picture evaluation is done by image analysis using a special developed analysing program. User defined parameters allow an adjustment of the evaluation algorithm, so that a fully automated picture processing is possible. Furthermore the algorithm uses a mathematical regression, which dramatically minimises the experimental error.

A major problem when using polished cross sections to determine the fibre orientation is, that from a cutting ellipse the orientation of a fibre is not determined uniquely. Two states of orientation are possible. Because of this, not all tensor components can be determined from one polished cross section. The problem can be overcome, if the cutting plane is taken under a certain angle to the 3-axis (Fig. 1) and some assumptions are made for the fibre orientation state: Either a symmetric fibre orientation with respect to the 1-2 plane or a „nearly planar“ orientation state has to be given.

Whilst the utilisation of the first condition needs a mathematical treatment [5], the consequence of the second is obvious: If we hit a fibre and determine the two possible orientations, the one which is nearer to a planar orientation is more likely. With this it is possible to determine all components from one cross-sectional cut.

2.2 Micro mechanical modelling

The traditional method of determining the material constants by testing soon reaches its limitations, because on the one hand the number of independent values increases for anisotropic materials and on the other, measurements for different fibre orientations are necessary. Therefore micromechanical modelling provides a comfortable solution method to determine the complete information which is needed for the stress-strain analysis of SFRTP-components.

If linear behaviour is assumed, the purpose of the micromechanical modelling is to find the effective constitutive equation of the composite, which is written, for example, in compliance form:

$$\underline{\varepsilon} = \underline{\underline{C}}^{V}\,\underline{\sigma} + \underline{\alpha}^{V}\,\Delta T , \tag{6}$$

where C^V is the compliance tensor (4th-order), ε is the strain tensor (2nd-order), σ is the stress tensor (2nd-order, α^V is the expansion tensor (2nd-order) and ΔT is the temperature difference. Input parameters for the calculations are the elastic constants of the matrix and the fibres, together with parameters characterising the geometry of the micro-structure. For the latter the fibre volume fraction, the fibre aspect ratio and the second and forth order orientation tensor are needed.

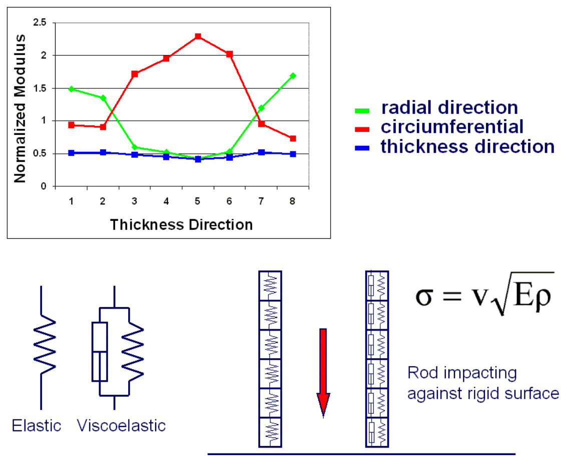

Figure 2: Typical modulus distribution over thickness in SFRTP materials. Fundamental

difference between elastic and viscoelastic material behaviour.

The used micromechanical model solves the thermo-elastic problem in a way, that not only the stiffness but also the expansion tensor of the composite can be calculated. It is based on the theory of Maewal and Dandekar [6] and was extended in [5]. As starting point an ellipsoidal inclusion, with the same effective aspect ratio as the cylindrical fibres, in an infinite matrix is considered [7]. Although the solution is only exact for vanishing fibre volume fractions, very reasonable parameters are predicted for real composites, at least for the low volume fractions encountered in SFRTP [5,6]. The generalisation to arbitrary fibre orientation-states is done by the mathematical procedure of orientation averaging. This tensorial technique gives exact solutions and eliminates the need for numerical integrations.

2.3 Material data for FE calculation

The following materials have been investigated: HOERBIGER PK (PEEK GF30) and HOERBIGER MT (Polyamide with 30% glass fibres, composition details are classified and not published). The analysis of the cross sections was performed by scanning electron microscopy. For the analysis the thickness is divided into eight different layers. Figure 2 shows the calculated results for the Young's modulus in normalized form.

The results for the normalized modulus in figure 2 reveal the strong orientation dependency of the modulus due to the fibre orientation. For impacts against stiff surfaces the stiffness of the material perpendicular to the surface is of importance. In case of valve plates that means that the impact stress levels are still highly determined by the matrix material even if the content of fibre reinforcement is high.

Polymers and especially polymers at higher temperature behave viscoelastic. Beside the decrease of stiffness the material exhibits better damping properties. In case of impact calculations the incorporation of this unique behaviour is essential.

2.3.1 Orthotropic viscoelastic material data generation

Similar to the stiffness the viscoelastic behaviour is not isotropic. In direction of the fibre orientation the material properties are strongly governed by the fibres with little viscoelastic influence. The measurement of viscoelastic properties in all directions to fill a stiffness tensor for FE calculation is not possible with the equipment available today. On the other hand the viscoelastic material data is typical generated in the frequency range or 0.02 to 20 Hz. These frequency levels are far away from the shock loading frequencies during impact.

In order to introduce the viscoelastic polymer behaviour the viscoelastic data of the material needs to be measured for the unreinforced material at different temperatures (Fig. 3, left). By the help of the so called "Time-Temperature Shift" it is possible to generate master curves for certain temperatures by shifting along the time axis. By this procedure it is possible to generate curves for the relaxation modulus in the needed time or frequency range with sufficient accuracy.

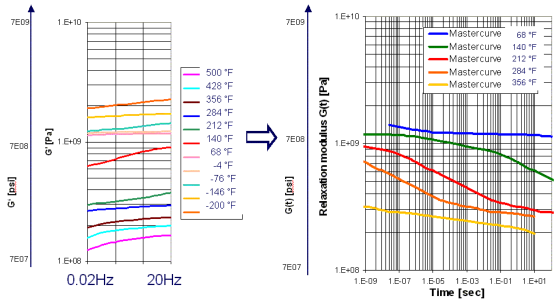

$$S_{ij} = S_{ij}^{\infty} + \sum_{k=1}^{m} S_{ij}^{k} e^{(\tau'-\tau)/\tau_{ij}^{k}}$$

Figure 3: Storage modulus for unreinforced PA46 at different frequencies and temperatures (left), Relaxation modulus for short times derived from measurements (right), expression for the orthotropic viscoelastic stiffness tensor used in finite element calculation.

The time dependency of the relaxation modulus is expressed by the help of Prony- series (Fig. 3). The orthotropic viscoelastic stiffness tensor is derived by micro mechanical modelling and assuming that each component of the tensor behaves similar, thereby having the same relaxation time.

3 Stress calculation

The question concerning the stress levels occurring during impact of a valve plate on a seat or guard are as old as the valves themselves. The high number of influencing factors like speed, geometry, oil stiction, tilted motion together with multidimensional stress stage inside the valve plate never allowed clear statements on the stress levels. Since the introduction of non metallic fibre reinforced materials the situation has become more complicated.

In order to get best insight into the occurring stresses during impact two different models are used: a cross section model to investigate the stresses near the seat and a model of a complete valve plate.

For the model the orthotropic viscoelastic material behaviour is taken into account. The models consist of eight layers. For each layer the fibre orientation was measured and the orthotropic viscoelastic material data was calculated and assigned to the FE elements.

The calculations were performed with the finite elements program ABAQUS Standard and EXPLICIT. For the material a user defined material (UMAT) was implemented.

3.1 Simulation with cross section model

The results from FE-Calculations of the cross-section model show that high stress concentrations in the contact region can be observed. It is obvious that the occurring stresses in the contact region strongly depend on the form of the valve seat and are thereby influenced by the mesh geometry.

A chamfer as it is shown in Fig. 4 does not lead to remarkable stress reductions in the contact area. The observed stresses are in an order of magnitude that plastic deformation and crack initiation can occur. Careful finishing of sharp edges is essential to reduce stress levels.

An optimisation of the valve seat by an adjustment of the contour according to the deflection of the valve plate smoothes and reduces the occurring stress levels (Fig 4) significantly. As a further advantage the location of the highest stresses is moved into the inner of the valve plate and thereby the possibility of crack initiation is decreased.

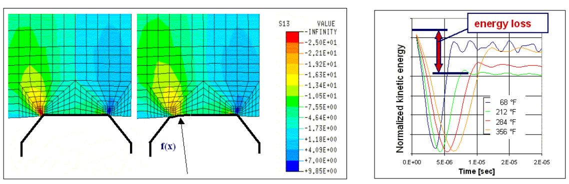

Figure 4: Stress distribution in seat land area with 3 m/s impact speed. Viscoelastic damping effect at different temperatures for HOERBIGER MT Material.

The performed analysis shows higher stresses in the contact region. However the dependencies in the given equation (Fig. 2) are confirmed. In the case of SFRTP`s the Young`s modulus is replaced by the stiffness of the composite in thickness direction. In addition, especially the stiffness in thickness direction is strongly influenced by the temperature dependent modulus of the matrix. As a result of the increased temperature the composite stiffness in thickness direction is reduced and thereby the maximum stresses are decreased. In Figure 4 on the right the viscoelastic damping effect and the dependency of this effect on temperature can be seen by looking at the kinetic energy during impact. At 180°C the damping effect is again reduced because this material exhibits the highest damping in the range of 100°C.

3.2 Valve plate model

For an estimation of the stresses in the whole valve plate, especially in web and ring areas it is necessary to model the whole valve plate together with the surface of the seat. Under the assumption of a plane parallel impact the stresses in the valve plate are almost the same as observed with the cross section model.

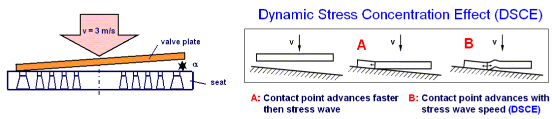

Figure 5: Model used for simulation, explanation of the Dynamic Stress Concentration Effect (DSCE) [8].

This situation changes dramatically if an oblique impact is considered. This impact situation can be confirmed by measuring the valve motion at different places on the valve plate. In this case a critical condition occurs when the location of the contact moves with almost the same speed as the shear / bending stress waves propagate through the material (Fig. 5). Stress waves generated at successive contact front positions move at the same speed as the contact front itself [8]. Instantaneous energy input at the contact front is always in phase with the oncoming stress waves from previous contacts. This effect is called dynamic stress concentration effect (DSCE) and causes high stresses and deformations through the interference of stress waves on the opposite side of the first contact (Fig. 6).

A higher contact angle than the critical one allows the stress wave to advance faster than the contact point and thereby reduces the DSCE. Otherwise, in case of a small contact angle the development of the DSCE is prevented because as the point of contact advances with higher speed than the speed of the stress waves.

Fig. 7 shows the normal stress in radial direction in an element out of the web region (see Fig. 6) over time for parallel impact and impact under critical condition for the material HOERBIGER MT at 230 °F. For this specific valve plate, geometry and load case a critical contact angle between 0.75 and 1° is found.

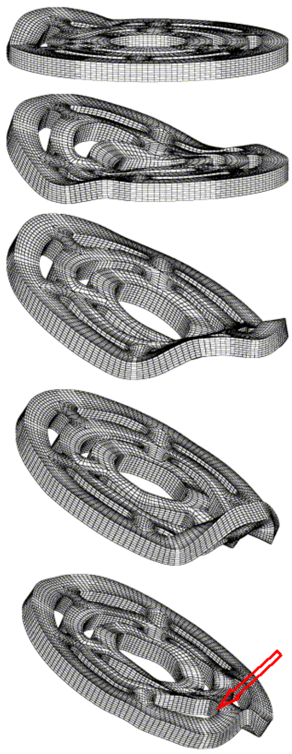

Figure 6: Magnified deformation of a valve plate under oblique impact and critical conditions.

The stresses caused by the DSCE are many times higher than the stress from a plane parallel impact against the valve seat (Fig. 7). The observed normal stresses lie in an order of magnitude above the fatigue strength for that material and explain premature failure of valve plates especially in the web and ring sections near the outermost diameter. High shear deformation can be observed which supports delamination processes of layered materials like SFRTP.

The interference of stress waves on the opposite site of the first contact produces high deflections and subsequently an acceleration of the deflected areas against the valve seat. Thereby much higher contact velocities occur. High impact speeds support a breaking out of fragments or fretting fatigue of the valve plate (Fig. 8).

Calculations with material damping or polymer specific viscoelastic material behaviour reveal that damping effects reduce the ability to develop the DSCE and also its magnitude. This is coincident with the experience that valve plates operating above their glass transition temperature show remarkable better fatigue performance in spite of reduced strength [1,9].

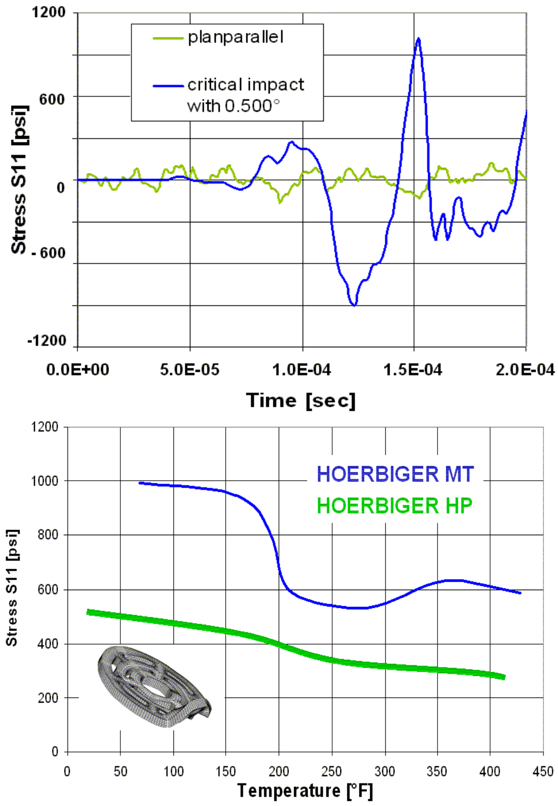

Figure 7: Up: Stress levels under plane parallel impact compared to impact under critical conditions in the web section (Fig. 6). Down: Dependency of maximum stress under critical conditions over temperature for standard material (MT) and a new developed material (HP).

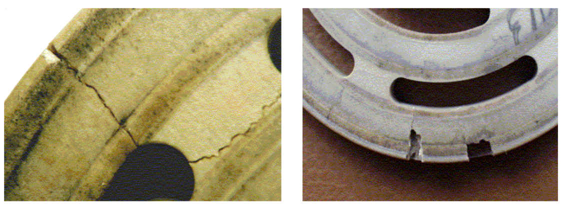

Figure 8: Typical valve failure modes resulting form Dynamic Stress Concentration Effect (DSCE) [8].

Its mentioned above, that a significant decrease of the matrix modulus by increasing temperature has a great influence on the stiffness and shear modulus of the SFRTP valve plate because of the lack of fibres in thickness direction. The development of the DSCE strongly depends on the stiffness values in thickness direction and is thereby significantly influenced by the temperature. A reduction of the stress wave propagation speed needs a higher contact angle to develop a critical condition and therefore the probability for this condition to occur is reduced.

3.3 Residual stresses in valve plates

The different layers of SFRTP components behave anisotropic concerning stiffness and strength as well as in thermal expansion. Improper processing conditions can lead to different thermal expansion coefficients of the complete structure in radial and circumferential direction for centre gated SFRTP plates. This produces high residual stresses by cooling down from processing temperature. If these stresses exceed a certain level unstable warpage may result. In the case of high residual stresses resulting from wrong processing parameters the complex residual stress state in SFRTP discs is worsened through stress transfers by machining slits into the plate.

Calculations and measurements show that improper processing may lead to residual stress levels up to 20 MPa. Furthermore, if areas of high residual stresses coincide with regions of high stresses due to DSCE crack nucleation, or in the case of existing cracks, crack growth is evident.

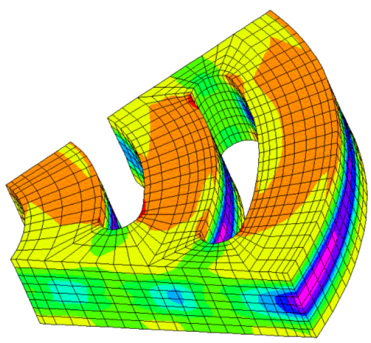

Figure 9: Residual stress distribution in circumferential direction of a typical valve plate machined out of a SFRTP slug.

4 Design of purpose built materials and optimized SFRTPs for compressor applications

The simulation of the impact and generation of the orthotropic material data already show clear areas for improving the material structure like: - reduced stiffness in thickness direction and damping behaviour - in order to reduce the occurring stresses and the DSCE during impact. Another area for optimization is to prevent crack initiation on the surface. By increasing the degree of isotropy the residual stresses in the material can be reduced.

Fracture mechanics (Fig. 10) and the investigation of crack advancement in the material (not shown in this paper due to space limitations) gives a number of advices how to improve existing material in the area of:

- Fibre diameter, fibre length, fibre aspect ratio
- Fibre bonding, fibre sizing, fibre surface structure (carbon fibre)
- Fibre content, polymer and fibre interaction
- Matrix viscosity
- Polymer processing

Some of the areas for improvement are further outlined in the following chapters.

4.1 Stress reduction

The most simple approach to increase lifetime is to reduce the occurring stresses. In case of valve plates the stress level is determined by the impact loading. Different measures can be applied to bring down the impact speeds in a valve – but this is a compressor and valve engineering issue. For a given application and valve the challenging part is to reduce the maximum stress levels by material improvements.

Based on the results out of the simulation in case of the HP material the degree of anisotropy has been increased, the modulus in thickness direction reduced and overall damping behaviour in the temperature range of operations optimized. This was done by selection of a proper matrix material, new type of fibre reinforcement and orientation. The simulations with the new “designed” material proves the effectiveness by reducing the maximum stresses during critical oblique impact by 60% (Fig. 7) without any changes on the valve design and springing – just by introducing a new valve plate material.

4.2 Crack stopping

The most common reason for premature valve failure is material fatigue or fatigue crack growth. Small cracks in the material or on the surface, for example caused by impact on sharp seat lands, increase in size by high load frequency and are supported by residual stresses (Fig. 9) in the material. The crack propagates through the reinforced material mainly by surrounding the short fibre reinforcement. Crack advancement is thereby also supported by the coalescence of material flaws preferably at the fibre ends of the short fibre reinforced material. Even if fibres themselves have high fatigue strength, the fatigue behaviour of standard short fibre reinforced materials at high load cycles it is still determined by the non metallic surrounding matrix.

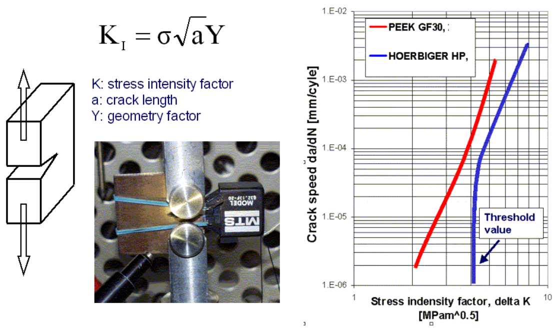

Figure 10: Fatigue crack propagation testing of valve plate materials under different cyclic load levels at room temperature

In order to overcome the limitations of commonly used short fibre reinforced materials, for the new HP material a very special type of reinforcement is used. A special planar long carbon fibre reinforcement prevents a potential crack from going around the fibre reinforcement. To improve the crack resistance the bonding levels between the carbon fibres and the polymer matrix is adjusted in that way that a certain amount of sliding on the fibre surface is allowed (Fig. 11).

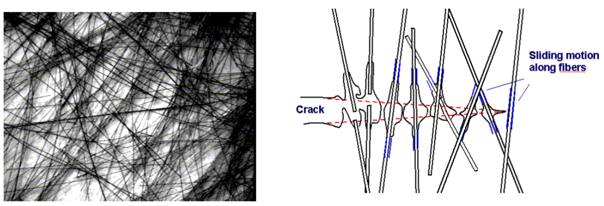

Figure 11: Special long carbon fibre reinforcement. Explanation model for exceptional fatigue crack resistance of HOERBIGER HP material.

This spreads the stress concentration near the crack tip and thus preventing crack advancement up to high load levels – creating a “threshold” value below which no crack advancement can be found. This exceptional crack stop ability was proven by fatigue test probes (Fig. 10). The HP material does not show crack advancement up to very high cyclic stress levels – at these stress levels standard short fibre reinforced material would fail after short operation time. This feature works like a shock absorber and forms the basis for HP’s unique crack stopping ability. Due to this HP specific property no more fatigue crack growth can be found in valve plates any more.

4.3 Functional skin layers

Very often damages caused by seat lands or particles on the seat are responsible for crack initiation at the surface or at the edges (Fig. 4, 8). The FE simulation of the stress concentration at the seat lands reveals high deformations in the micro scale. Modern polymers like PA and PEEK can survive this strain – but not the stiff reinforcing fibres near the surface. Fibres get broken and micro cracks coalesce forming a macroscopic crack advancing into the valve plate.

To prevent crack initiation on the surface the HP material was equipped with fibre free functional skin layers. These skin layers are softer and thereby in addition improve the sealing and damping behaviour. This feature eliminates seat wear as well.

4.4 Thermal Expansion and dimensional stability

Beside the requirements on mechanical strength and fatigue resistance there also exist strong needs in terms of thermal expansion and dimensional stability. Standard materials tend to have higher thermal expansion than the steel seats. This causes problems with large valves preferably in discharge valves. Ring valves with contoured seat lands suffer of severe leakage problems if dimensional stability is poor.

In the HP material the thermal expansion was adjusted to match the thermal expansion of steel. This makes sure, that there is no dimensional deviation even at higher temperature and it gives good sealing performance in ring valves. No moisture pickup additionally improves the stability.

4.5 Proven lifetime extension of optimized SFRTPs on lifetime tester

Short fibre reinforced materials for valve applications were improved by optimizing fibre reinforcement, fibre aspect ratio, fibre diameter, fibre sizing, fibre content and production. The new materials (called HOERBIGER X-materials, like LTX, MTX, HTCX) show significantly higher robustness and lifetime on the inhouse slap tester and in operation.

Figure 12 shows the lifetime tester used for material development. The tester allows fatigue testing of valve plates and valve design under different speeds (up to 3000 rpm), lifts and temperatures. Under typical operating conditions a more than 4 times higher lifetime of the new optimized MTX grade compared to standard MT can be found.

The newly developed material grade for high temperature use und critical process gas applications and new ring valves, HOERBIGER HTCX, achieves 5 times longer lifetime compared to standard PEEK GF30.

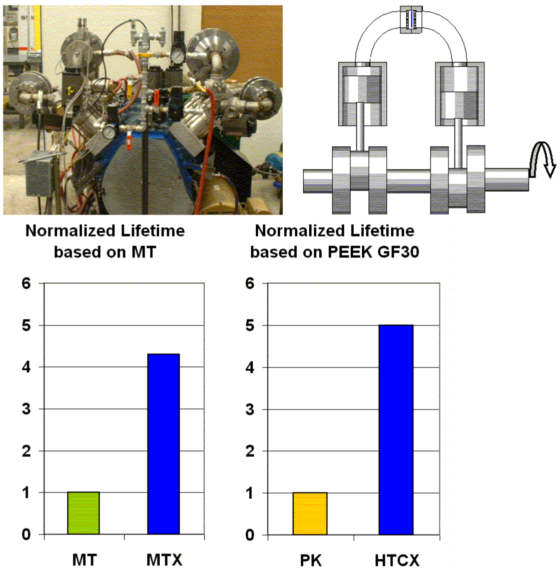

Figure 12: Lifetime tester for accelerated life time testing of valve plate materials. Lifetime comparison between HOERBIGER MT and optimized MTX grade. Lifetime comparison between standard PEEK GF30 (HOERBIGER PK) and newly developed material grade HOERBIGER HTCX.

5 Field experience

The new, “designed”, HP compressor valve material was submitted to worldwide field test. For 5 years more than 10000 valve plates and ring sets have been successfully running predominantly in demanding installations (oxygen, low temperature, oil stiction, high impact, high corrosive gas, leakage critical, HydroCOM,…) and were able to cure persistent problem applications. None of the test valves has failed or shows any form of fatigue or aging (Fig. 13).

Due to the usage of a base material with reduced shear strength and shear stiffness the application envelope of HP is actually limited to medium pressure applications (depending on valve type). Developments to extend the pressure limitations are ongoing.

In parallel the optimized SFRTPs like LTX, MTX and the newly developed material grade HTCX are running successfully in more than 1000 field installations in gas gathering, gas storage and gas transport. HTCX proves its outstanding properties as new material for performance ring valves in several demanding field installations globally and will be the standard material for all new ring valves.

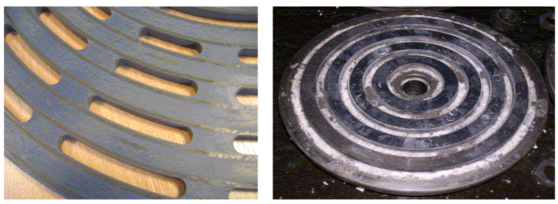

Figure 13: HOERBIGER HP valve plate and rings after 12000 h successful service in demanding compressor installation. No indication of fatigue, aging or crack growth.

6 Conclusions

Fundamental research on valve materials opens a window of opportunity for material improvement. Design guidelines derived form dynamic finite element calculation, micro & fracture mechanics allowed to significantly improve valve materials.

A new purpose built high performance (HP) composite with tailored structure, reinforcement and surface has already proven its outstanding properties in a high number of field tests in critical installations all over the world in a 5 years’ field test.

Material optimization of existing material grades based on the fundamental findings led to improved and new material grades (LTX, MTX, HTCX) showing more than 4 times higher lifetime potential and higher robustness in critical applications. This new material series will allow compressor operators to run their compressors more reliably and efficiently in future.

References

[1] B. Spiegl, B. Mlekusch, D. Artner; Stress calculations in short fibre reinforced thermoplastic (SFRTP) compressor valve plates; ImechE Conference, London 1999

[2] Steinrück P.,„Kunststofftechnik für Kompressorenventile„ Industriepumpen und Kompressoren, Heft 3, September 1997

[3] Mlekusch B., „Fibre Orientation of Short Fibre Reinforced Thermoplastics II: Quantitative Measurements by Image Analysis“, Journal of Composite Materials, (1998).

[4] Advani S.G., Tucker C.L, „The Use of Tensors to Describe and Predict Fibre Orientation in Short Fibre Composites“, Journal of Rheology, 31(8), 751-784 (1987).

[5] Mlekusch B., „Thermoelastic Properties of Short Fibre Reinforced Thermoplastics“, Journal of Composite Materials, (1998).

[6] Maewal A., Dandekar D.P., „Effective Thermoelastic Properties of Short-Fibre Composites“, Acta Mechanica, 66, (1987).

[7] Eshelby J. D., The determination of the elastic field of an ellipsoidal inclusion, and related problems. Proc. Roy. Soc. London. Ser. A 1957; 241:376-96

[8] Böswirth L., Zur Frage der Brüche von Ventilplatten in Kolbenverdichtern, Konstruktion 32, Heft 12, 481-486, 1980

[9] B. Spiegl, G. Machu, P. Steinrueck; Role of improved valve technology in the utilization of natural gas resources, EFRC Conference, Prague, March 2007

Case Study of a Bearing Failure Analysis

by:

Dr.-Ing. Marcel Hempen
Central Division of Technology
NEUMAN & ESSER GmbH & Co. KG
Übach-Palenberg
Germany
marcel.hempen@neuman-esser.de

Bernd Wagner
NEAC Compressor Service GmbH & Co. KG
Übach-Palenberg
Germany
bernd.wagner@neac.de

6th Conference of the EFRC
October 28th / 29th, 2008, Dusseldorf

Abstract:

Analysis of bearing failures is very time-consuming and expensive because different interdisciplinary fields like oil grade, hydro-dynamic bearing calculation, service conditions, fatigue of material, structural design and compressor alignment must be taken into account.

In the presented report the course of action is shown as an example for the investigation of bearing failures at a NEA compressor, type 1 SVL 320. The case study will show the options and limits of SEM (scanning electron microscope) investigations for analysing bearing failures and present technical measurement options to check and verify the geometric installation of a compressor.

1 Introduction

Modern construction methods with finite element methods allow an increase of the work load of mechanical components. Also the development of new bearing materials resp. modified fabrication methods at the bearing production allow an increase of the maximum load, being seeming impossible some years ago. **Figure 1** shows an overview of the allowable maximum loads of different bearing materials.

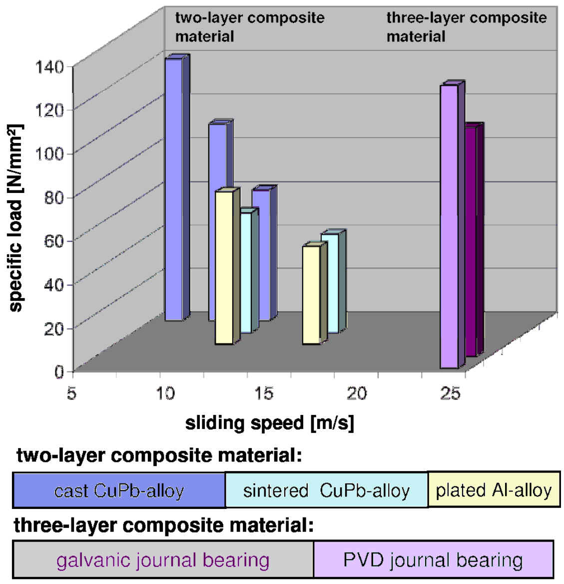

Figure 1: Typical journal bearing materials [1]

The chart shows that the bearing material as well as the fabrication method have a serious impact on the bearing material properties. Especially the PVD (**P**hysical **V**apour **D**eposition) technique has to be mentioned, achieving with its thin material layers a high specific load in combination with a possible high sliding velocity.

Today increased computer performance enable to solve the differential equation of Reynold, **figure 2.** Hence bearing calculations with classical materials, e.g. white alloy bearings, will be more accurate.

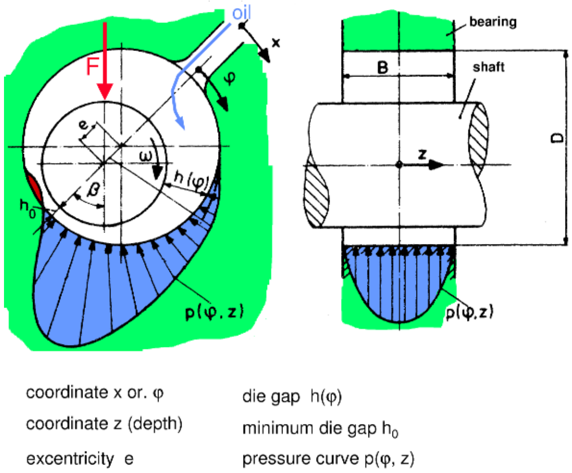

$$\frac{\partial}{\partial x}\left(h^3 \frac{\partial p}{\partial x}\right)+\frac{\partial}{\partial z}\left(\frac{h^3}{\eta}\frac{\partial p}{\partial z}\right)=6\eta\left[(U_1+U_2)\frac{\partial h}{\partial x}+2\frac{\partial h}{\partial t}\right]$$

Figure 2: Differential equation of Reynold [2]

Still bearing failures occur on machines with several thousand flawless running hours as well as on new installed machines. Normally bearing failures will be detected only at the final and last moment, e.g. by Δp indicator at the oil filter or increased bearing temperatures.

Figure 3 shows a typical bearing failure of a white alloy bearing.

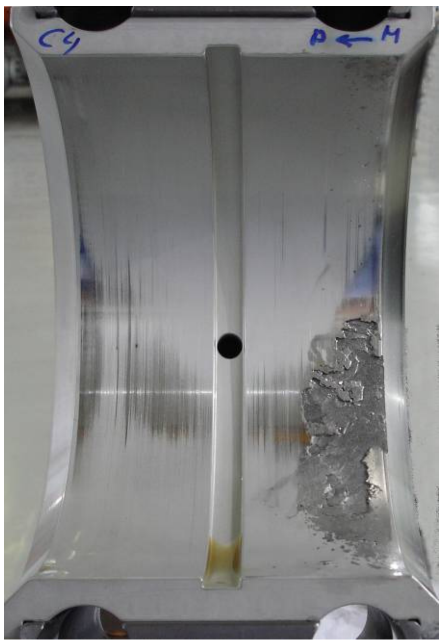

Figure 3: Typical cracked-off bearing metal

2 Failure Investigation

2.1 Interpretation of Bearing Failures[3]

A bearing failure investigation especially at an early stage of damage can give important hints to the damage reason due to the specific damage symptoms of the bearing failure. A bearing failure at a final stage will give nearly no information and only general statements can be made like: bearing failure, jammed bearings, worn out or broken-down. A meaningful evaluation with states of failure type (damage symptom) and failure mechanism (kind of damage) is mostly not possible any more.

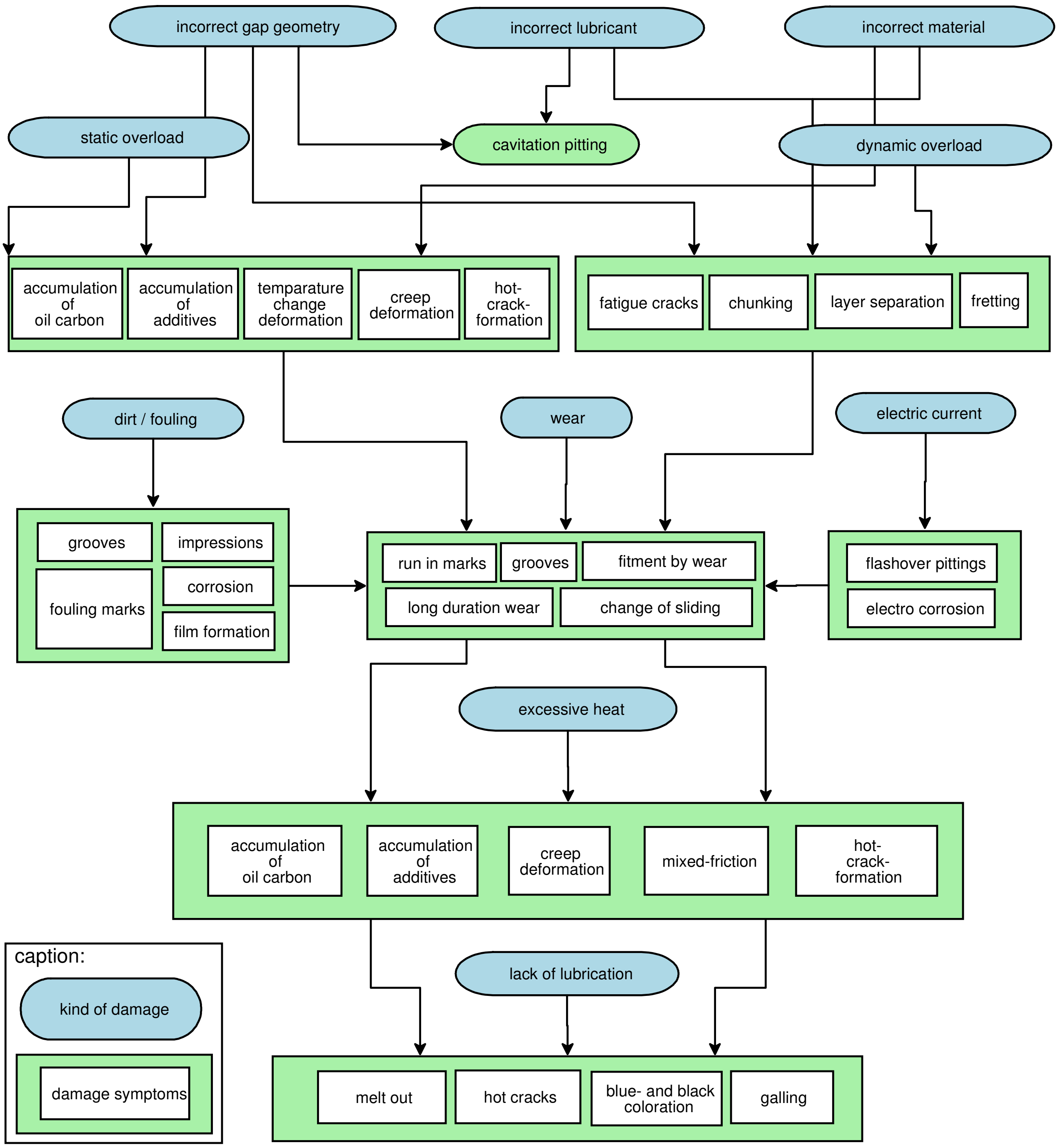

Figure 4: Kind of damage and damage symptoms in dependence of failure stadium

Hence to this situation, it is important to check several different parameters, properties and continual influence of operations. With this methodic course of action it is possible to achieve further technical expertises. Typical parameters are for example:

- construction of bearing (material, bearing clearance, bonding, …)
- dynamic and static Load (bearing calculation, nonstandard load conditions..)
- bearing monitoring (e.g. oil temperature, bearing-temperature, oil-pressure, …)
- lubrication (oil quality, viscosity, particles, type of oil pump, emergency supply, total acid number, base number, type of filter, filter condition, recent oil change, …)
- course of events (course of failure, extent of damage, operating conditions during failure and operating conditions history, …)
- sliding surface (primary modification, secondary modification)
- back side of bearing (contact pattern, marks of friction, fretting, oil carbon, impressions, cracks, corrosion, …)

It is very important to know that the bearing failure analysis includes some major problems and the following fact has to be considered:

- Different failure reasons can show the same damage symptoms.
- Identical failure reasons may have different damage symptoms depending on the bearing construction or lubrication.
- A certain failure reason can show different damage symptoms depending on the stage of failure.

Figure 4 illustrates this fact, e.g. a mixed-friction situation can occur due to electrical current, overheating or oil contamination.

The damage symptoms of the above mentioned, very different failure reasons are quite the same. A technical distinction can only be seen at an early stage of damage.

3 Case Study NEA 1 SVL 320

In the following the methodic course of action of bearing failure investigations, **figure 5**, and the drawn conclusions at an NEA 1 SVL 320 compressor for natural gas storage are described.

3.1 History

After properly working for several years, more and more bearing failures occurred at main bearings and crankpin bearings of a total of 6 compressors of type NEA 320 at the same location. First investigations focused on possible changes in state that could appear simultaneously at all 6 machines. Leads with regard to sulphur corrosion, i.e. a corrosion of white metal bearings due to sulphur compounds in the driving mechanism oil, could not be confirmed since the oil brand was changed, but the type of damage occurred again at the end of storage period of appr. 6 – 8 months (700h).

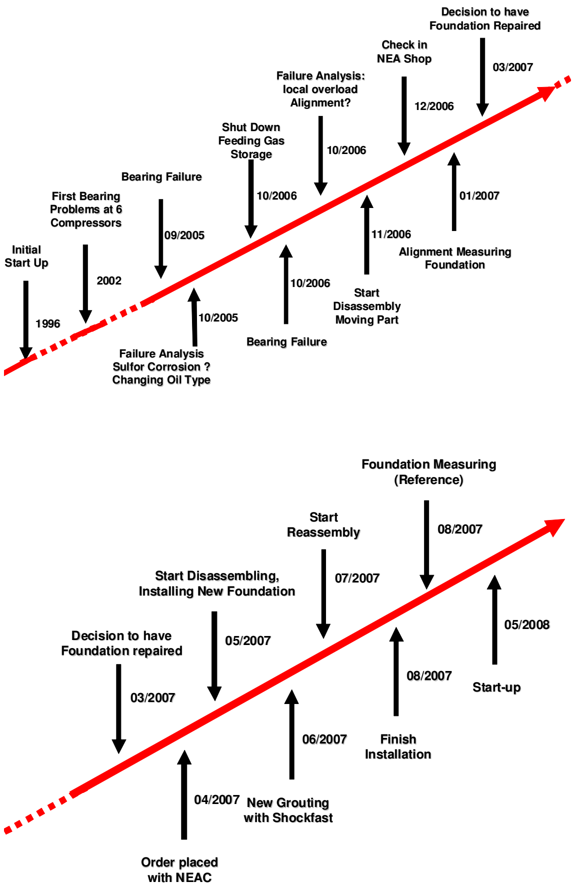

Figure 5: Complete Compressor History

Than inspections carried out in that context concentrated on apparently perfect bearings in order to assess a bearing damage at its beginnings. **Figure 6** shows such a ‚perfect' main bearing.

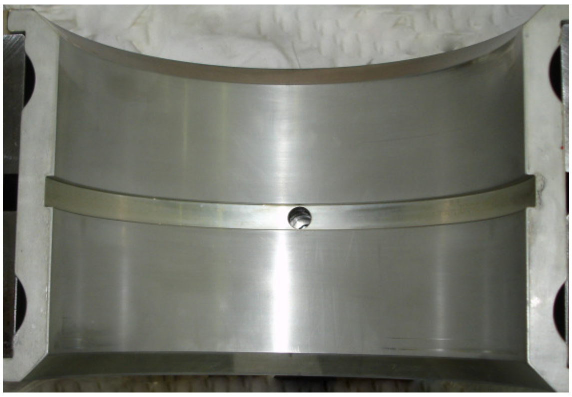

Figure 6: Apparently perfect bearing

However, when looking at the back side more in detail, it becomes obvious that the contact pattern is not uniform, **figure 7**.

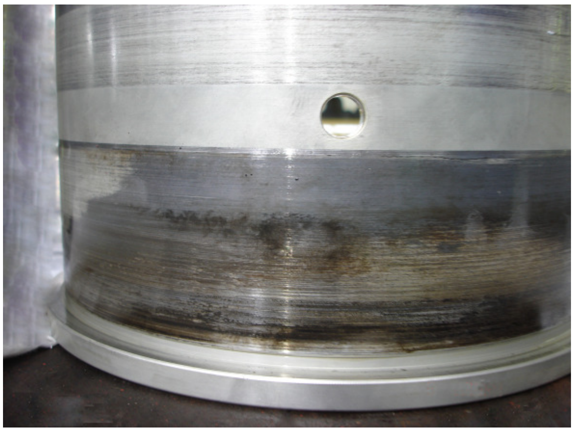

Figure 7: Nonuniform contact pattern

Moreover that bearing showed one oddity. In the upper right-side area of the bearing a small dent was found one could also interpret as an assembly error. **Figure 8** shows a detail photo of that area. Further analysis of this "dent" became necessary.

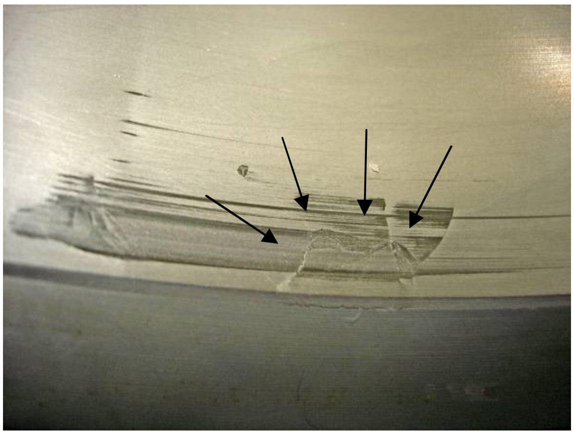

Figure 8: Buckle at the journal bearing

3.1 SEM analysis

The scanning electron microscopy (SEM) analyses were made at the Institute for Materials Science of the RWTH Aachen University. For the analysis a section of abt. 20 mm x 30 mm was removed, **figure 9**.

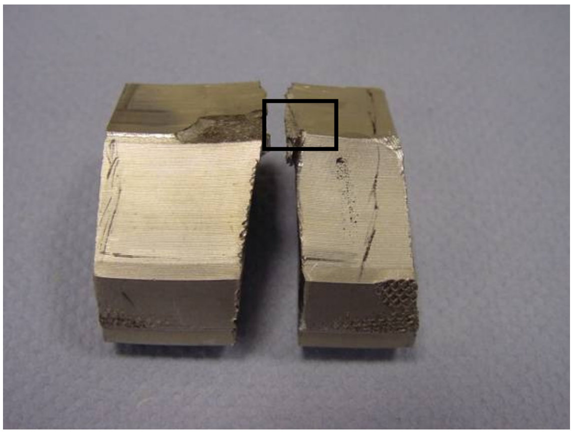

Figure 9: Analysed sections

The sections' surface was scanned. The **figures 10** to **13** are examples for the analysis of the sections shown in **figure 9**. In wide areas pitting were found from which sporadial cracks spread that combine to one big crack.

Summing up, it could be found out that there was a fatigue failure as a result of too high local load. In this case, the failure of the bearing shell due to the formation of pitting was at its beginning; however, after some longer operation it would have resulted in the bearing's failure.

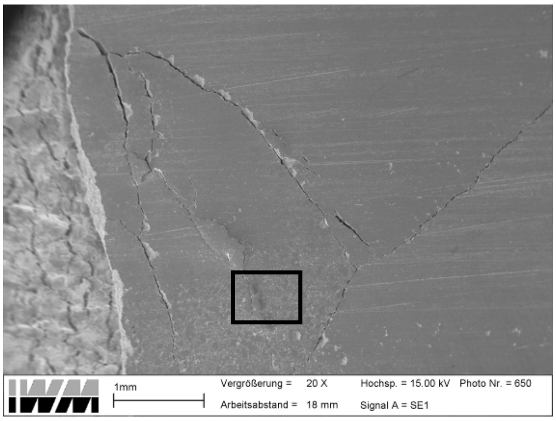

*Figure 10: Section out of **figure 9***

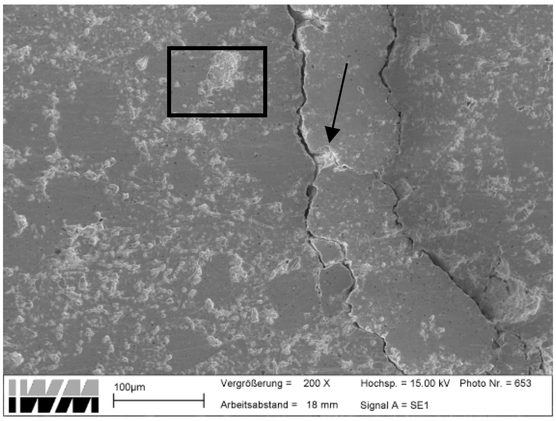

Figure 11: Destructive pitting, origin of the cracks

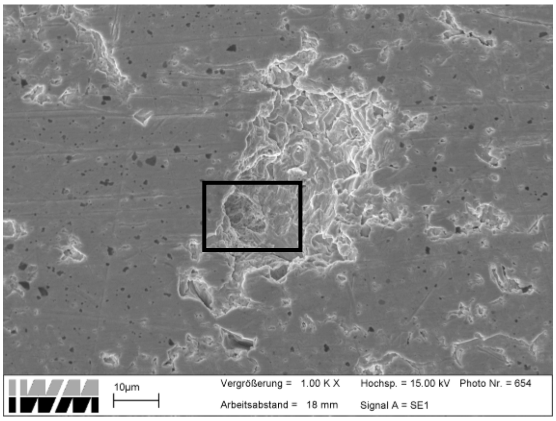

Figure 12: Section out of **figure 11**, *pitting*

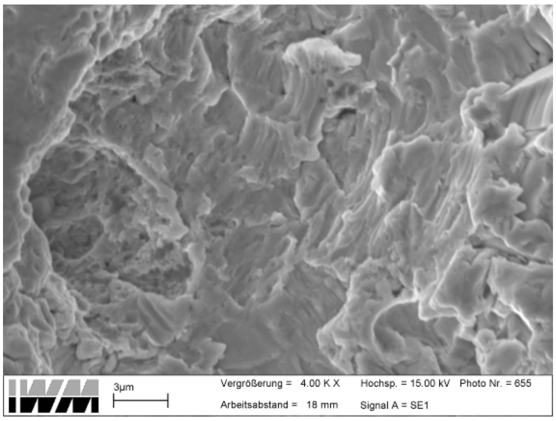

Figure 13: Section out of **figure 12**

The sum of all findings, i.e. the compressor's history, the nonuniform contact pattern as well as the SEM-analysis suggested a structural problem.

3.2 Laser measuring of the crankcase

In order to isolate a structural problem and in order to find the reason for the local excessive load, crankshaft, connecting rod, crosshead and piston were checked with regard to their form and their position. All components were in perfect condition whereupon inspections were extended to the crankcase. By means of Easy-Laser (**figure 14** and **figure 15**) the concentricity of the compressor's main-centreline as well as the rectangularity of the cylinder shaft to the main centreline were measured[4]. For this it is first necessary to align the measuring system. Then the y/z-coordinates of the main bearing seats are measured. In the present case the reproducibility of the y/z-coordinate was 0.1 mm.

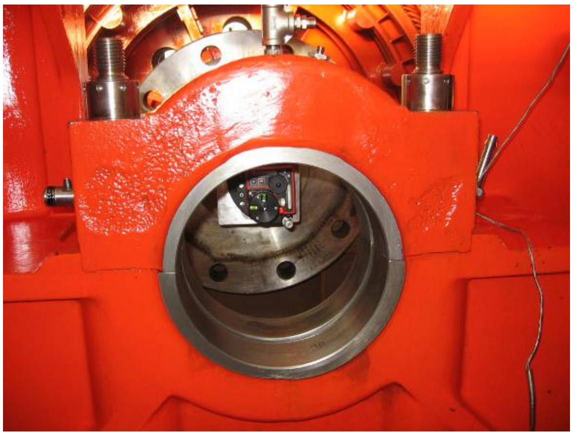

Figure 14: Laser of Easy-Laser measuring system in NEA crankcase

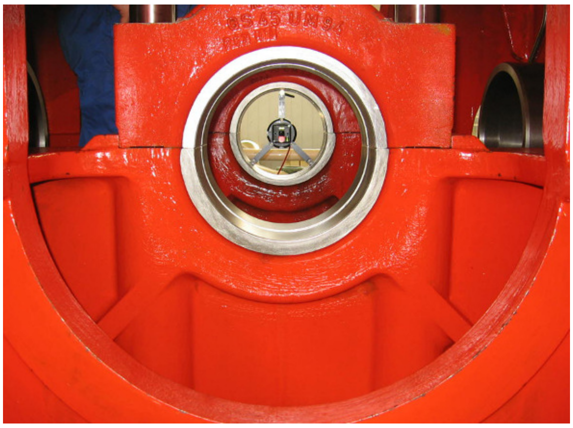

Figure 15: Detector of Easy-Lasers measuring system in NEA crankcase

Figure 16 shows the positions of the machine measuring as well as its results. For calculating the straight lines, the first and the last bearing position was chosen as reference zero. It becomes obvious that the crankcase is sagging in the middle by 0.175 mm – corresponding approximately to the mean bearing clearance.

It is important to mention that in this case the sagging of the crankcase was not detectable by measuring the web deflection of the crankshaft.

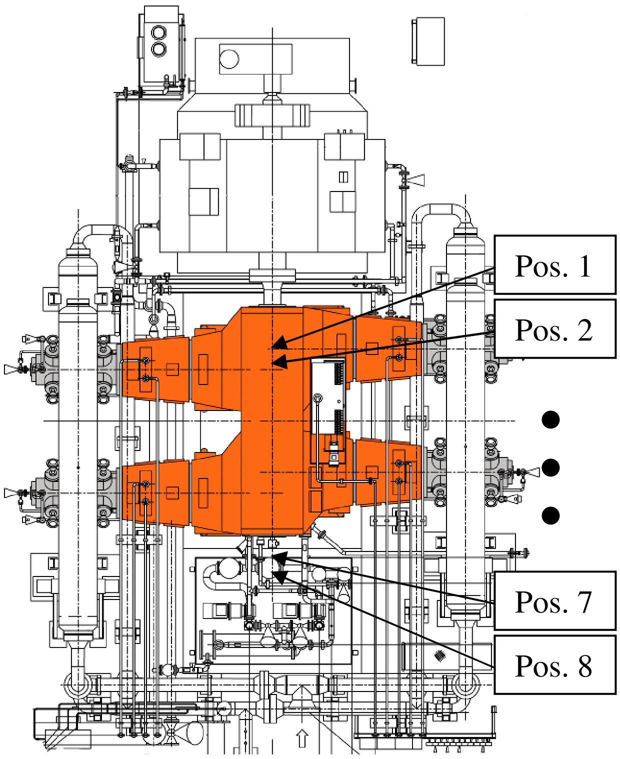

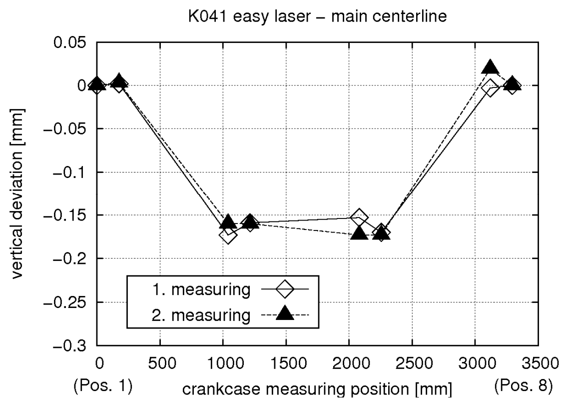

Figure 16: Results of the measuring of the main centreline

A measurement of the crankcase cover confirms the deformed installation of the compressor's crankcase centreline, **figure 17**. In this context it also appears that the driving mechanism is not only 'sagging', but also twisted.

In order to correct the insufficient alignment, it was not only thought about to bore out the crankshaft axis, but also to completely re-install the compressor. Finally a decision in favour of the second alternative was taken since another subsiding of the foundation cannot be excluded and since thus in case of a completely new alignment all options for later possibilities are kept.

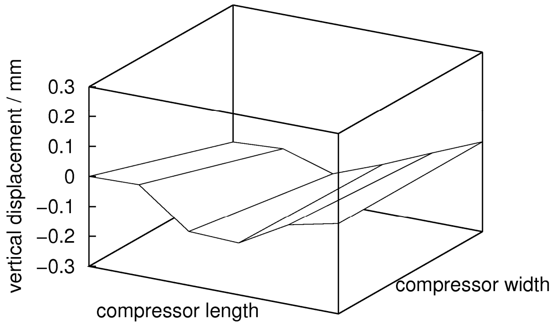

Figure 17: Measuring results of crankcase cover

4 New alignment of the compressor

The compressor was taken of the foundation for the re-alignment, the grouting was removed and re-installed with Chockfast. **Figure 18** shows the compressor during the installation procedure.

Figure 18: NEA compressor during re-installation

During as well as after the installation the compressor's alignment was controlled. **Figure 19** shows the deviations of the main centreline after the re-installation in direct comparison with the original, sagged state. It becomes obvious that the vertical deviation is within the range of the measuring system applied and has improved by the factor 3 to 4 referred to the initial state.

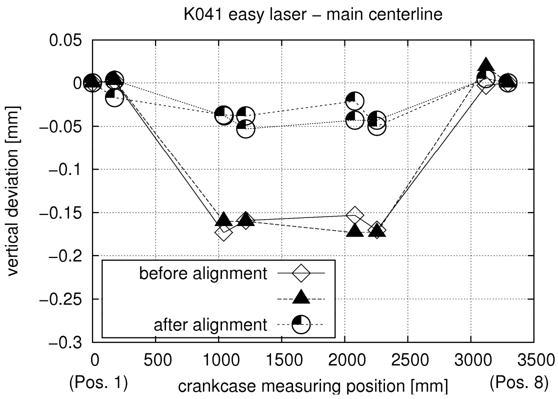

Figure 19: Results of the measuring of the main centreline after the driving mechanism installation has been finished

5 Conclusion

In most cases the analysis of bearing damages is cost and time-consuming and can partly be controversial due to the different forms in which damages can appear during their various stages of development. Therefore it is important to analyse the bearing damages in their initial stage in order to draw reliable conclusions as to their cause.

In the present case the systematic assessment and analysis of damage was described in order to explain and repair the increasing number of bearing damages at several compressors with the objective to ensure a safe and reliable operation.

The compressor was realigned and installed by means of Shockfast. Comprehensive measurings were made at the crankcase and at the foundation in order to gain long-term experience from the soft foundation.

6 Acknowledgement

Herewith we would like to thank all colleagues of the NEA GROUP who have supported this study. In particular we would like to express our thanks to F. Mainz (NEA-QP) und L. Bedekovics (NEAC) whose personal commitment have contributed considerably to the successful execution of the study. Moreover we would like to thank Mr. Idler (MIM) who was always there to help with words and deeds when questions regarding Shockfast arose.

[1] Federal-Mogul,
GLYCO-Ingenieur Bericht - Nr. 1 / 91

[2] P. Gold, Maschinenelemente I,
Universität der RWTH Aachen

[3] R. Kreutzer, Allianz-Zentrum für Technik GmbH:
Schäden an Gleitlagern

[4] H. Ochs (BASF), H. Zachmann (BASF),
B. Wagner (NEAC): - An old Product still fresh - Exchange of crankcases on a 325 bar “CO-Einheitsverdichter”, 4th Conference of the EFRC June 9th / 10th, 2005, Antwerp,
available by e-mail to info@neac.de

Machinery protection for recips: experience and outlook

by:

Roland Schuhmann
Rotating Equipment
BASF AG
Ludwigshafen
Germany
roland.schuhmann@basf.com

Christian Prinz
Monitoring, Controls & Services
HOERBIGER Ventilwerke GmbH
Vienna
Austria
christian.prinz@hoerbiger.com

6th Conference of the EFRC
28–29 October 2008, Düsseldorf

Abstract

Machinery monitoring and protection systems are as important for reciprocating compressors as they are for turbomachines. Because of the special requirements of reciprocating equipment, however, they are considerably harder to design. BASF AG (Ludwigshafen, Germany) has found from past experience that systems not specifically designed for reciprocating machinery perform unsatisfactorily.

Accordingly, BASF joined forces with reciprocating compressor specialist HOERBIGER (Vienna, Austria) to develop a monitoring and protection system purpose-designed for recips. The designers took into account the wide range of applications and types of compressors in use, as well as new standards for safety-critical systems, notably IEC 61508.

The resulting system is reliable, versatile, and fast: it can trip a malfunctioning compressor within a single revolution, if necessary. It uses a combination of embedded systems for speed and robustness, and Windows®-based software for ease of use and powerful data analysis. Appropriate techniques allow rapid (20 kHz) sampling without generating unmanageable amounts of data.

Designing to the IEC 61508 methodology took longer and cost more than would otherwise have been the case. As automated monitoring and protection systems extend to more and more classes of equipment, however, the future lies with IEC 61508, and perhaps also with higher-level standards to promote the uniform handling of data from different types of monitoring systems.

1 Recips need monitoring

Machinery protection systems have been used for many years to protect against product leakage or human injury by shutting down equipment automatically in the event of problems.

These systems typically use measurements of flow, pressure, temperature and vibration to judge the status of the equipment they protect. Vibration monitoring to assess reciprocating compressors is the subject of this presentation.

Almost every item of turbomachinery has a vibration measurement system installed, in most cases with the ability to trip the machine immediately it detects a fault. By comparison, vibration-based shutdown systems for reciprocating equipment such as compressors and metering pumps are rare.

Reasons for this include the fact that reciprocating machines are often used in redundant configurations and maintained at relatively short intervals. Plant personnel often believe that it is easier to hear problems with reciprocating than with rotating machines. Perhaps most importantly, vibration monitoring of reciprocating machinery is simply more difficult.

But unplanned shutdowns are expensive regardless of the type of machinery that causes them. Fewer plant personnel; more and more equipment required to operate unsupervised; a shift from time-based to condition-based maintenance; longer service intervals made possible by new materials for wear parts such as rider rings: all these factors make condition monitoring and fault diagnosis of prime importance for reciprocating machines.

2 How to analyse vibration

2.1 Rotating and reciprocating machines

Turbomachines operate at speeds of thousands or tens of thousands of rpm. Their vibration signatures are stable over millions of revolutions, with amplitudes that in most cases change only slowly over time. Identification of a problem is usually done in the frequency domain. Figure 1 shows a steady vibration signal, a trend curve showing increasing vibration amplitude, and the corresponding frequency spectrum. If we know the steady-state peak or RMS amplitude, the appropriate alarm and trip settings are relatively easy to calculate using approved procedures.

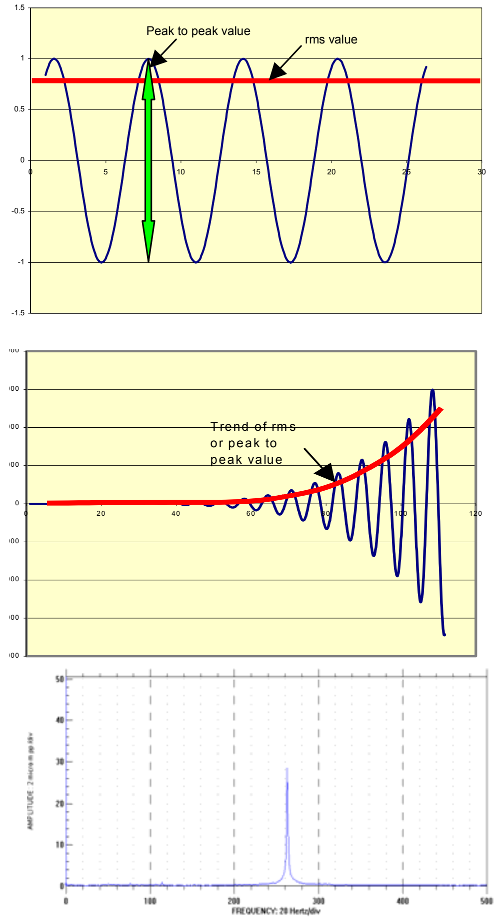

Figure 1: (Top to bottom) a basic turbomachinery vibration waveform; a trend curve showing increasing amplitude; and the corresponding frequency spectrum

Reciprocating machines are much harder to monitor because the signal changes significantly over the course of each revolution (Figure 2).

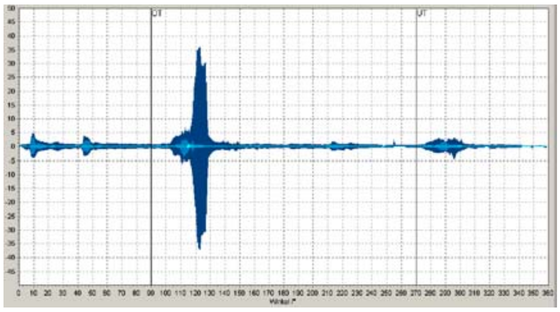

Figure 2: Vibration amplitude signal from a reciprocating compressor

The mechanical impacts which occur normally during the operation of a reciprocating compressor produce a frequency spectrum containing many harmonics (Figure 3). As a result, fault diagnosis in the frequency domain is almost impossible.

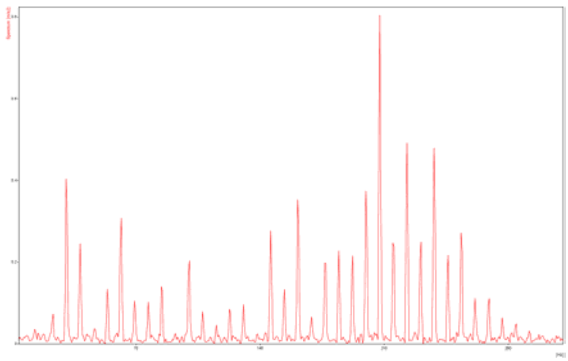

Figure 3: FFT frequency spectrum from a reciprocating compressor: the harmonics make fault diagnosis difficult

Measuring the overall level, which is very common for rotating machines, is also not very suitable, because the impacts make reciprocating compressors inherently noisy. The alarm levels therefore need to be set quite high, and as a result, changes in vibration amplitude are unlikely to be discovered at an early stage.

Clearly, monitoring and protection systems for reciprocating machinery need a different strategy.

2.2 Time-dependent alarm thresholds

Since the frequency domain is obscured by harmonics, and simple amplitude measurements are dominated by impact signals, the answer is to use alarm values that track the amplitude signal over time (Figure 4). During the quiet parts of the cycle the alarm (green) and trip (red) thresholds have low values; during noisy events such as valve movements and crosshead impacts, the thresholds are raised accordingly.

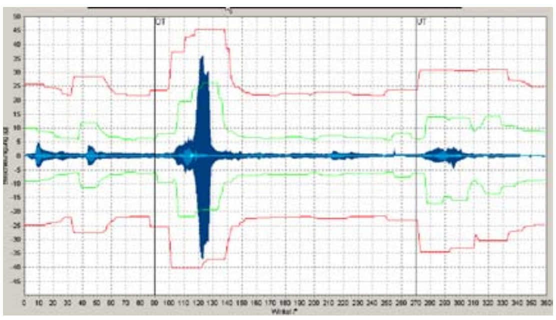

Figure 4: Amplitude signal (blue) with alarm (green)and trip (red) bands over a complete cycle

The protection system can identify these events because they correlate with the crank angle, but this is not as simple as it sounds. Experience shows that the amplitude and timing of impacts can differ greatly depending on the speed, suction pressure and load. To be successful, a monitoring and protection system must be able to use different alarm bands for different operating conditions.

Figure 5 shows an example of a "normal" signal moving out of its alarm band as a result of a change in conditions. Although in this case a dangerous condition does not exist, an alarm will be sent because the alarm band cannot adapt to the change.

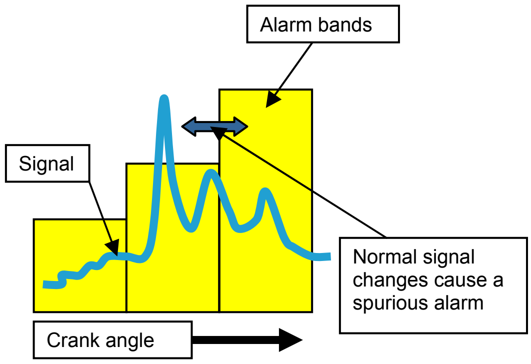

Figure 5: Faulty alarms due to the use of time increments that are too coarse

To eliminate this problem it is necessary to measure the amplitude, and set the alarm band, with high time resolution (for example, one degree of crank angle), giving the ability to "stretch" the alarm bands around the impacts.

Since failures in reciprocating compressors can progress very rapidly compared to rotating machines, the system must measure the signal, and compare it with the alarm band, on every revolution.

3 Designing a practical system

3.1 System requirements

A successful monitoring and protection system for recips should be able to:

- Meet the relevant safety standards for reliability and operation in potentially hazardous atmospheres (see Section 3.2 below).
- Measure and analyse vibration (acceleration), indicator pressure and rod motion during the course of every revolution.
- Synchronise measurements with the compressor's crank angle using a trigger sensor installed at the flywheel or coupling.
- Adapt to the many different conditions under which a particular reciprocating compressor can operate, with appropriate alarm levels.
- Monitor every revolution, compare all measured and calculated data with the appropriate limit

values, and generate near-instantaneous alarms and trips in the event of abnormal conditions.

- Record all measurements and analyses continuously and at high enough time resolution to help in subsequent analysis, for instance in determining the cause of an alarm or shutdown, and store this data for at least three years, without averaging.
- Communicate with programmable logic controllers (PLCs) and distributed control systems (DCSs) via standard interfaces such as MODBUS, OPC, and TCP/IP.

3.2 Standards and certification

A practical monitoring and protection system must be capable of reliably shutting down the compressor on detecting a dangerous condition, but at the same time it needs to minimise the risk of spurious trips. The resulting combination of hardware and software must also be smart enough to recognise a sensor or system failure.

As programmable electronic protection systems gain acceptance, certification to standards such as IEC 61508 is becoming important in meeting health and safety requirements. IEC 61508 requires each certified system to have a defined "safety integrity level" (SIL) which describes the probability of failure and makes it easier for users to select the correct system. From the start, this system was designed to be certified to IEC 61508 with SIL 1. Section 5.1 below discusses this in more detail.

Reciprocating compressors are widely used in areas with potentially explosive atmospheres, so Ex certification is mandatory. The system is designed to be certified to European (ATEX), US (FM), Canadian (CSA) and Japanese standards for equipment operating in hazardous areas.

3.3 Hardware and software

To meet the system requirements outlined above, the best solution is a combination of a hardware-based ("embedded") system and a personal computer (PC) that relies on software.

The embedded system is fast and robust, guaranteeing real-time performance and the reliability required to meet IEC 61508. The embedded system is responsible for all the machinery protection functions of the complete monitoring and protection system.

The PC platform, on the other hand, is ideal for data recording, trending and sharing, with a friendly user interface based on Microsoft® Windows®. It provides all the monitoring functions needed to analyse and diagnose problems as they develop.

The complete system recognises three levels of notification; in order of increasing severity, these are known as "Warning", "Alarm" and "Safety Alarm". All three alarm levels are generated by the embedded system, which then passes them on to the PC. Warning signals are used only by the PC software, to inform maintenance and reliability engineers that a problem may be developing. Alarms and Safety Alarms are also available as relay contacts, in accordance with IEC 61508, to provide automatic shutdown via a safety-critical PLC or DCS.

Modular design of both hardware and software allows the system to be designed such that it provides an economic solution for both large and small compressors. To reduce installation costs, especially for compressors operating in potentially hazardous atmospheres, the main hardware unit mounted in the safe zone communicates with a field-mounted data acquisition device, which in turn links to individual accelerometers and other field sensors. This approach uses just a few safety barriers (typically two or three), in contrast to the many that would be required if all the sensors were hard-wired directly to the main hardware unit.

4 Detailed system description

4.1 Overview

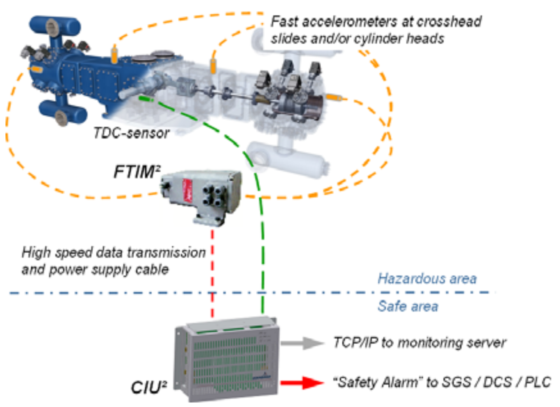

Figure 6: System layout

Figure 6 shows the overall layout of the system. The raw vibration data comes from accelerometers mounted on the crosshead slides and the cylinders. Other data such as temperature and pressure is provided by standard 4–20 mA sensors.

Up to eight field sensors are connected to a field-mounted data acquisition device, the Fast Transmitter Interface Module (Fast-TIM² or FTIM²). A large installation will typically use several Fast-TIM² units.

The Fast-TIM² connects to the main hardware unit, known as the CIU², which is mounted in the safe area. The CIU² also takes a direct input from the trigger on the flywheel that is used to calculate the crank angle for timing purposes.

The CIU² sends hard-wired binary signals, including Alarm and Safety Alarm signals, to the safety-critical PLC or DCS. The CIU² also sends data to the monitoring server via TCP/IP.

4.2 Data acquisition and Fast-TIM²

The sensors used to gather compressor data include ICP® (integrated circuit piezoelectric) accelerometers for vibration, standard 4–20 mA sensors for variables such as temperature, dynamic 4–20 mA sensors for the indicator pressure, and 3-wire voltage-based sensors to measure rod motion.

Up to eight sensors are connected to each field-mounted Fast-TIM² module (Figure 7), whose task is to collect and transfer the resulting data via a single high-speed data line to the main hardware unit mounted in the safe zone.

Almost all the sensors required for compressor monitoring are intrinsically safe (Ex i). To simplify installation while maintaining safety in the potentially explosive atmosphere around the compressor, the Fast-TIM² incorporates Ex barriers for each data channel and power line.

Figure 7: Two Fast-TIM² modules mounted on a compressor

An important task of the Fast-TIM² is to reduce the bandwidth required for sensor measurements without compromising accuracy. The need to do this stems from the high sampling frequency required.

To allow its use on high-speed natural gas compressors as well as the slower compressors typically used for process gases, the system must be capable of working at speeds up to 1200 rpm. Indicator pressure and rod motion can be measured at a relatively slow sampling rate, but to detect incipient damage, the system must be able to listen out for high-frequency peaks in the phased acceleration pattern (time waveform). Doing this at high enough time resolution to allow accurate and reliable analysis requires a sampling rate of 20 kHz.

Such a high sampling rate poses bandwidth challenges for data transfer between the various parts of the system, and also requires a large amount of storage space for archived data.

To reduce the amount of data without losing information, especially during high-frequency peaks, we use a method known as enveloping. Figure 8 shows the raw acceleration signal sampled at 20 kHz:

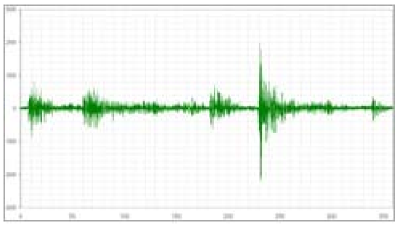

Figure 8: Raw acceleration signal

First, the data is rectified to ensure that both positive and negative peaks are taken into account (Figure 9):

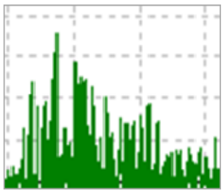

Figure 9: Rectified acceleration signal (zoomed)

Next, the “maximum peak hold” method is used to compress the data into 504 points per revolution. Each point represents the maximum vibration amplitude over a crank angle (CA) increment of 0.71° (504 × 0.71° = 360°) (Figure 10):

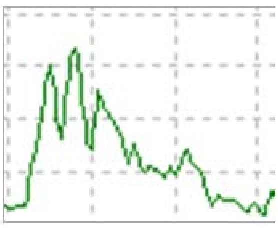

Figure 10: Building the envelope

The last step is to compare each value with its corresponding threshold values for Warnings, Alarms and Safety Alarms (Figure 11).

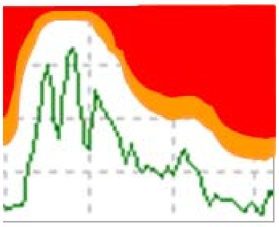

Figure 11: Acceleration peaks are monitored 504 times on every revolution

Done correctly, the envelope method greatly reduces the amount of data that the Fast-TIM² needs to transmit, without degrading the accuracy of the system.

4.3 Quick thinker: the CIU²

The central hardware unit or CIU² (Figure 12) serves as the interface and power supply for up to six Fast-TIM² modules. The CIU² synchronises incoming data with the crank position of the compressor, validates it, and transfers it to the monitoring server for display and storage. The CIU² also monitors its own internal status to prevent false alarms.

Figure 12: CIU² installed in a cabinet in the safe area

Data received from the Fast-TIM² modules must first be synchronised to the crank angle using the pulses from the trigger sensor. Between these synchronisation pulses, the measured data is sent to the CIU² where it is immediately checked for plausibility.

This validation process controls a binary output known as “Trust”, which reassures the safety-critical PLC or DCS that the alarm signals are reliable. If the CIU² detects a system failure or implausibility in the data, it resets the Trust output to avoid nuisance alarms and spurious trips.

Another potential source of spurious trips is a change in operating conditions such as load, speed, pressure or gas composition—a frequent occurrence with many reciprocating compressors. To get around this, the operator chooses the correct set of alarm thresholds for the current operating conditions. This is done via a manual control that is marked with a number of predefined operating conditions; changing the position of this control varies a 4–20 mA signal that acts as a limit selector for the CIU². This arrangement ensures compliance with the requirements of a fully embedded system, while providing the flexibility that reciprocating compressors typically require.

Data from each revolution is compared with the current operating condition and monitored for possible threshold violations. The system is fast enough to trigger the alarm output from the CIU² immediately after the first revolution that violates a limit. To avoid false alarms, however, a “smart counter” usually that the violation is also present during the next 3–10 revolutions. If it is, the CIU² generates an Alarm or Safety Alarm signal; if not, the counter is reset and the violation ignored.

5 Standards and the future

5.1 Challenges of IEC 61508

The Ex standards for equipment operating in potentially hazardous atmospheres specify design rules and performance criteria, but say nothing about *how* the finished design is arrived at. A product that is to be Ex-certified requires only to be handed over to an independent authority for testing and certification.

IEC 61508 is different: a key point is that the complete life cycle of the product, from concept to decommissioning, has to be certified as complying with the standard. On this project, the main effects were felt in the development phase. IEC 61508 influenced the design, testing, verification and finally validation of the project, and required the use of a so-called V-model (Figure 13):

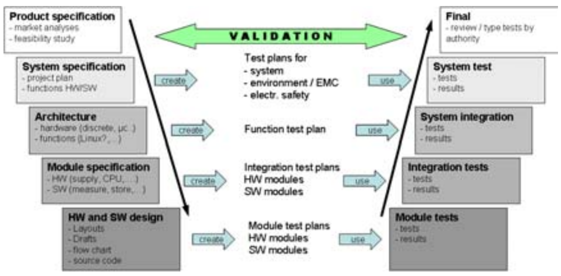

Figure 13: V-model of the development process as required by IEC 61508

Starting with a product specification and a general system requirement specification (SRS), work proceeds down the left-hand side of the V. First come specifications for individual modules, followed by detailed specifications for the hardware and software used. In parallel with this, test plans for all the specifications have to be developed.

At the bottom of the V, as soon the first prototype modules are available they are tested in accordance with the corresponding plans. Work then proceeds up the right-hand side of the V until the complete system has been tested in-house and finally by an independent authority.

Working to the IEC 61508 model required considerably more staff, time and money than would otherwise have been the case, and generated an extra 500 pages of documentation.

Achieving the high reliability specified by IEC 61508 also posed some technical challenges. The need for hardware self-testing introduced a requirement for two-out-of-three redundancy, while the validation process carried out by the CIU^2 during every revolution ensures the plausibility of the measured data. Safe communication between the F-TIM^2 modules and the CIU^2, and the combination of high-speed data transfer and power supply in a single cable, required clever thinking in areas such as EMC.

Finally, the designers took care to leave the platform open for later extensions. In the future, for instance, it could be used to monitor engines and other types of reciprocating machinery.

5.2 Future higher-level standardisation

Rotating and reciprocating machines need different strategies for protection and condition monitoring, and so too do different types of machine, such as compressors, pumps, and turbines. There is rapid progress in the development of such systems, and in the future users will be able to buy machines from OEMs with built-in protection and monitoring. However, this proliferation is likely to generate further complexity.

Refineries and chemical plants require many different types of machines to work together, so operators are now confronted with many different types of protection systems. The maintenance expert for each type of machine needs a detailed understanding of the signals provided by the monitoring system in order to give comprehensive advice, but it is not reasonable to expect the operator to understand the many different systems at such a deep level.

We therefore see the need to standardise the signals produced by these “specialised diagnostic units” and supplied to large control systems (DCSs). Especially for smaller machines, which are more and more commonly connected via fieldbuses, such standardisation, plus reliability ensured by IEC 61508 compliance, is becoming increasingly important.

Paper for the conference proceedings 6.EFRC Düsseldorf

Authors: Dipl.Ing. Horst Becker (RWE), Dipl.Ing.Werner Schulte (GOC)

Liquefaction Process with Reciprocating Compressors in a small LNG Peak Shaving Plant

- Start
- The liquefaction process of the RWE LNG Peak Shaving Plant Nievenheim
- Natural gas flow to be liquefied
- Regeneration gas flow
- Coolant gas flow
- Compressor C21601
- Problems and basic considerations to optimize the liquefaction process
- Solutions to be discussed
- The way to do in Nievenheim
- Conclusion

Start

In large LNG liquifaction plants a deep-cooling process with cascade circuits and different coolants is used to liquefy natural gas. These configurations optimize the energy consumption, but for that a lot of equipment (compressors and other instruments) is necessary.
This is a serious disadvantage for small plants.

For small scale LNG plants and their liquefaction processes the target is a small number of equipment and instruments, so that the investment is also small. This can be done with a mixed refrigerant loop (MRL) in the deep-cooling process. Especially the number of compressors can be kept down to just one if you compress the different mass flows simultaneously. However, these solutions have a lot of difficult problems.

The liquefaction process of the RWE LNG Peak Shaving Plant Nievenheim (Germany)

-Figure 1 (LNG Plant Nievenheim)-

To produce LNG in the LNG Plant Nievenheim a closed mixed refrigerant loop was installed. The coolant -a mixture of propane and methane- and the product are always in different circuits (pipes and other devices). The liquefaction ratio is only approx. 2,400m³/h gas or 4 m³/h LNG.

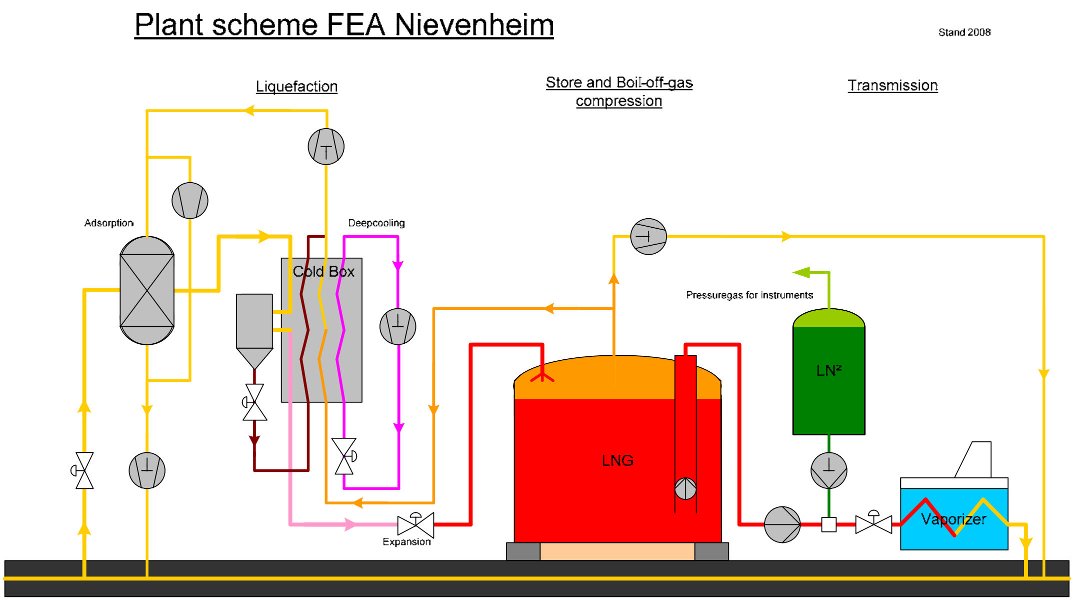

-Figure 2 (Plant Scheme)-

Natural gas flow to be liquefied

Gas to be liquefied is taken from the high pressure grid. The mass flow, approx. 10,000m³, is passed through filters first to remove dust and in a second step it is passed through adsorption filters to remove moisture, aromatics and carbon dioxide. These components are frozen or stiffened by the cryogenic liquefaction temperature and the process equipment is blocked, especially the cold box with its narrow passages.
After passing through the gas treatment plant there is only methane and a little bit heavy hydrocarbons in the mass flow, called now “Clean gas”. This mass flow enters the cold box at ambient temperature (approx. 20 – 35°C). In the centre of the cold box the temperature is nearly -90°C and via a bypass the Gas passes through a separator for heavy hydrocarbons because they are liquefied at this temperature. The Clean gas devoid of heavy hydrocarbons enters the cold box again. The pressure of the liquefied heavy hydrocarbons (approx. 40 bars) is reduced with a “Joul-Thomsen-valve” to ambient pressure. Now the liquid has a temperature of approx. -145°C. It enters the cold box in reverse flow to the Clean gas and supports the cooling process with the coolant MRL. The Clean gas exits the cold box with a temperature of approx -130°C, at a pressure of approx. 39 bar.
A Joule-Thomson-valve reduces it to ambient pressure. Thus the temperature drops to -164°C, the Clean gas enters the tank and approximate 30 % of the mass flow will be liquefied, called LNG. The other 70%, called Flash gas, is needed to regenerate the adsorbers.

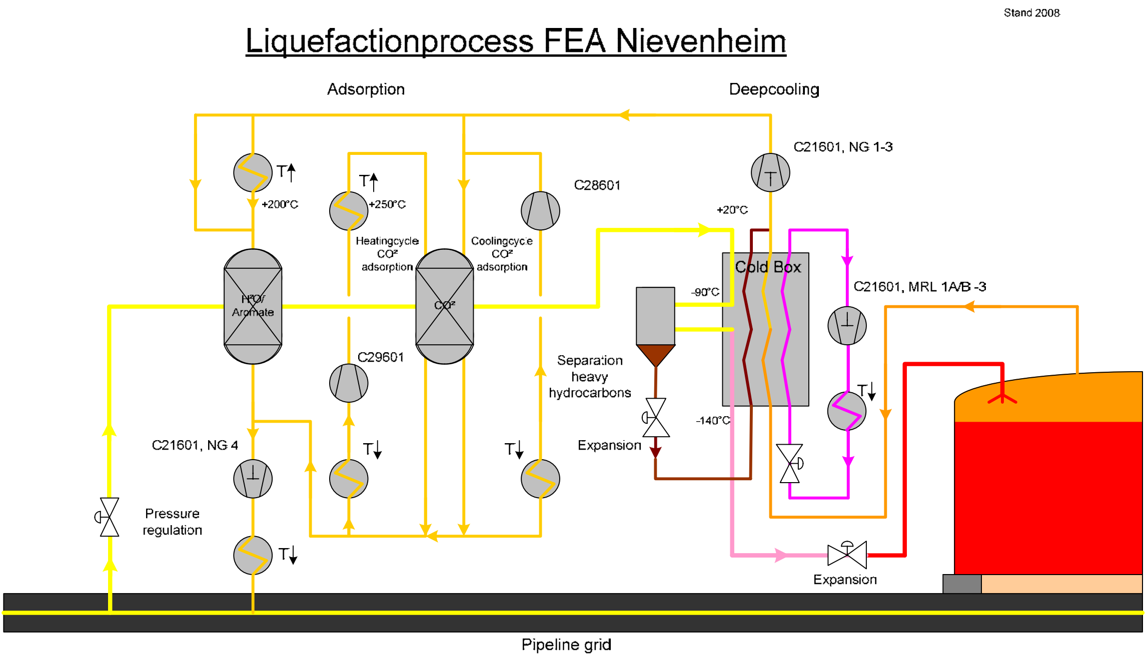

-Figure 3 (Liquefaction-scheme)-

Regeneration gas flow (REG)

The Flash gas is channelled through the cold box (entering temperature approx. -135°C) to support the cooling process like the heavy hydrocarbons do. During this process the temperature rises up to approx. +20°C. Both mass flows are unified, called now "Regeneration gas" and fed into the compressor C21601 (regeneration gas site).
The adsorbing process is a pressure swing process with hot regeneration. The unified mass flow is compressed from approx 1 barg to 22 bar in stages 1 to 3 while the temperature rises to approx +100°C. After that it is heated further to approx.+280°C in a heat exchanger by hot thermal oil from an oil plant. This hot regeneration gas flows through the adsorbers to regenerate them.
The gas including the adsorbents (moisture, aromatics and carbon dioxide) is compressed to a level slightly above the pressure of the grid, cooled down to ambient temperature in an air cooler and fed into the high-pressure grid. This small gas flow, approx. 7,600m³/h, blends with the main flow of pipeline gas, more than 50,000m³/h. Therefore the quality does not change.


-Figure 4 (picture Adsorber)-

Coolant gas flow

To cool down the natural gas flow a coolant circuit is necessary. In Nievenheim a Mixed Refrigerant Loop has been installed. The coolant is a mixture of methane and propane. It is usable throughout the relevant temperature range from approx. +100°C down to -150°C. The MRL first enters the compressor in stage 1, which is built with two parallel cylinders (MRL 1A and MRL 1B), and compressed from approx. 0 barg up to 2 bar. The temperature is raised up to +70°C. After cooling down to approx. +25°C via an air cooler the mass flow is compressed further in stage 2 up to 10 bar. The temperature rises up to +95°C and is cooled down via another air cooler.
The last compressing stage is the third. The MRL is compressed up to 39 bar, temperature rises up to approx. +100°C. The hot gas is cooled down again to approx. +20°C by an air cooler and in a second stage in a bypass of the cold box down to -20°C. The following Joule-Thomson-expansion to approx. 1 bar cools the MRL down to -150°C. The MRL is fed into the cold box to liquefy the clean gas in a counter flow. After passing the cold box the circuit starts again by entering the compressor, cylinder MRL 1A/B.

One of the main parts of the liqufactionprocess, compressor C21601

For all described mass flows it needs only one machine to compress.


-Figure 5 (picture C21601)-

Problems and basic considerations to optimize the liquefaction process

There is only one reciprocating compressor installed for the liquefaction process.
Both mass flows (MRL and REG) are simultaneously compressed. It is difficult to control each mass flow without reaction to the other.
The risk is to get a thermal shock in the cold box, thereby shortening lifetime of the unit.

The arrangement of the equipment with the main compressor, consisting of two process parts causes some difficulties:

- Because of the cast iron material and the oil lubrication the compressor must not get temperatures below zero degrees. The cold gases have to be warmed up, which lowers suction capacity thus making the process inflexible.

- The lubrication oil used for the cylinders of the refrigeration cycle has to be separated very accurately from the refrigerant because it would stiffen due to the conditions in the cold box heat exchanger of -140 °C. The oil has to be removed directly after the third compression stage at high temperatures (110 to 130 °C), because after condensing of the refrigerant the separator would remove the liquid phase of the refrigerant, too. These conditions mean very high requirements for the separators, which are only achieved by a two stage design.

- Driving all process cycles of the plant with one crankshaft means wasting energy at the start-up phase of the liquefaction, where only the purifying process is run for several days without using the refrigeration cycle.

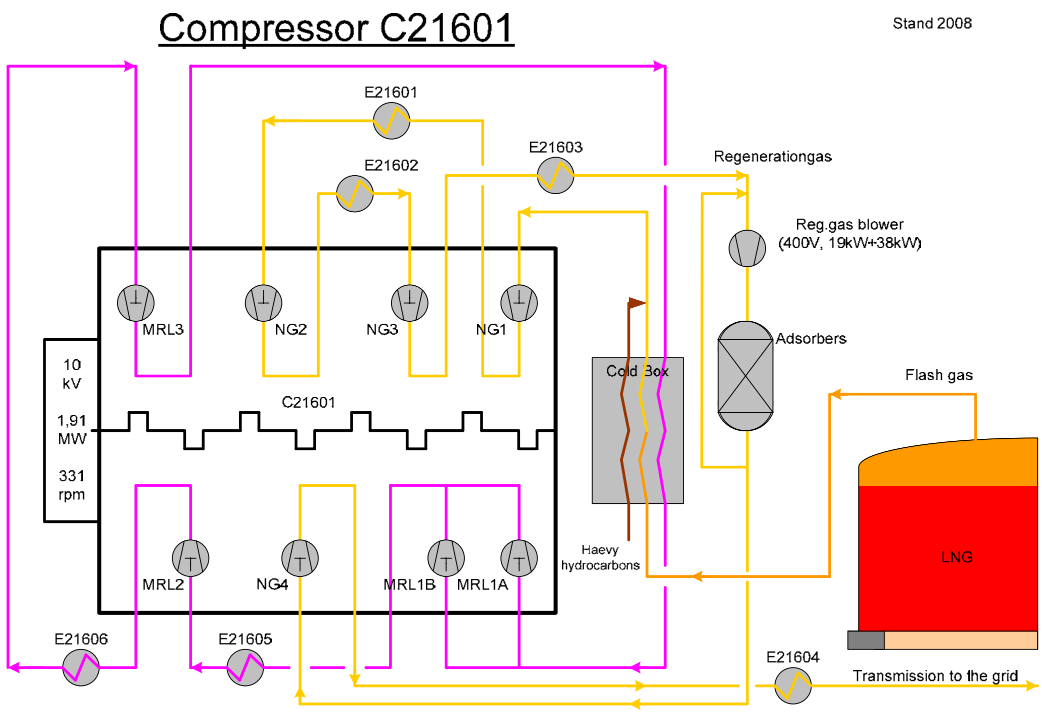

-Figure 5 (Scheme C21601-massflows)-

Solutions to be discussed

1. The ideal compressor would be suitable for cryogenic suction temperatures with the possible use for optimizing the thermodynamics of the liquefaction process. However, to take advantage of that, would lead to a completely new design of the process including the apparatuses. – that is impossible

2. The lubrication oil is not a big problem in the NG-part, because the compressed gas is cleaned from oil and need not be cooled down afterwards to temperatures lower than ambient. The waste gas of the process is sent out to the pipeline, where rests of vaporized lubricant will be diluted.

However, in the refrigerant cycle the lubrication oil causes trouble and sometimes breakdowns of the process. So the ideal compressor would be equipped with non-lubricated cylinders in order to avoid the above mentioned problems. Rebuilding the compressor to a dry working system with Teflon piston rings could be a possible solution.

3. Dividing up natural gas line and the refrigerant cycle on three separated machines would save first of all the waste energy of the unused refrigerant cycle during start-up of the process. In theory this would not be too much, because the liquefaction process should be started once a year and should be driven continuously. But in reality the whole process is sensitive to pollution of the cycles and has to be stopped sometimes to clean the system and readjust parameters, which cannot be switched during the ongoing process. So energy would be saved if the refrigerant cycle could stand still during those phases. At the natural gas line the fourth stage, which sends out the waste gas from the purifying process, there is need for overcapacity due the expansion during relieving of the adsorbers. During these phases the fourth stage has to suck off the normal flushing capacity together with the expansion volume. This occurs twice an hour for some minutes. During the main time the stage is driven with a kickback cycle in order to keep the suction pressure at a constant level. During optimizing the process it will be useful, to investigate possibilities of unloading one side of the double acting stage, or to install a separat compressor.

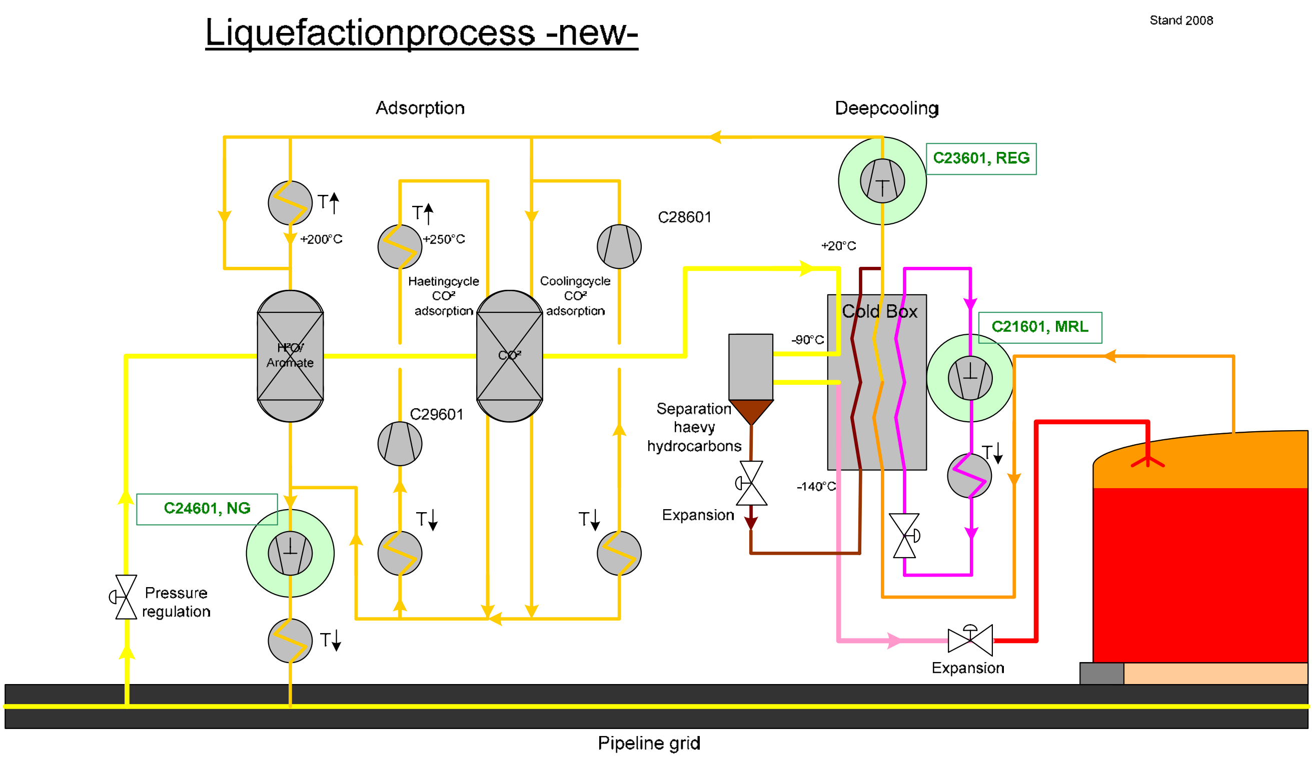

-Figure 6 (Scheme with three Compressors)-

The way to do in Nievenheim

The LNG Plant Nievenheim is a Peak shaving plant. The liquefaction ratio is very low against the transmission ratio. This will not change. So all apparatus will not be changed, only the compressor C21601!

As a first step we have to start with a visibility study to fix the technical solution. Secondly, the basic ingeneering with budget planing has to be done. The third step is the project detail planning…and so on.
Today the main problem for realising this optimization project is the delivery time of the compressors.

We may need at least three smaller compressors with 2 or 3 stages. The power consumption will be decreased to approximate 1.7 MW instead of 1.9 MW. Two of the compressors are of similar designe: 3 stages , pressure range from 0 bar – 25 bar and from 0 bar to 40 bar. The third compressor will be used to transmit the regeneration gas into the grid; pressure ratio is approx. 20 bar – 67 bar. Therefore a two stage compressore is a possible solution.

Conclusion

With regulated compressors on different parts of the process it is possible to control the liquefaction process easily. Lifetime of the coldbox and plant availability will be increased and energy consumption will be decreased.

Technical and economical aspects in the evaluation for upgrading a reciprocating compressor installation

Giving your reciprocating compressor a second life

by:

Rob Vieverich and Gerard van Bergen
Revamp Reciprocating Compressor Department
THOMASSEN COMPRESSION SYSTEMS BV
Rheden
The Netherlands

6th EFRC Conference
28-28 October 2008, Dusseldorf

Abstract:

The markets and operational demands facing refineries and other players in the petrochemical industry change constantly. Such changes may be triggered by a process, a product, a more pronounced focus on performance, or alterations to HSE controls. Some of these changes require compression equipment to be modified. In these instances, it makes sense to compare the replacement of a compressor to the modernisation or re-rating of existing equipment. This paper, which is based on a case study, explains the relevance and importance of such a comparison.

The paper offers a detailed explanation of how an existing compressor may be modified by creative thinking and extensive calculations, allowing it to accommodate different process requirement. The possibility of improving the operational availability and useful life of a compressor by upgrading and overhauling its components using the latest technology will also be discussed. Other topics include the economic life of the compressor, inherent risks, operational availability, the total cost of ownership and investment considerations. As there are no golden rules, it always makes sense to investigate the feasibility of re-using existing equipment.

1. Introduction

Reciprocating compressors typically have a long operating life. During this life, markets change while new technological developments emerge. The modification of machinery in response to new market requirements or process conditions is commonplace and allows operators to benefit from the latest technology. The usefulness of, and scope for, modifying a compressor during its operating life is best demonstrated using a case study.

2. The objective

The case study described in this document involves a client that initiated a study into the feasibility of increasing production levels by 50% (or 6.000 Kg/hr) using its existing propylene plant.

The study, which was conducted in 2002, focused on economic feasibility in particular. As a consequence, the client asked its engineering contractor to calculate the cost of three options (within an accuracy of +/- 15%). All three had to facilitate the client's wish to increase production from 4.000 Kg/hr to 6.000 Kg/hr. The client was primarily interested in establishing whether it would be able to realise the desired production increase within prevailing budget constraints.

The following (3) options were reviewed:

- Installation of an additional reciprocating compressor upstream of the existing (reciprocating) compressor.
- Replacement of the existing compressor by a unit having the required capacity.
- The refurbishment / revamping of the existing compressor.

Based on cost estimates prepared by the engineering contractor, it soon emerged that only the third option proved feasible. To verify that the equipment could be modified, the contractor got in touch the OEM (Thomassen).

3. Approach

The first step to take in these circumstances is to investigate how much of the production increase the existing compressor is able to accommodate. This is done by placing the new operating envelope over the existing design and by simulating a performance run. The analysis highlights any bottlenecks in the existing design.
Based on the first performance run, it was determined that the new operating envelope could not accommodate the revised process conditions. However, other essential design criteria, including discharge temperature and volumetric efficiency (swept volume), were within the norm.

In addition to limitations in the existing design, the new configuration can also be affected by user-defined parameters, including operating speed (rpm), piston speed, etc. In this case, the client was unable to increase piston speed given that it wanted to minimise operating costs as a result of component wear (during normal use). In practice, this prevented the piston stroke or the number of revolutions (rpm) from being changed.

Given the outcome of the performance run and the parameters defined by the client, it was concluded that the required production increase could only be achieved by increasing the diameter of the first as well as the second-stage cylinder. More detailed information on how we executed this can be found in section five.

Increasing the cylinder diameter also raised the forces exerted on the piston rod. Additional calculations showed that the mechanical design of the original compressor (as delivered) would be exceeded.

This problem could only be resolved by modifying the compressor, allowing it to withstand greater loads. In turn, this required the complete design to be reviewed in order to identify the compressor components that would need to be modified to accommodate these loads.

4. Compressor design

How the compressor was upgraded is best demonstrated by explaining the status of the various components.

The compressor - a model C-12 - was originally delivered in 1980. Thomassen has upgraded this model twice since then, as part of our ongoing drive to improve the quality and capacity of all compressors. This allows us to meet the latest standards (API 618 final revision) and operating conditions. We adopt a similar approach to CE regulations (including the related Machinery Directive), as well as ATEX and PED requirements.

The compressor in question was manufactured in 1980 based on the API 618 2nd edition. It was designed for a maximum continuous rod load of 120KN.

Both model upgrades were preceded by extensive studies, conducted by our R&D department. The subsequent modifications allowed the maximum mechanical load to be increased to 185KN.

4.1. Frame & Crosshead Guide Arrangement

4.1.1. Frame. The original frame was developed based on resistance strain measurements taken at high-strain locations. Strain levels were sufficiently low - by design - to facilitate higher loads without having to modify the frame. Improved procedures for assessing metal fatigue have since confirmed this. Using several research methodologies, it was established that the existing design would be able to endure a load of 240KN. In other words, the existing frame could be retained.

4.1.2. Crosshead Guide. The original design of the crosshead guide was studied in the same way as the design of the frame. The study, which reflected the latest load-bearing know-how, also concluded that the original design would not prove a limiting factor.

The existing bolting attachments (flanges) of the cross-head guide are the same as those presently used to achieve a rating of 185KN. No modifications were required here either.

4.2. Motion work

Unlike the frame and the crosshead guide arrangement, the crank shaft, connecting rod and crosshead head fixture had to be replaced, as these components were designed for a mechanical load of 120KN.

4.2.1 Crankshaft. During the up-rates, only minor changes were made to the crankshaft (involving modifications to radii, geometry and tolerances). Moreover, the original forging material was changed from Ck45N to 42CrMo4, allowing fatigue strength to be increased by approximately 20% (over and above the maximum design limit for a crankshaft made of Ck45N material).

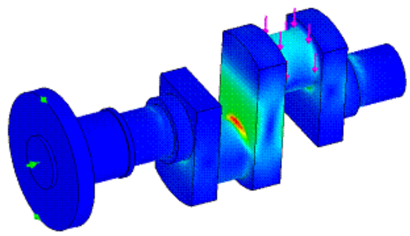

4.2.2. Connecting rod and crosshead. During the 1988 up-rate, the following changes were made to the connecting rod and crosshead: (i) the radii were adjusted, (ii) the small and big-end heads were enlarged, (iii) a so-called floating crosshead pin was fitted, and (iv) the tolerances were tightened.

4.2.3. Tri-metal layer bearings. A new set of tri-metal layer bearings - for both the big and the small end - were fitted during the most recent upgrade.

These tri-metal layer bearings, which have a layer thickness of 35-40um, were needed to accommodate the up-rating requirements.

Tri-metal plain bearings are made of a combination of steel, lead, bronze and nickel dam, which are added by means of electroplating.

The advantage of tri-metal layer bearings is that fatigue strength is increased. The bearing is therefore able to withstand the higher loads exerted as a result of the upgrade as required for [caused by] the motion work upgrades.

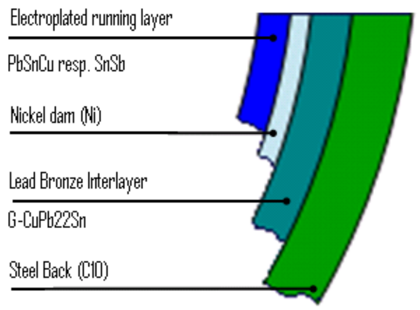

Filter:

The introduction of new tri-metal bearings for the frame, crank and crosshead pins also required the existing oil filter and 25 micron cartridge to be replaced by a filter with a 10 micron mesh.

4.3. Hydraulic Fit connection

The compressor was up-rated in accordance with API 618 4th edition, which recommends the use of hydraulic and/or thermal methods for tightening piston rod nuts with a diameter in excess of 75mm (see paragraph 2.8.1)

This hydraulic tightening method was implemented during the first up-rate and is used on all our reciprocating compressors regardless of piston rod diameter or compressor model.

We were able to increase the permissible rod load and improve reliability by using pre-loaded connections and by optimising the rod geometry.

The rod end is tensioned within the coupling flange using a hydraulic tensioning device, pressurized by a separate, external hose coupled to a pump.

The special nut is positively locked (as is the piston nut).

4.4. Dynamically loaded studs and or bolts

We recommended the use of studs with rolled threads and a minimum stud length (under torque) of 1.5 times the stud diameter. In other words, studs that comply with API 618 4th edition, paragraph 6.8.1.9.

As indicated, the compressor was manufactured in 1980, at which time the second edition of API 618 applied.

We also advised the client to use fasteners with rolled threads (quality Grade B7) rather than their machined predecessors (quality 5.6). We made this recommendation for two reasons:

Primary reason - reciprocating compressor generate large alternating or cyclic forces. The majority of fasteners are therefore subjected to substantial cyclic loads and stresses. The fatigue strength of rolled threads is 2.5 times higher than that of machined or ground threads. From a safety and reliability perspective, rolled threads are much preferred.

Secondary reason - in our capacity of OEM, we always recommended the replacement of old studs and nuts. After 20+ years of operation, maintenance and corrosion, the reliability of the 'main' fasteners is reduced. Replacing the nuts and bolts with rolled-thread equivalents not only raises reliability (to a level at least comparable to that of a new machine), it also creates an additional margin over and above the original specifications. We even recommend this change if the compressor's performance is satisfactory. Again, this should be seen as a preventive measure.

Several studs did not meet the specified length (for instance between crosshead guide and the distance piece, and the distance piece and the cylinder(s)). As a consequence longer studs - paired with extension bushes to provide higher safety margins against joint relaxation - were also installed.

5. New modifications

5.1. Cylinder(s)

To achieve the required 50% capacity increase, two new cylinder assemblies had to be installed. The customer additionally asked for cylinder materials capable of withstanding external temperatures of -46 ^{o}C.
This required the nickel content of the metal to be raised, increasing the material's impact values.

5.2. Process piping

The flow increase also impacted the dimensions of upstream, inter-stage and down stream process pipes. To give an example, the diameter of the 1st stage suction line had to be increased from 10" to 16". This increase facilitates a flow velocity that permits the use of pulsation dampening orifices in the system without incurring excessive pressure drops when installed. Maintaining the present line diameters (as requested by the client) made the use of existing damping orifices more or less impossible as orifice damping itself will be less effective, generating an excessive pressure drop. Thomassen was asked to compensate the absence of an orifice by using oversized dampeners. This approach has several drawbacks and does not guarantee that API 618 standards and specifications are met.

An examination of the existing system revealed that without a damping orifice in the line connection of the 1st stage dampener, pulsation levels could reach nearly five times the recommended maximum at 50% load step. This can easily be reduced to within the recommended value by fitting a damping orifice (with a suitable larger" line size). If the same result is to be achieved using an oversized volume bottle, its volume would have to be nearly five times the normal amount, resulting in considerable vibration while requiring much more space. Not an efficient solution as it does not alleviate the problem at source.

To resolve the situation, the size of a relatively small section of the 1st stage suction line up to the first main T piece was increased to 16 inch (previously 10 inch). At the same time, the size of the volume bottles was increased (in accordance with API 618 4th Edition design approach III) while a pulsation and mechanical response study was initiated.

5.3. Heat Exchanger

A new inter-stage heat exchanger was installed to accommodate the larger flow requirement. All components exposed to internal pressure were calculated and constructed to comply with the prevailing Pressure Vessel Code for the district or industry in which this pressure vessel (Heat Exchanger) is operational.

Although the majority of heat exchangers delivered within European Union are nowadays constructed in accordance with the PED, the heat exchanger in question had to be designed in accordance with EN 13445, which had only been introduced shortly before.

From a physical perspective, the heat exchanger needed to be constructed so that it could be positioned and fitted within the same space and onto the existing foundation columns (supports). At the same time, account had to be taken of the new e-motor extension.

The above was achieved using an eccentric support design, fitted underneath the heat exchanger.

5.4. Inter stage Separator

The existing inter-stage cooler also had to be replaced (the new cooler mirrored the design philosophy used for the heat exchanger).

5.5. E-motor arrangement

The need to increase compressor capacity also necessitated the installation of a new motor with a higher power rating.

One of the key challenges was to re-fit the larger e-motor onto the existing footprint without making any adjustments to the foundation.

The solution took the form of a pallet-type base plate, also known as a 'skid', which was placed underneath the e-motor. The use of a skid:

- allowed the new e-motor shaft to be elevated to the original position.
- provided an accurate interface between the existing foundation bolts and the new e-motor foot print. The skid was also equipped with sled-type runners for easy and rapid installation.

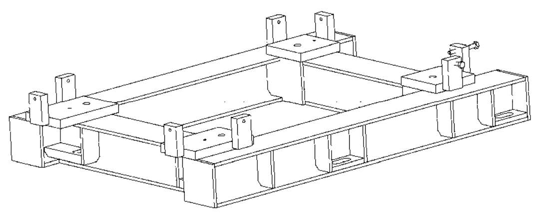

The main junction box for the high voltage cable was placed in the same location, allowing the existing power cable to be easily re-fitted.

6. Installation

The compressor was fully dismantled and re-built by Service engineers working in two shifts. The task was completed in 12 days, with the client assuming responsibility for the modifications to the foundation. The client also made the necessary changes to the process pipes.

7. Summary and conclusions

Thomassen's engineers were only able to modify the compressor to meet new production flow requirements by replacing the existing cylinders, allowing the total load to be increased from 120 KN to 185KN.
The frame (except for internals), the crosshead guides and the oil system were all re-used. The following new components were fitted: a crankshaft, bearings, connecting rods, crossheads, piston rods, complete cylinders including pistons, lubricating equipment, pipes for coolants and lubricants, suction and discharge vessels, an inter-stage cooler, a moisture separator, a skid-mounted e-motor, and a flexible coupling.
The decision to modify the existing compressor – as opposed to replacing the existing compressor or acquiring an additional compressor – offered the operator several important advantages, including:

- Quick turnaround through maximum component re-use.
- Minimal modifications to the existing foundation (the original bolt hole pattern was used).
- The use of an 'easy fit' base frame allowed the main motor to be set up quickly.
- Changes to the process gas system were minimal (and calculated in advance using a pulsation study).
- No new power cables were installed. The existing MCC was re-used.
- The entire unit meets EU Directives, allowing us - in our capacity of OEM - to issue us a letter of conformity.

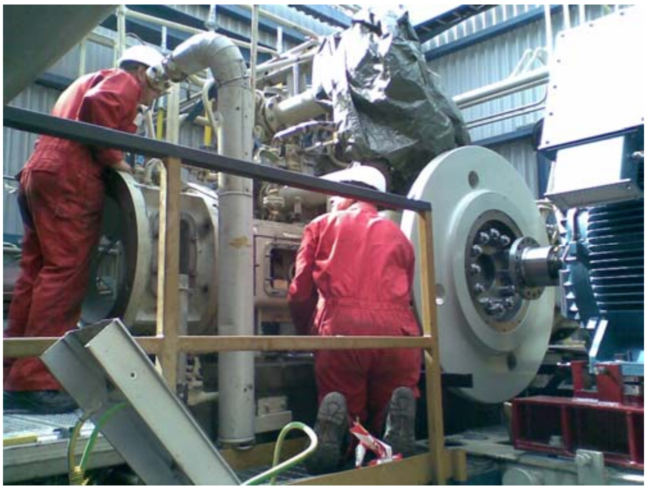

The case study outlined in this document emphasises the importance of investigating all options before selecting the most suitable or cost effective solution. The modification of the existing compressor has given it a second life (subject to the same guarantees as the first life). In this case, it was faster, easier and considerably less expensive to modify the compressor than it was to acquire a new unit!

The re-launch of the BORSIG BX series: examples drawn from the options and possibilities in the technical implementation of, and experiences during, the re-activation of long-standing design documents

by:

Dipl.-Ing. Steffen Gast, Dipl.-Ing. Knut Sponner
and Dipl.-Ing. Jürgen Ilgner
Sales/ Service Department
BORSIG ZM Compression GmbH
Meerane
Germany
info@zm.borsig.de

e.g. 6th Conference of the EFRC
October 28th / 29th, 2008, Dusseldorf

1.0 Introduction

Most of the machine and plant engineering and construction companies have been changing their CAD systems to modern 3D systems in the last few years.

Some manufacturers, however, still today have to decide if they want to take existing, well-established compressor series into modern 3D systems.

In this report BORSIG ZM will present its experiences with the transfer of old design documents to enable current production.

2.0 Reasons for re-launch of a series drawing on the example of the BX series

Not every compressor manufacturer is put in a position to take over an existing, well-established and famous compressor series and put it on the market again.

The production of BORSIG reciprocating compressors was stopped in the mid 1990's due to a political decision and had nothing to do with the competitiveness of the product.

Thereafter, there were always customer inquiries regarding these machines.

After the BORSIG Group decided to fully resume the process gas compressor business by taking the former Zwickauer Maschinenfabrik (ZM) into the BORSIG Group, a chance emerged to re-introduce to the market a well-established BORSIG compressor frame series.

The current ZM compressor frame series was, therefore, significantly extended up to a stroke of 500 mm.

The access to the complete design documents such as drawings, parts lists, design guidelines and basic calculations was enabled since all these documents were well archived, were not sold or destroyed.

In addition, some former BORSIG employees are still available who were responsible for the development and design of this series.

The competitiveness of the new BORSIG ZM is significantly strengthened by the re-launch of the BX series.

3.0 Technical options and possibilities for integrating long-standing design documents into an existing production system

The following paragraph is a reflection of the possibilities for the integration of long-standing design documents respectively into existing design and production systems.

3.1 Utilization of archive documents for purchase orders and manufacturing processes

For the components to be manufactured, the existing parts lists have to be transferred into the current PPS system and adapted to current conditions (titles of standards and tests etc.).
The drawings and documents mentioned in the parts lists have to be compiled from the archives, checked and approved. Picture 1 shows an example for archived documents.

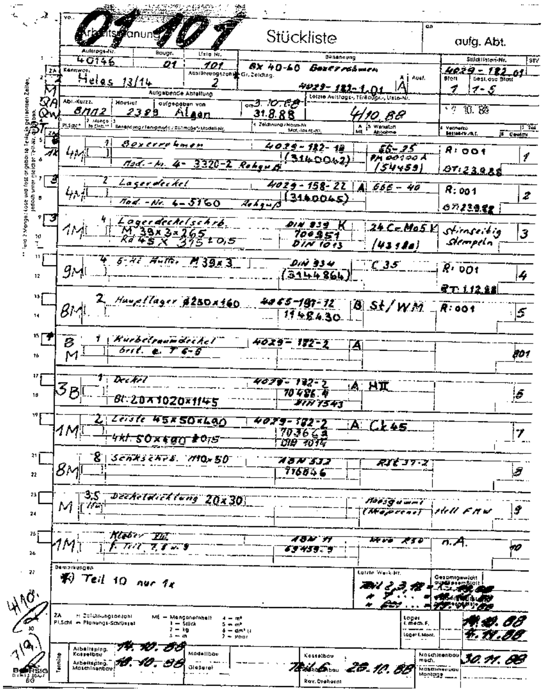

Picture 1: Example: archived parts lists from 1988

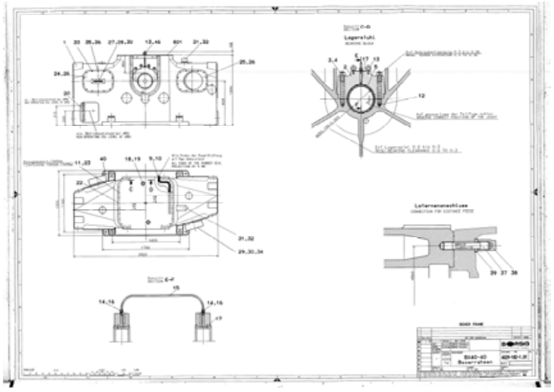

Picture 2: Example: archived assembly drawing for horizontal (boxer-type) compressor frame

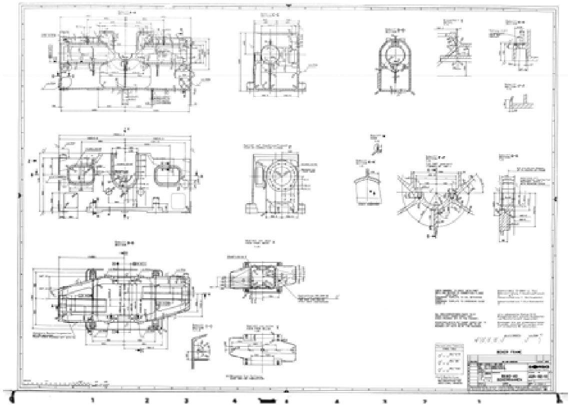

Picture 3: Example: archived manufacturing drawing for horizontal (boxer-type) compressor frame

Advantages:
This option is the most cost-effective and is the fastest to reintegrate former components or assembly units into production, since it requires the least effort.
The existing component's drawings are in the main suitable for both placing orders and manufacturing the frame components.
Archived original drawings are of sufficiently good quality and in most cases can be used for production processes without larger corrections and extra work.

Disadvantages:
The documentation of the complete assembly unit or complete compressor unit is complicated because no CAD model is available. In these cases a non-parametrical dummy model has to be generated for the documentation.

In addition, for the component's manufacturing and foundry technology, CAD model data is missing which has to be compensated for by expenditure of time and money.

FEM analyses, modifications and further developments are not really feasible.

3.2 Transmission of designs into an extant CAD system

A professional, frame size dependent compilation of the archive documentation has to be made.
Following this comes the remodelling of the components or assembly units and the integration of the complete unit in a current 3D CAD system.
Experienced employees are very helpful in checking the modelling by comparing the old with the newly generated drawings. The ideal case is to attain the services of former design engineers of the respective compressor series for this task.

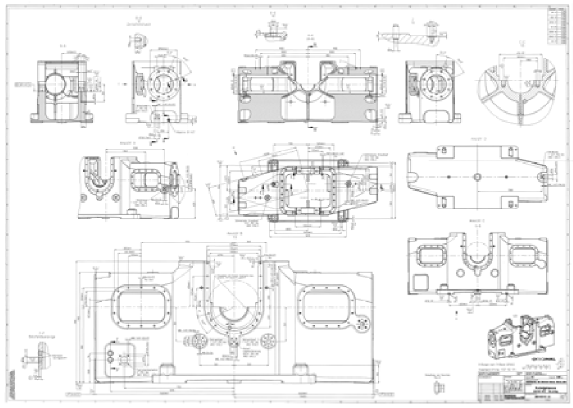

Picture 4: Example of the derivation of a manufacturing drawing from a 3D CAD model

The newly generated and approved 3D models (casting and finished parts) are then provided to the model-makers and casting manufacturers.

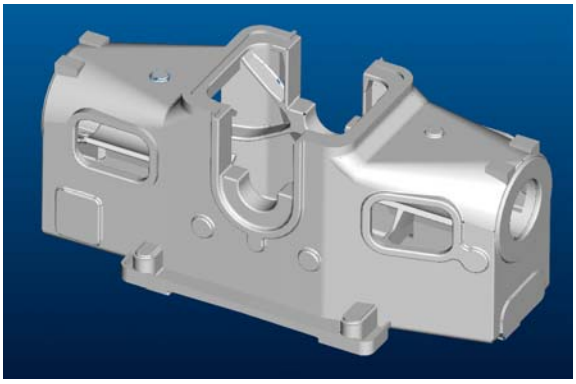

Picture 5: CAD model of raw casting

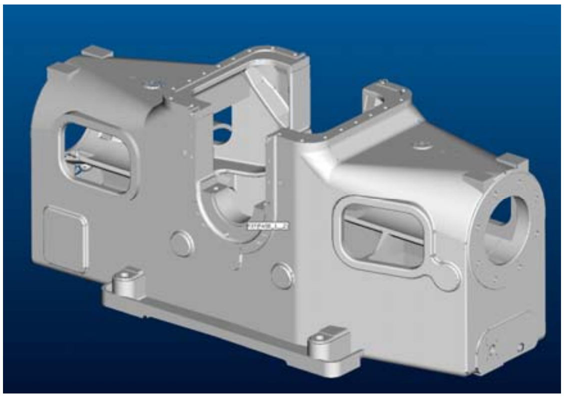

Picture 6: CAD model of finished part

Advantages:
Since the old component's drawings "only" have to be transferred into the current 3D CAD system, no reciprocating compressor experts are required for the modelling work. This work can be carried out by qualified staff under skilled supervision.

The documentation of the complete assembly unit and complete compressor unit is facilitated since the "real" image of the assembly unit is available as a parameterized CAD model.

In addition, the CAD model data can be handed over to the component manufacturing and foundry saving time and effort and, in addition, involving significant quality assurance.

The existence of the 3D data enables the performance of FEM analyses, modifications and further developments.

Disadvantages:
This option requires a great deal of support, which results in exposure to higher costs and time.
Engineering work is not yet implemented via this option, i.e. existing mistakes are neither detected nor eliminated.
With this option further development of the components and assembly units are not yet up for discussion.

3.3 Re-engineering of a series

The professional, frame size dependent compilation and evaluation of the archive documentation is made just as described in paragraph 3.2.

The modelling of the components or assembly units on the basis of selected models is carried out, as far as is possible, by in-house design engineers, including former experts.

Advantages:
Please see paragraph 3.2

At the same time, during the modelling process the components are optimized and adapted to the current design and manufacturing facilities.

The use of modern analysis procedures (FEM) and the comparison of the results with, respectively, former design guidelines (KR) or calculation bases, enable design engineers to comprehend the design of the component and, if necessary, to optimize it.

The components and assembly units generated by this process may be further developed and improved and, therefore, established on the market.

Disadvantages:
Compared with the option described in paragraph 3.2, there is even higher exposure to time and costs. Expert manpower is involved to a great extent and is scarcely available to order processing work.

4.0 Selection of option

4.1 Rating of in-house criteria

Criteria		A	B	C	D	E	F	G	Rate
A	Provision of documentation for PP system (parts lists and drawings)		2	2	2	2	1	1	**10**
B	Provision of CAD data for CNC machining and foundry technolgoy	0		1	1	2	0	0	**4**
C	Provision of models and drawings for customer's documentation	0	1		2	2	1	2	**8**
D	Possibility for component alteration	0	1	0		1	0	0	**2**
E	Possibility for analysis	0	0	0	1		0	0	**1**
F	Staff requirement	1	2	1	2	2		1	**9**
G	Cost requirement	1	2	0	2	2	1		**8**

0- less important
1- equally important
2- more important

Table 1: Rating of criteria

4.2 Comparison of options and aid to decision-making

Options		Option 3.1		Option 3.2		Option 3.3	
Criteria	Quf[1]	EAt[2]	Quf*EAt	Quf	Quf*EAt	Quf	Quf*EAt
A) Provision of documentation for PP system (parts lists and drawings)	10	4	40	7	70	10	100
B) Provision of CAD data for CNC machining and froundry technolgoy	4	1	4	6	24	10	40
C) Provision of models and drawings for customer's documentation	8	1	8	10	80	8	64
D) Possibility for component alteration	2	1	2	7	14	10	20
E) Possibility for analysis	1	1	1	7	7	10	10
F) Manpower	9	10	90	3	27	1	9
G) Costs	8	10	80	3	24	1	8
Total:		225		246		**251**	
Ranking:		3		2		**1**	

Table 2: Comparison of options and aid to decision-making

[1] Quf=quantifier
[2] EAt= earmarked assets

4.3 Reasons for decision-making

The priorities determined by the company led to a clear result in favour of option 3.3 "re-engineering".

For this reason we decided to choose the option which was supposed to require the highest effort. However, this future-orientated decision justified the increased expenses and need for engineering work.

In addition to the excellent development options in the new compressor manufacturing sector, the service department will profit from the engineering and development achievements of the re-activated series.

As a result, the further operation of a continuingly active series with possibilities for modification and updates are ensured in the long term for compressor and plant operators.

5.0 Experiences during the implementation process using the re-activation and re-launch of the BX frame series as an example

After deciding which option was to be used for the activation of the BX series, the following works were carried out.

5.1 Definition of project objectives and determination of priorities

There was a determination to provide all material and technical prerequisites necessary to get production of the BX compressor frame series started rapidly.

A project team was established including active and former BORSIG reciprocating compressor experts.

It was recognised that it was necessary to increase manufacturing and assembly capacities and in the short term a large building extension has been completed.

The re-engineering of the series should have a strong future-orientation.
Together with the sales department, priorities have been determined for the selection and processing of orders for the frame sizes.

5.2 Sighting of the archives and provision of the example documents

The BORSIG archives contain approx. 200,000 drawings and approx. 40,000 pages of parts lists with respect only to the reciprocating compressor division of the former Berlin series. Some examples are shown above in pictures 1 to 3. In addition, there are approx. 1,000 archived orders for new compressors with approx. 3 million pages of documentation.
Looking at these figures it soon becomes clear that only those employees who are familiar with the process flows and document archives can work effectively within them. Such employees are available to BORSIG ZM Compression. The necessary example documents can, therefore, be provided at short notice for the relevant frame sizes.

5.3 Recalculation of the components on the basis of the classical design guidelines and calculation basics

The recalculation of the compressor frame components was carried out on the basis of the calculation basics (KR) of former BORSIG design engineers.

The following example (pictures 7 to 10) shows the calculation results of the stress analysis of the "boxer frame" component by means of two selected cross sections.

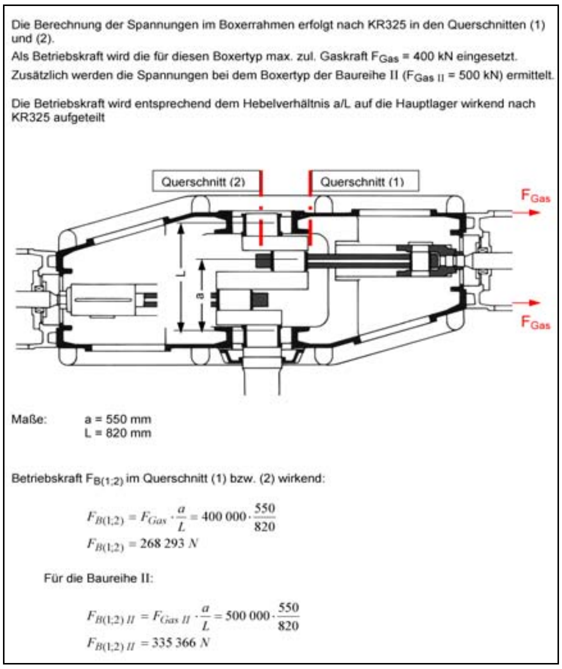

Picture 7

Querschnitt (1)

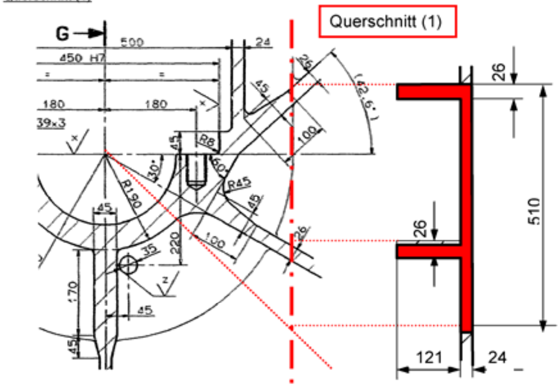

Fläche von Querschnitt (1)

$$A_{(1)} = 510 \cdot 24 + 2 \cdot 26 \cdot 121 = 18532\ mm^2$$

Spannung im Querschnitt (1)

bei max. zul. Gaskraft $F_{Gas} = 400$ kN

und Betriebskraft $F_{B(1;2)} = 268\,293$ N

$$\sigma_{(1)} = \frac{F_{B(1;2)}}{A_{(1)}} = \frac{268\,293}{18532} = 14{,}5\ N/mm^2$$

für Baureihe II

bei max. zul. Gaskraft $F_{Gas\ II} = 500$ kN

und Betriebskraft $F_{B(1;2)\ II} = 335\,366$ N

$$\sigma_{(1)\ II} = \frac{F_{Gas\ II}}{A_{(1)}} = \frac{335\,366}{18532} = 18{,}1\ N/mm^2$$

Picture 8

Querschnitt (2)

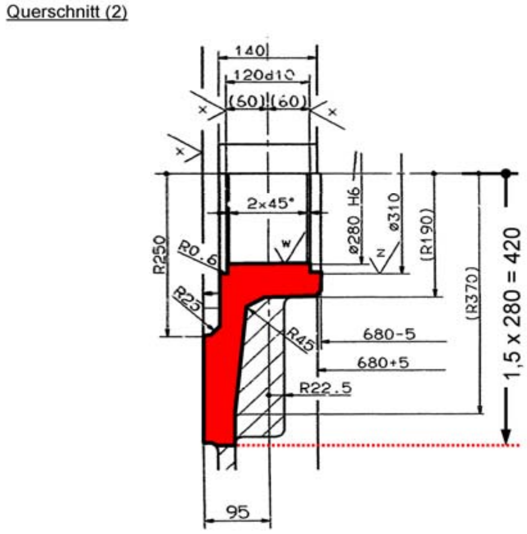

Fläche von Querschnitt (2)

$$A_{(2)} = 17570\ mm^2$$

Spannung im Querschnitt (2)

bei max. zul. Gaskraft $F_{Gas} = 400$ kN

und Betriebskraft $F_{B(1;2)} = 268\,293$ N

$$\sigma_{(2)} = \frac{F_{B(1;2)}}{A_{(2)}} = \frac{268\,293}{17570} = 15{,}3\ N/mm^2$$

für Baureihe II

bei max. zul. Gaskraft $F_{Gas\ II} = 500$ kN

und Betriebskraft $F_{B(1;2)\ II} = 335\,366$ N

$$\sigma_{(2)\ II} = \frac{F_{Gas\ II}}{A_{(1)}} = \frac{335\,366}{17570} = 19{,}1\ N/mm^2$$

Picture 9

Zusammenfassung:

		Querschnitt (1)	Querschnitt (2)
Zugspannung für F_{Gas} 400 kN	N/mm²	14,5	15,3
Zugspannung für F_{Gas} 500 kN	N/mm²	18,1	19,1
Zul. Spannung nach KR	N/mm²	26,1 *)	

*) aus „zu erwartende Zugfestigkeit für GG-25" und Wanddicken bis 30 mm nach DIN 1691 (=235 N/mm²) und einer Sicherheit von S = 9.

Picture 10

The results show that the stress values at the selected cross sections are below the admissible values according to the KR.

The admissible minimum safety factor against fatigue failure has been determined with S=9 in BORSIG's design guidelines.

The theoretical margins against fatigue failure amount to S=15 with the currently applied load limits. From these values a potential for higher loads might be expected which are analysed more detailed way below by means of modern analysis methods.

5.4 Evaluation of the modelled components by means of the FEM analysis

An FEM analysis was performed on the CAD model of the boxer frame which again served as example. For the purpose of the analysis the component was stressed 25 % higher than is currently specified for this frame size to ensure better recognition of the load impacts.

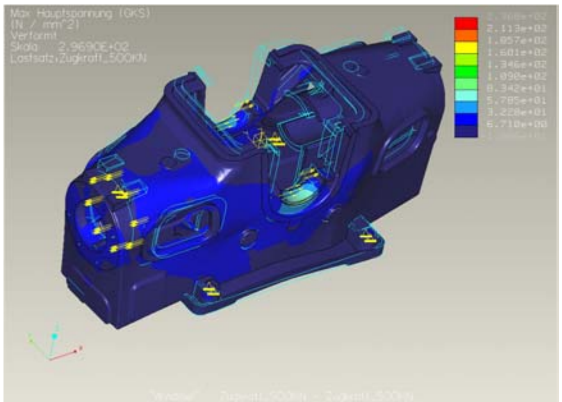

Picture 11: Distribution of stress and displacement

Picture 11 shows the graph of the resulting displacement in a highly excessive manner to improve presentation of the effects of the load impact.
The maximum principal stresses for the tensile loading are within the estimated range. Stress peaks can be recognized.

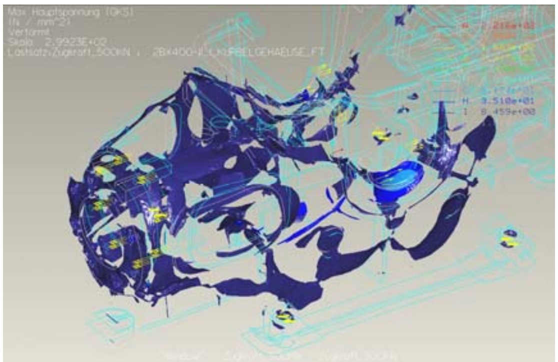

Picture 12: Sections of similar stress

Picture 12 shows the stress distribution in the structure. It can be seen that there is a very good and relatively homogeneous distribution of the flux in the component.
This may be taken as an indication of the successful design of the component.

5.5 Comparison of results of both evaluation methods

The comparison of the results of the classical component calculation and the structural FEM analysis had the following findings:

- The classical calculation method (pictures 7 to 10) may only evaluate previously selected cross sections and does not describe the complete structure of the component. For this reason, in former times relatively high admissible safeties were worked out which proved very worthwhile in practice.

- The comparison of the selected cross sections shows nearly similar values (approx. 18 N/mm²), i.e. the limiting conditions of the FEM analysis have been chosen properly and the analysis of the complete structure comes close to reality.

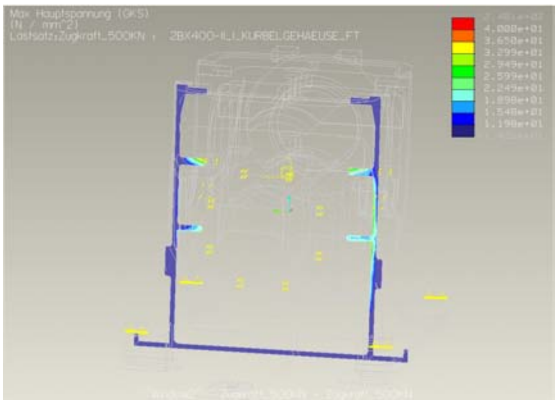

Picture 13: FEM analysis of cross section 1

- In any case the results of the FEM analyses have to be evaluated usefully. There is a high risk of deviating considerably from the reality due to the determination of possible unfavourable model simplifications and/or incorrect limiting conditions.

- However, in contrast with the classical method, the FEM analysis may describe the complete structure of the component and also goes into interactions, such as deformations.

- Stress peaks could be located which were unrecognized before.

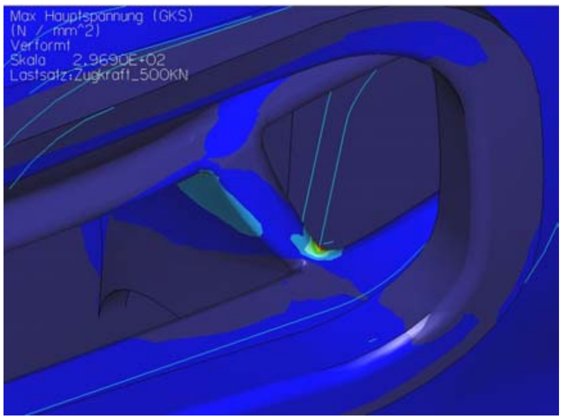

Picture 14: Recognition of stress peaks

- Evaluation the directions and magnitudes of the component deformation caused by stress was possible.

- It was clear that the assessed component "boxer frame" had been designed by very experienced design engineers. It was easy to comprehend the excellent consideration of the flux as well as the compliance with the requirements concerning casting.

- The component was not designed within value limits and may therefore be considered as a solid structure which proved to be true in practice.

5.6 Evaluation of model modifications and alternatives for the optimization of the BX series

Even where the design of the component was already very good, as experienced in paragraph 5.5, we were looking for potential improvements in the component.
One reason for the development of alternatives for modification was to further optimize the complex

casting component and hence increase the reliability of our compressor frames.
The variants were modelled, analysed and evaluated separately to find out which modifications of the component's design would achieve the best improvement of the component's structure.

At the same time we dealt with the history and the stages of development of the "boxer frames".

We were surprised to see that in the course of the decades of development some design modifications were performed which, from today's point of view, are considered to be disadvantageous for the component's structure.

Two variants have thus been analysed reflecting a former design stage. It was proved that in these cases the design of the previous stages of the development was more favourable because of lower stress peaks occurred.

At this point we shall not expand in particular on the detailed design modifications. However, it is worth noting that the structural FEM analysis is an excellent instrument for design evaluation.

In the first instance we evaluated the variants with respect to their benefits for the component's structure and recognized clear potential for improvement.

At the moment the options for implementation are being evaluated, i.e. the pattern-making, foundry technology and manufacturing technology have to be analysed with regard to the variants of the model modifications. As a result of these tests a combination of several variants will be analysed and evaluated.

After this evaluation the implementation of the model modification will be decided and transferred to the new compressor design.

6.0 Conclusion

The re-launch and modernisation of an approved compressor frame series put the manufacturer in the position of having to make fundamental decisions which will have an influence, to a greater or lesser degree, on the future sales prospects and possibilities for development of the series to be activated.

Thus BORSIG ZM Compression decided to choose the option which it supposed was the most expensive. This strictly future-orientated decision implies increased expenses and engineering effort.

It turned out that it was very beneficial to include former design engineers - some of them already retired – during the transfer of the components. These employees are highly motivated since their former designs are the basis for a new manufacturing series and, therefore, their lifework is properly appreciated. In addition, the delicate transfer of complex castings proved considerably easier with the help of former experts since not all outlines were shown clearly on the old 2D manufacturing drawings and rough casting drawings are not available. In the past pattern-making and casting technology was left in the model-maker's and casting supplier's care.

In this way engineering and manufacturing processes are interpenetrated by the new series and aligned with it. The existence of simple possibilities for analysis and development contributes to the long-term marketability of the series.

Based on the know-how of former BORSIG design engineers available to BZM and by means of the most modern design and engineering methods we are today not only able to resume manufacture of the solid and reliable BX frames but also to integrate improvements.
This development project will be continued since the potential of this compressor frame series is by no means exhausted yet.

Apart from the advantages for the manufacture of new compressors and the design department, the service department also profits from the engineering and design achievements and the possibilities for manufacture of the activated series.

We can, therefore, assure our customers, who have had BORSIG reciprocating compressors in operation for many years or even decades, of the long-term continuation of the series.
In addition, once again there are excellent possibilities for conversion and modernisation of those BORSIG compressors which are still in operation.

The manpower requirements and financial resources for the reintroduction of a former compressor frame series can already be considered to be both justified and worthwhile since the series was put on the market very quickly and successfully.

Advancement in Pulsation Control for Reciprocating Compressors

Authors:

Broerman, Eugene "Buddy"; McKee, Robert, Ph.D.; Scrivner, Christine

Southwest Research Institute®

Bourn, Gary

El Paso Western Pipelines

Presented by:

Scrivner, Christine

Fluids Engineering Department

Southwest Research Institute®

San Antonio, Texas, USA

christine.scrivner@swri.org

6th Conference of the EFRC

October 28th / 29th, 2008, Dusseldorf

Abstract:

Current acoustic manifold designs for reciprocating compressors require a balance between pulsation control, compressor performance, and mechanical vibration. The high amplitude pulsations associated with uncontrolled nozzle resonance can cause unacceptable vibration and poor compressor performance. Pressure drop elements, which are currently used to control cylinder nozzle pulsation amplitudes in combination with surge volumes, can significantly affect compressor capacity and horsepower requirements. For modern high-speed compressors units, nozzle resonance control with the use of an orifice is common but can significantly reduce unit performance and decrease capacity. As part of an ongoing, joint Gas Machinery Research Council (GMRC) and Southwest Research Institute (SwRI) research project, a pulsation control device designed to mitigate cylinder nozzle resonant pulsations without the losses typically associated with the installation of cylinder nozzle orifices was developed and field tested. This newly developed pulsation control device was named the Virtual Orifice, since this technology was essentially developed to replace the compressor nozzle orifice. The Virtual Orifice effectively reduces the nozzle pulsations without a pressure drop and a corresponding power and capacity loss. This paper presents results from the research and field trial of the virtual orifice with respect to pulsation control performance, efficiency improvements, and vibration reduction.

1 Introduction

Controlling pulsations associated with the cylinder nozzle response is a continuing challenge generally tackled through frequency avoidance or by pressure drop damping. Wide speed ranges and/or large variations in operating conditions (temperatures and pressures) often make the preferred design approach, resonance avoidance, impossible. Because it has become necessary to manage resonance rather than avoid it, orifice plates are commonly installed at or near the cylinder nozzle flange connection of most high-speed and many low-speed reciprocating compressors. A continuing need for increased operational flexibility with lower losses is driving today's pulsation control research.

Cylinder nozzle resonance is a simplified term for the quarter wave response associated with the acoustic length from the cylinder valves through the cylinder internal gas passages and compressor cylinder nozzle to the compressor cylinder bottle. When the frequency of the pulsations that are inherently generated by reciprocating compressors coincides with or is near the acoustic natural frequency of the cylinder nozzle response, the pulsations are significantly amplified.

In 2005, the Department of Energy (DOE), Gas Machinery Research Council (GMRC), and Southwest Research Institute (SwRI) formed a joint research program coined the Advanced Reciprocating Compressor Technology (ARCT) research program. This research program was continued by GMRC and SwRI in 2006. Pulsation control was one of many areas researched through the ARCT program. A primary goal of the ARCT pulsation control research program was to develop a low pressure drop method of controlling the cylinder nozzle resonance, thus eliminating the need for orifices in the nozzle region. The application of a Side Branch Absorber (SBA), or Helmholtz resonator, at or near the cylinder nozzle was conceptualized and later tested for the first time in February 2006. Because the novel application of the SBA near the cylinder nozzle was meant to replace the typical orifice plate, the device was named the Virtual Orifice (VO).

2 Development

Side Branch Absorber (SBA) technology has been used for many years to alter acoustic responses in compressor piping systems. SBAs have been industry proven to alter lateral resonances and acoustic filter responses, significantly reducing pulsations and vibrations. An example of the results that can be achieved through proper installation of an SBA are depicted in Figure 1. For the fixed speed (400 RPM) compressor piping system evaluated, the acoustic filter frequency was not adequately placed to limit pulsations in the adjacent centrifugal piping to acceptable levels. Additional pulsation control in the form of an SBA attached to the piping lateral resulted in significant reduction of the pulsations at one times the compressor running speed (1x). As an SBA applied in the compressor cylinder nozzle region, the VO has a similar impact on pulsations at the cylinder nozzle resonance frequency. For optimum reduction, the VO should be located as close as possible to the compressor cylinder valves (i.e., at the pulsation maximum of the cylinder nozzle quarter wave response).

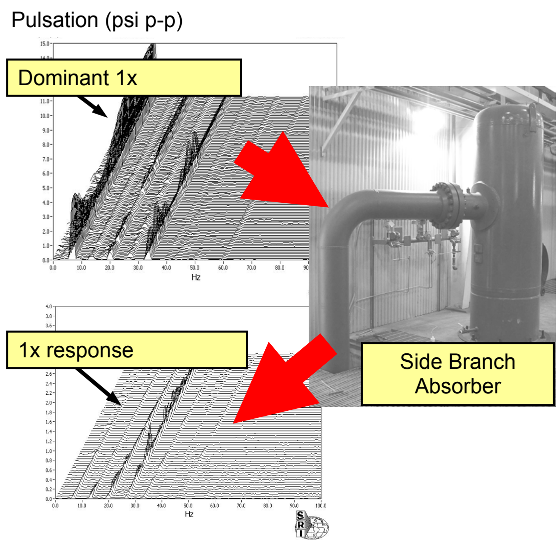

Figure 1: Effectiveness of a Side Branch Absorber

As with the SBA, the VO is comprised of a choke tube (relatively small piping) that connects a volume to the main piping. Initial sizing of the VO choke tube and volume is determined using the well-documented equation for the Helmholtz resonator. Frequency placement and effectiveness of the VO are then fine-tuned using proven acoustic simulation software to model the piping system. This sizing method has been successfully used throughout the development stages of the VO.

2.1 VO Testing at the Reciprocating Compressor Test Facility (RCTF)

Testing of the original VO design was performed at the Reciprocating Compressor Test Facility (RCTF) located at SwRI. Two VO devices were installed on an Ariel JGA/2 reciprocating compressor as indicated in Figure 2. The VO in the left circle is installed on the valve cap. The VO in the right circle is installed along the cylinder nozzle. As depicted in the figure, the choke tube of each VO included a full bore ball valve to allow quick installation or removal from the acoustic system. Because the data could be acquired quickly with and without the VO installed, this configuration provided valuable insight. It was possible to locate the cylinder nozzle resonance peak, then almost instantaneously open the valve and watch the resonance peak drop. For this configuration, a pulsation amplitude of 9.0 psi [62 kPa] at 50 Hz was measured with the valve closed (Figure 3). With the valve open (VO installed), the pulsation amlplitude at the cylinder nozzle resonance frequency dropped to 1.5 psi [10 kPa] at 50 Hz. Testing of the original VO designs showed a pulsation amplitude reduction of 60 percent over the entire 500 to 1,000 RPM speed range.

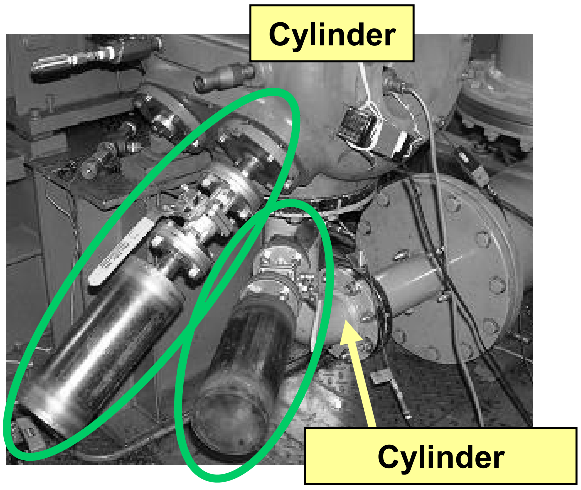

Figure 2: The Original Virtual Orifice

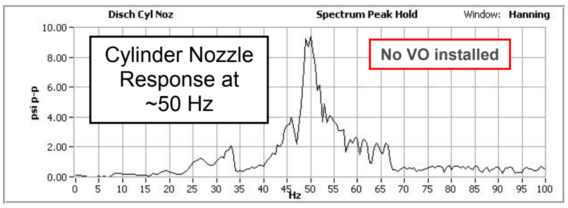

Figure 3: RCTF Cylinder Nozzle Resonance

Following successful testing of the VO in the RCTF, modifications were developed to improve the mechanical design. Some slight improvements to the acoustic design were also made. The more compact and mechanically stable VO design is depicted in Figure 4. The plot in Figure 5 presents the pulsations that were measured with the more compact and acoustically improved VO installed on one of the cylinder head-end valve caps. When compared with the plot in Figure 3 (no VO installed), an overall pulsation reduction of 67 percent is observed with the VO installed.

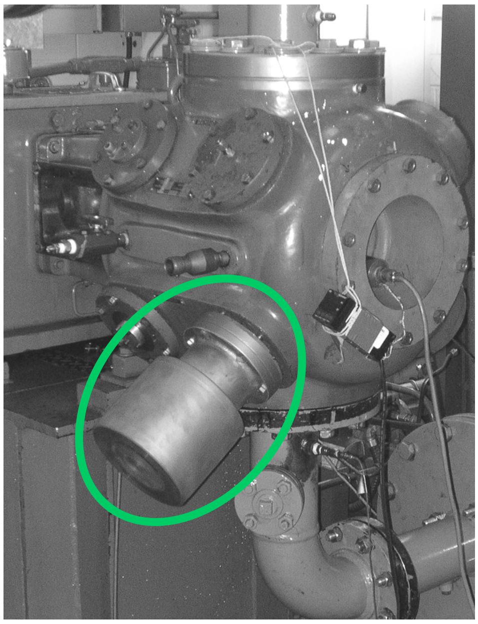

Figure 4: Improved Compact Mechanical Design

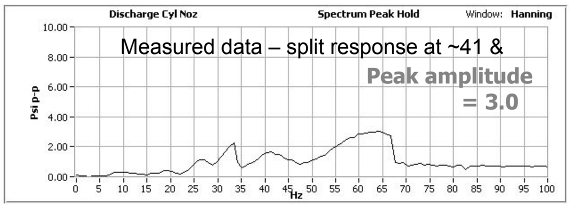

Figure 5: RCTF Test Results with Compact VO

2.2 VO Testing at the Advanced Reciprocating Compressor Technology (ARCT) Test Bed

Once initial testing of the VO on the small compressor at the RCTF was successfully completed, a similar VO design was installed and tested at the Advanced Reciprocating Compressor Technology (ARCT) Test Bed, also located at SwRI. For testing at this facility, the compact VO design was installed on an Ariel JGR/2 reciprocating compressor at a discharge valve cap. Cylinder discharge nozzle pulsation data without the VO are provided in Figure 6. Approximately 20 psi [138 kPa] was observed at 54.5 Hz. Measured pulsations with the VO mounted on the discharge valve cap are provided in Figure 7. Pulsations at the cylinder nozzle resonance frequency were reduced to less than 5 psi [34 kPa] with the VO installed. A reduction of 75 percent was achieved without the use of an orifice.

An orifice was also tested in the ARCT test bed in order to document the effects on efficiency for comparison purposes. Efficiency was measured for the relevant cylinder with the orifice installed and then with the VO installed (orifice removed). A comparison of the measured cylinder efficiencies is summarized for the entire speed range in Figure 8. At approximately 510 RPM, a 3 percent efficiency improvement was observed with the VO installed. At approximately 885 RPM, an 8 percent efficiency improvement was observed with the VO installed. Once the VO pulsations and efficiency improvement capabilities were confirmed through lab testing at the SwRI facilities, the VO was installed at El Paso Western Pipeline's Baxter Station in a field test application.

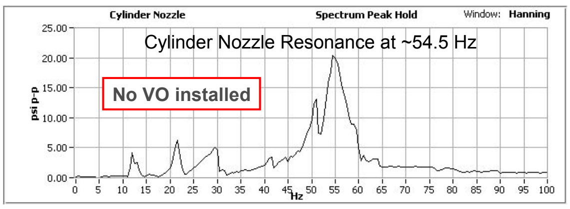

Figure 6: ARCT Test Bed Cylinder Nozzle Resonance

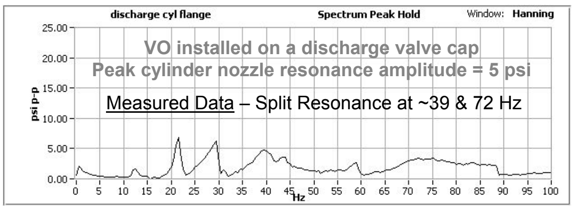

Figure 7: ARCT Test Bed Data with VO Installed

2.3 VO Field Testing

Field testing of the VO was necessary to further validate the design. A two-throw reciprocating compressor installed at El Paso Western Pipeline's Baxter Station had experienced excessive vibrations and cylinder nozzle failures as a result of uncontrolled cylinder nozzle pulsations. As a result of the nozzle failures, fairly restrictive cylinder nozzle orifice plates were installed at the suction and discharge cylinder flange connections. Although the orifices effectively reduced the vibrations and eliminated the nozzle failure issue, they also reduced unit throughput. Representatives from El Paso Western Pipelines welcomed the opportunity to install the VO with the hope that the unit efficiency would improve.

The two-throw 1,200 BHP compressor at the Baxter Compressor Station operates in a single stage natural gas transmission service over a speed range of 1,050 to 1,150 RPM. Each cylinder has a 7.5-inch [191 mm] bore and a 6.0-inch [152 mm] stroke. Operating pressures are 780 psi [5378 kPa] suction pressure and 1030 psia [7102 kPa] discharge pressure. Figure 9 shows the VO installed at the suction valve cap on one side of the compressor. Further improvements were made to the mechanical design prior to field installation. Figure 10 portrays two 3-D images of the improved VO design. In this figure, the VO volumes are transparent to show the internal details. The improved design incorporates the VO into the valve cap such that the valve cap and VO are now one assembly. Field test measurements of the compressor pulsation, vibration, and performance were acquired in July 2007 and are summarized in the following sections.

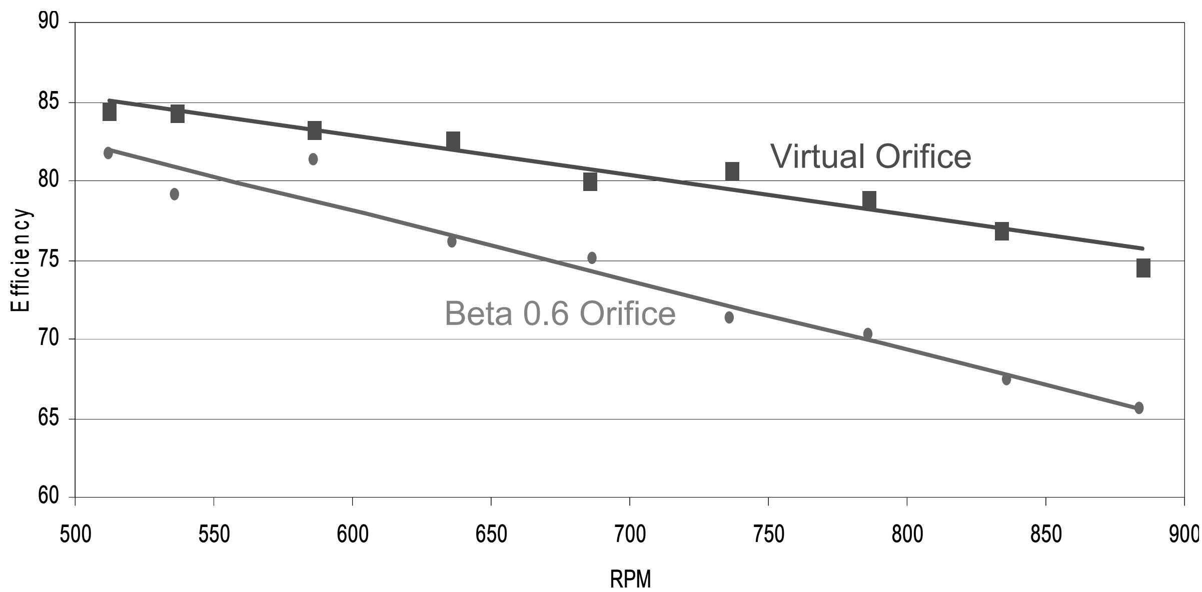

Figure 8: ARCT Test Bed Efficiency Comparison between the Virtual Orifice and a Conventional Beta 0.6 Orifice Plate

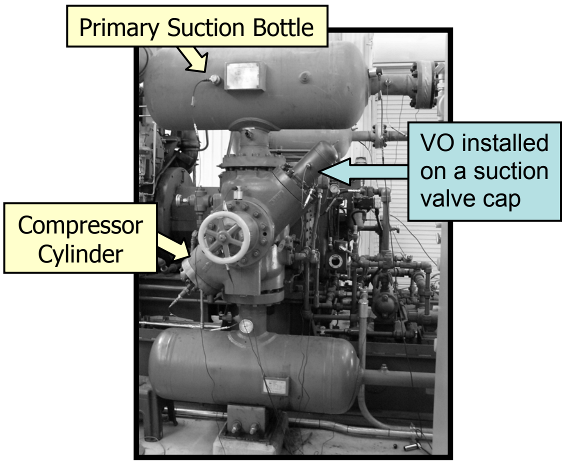

Figure 9: VO installed at GMRC Member Company Station

2.3.1 Pulsation Improvement

Pulsation measurements were obtained at a cylinder valve cap for each cylinder. Data were measured for the following configurations:

- with neither the orifice nor the VO installed,
- with only the orifice installed, and
- with only the VO installed.

Figure 11 summarizes the pulsation measurements for each of the three conditions described above, showing the benefits of installing the VO. With neither device installed, the cylinder nozzle response was just above fourth order (4x), and the maximum pulsations resulting from that response placement peaked at 52 psi [359 kPa]. Pulsation amplitudes at second order (2x) increased significantly with the orifice installed, resulting in a maximum pulsation amplitude of 30 psi [207 kPa]. The large increase in 2x pulsations is indicative of an undersized orifice. With the VO installed, maximum pulsation amplitudes were reduced to 15 psi [103 kPa]. Maximum pulsation amplitudes over the 0 to 200 Hz frequency range were reduced by 71 percent with the VO installed. Overall pulsations were approximately 50 percent lower with the VO than with the orifice. Pulsation improvements also resulted in vibration and efficiency improvements.

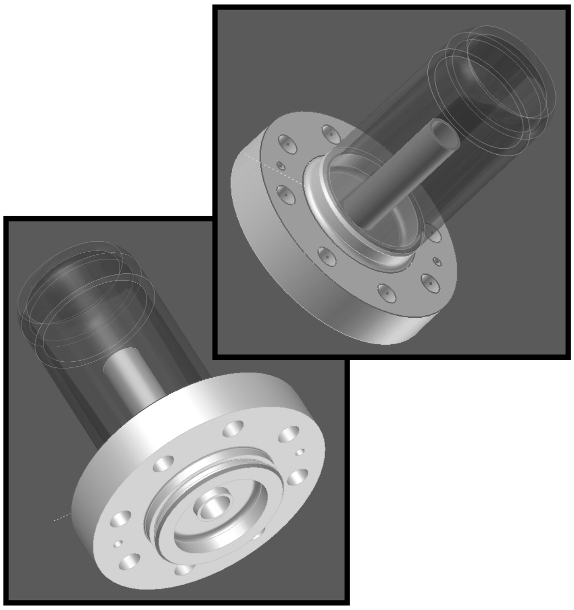

Figure 10: 3-D Model of the Field Tested VO

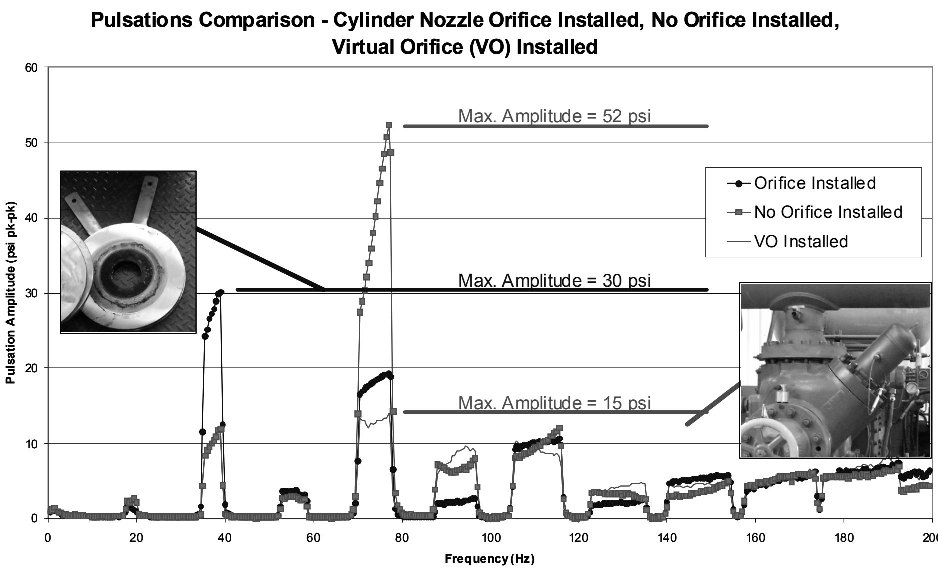

Figure 11: Field Data Show Reduced Pulsations with VO Installed

2.3.2 Vibration Improvement

Vertical cylinder vibration was measured for the three configurations described in section 2.3.1. It was clear upon review of the vibration and pulsation data that fourth order (4x) vibrations are directly related to the pulsations associated with the cylinder nozzle response. Fouth order (4x) vibrations were approximately 0.8 ips [20 mm/s] with neither device installed. With either the orifice or the VO installed, pulsations were reduced to 0.6 ips [15 mm/s] at the bottom end of 4x and 0.3 ips [8 mm/s] at the top end of 4x. The vibration data acquired at the Baxter Station are summarized in Figure 12. Maximum vibration amplitudes at the second (2x) and third (3x) orders were not affected by the system configuration changes. It was determined from the field test results that 2x and 3x vibrations were not pulsation driven and that vibration reduction at these frequencies would require modifications to the mechanical system. In this field test case, the VO did not significantly improve vibration compared to the orifice; however, because the improvements were similar to that of the orifice, these data provide further evidence that the VO could potentially replace the orifice.

2.3.3 Efficiency Improvement

Field testing indicated that the VO more effectively reduced pulsations than the orifice and that a similar reduction in vibration amplitudes was achieved with either device installed. Further analysis was then performed to determine if the VO would have a positive impact on cylinder efficiency. Overall thermodynamic efficiency and power per unit flow were calculated based on the measured Pressure-Volume (PV) cards. Figure 13 summarizes the changes in cylinder efficiency with an orifice installed versus the changes in cylinder efficiency with a VO installed. The upper plot depicts a 2.5 to 4 percent efficiency improvement with the VO installed. The lower plot depicts a 1.7 HP/MMSCFD [1416 kW/(Nm^3/hr)] reduction in power per unit flow with the VO installed. Based on the fuel savings generated by installing the two VOs on the test compressor, a payback time of less than two years is estimated.

3 Summary

Through the GMRC research program, the Side Branch Absorber (SBA), an industry proven pulsation control device, was adapted for use at a novel location in the piping system. Efforts to control cylinder nozzle pulsations with minimal losses resulted in a very useful device called the Virtual Orifice (VO). The VO can be installed on both low-speed and high-speed compressors to replace any cylinder nozzle orifices that are consuming large amounts of horsepower. Installation of the VO on a gas transmission compressor has shown significant pulsation reduction and improved efficiency.

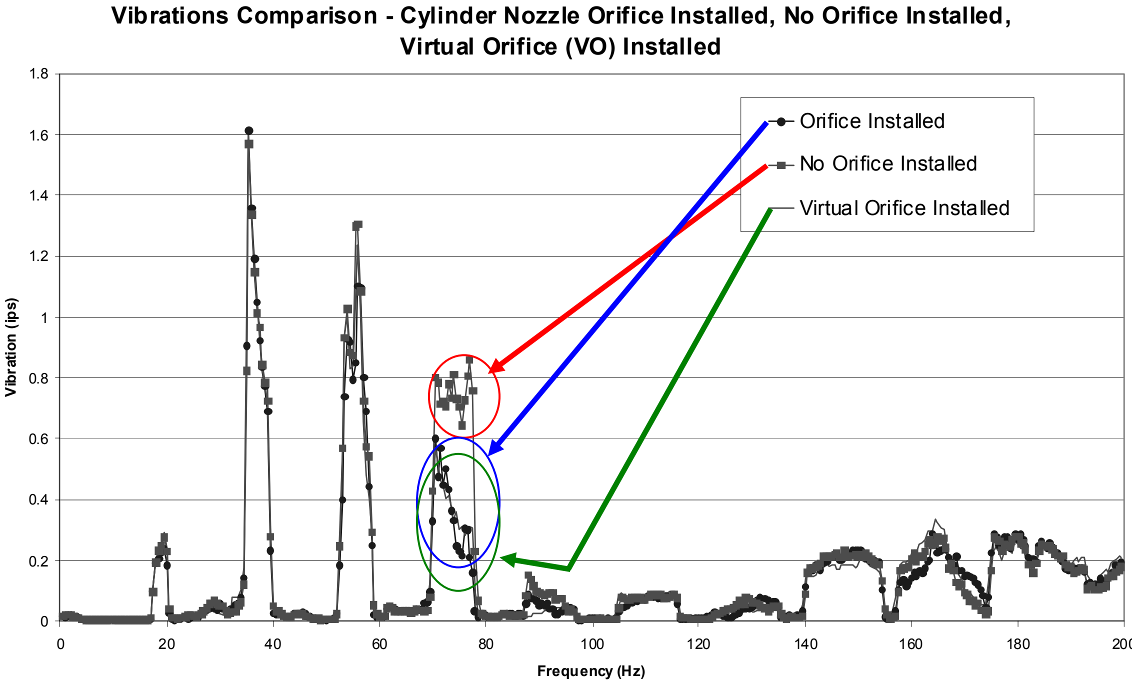

Figure 12: Field Data Show Reduced Vibrations with VO Installed

Vibration reduction achieved with a VO installed was similar to that achieved with an orifice installed. Reciprocating compressor installations require a balance between pulsation control, compressor performance, and mechanical vibration. The VO offers a solution that more effectively manages the cylinder nozzle resonance, thereby maintaining the required system balance.

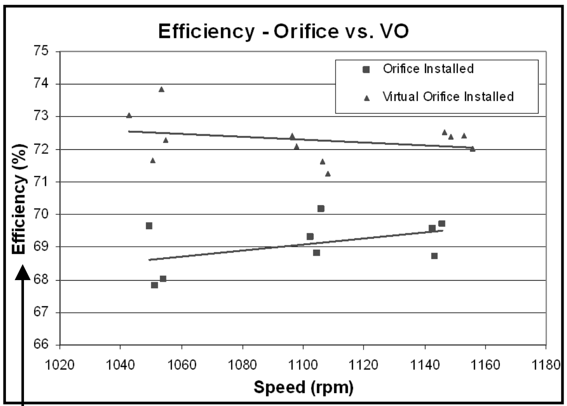

Overall thermodynamic

Values for one of the 2

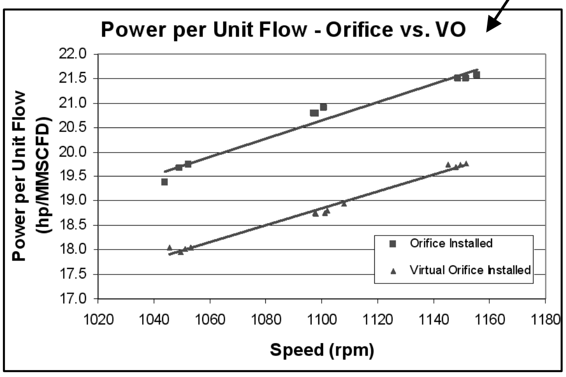

Figure 13: Field Data Show Improved Efficiency with VO Installed

4 Acknowledgements

SwRI and El Paso Energy would like to acknowledge the Gas Machinery Research Council (GMRC) for funding the research and development described in this paper.

References

Broerman, E.L., M.G. Nored, R.J. McKee, Ph.D., "New Solution – Virtual Orifice, Old Problem – Pressure Drop Used for Controlling the Cylinder Nozzle Resonance," GM Journal, May 2008.

Nored, M.G., E.L. Broerman, D.M. Deffenbaugh, R.J. McKee, "Advancements in Pulsation Control Technology," presented at the 2007 GMRC Gas Machinery Conference, October 1-3, 2007, Dallas, TX.

Smolik, M.A., E.L. Broerman, C.M. Scrivner, "Helmholtz Absorbers: Experiments in Controlling Resonant Pulsation Without the Use of Orifice Plates," presented at the 2007 ASME Pressure Vessels and Piping (PVP) Division Conference, July 22-26, 2007, San Antonio, TX. (paper reference number PVP2007-26246).

Broerman, E.L., R.J. McKee, C.M. Scrivner, "GMRC Advanced Reciprocating Compressor Technology (ARCT)," Compressor TechTwo, Two-Part Series published June 2007 and July 2007.

Broerman, E.L., R.E. Harris, C.M. Scrivner, "ARCT & GMRC Pulsation Control Project: Current Results," presented at the 2006 GMRC Gas Machinery Conference, October 2-4, 2006, Oklahoma City, OK.

Smalley, A. J., R.E. Harris, C.M. Gehri, and G.W. Weilbacher, “Dynamic Characteristics of Large High-Speed Reciprocating Compressor Systems,” presented at the European Forum for Reciprocating Compressors (EFRC-Conference), March 27-28, 2003, Vienna, Austria.

Weilbacher, G.W., C.M. Gehri, R.E. Harris, B.A. White, C.R. Sparks, P.J. Pantermuehl, A.J. Smalley, and R. Goodenough, “Acoustic and Mechanical Dynamics Issues for High Horsepower, High-Speed Compressors in Gas Transmission Service,” presented at the Gas Machinery Conference (GMC), October 7-9, 2002, Nashville, TN.

Gehri, C.M. and R.E. Harris, “Technology for the Design and Evaluation of High-Speed Reciprocating Compressor Installations,” presented at the European Forum for Reciprocating Compressors (EFRC-Conference), November 4-5, 1999, Dresden, Germany.

Gehri, C.M. and R.E. Harris, "High Speed Reciprocating Compressors - The Importance of Interactive Modeling," presented at the Gas Machinery Conference (GMC), October 4-6, 1999, Houston, TX.

Pierce, Allan D., “Acoustics – An Introduction to Its Physical Principles and Application,” McGraw-Hill, 1981.

Torsional Vibration Case Study Highlights Design Considerations

by:

Howes, Brian
Beta Machinery Analysis
Calgary, Alberta
Canada
bhowes@BetaMachinery.com

King, Tony
AG Equipment
Broken Arrow, Oklahoma
USA
tking@agequipmentcompany.com

Pearsall, David
Dresser-Rand
Tulsa, Oklahoma
USA
dpearsall@dresser-rand.com

6th Conference of the EFRC
October 28th / 29th, 2008, Dusseldorf

Abstract:

A large compressor installation in a remote location of Russia experienced rapid crankshaft failures. Due to the very high costs and logistics involved, a root cause failure analysis was conducted. Field measurements obtained at site identified an unexpected situation where the first two torsional natural frequencies occurred at essentially the same speed. This resulted in a double resonance condition – something very rare in the field of Torsional Analysis. Detailed modeling using the field data confirmed the cause of the failure and was instrumental in finding a quick solution.

This technical paper highlights a number of important considerations for the torsional system in new or revamped compressors, as well as design philosophies to assess and mitigate the risk of torsional failures.

1 Introduction

The authors of this paper represent the manufacturer of the compressor, the packager of the unit, and the third party consultant that provided assistance to solve the problem.

The unit was a reciprocating compressor driven by a motor, as described in more detail below (the delivered unit):

- fixed speed, induction motor, 1500 RPM synchronous speed, 1480 loaded, 500 kw;
- shim pack coupling;
- flywheel (32,724 lbf in^2, original design);
- horizontally opposed reciprocating compressor, 4 throw, 3 stage.

The cause of failure was clearly torsionally-induced alternating stress. Refer to Figure 1 for a view of the failed surface at the drive end of the compressor. The classic 45 degree crack is consistent with a torsional failure. The crack appears to have initiated at the end of the keyway, close to the flywheel. Having the keyway causes a slightly greater stress concentration than without (2.85 versus 2.2).

Figure 1: Broken Shaft End

It would be logical to assume that the presence of the keyway was the cause of the failures. Evidence given below shows that the presence of the keyway is not sufficient to explain the failures. Stresses predicted for the original system without the keyway are still high enough to cause a failure. By way of explanation, stresses will be high at a node (defined as a point of zero motion). Typically, a node for the torsional deflections and, therefore, a plane of maximum stress, will occur near the flywheel. Refer to the mode shape plot in Figure 2 (shown for the model tuned to field conditions for Scenario B). A node occurs for the second mode close to the flywheel.

The sharp change in the slope of the second mode line at the flywheel also suggests a stress maximum is present at that location. The actual stress contribution depends on amplitudes of vibration at or near the second mode. The node for the first mode is closer to the motor, but there is a significant change in slope for the first mode at the flywheel, indicating that a significant contribution to stresses at the failure location could also come from torsional vibrations at or near the first mode.

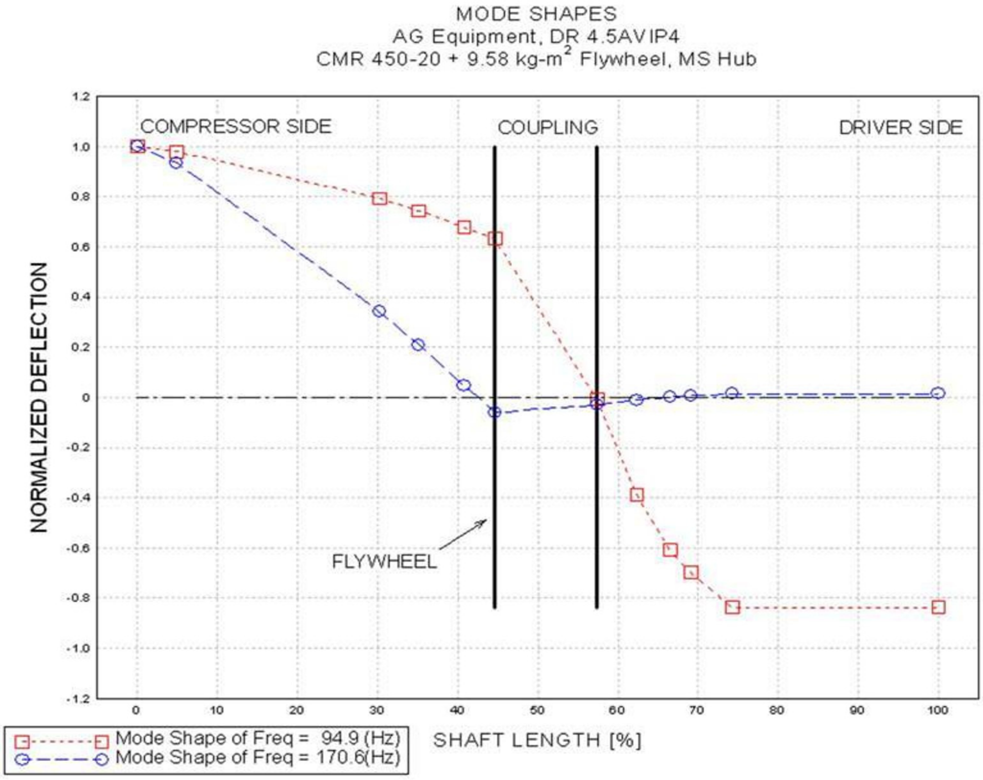

Figure 2: Mode Shape Plot

2 Case History

2.1 Original Design and Operation Resulting in Failures

The original design analysis resulted in a system with a flywheel on the compressor side of the coupling. The calculated torsional natural frequencies (TNFs) were placed between 3 and 4 times run speed for TNF1, and between 7 and 8 times run speed for TNF2. See Figure 3.

Despite the predictions of non-resonant performance, the system design factors (DFs) were assessed assuming that resonance would occur. This is a conservative design philosophy that is usually sufficient to avoid torsional failures. The stresses assuming resonance at TNF1 or resonance at TNF2 were found to be acceptable. Since the expected operation was not going to be resonant at either TNF, the design was accepted.

In due course, the system was packaged and shipped to Siberia for installation and startup. The first failure occurred after 375 hours of operation. (Note that many of those hours were under very light load while the process was being purged.)

After the failure, it was noted that there was a keyway in the compressor crankshaft. This had not been intended, but the DF with the keyway was still very good. It was decided that the failure was likely a rogue failure and a replacement crankshaft was shipped to site and installed. The replacement also had a keyway, but was considered acceptable as no alternative spare was available in a short timeframe and since calculations indicated that the keyway was not critical.

The second failure occurred after another 111 hours of operation (about 32 hours were under full load).

2.2 Post-Failure Design Audit

A third crankshaft was shipped to site. This one did not have a keyway. However, in an effort to prevent a third failure, a second opinion was requested from a consulting engineering organization with extensive experience analyzing torsional response of reciprocating compressor systems.

The first observation from the design audit was that the first TNF was predicted to be resonant at 4 times run speed. See Figure 3. (Note that the analysis methods used by the consultant included tolerances for system stiffnesses and inertias, as described in papers found in the Bibliography at the end of this paper. Scenarios A, B, and C are calculated for the low, the average and the high natural frequencies based on the tolerances for stiffness and inertia.) The apparent reason for the difference in the predictions of TNF1 was the way the motor rotor was modelled. However, even at resonance for the first mode, the design factor (DF) for the system was acceptably high.

The second TNF was not observed to be close to resonance. Note that in both models (original design and design audit) there was no added inertia for the oil pump. The oil pump used in this model of compressor is driven directly through a coupling at the outboard end of the compressor crankshaft.

In a normal modelling job in the design stage, the reaction to having predicted operation at resonance would have been to change the system to avoid this resonant condition. Uncertainties associated with

- defining damping values,
- defining the torque effort from the compressor under upset conditions, as well as
- the unknown level of acceptable torsional vibrations for auxiliary equipment, such as motor fans and compressor oil pumps,

generally lead to a conservative design philosophy of avoiding resonant operation, if practical, on fixed speed motor driven units.

In this case, however, due to the lack of a clear indication from the design audit models as to why the failures had occurred, it was concluded that a visit to the field to measure the actual TNFs and amplitudes of torsional vibrations in operation was required to determine the root cause of failure.

Due to the remoteness of the site and the delays that would have ensued getting travel documents, it was decided that the consultant would train and equip the packager's representative (already possessing travel documents) to collect the required data. The data were transferred via electronic mail to the consultant's office for analysis.

3 Field Measurements and Design of Solution using Tuned Model

Field data were collected by the packager's representative. A team effort, including the end user's personnel, the packager's representative and the consultant, was required to overcome various hurdles. For example, the only location available to measure torsional response with the test equipment available was the opposite drive end (ODE) of the motor. A special adapter had to be manufactured in the field to accomplish this measurement. The compressor ODE was not available due to looseness in the coupling (by design) between the crankshaft and the oil pump.

The first TNF was measured close to resonance at the 4th order of run speed - consistent with the design audit model (Scenario C, see Figure 3). However, the second TNF was found to be close to resonance at the 7th order – not consistent with the audit model.

An interesting aside: It was observed that TNF1 was about 3 Hz (2.8%) higher when the system was started cold, compared to starting the system in a "warm" condition. Consistent with this observation, the amplitude of torsional vibrations at 4th order increased as the system warmed up under load. These behaviors are consistent with the motor rotor being stiffer when cold – an observation that has been made in the past by the consultant's personnel.

The results from the field measurements immediately pointed toward the idea that having both TNFs resonant at the same speed would lower the design factor for the system. How to model this simultaneous resonance was a problem.

Experience with modelling other compressor packages suggested that the addition of inertia for the oil pump might correct the second TNF discrepancy between field and model. Addition of a representatively small inertia to the model at the compressor ODE lowered the predicted second TNF to resonance with the 7th order without changing the first TNF. The design factor with both TNFs resonant at the same speed was at a failure level (0.9 with and 1.1 without the added stress concentration due to a keyway!). The technical explanation of the failures (the root cause) was now understood.

Using the tuned model, the size of the flywheel was changed to see if resonance could be avoided at both TNFs. In fact, both modes were sensitive to the removal of inertia from the flywheel. The flywheel inertia was reduced in the model to about 50% of the original flywheel size. This change was predicted to move the TNFs midway between orders and raise the design factor above the target minimum of 2 for all conditions.

This change was implemented in the field and no crankshaft failures have been reported since.

Figure 3 below summarizes model and field TNF and DF results for the three project phases described in the case history.

Note the design factors for the design audit (Phase 2). The DF goes up as the predicted TNF1 approaches resonance. At the same time, the TNF2 gets further away from resonance. This is an indication that resonance at the second TNF is of more concern than at the first.

For Phase 3, the design factors are given for Scenario C, which was the worst for the tuned model.

Design Phase	Design Factor*2	TNF1 (Hz/Order*3) 1480 rpm	TNF2 (Hz/Order*3) 1480 rpm
Phase 1 design before construction			
Design	2.4	88 / 3.6	186 / 7.5
Resonant at TNF1*1	2.7	Resonant at 4X 1320 rpm	
Resonant at TNF2*1	2.0		Resonant at 8x 1394 rpm
Phase 2 design audit after two failures			
Scenarios A/B/C	2.1 2.2 2.2	89.8 / 3.64 94.4 / 3.8. 98.1 / 3.98	183.0 / 7.42 186.8 / 7.57 189.1 / 7.66
Phase 3 field measurements and tuned model			
Field data*4	----	105/ 4.25(C)*4 102 / 4.1(W)*4	177 / 7.17
Tuned Design*6 As Built Scenario C	0.9 1.1*5	98.6 / 4.0 98.6 / 4.0	172.7 / 7.0 172.7 / 7.0
Modified*6,7 Scenarios A/B/C	2.0*5 2.1*5 2.2*5	103.0 /4.17 107.8 / 4.37 111.7 / 4.53	176.9 / 7.17 180.6 / 7.32 183.0 / 7.42

Figure 3: Model and Field TNF and DF Summary

Notes for Table in Figure 3:

*1. "Worst case" calculation assuming one TNF is resonant at the nearest order of run speed.

*2. Design Factor (DF) is the minimum for the compressor crankshaft, based on overall stresses. DF > 2 is good, and DF <1 is a guarantee of failure. Unless otherwise noted,

- a keyway was included in the design factor calculation,
- a flywheel (inertia = 9.58 kg-m^2) was present at the compressor drive end, and
- no inertia was present to represent the oil pump at the compressor outboard end.

*3. An "Order" is an integer multiple of run speed. Run speed is 1500 to 1480 rpm.

*4. Measured TNFs reported here were at "cold" (C), (ambient), and "warm" (W) temperatures.

*5. A keyway was not included in the stress calculation for this model.

*6. An inertia representative of the oil pump at the outboard end of the compressor was added to the model.

*7. The flywheel inertia was changed in this model to 4.83 kg-m^2)

4 Philosophy for Deciding to Perform a Torsional Design Study on a New Unit

End users and packagers of reciprocating compressor systems need to make the decision whether or not to perform a torsional dynamic design study for each new compressor package that is ordered.

The following considerations are offered from the consultant's experience with fixed speed electric motor driven reciprocating compressors. If the answer to any of the following questions is yes, then a design study should be performed.

1. **Is the unit critical?** A definition of a critical unit is required. It is suggested that the cost of one day of down time or lost production ($lp) is compared to the cost of performing the design study ($ds). Usually, this ratio ($lp/$ds) is greater than one. Problems caused by torsional issues with a unit will cost many days of lost production, as well as other costs. Therefore, a conservative definition of a critical unit would be one for which the above mentioned ratio is greater than one. Remote sites will always have a high cost per day of down time, if only for the repair process. New installations are likely to have subtle differences that only a torsional study can identify.

2. **Is the new package a different combination of compressor and driver from what has been used in the past?** For example, a change in motor manufacturer between an existing package and a new package could justify a model study, even if the motor is nominally the same size. There are usually subtle differences.

3. **If the new package is not a new combination, are there significant differences in cylinder size, staging, operating conditions, or load steps, compared to existing packages?** A definition of significant is required. How can the significance of the differences be determined? One way is to compare the predicted compressor torque effort of the new package to that of the existing package. Both overall torque and individual orders of torque should

be compared with an emphasis on torque orders close to the first and second TNFs. A simple ratio of the old to new torque efforts times the DF of the existing system will be useful as a guide.

4. **If none of the other questions have been positive, are speeds going to be different for the new package, compared to the existing package?**

5 Conclusions

Tolerances associated with fabrication cannot be avoided and must be considered in the design stage when tuning of TNFs is required.

In the design stage, it is important to make “worst case” assumptions to avoid bad surprises after startup. In the case study provided, a failure would have been predicted in the design stage if a “worst case” design approach (a model with resonance occurring at both TNFs at the same speed) had been used.

Clients who have not had experience with torsional failures may be critical of the excessive conservativeness of the “worst case” approach to design. This conservativeness has to be weighed against the huge costs from lost production, problem identification and repairs that can result after a failure.

If predicted torsional problems are

- expensive to eliminate as a possibility in the design stage,
- destructive if they do occur, but
- easily corrected in the field once the exact response is known (for example, by addition of mass rings on the crankshaft to avoid resonance),

then, torsional vibration measurements at startup should be performed.

The cost-effectiveness of this design philosophy must be judged on a case by case basis. Consideration should be given to the cost of

- an extended outage in the event of a failure, versus
- making expensive design changes (typically a soft coupling), versus
- torsional measurements at startup with fine-tuning at site, as required.

The actual system can turn out to be satisfactory after torsional measurements are made. Then, no additional costs beyond the testing will be incurred. However, if a condition that will lead to failure is detected at startup, relatively inexpensive changes (compared to the cost of a failure) can be implemented.

As demonstrated in the case study;

- torsional systems are complex and sensitive to small errors,
- the feedback of data from field measurements to designers can lead to improved design methodology which will help prevent future problems, and
- cost-effective ways are available to allow packagers and end users to perform baseline startup checks instead of waiting for expensive failures to occur.

The job of the designer should be to identify those systems for which the expense of a torsional analysis check at startup is justified. This job can be accomplished by assessment of system tolerances and by using “worst case” analysis methods.

6 Bibliography

Lateral and Torsional Vibration Problems in Systems Equipped with Variable Frequency Drives. Howes, B., P. Eng.; De la Roche, L., P. Eng.; presented at the Gas Machinery Conference, Covington, KY, USA, Oct. 2005.

Torsional Vibration: The Value of Field Verification. Varty, R.; Harvey, J., P. Eng.; presented at the Gas Machinery Conference, Albuquerque, NM, USA, Oct. 2004.

Torsional Vibration Modelling and Analysis Continued. Varty, R.; Harvey, J., P. Eng.; presented at the Gas Machinery Conference, Salt Lake City, UT, USA, Oct. 2003.

A New Shaft Alignment Technique. Howes, B., P. Eng.; presented at a Canadian Machinery Vibration Association Meeting, Canada, 2000.

Compressor Operating Conditions & Loading: A Torsional Perspective. Murray, B. D.; Fofonoff, B.; Howes, B., P. Eng.; Zacharias, V.; presented at the Gas Machinery Conference, Denver, CO, USA, Oct. 1996.

Sensitivity of Torsional Analyses to Uncertainty in System Mass-Elastic Properties. Murray, B. D.;

Howes, B., P. Eng.; Zacharias, V.; Chui, J.; presented at the International Pipeline Conference, Calgary, AB, Canada, June, 1996.

A Systems Approach to Torsional Analysis. Murray, B. D.; Howes, B., P. Eng.; Zacharias, V.; presented at the Gas Machinery Conference, Corpus Christi, TX, USA, Oct. 1995.

7 Acknowledgements

The authors acknowledge the assistance of Michael Cyca, Rodney Varty, and Jackie Walters, all with Beta Machinery Analysis, in the preparation of this paper.